



Signaling, Cooperation, and Conflict in Animals



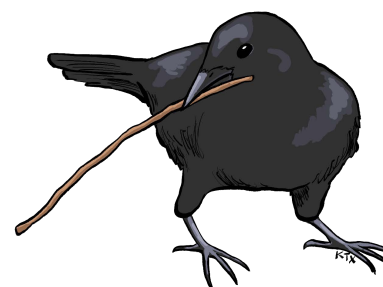
A DISSERTATION PRESENTED
BY
DAKOTA E. MCCOY
TO

THE DEPARTMENT OF ORGANISMIC AND EVOLUTIONARY BIOLOGY



IN PARTIAL FULFILLMENT OF THE REQUIREMENTS
FOR THE DEGREE OF
DOCTOR OF PHILOSOPHY
IN THE SUBJECT OF
BIOLOGY

HARVARD UNIVERSITY
CAMBRIDGE, MASSACHUSETTS
MAY 2021



©2021 – DAKOTA E. McCOY
ALL RIGHTS RESERVED.



Signaling, Cooperation, and Conflict in Animals

ABSTRACT

Animals spend their lives sending and receiving signals. Before birth, embryos converse with mothers through hormones and receptors; in adulthood, many animals attract and assess partners through colorful mating dances. In this dissertation, I used experimental optics and evolutionary theory to analyze the physical makeup and evolutionary purposes of animal signals—from placentas to birds-of-paradise. **In Chapter 1**, I show that ornate male birds-of-paradise evolved “super black” feathers with microstructures that absorb up to 99.95% of light. Super black is an evolved optical illusion which makes males’ bright colors appear brighter, even glowing, to observing females. **In Chapter 2**, I find that colorful peacock spiders—the alluring arachnid analogue of birds-of-paradise—have super black microlens arrays, bumps that are optimally sized and shaped to absorb more, and reflect less, light. **In Chapter 3**, I demonstrate that super black evolved convergently in 15 families of sexually-selected, brightly-colored birds. Super black is not the only adaptation to harness physical rules of light for evolutionary purposes. **In Chapter 4**, I show that some carotenoid-colored male birds (an archetypal example of honest signaling) fly under false colors: male tanagers use microstructures to deceptively amplify their appearance. These lessons about deception in mate choice also apply to mammalian pregnancy, where selective mothers evaluate embryos and automatically terminate low-quality embryos (akin to selective female birds choosing a mate). **In Chapter 5**, I describe evidence that human embryos exaggerate their own quality to satisfy choosy mothers: in primates and convergently in horses, embryos produce signalling hormones (i) in massive quantities and (ii) with biochemical changes to extend half-life (two evolutionary signatures of deception and escalation). Beyond maternal-embryo conflict, siblings can also clash during pregnancy. **In Chapter 6**, I analyze a large dataset ($n = 27,080$) of marmoset monkey births to show that conflicts of interest between same-sex co-gestating siblings harm health and survivorship. Finally, **in Chapter 7** I close on an optimistic note by presenting experimental evidence that tool-making New Caledonian Crows feel happier after they have used tools, like humans who are intrinsically motivated to play chess or solve crosswords. All of these projects included collaborators to whom I am grateful.





Contents

o	INTRODUCTION	I
1	SUPER BLACK IN ORNATE BIRDS-OF-PARADISE	8
2	SUPER BLACK IN COLORFUL PEACOCK SPIDERS	17
3	SUPER BLACK EVOLVED CONVERGENTLY IN 15 BRILLIANT BIRD FAMILIES	27
4	MICROSTRUCTURES AMPLIFY CAROTENOID PLUMAGE SIGNALS IN TANAGERS	41
5	EMBRYO SELECTION & MATE CHOICE: CAN ‘HONEST SIGNALS’ BE TRUSTED?	69
6	EFFECTS OF LITTER SIZE AND SEX COMPOSITION IN CALLITRICHINE MONKEYS	81
7	NEW CALEDONIAN CROWS BEHAVE OPTIMISTICALLY AFTER USING TOOLS	97
	REFERENCES	115



Author List

THE FOLLOWING AUTHORS CONTRIBUTED TO THIS DISSERTATION:

CHAPTER 1: Teresa Feo*, Todd Alan Harvey, and Richard O. Prum

CHAPTER 2: Victoria E. McCoy, Nikolaj K. Mandsberg, Anna V. Shneidman, Joanna Aizenberg, Richard O. Prum, and David Haig

CHAPTER 3: Richard O. Prum

CHAPTER 4: David Haig

CHAPTER 5: Allison J. Shultz, Charles Vidoudez, Emma van der Heide, Jacqueline E. Dall, Sunia A. Trauger, and David Haig

CHAPTER 6: Brett M. Frye*, Jennifer Kotler, Amanda Embury, Judith M. Burkart, Monika Burns, Simon Eyre, Peter Galbusera, Jacqui Hooper, Arun Idoe, Agustín López Goya, Jennifer Mickelberg, Marcos Peromingo Quesada, Miranda Stevenson, Sara Sullivan, Mark Warneke, Sheila Wojciechowski, Dominic Wormell, David Haig, and Suzette D. Tardif

CHAPTER 7: Martina Schiestl, Patrick Neilands, Rebecca Hassall, Russell D. Gray, and Alex H. Taylor

* co-first author.

TO MY FAMILY.
AND TO THE BIRDS, SPIDERS, AND MAMMOSETS.

Acknowledgments

My acknowledgements must start with David Haig, my PhD supervisor. After meeting David for the first time, I rushed out of his office full of energy and jotted down the following note: “David Haig: an absolutely awesome guy who studies all sorts of things, puts jokes in his paper, and even writes about stuff like philosophy.” I decided on the spot I would join his group if I could, and, luckily, I did. At our first lunch, David and I sat down and talked for an hour. Many memorable conversations followed, each brimming with tangents, visits to the Oxford English Dictionary, forays into books ancient and new, and lots of laughter. Through his kindness and brilliance, David has fundamentally changed the way I view evolution, life, and mentorship. While I will not be able to pop my head around the corner to say hello anymore, I look forward to many more conversations in our future. Anyone who has not met him: go! Run, at top speed! Have a conversation with David Haig!

I have to convey my immense gratitude to my mentors. First, I am grateful for my brilliant and supportive committee—Catherine Dulac, Scott Edwards, and Naomi Pierce—with whom I have had so many illuminating conversations. Thank you also to George Lauder for his strong support and for our conversations about biophysics. Thank you to Lydia Carmosino for being an organizational genius. My dissertation would not have been possible without Brett Frye, Allison Shultz, and Martina Schiestl. Finally, I am a biologist because Leo Buss showed me the joys of scientific research through the Collections of the Peabody Museum at Yale. Rick Prum and Kristof Zyskowski introduced me to the beauty of birds, and Laurie Santos supported my curiosity about animal minds. And I will not soon forget learning from Chris Norris in the paleontological catacombs.

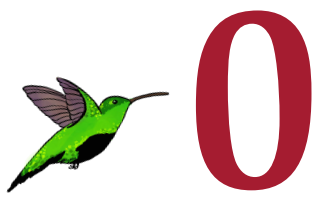
My labmates, and the members of our weekly FIAT group, greatly enriched my PhD experience both socially and academically. Special thank you to Jenna Kotler, Ava Mainieri, Holly Elmore, Brianna Weir, and Arvid Ågren. In MCZ #410 the tea kettle (and the conversation) never got cold.

Graduate school would have been a pale imitation of what it was if not for my wonderful cohort! We met during the Snowpocalypse of 2015, got stuck on campus, and then stuck together ever since. Thank you Sam Church, Molly Edwards, Brandon Enalls, Jess Gersony, Ben Goulet-Scott, Eadaoin Harney, Alyssa Hernandez, Nick Herrmann, Milo Johnson, Sang Il Kim, Vanessa Knutson, Phil Lai, Amaanet Lochab, Sofia Prado-Irwin, Jonathan Schmitt, Kristel Schoonderwoerd, Dan Utter, Yang Wang, Brock Wooldridge, James Xue, and Min Ya.

Friends make life richer. Tom Barron has helped me see more clearly and enjoy the wonders of nature. Sean and Judy Palfrey made Adams House not just a House but a Home. Cellar Thursday was a high point of every week; thank you Liz Asai and the rotating cast that made Thursdays sparkle. Finally, thank to the friends I’ve gotten to spend time in Cambridge— to name just a few, Priyanka deSouza, Ed and Imo Doddridge, Allan Hsiao, Rachel Kolb, Ela Leshem and Doni Bloomfield, Charles Masaki, and Mubeen Shakir. Finally, Voicelab has brought music and joy to my life beyond measure.

Thank you to my partner, William Burke. You make life so fun and special.

And thank you to my family: Mom (known to the world as Mary L. Marazita), Dad (Richard T. McCoy III), Marty, Tory, Tom, and Sammie.



Introduction

Signals abound in nature. From dense forest to deep ocean, ecosystems buzz with chemicals, calls, and colors in a cacophony of communication. In this dissertation, I focus on signals in two domains: mate choice and pregnancy. By studying the physical makeup and evolutionary purpose of signals, my work has helped unravel secrets about earth's biodiversity. Beyond basic science, my research touches three other areas: colorful animals inspire new solar power technologies, hormone signals help explain medical complications of human pregnancy, and animal behavior reveals what is going on inside non-human minds. Below, I will give a brief background to the themes I cover in my dissertation. Taken together, the seven chapters illustrate the unofficial name of David Haig's research group: the Fundamental Inter-connectedness of All Things.



1. COLORFUL MATING DISPLAYS

Colorful animals, particularly birds, are a model system for evolutionary biology. Two questions stand out. First, why are some animals colorful when it seems safer to be brown? Second, what is the physical, optical basis of fantastic animal colors? In addition to these fundamental questions, by studying how animals manipulate sunlight for their own purposes, we can develop new solar-powered technologies of our own. In Chapters 1-4, I consider colorful signals in elaborate mating displays. I started this work in birds, at Yale, with Rick Prum's mentorship, and then brought it to my PhD with David Haig.

1.1 Sexual Selection

For many years, biologists have tried to explain why some animals are brilliantly colorful (often only in one sex). There are three major theories. First, the choosing sex may have aesthetic preferences that could be arbitrary¹, shaped by Fisherian runaway selection², or influenced by selection on another domain such as foraging (sensory bias)³. Second, bright colors could help species identify mates of the same species rather than fruitlessly mating with the wrong species⁴. Third, and most commonly discussed, “honest signaling theory” posits that color is an honest signal of quality, either as a costly signal (e.g., due to parasite load⁵ or general handicap⁶) or as an index of health^{7,8,9,10,11}. All of these sexual selective pressures likely operate in concert with the demands of natural selection^{12,13}.

Counter to honest signaling theory, evolutionary game theory predicts that males have an incentive to appear better than they are^{14,15,2,16,17}. Carotenoid pigments—the red, orange, and yellow objects of my research in Chapter 4—are a textbook example of honest signaling¹¹ because they must be eaten rather than synthesized and have some links to metabolic or immunological activity^{8,18,10,19,11}. In Chapter 4, I study carotenoid-colored tanager birds and show that mate choice is subject to subtle deceptions (consistent with the predictions of evolutionary game theory rather than honest signaling theory).



1.2 Physics of Color

Color in nature arises from either pigments or structures. Pigments make color by absorbing certain wavelengths of light but reflecting others. In birds, the most common pigments are melanins (blacks, browns, and reddish-browns) and carotenoids (reds, oranges, and yellows), but some birds also have porphyrins (red, brown, green, and pink) and psittacofulvins (yellow, green, and red)^{20,21,22}. Structures make color by physically interfering with light. Usually, researchers study nanostructures²³, or features that are at the same size scale as wavelengths of visible light (400-700nm). Nanostructures cause iridescent colors and usually cause blue colors in nature. In birds, lattice-like arrangements of melanosomes make feathers iridescent^{24,25}, like a peacock's tail, and spongy keratin matrices underpin blue color in many birds²⁶.

While pigments and nanostructures are the most commonly-studied drivers of color, there is a third physical mechanism—the focus of my research in Chapters 1-4—that is comparatively understudied: microstructures between 1 μm and 1 mm in size. A handful of studies show that microstructures are important in plant and animal color, from emerald-colored cuckoos²⁷ to glossy cassowaries²⁸; from saturated flower petals²⁹ to velvet-black snakes³⁰. In Chapters 1-3, I show that microstructures play a major role in producing super black color in birds and spiders (reflecting less than 99% of light). Further, these antireflective signals tell us about the receiver's sensory experience. I propose that super black color creates an optical illusion fundamental to many animals with color-vision, from birds to spiders.

1.3 Bio-inspired Technology

By studying the physical cause of unusual coloration in animals, scientists can inspire new technologies for optical equipment, thermal technology, textile design, and solar panels³¹. For example, butterflies of the genus *Pieris* helped improve solar panel output by more than 40%. *Pieris* butterflies have ultra-white, lightweight wings³²; before taking flight, they bask with angled wings to focus light onto their body and warm their flight muscles³³. In an ingenious experiment, researchers mounted actual *Pieris* butterfly wings onto solar panels—and found that

the lightweight butterfly wings concentrated light and increase power output by 42.3%³⁴, a gigantic improvement over heavy, expensive metal concentrators^{35,36}. Likewise, our work on super black spiders in Chapter 2 led my colleague Nikolaj Mandsberg and his team to fabricate spider-inspired arrays for solar panels (with promising early results).

We face twin perils on the road to sustainability: the catastrophic loss of biodiversity and the looming threat of climate change. Every time a species is lost, we lose something ineffable and indescribably important. We lose critical ecosystem services. But we also lose the tangible, direct value of bioinspiration for sustainable engineering. We should learn all we can about how wild animals harness solar power, because our future—just like theirs—might depend on it.



2. PREGNANCY IN HUMANS AND OTHER MAMMALS

Pregnancy is the only time of human life where two (or more) distinct genetic individuals—with their own evolutionary agendas—cohabitiate the same body. While many features of pregnancy are joint adaptations, benefiting both mother and embryo, some adaptations of the embryo during pregnancy favor its own development even at a health risk to the mother³⁷, akin to resource wars between humans and our microbiota³⁸. Mothers face a fundamental evolutionary tradeoff: they may either invest more in one offspring or save resources to invest in other offspring. A given embryo values its own health over that of its siblings. This “altercation of generations”³⁹ can harm maternal and/or fetal health.

2.1 Embryo Selection

Most mammalian mothers invest substantial resources in their offspring before and after birth. Therefore, it is worth their while to assess embryo quality and terminate sub-par embryos early^{40,41}. In all of human life history the highest mortality occurs in the first month after conception^{42,43}. In order to be carried to term, embryos must pass signaling “checkpoints”⁴⁴. Embryos “audition” for the role of a lifetime⁴⁵ and mothers are unforgiving judges. One way



that maternal bodies select healthy embryos is to assess hormonal output. Selection favors mothers who gestate high-quality offspring, but selection favors embryos who can amplify their apparent quality⁴⁶. The placenta-maternal interface is “a battleground that has shaped remarkable rates of evolutionary change”⁴⁷. . Beyond placental mammals, many marsupials⁴⁸ and plants^{49,50} audition embryos and neonates.

In Chapter 5, I show that hormone signals during pregnancy can be thought of as a coevolutionary arms race where placenta produce high amounts of hormones and maternal bodies respond less³⁹. Placentas show “bewildering” diversity in structure and physiology across mammals⁴⁷, akin to the diversity of birds-of-paradise.

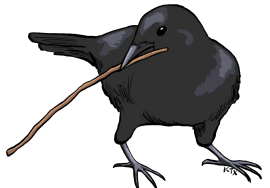
2.2 Sibling Competition

Siblings compete intensely in many taxa^{51,52,53,54}; e.g., siblings fight over space in the uterus⁵⁵, access to nipples⁵⁶, and alloparental care⁵⁷. Pronghorn fetuses (*Antilocapra americana*), implanted in groups of 5-8 in each of two uterine horns in the mother; however, the fetuses grow a “necrotic tip” which impales all fetuses except one pr horn⁵⁸. There is some evidence that same-sex sibling competition is stiffer; in spotted hyenas (*Crocuta crocuta*) same-sex litters have higher rates of aggression than do mixed-sex litters during infancy⁵⁶ and same-sex human siblings have lower reproductive success^{59,60,61}, but see⁶². These sibling conflicts can have major impacts on health and reproductive success. In Chapter 6, I find evidence that having siblings, particularly same-sex littermates, harms lifespan and reproduction in a peculiar bunch of monkeys (the Callitrichidae).

1.3 Pathologies of Pregnancy

It is a seeming paradox that pregnancy— required for the furtherance of human life— so often risks the life of mother and/or offspring. In humans, healthy pregnancies cause significant physical stress; pathological pregnancies can lead to severe bleeding, diabetes, high blood pressure, and death. In 2017, the World Health Organization reported that the lifetime risk of ma-

ternal death worldwide was 1 in 190. Traditionally, it is argued that pregnancy complications are the unintended evolutionary by-products of having large heads (we are smart) but narrow hips (we are bipedal). However, leading causes of pregnancy-related maternal deaths – such as hemorrhage and high blood pressure⁶³ – cannot be explained by head and hip size. Instead, the most common complications of pregnancy result from parent-offspring conflict over resources: hemorrhage, high blood pressure, and gestational diabetes are an overexpression of embryonic adaptations to promote more nutrient-rich blood flow to the placenta³⁷. In Chapters 5-6, I examine health complications of pregnancy in mammals. The lens of conflict explains why the best treatment for some life-threatening maternal problems, such as preeclampsia, is to deliver the baby.



3. ANIMAL MINDS

In the preceding two sections of this introduction, I have described how we can study signals to learn something about evolution. How hormones and receptors evolve during pregnancy tells us about parent-offspring conflict; the optical basis of signals in birds and spiders tells us about honesty and deception in mate choice. But these studies only make inferences about animal minds. What are the females actually feeling when they see a brilliantly-colored male framed by super black? How do genomic conflicts (say, between paternally-imprinted and maternally-imprinted genes) translate into subjective experience of a divided self⁶⁴? I hope to tackle these specific questions in my future work, but a related question about the subjective experience of New Caledonian crows forms the final chapter of my dissertation. I first learned about the rich inner lives of animals thanks to two mentors: Laurie Santos at Yale and a parrot named Penny who taught me how to speak. After several summers of fieldwork on the unforgettable island of New Caledonia, I can contribute some experimental data about the inner lives of animals.

3.1 Testing Animal Mood

Animals cannot tell us how they are feeling. However, cognitive scientists have developed a clever tool to peek into the subjective experience of animals based on the “glass half-full” paradigm. Happy people see a half-full glass where sadder people see the same glass as half-empty. Our mood—our subjective feelings—influence our interpretation of ambiguous stimuli (the glass). Likewise, we know from substantial past experimental work that animals in a better mood are more optimistic about ambiguous stimuli^{65,66,67,68,69,70,71,72,73} (see Chapter 7 for experimental details). Previously, most studies of animal mood have tested how circumstances, or manipulation, influence animals. For example, starlings^{74,75}, and pigs⁶⁷ are in a better mood when housed with enrichment. Calves separated from their mothers⁷⁶, socially isolated chicks⁷⁷, and shaken-up flies⁷⁸, are pessimistic. More happily, you can put rats in a good mood by tickling them⁷⁹.

Circumstances make animals happy or sad, but a rich life is defined not only by circumstantial comfort. Human welfare depends on a sense of purpose and meaningful intellectual stimulation. In my final chapter, I test whether wild New Caledonian Crows, like humans, enjoy tool use for the sake of tool use—akin to humans who enjoy playing bridge or solving crosswords. At the end of the experimental study, we released the birds back into the wild. I like to think that they tell their friends about their strange winter—the winter when they ate steak three times a day, stole bottle caps from scientists, and taught some humans how to use tools.



The people told us that those birds came from the terrestrial paradise, and they call them bolon diuata, that is to say, "birds of God".

Antonio Pigafetta



1

Super Black in Ornate Birds-of-Paradise

REPRINTED FROM: McCoy, D.E.*; Feo, T.*; Harvey, T.A. and Prum, R.O., 2018. Structural absorption by barbule microstructures of super black bird of paradise feathers. *Nature Communications*, 9(1), pp.1-8.

ARTICLE AND SUPPLEMENT AVAILABLE AT: <https://doi.org/10.1038/s41467-017-02088-w>



ARTICLE

DOI: 10.1038/s41467-017-02088-w

OPEN

Structural absorption by barbule microstructures of super black bird of paradise feathers

Dakota E. McCoy¹, Teresa Feo², Todd Alan Harvey³ & Richard O. Prum³

Many studies have shown how pigments and internal nanostructures generate color in nature. External surface structures can also influence appearance, such as by causing multiple scattering of light (structural absorption) to produce a velvety, super black appearance. Here we show that feathers from five species of birds of paradise (Aves: Paradisaeidae) structurally absorb incident light to produce extremely low-reflectance, super black plumages. Directional reflectance of these feathers (0.05–0.31%) approaches that of man-made ultra-absorbent materials. SEM, nano-CT, and ray-tracing simulations show that super black feathers have tilted arrays of highly modified barbules, which cause more multiple scattering, resulting in more structural absorption, than normal black feathers. Super black feathers have an extreme directional reflectance bias and appear darkest when viewed from the distal direction. We hypothesize that structurally absorbing, super black plumage evolved through sensory bias to enhance the perceived brilliance of adjacent color patches during courtship display.

¹Department of Organismic and Evolutionary Biology, Harvard University, Cambridge, MA 02138, USA. ²Department of Vertebrate Zoology, MRC-116, National Museum of Natural History, Smithsonian Institution, Washington, DC 20013, USA. ³Department of Ecology and Evolutionary Biology, and Peabody Museum of Natural History, Yale University, New Haven, CT 06520, USA. Dakota E. McCoy and Teresa Feo contributed equally to this work. Correspondence and requests for materials should be addressed to D.E.M. (email: dakotamccoy@g.harvard.edu)

Bird coloration is a model system for understanding evolution, speciation, and sexual selection¹. Color-producing mechanisms are generally assigned to two categories¹: (i) pigmentary colors produced by molecules and (ii) structural colors produced by light scattering from nanoscale variation in refractive index (e.g., channels of air within a keratin matrix). In addition to color, the directional distribution of scattered light can also affect plumage appearance. The shape, orientation, and smoothness of the feather barbs and barbules create directionally dependent appearance, such as with glossy or iridescent plumage^{2, 3}.

However, the mechanism of “structural absorption”^{4–8}, which occurs when superficial features cause multiple scattering of light^{5, 9}, can also influence visual appearance. Each time light scatters at a surface interface, a proportion of that light is transmitted into the material, where it can be absorbed⁹. By increasing the number of times light scatters, structurally absorbing materials can increase total light absorption to produce a profoundly black appearance. For example, a shiny metal with a smooth surface that reflects 30–70% of visible light can be converted to a matte black material that reflects less than 5% of light by adding microstructural surface complexity that increases structural absorption⁵. Natural examples of structural absorption have been described in the wing scales of butterflies^{10–12} and the body scales of a snake¹³. Structurally absorbing, “super black”^{14, 15} materials (which have extremely low, broadband reflectance) have important applications for a wide range of optical, thermal, mechanical, and solar technologies, including thin solar cells⁴ and the lining of space telescopes⁸.

Decades of previous research have focused on the physics, chemistry, social function, and evolutionary history of bird plumage coloration^{1, 16}. The polygynous birds of paradise (Aves: Paradisaeidae) have evolved some of the most elaborate mating displays and plumage ornaments in all animals¹⁷ (Fig. 1). In multiple species from multiple genera in the family, males have deep, black, and velvety plumage patches immediately adjacent to brightly colored, highly saturated, and structurally colored plumage patches (Fig. 1c–g). These black plumage patches have a strikingly matte appearance (i.e., lacking specular highlights) and appear profoundly darker than normal black plumage of closely related species¹⁸ (Fig. 1a, b).

Here we use spectrophotometry, scanning electron microscopy (SEM), high-resolution synchrotron tomography (nano-CT), and optical ray-tracing simulations to investigate the role of structural absorption in black feathers from seven species of birds of paradise. Unlike normal black feathers with typical barbules, we find that super black feathers have highly modified barbules arranged in vertically tilted arrays, which increase multiple scattering of light and thus structural absorption. Super black feathers reduce specular reflection by one to two orders of magnitude compared to that of normal black feathers and have extreme directional bias corresponding to the viewing direction of a female observing a displaying male. Therefore, we hypothesize that these feathers evolved to enhance the perceived brilliance of adjacent color patches by generating an optical/sensory illusion during mating displays.

Results

Reflectance spectra. We visually selected five species of polygynous birds of paradise with profoundly black plumage from five different genera—*Ptiloris paradiseus*, *Seleucidis melanoleucus*, *Astrapia stephaniae*, *Lophorina superba*, and *Parotia wahnesi*—and two species with normal black plumage—*Lycocorax pyrrhopterus* and *Melampitta lugubris* (a Papuan corvoid related to birds of paradise)—to serve as comparative controls

(Supplementary Table 1). For *Lophorina*, we examined both the profoundly black plumage of the display cape and the normal black plumage of the back, which is not used in display.

We measured the spectral reflectance of each plumage patch using two methods: (1) total integrated (specular and diffuse) reflectance was measured using an integrating sphere with a diffuse light source, and (2) normal directional reflectance was measured with a directional light source and a detector oriented normal to the feather vane (see “Methods” for details). Both the total integrated and normal directional reflectance measurements confirmed that the profoundly black plumage patches were darker than normal black plumage (Fig. 2, Supplementary Figs. 1 and 2, and Supplementary Table 1). The directional reflectance of the profoundly black plumage patches was extremely low (0.05–0.31%), and was one to two orders of magnitude less than the normal black plumes (3.2–4.7%) (Fig. 2b, Supplementary Fig. 2, and Supplementary Table 1). The extremely low directional reflectance of these five plumes is comparable to that of other natural and man-made super black materials^{4–8, 10–15}.

Reflectance spectra differed between normal and super black plumage: spectra of normal black plumes sloped upward above ~600 nm (Fig. 2 and Supplementary Figs. 1a–c and 2a–c), which is typical of melanin pigments¹⁹. In contrast, reflectance spectra of all five super black plumes were nearly flat (Fig. 2 and Supplementary Figs. 1d–h and 2d–h), which is reminiscent of super black carbon nanotube materials with exceptionally low reflectance over the entire visible range¹⁴. Super black plumage reflectance curves were also flatter than many man-made velvet fabrics (Supplementary Fig. 3), profoundly black snake scales¹³, and butterfly scales¹². Super black plumes of birds of paradise appear to have a more efficient, broadband absorption than other biological examples of structural absorption.

Feather microstructure. SEM and nano-CT revealed striking differences in microscopic barbule morphology between normal black and super black feathers (Fig. 3a, b and Supplementary Figs. 4–6). Barbules of normal black feathers had a typical, open pennaceous morphology with smooth margins and a horizontal orientation restricted to the plane of the barb rami (Fig. 3a and Supplementary Figs. 4a, b, 5a, b, and 6a, b). In contrast, barbules of all super black feathers had a highly modified morphology, with microscale spikes along the margins, reminiscent of dried oak leaves. Super black barbules curved up from the plane of the barb rami to form a densely packed array tilted ~30° toward the distal tip of the feather (Fig. 3b and Supplementary Figs. 4c–g, 5c–f, and 6c–f). The resulting morphology—an array of deep, curved cavities between the smallest branches of the feather vane—is distinct from the microstructure of super black snake and butterfly scales¹³ and from man-made super black materials^{4–8}.

Often, color-producing feather pigments or nanostructures are restricted to the exposed tips of overlapping feathers in the plumage¹. We found a similar pattern with super black barbule modifications. Barbules toward the tip of super black feathers were highly modified, whereas barbules toward the base of the same feathers had a typical normal morphology (Supplementary Fig. 7). Also, black feathers from the back of *Lophorina superba*, which are not used during display, had a typical normal morphology and were more reflective than super black feathers from the display cape with modified barbules (Supplementary Figs. 1c, h and 2c, h and Supplementary Table 1). These observations support the conclusion that the modified barbule morphology of super black feathers serves an optical, signaling function.

Structural absorption can occur when superficial cavities that are much greater in width than the wavelength of visible light

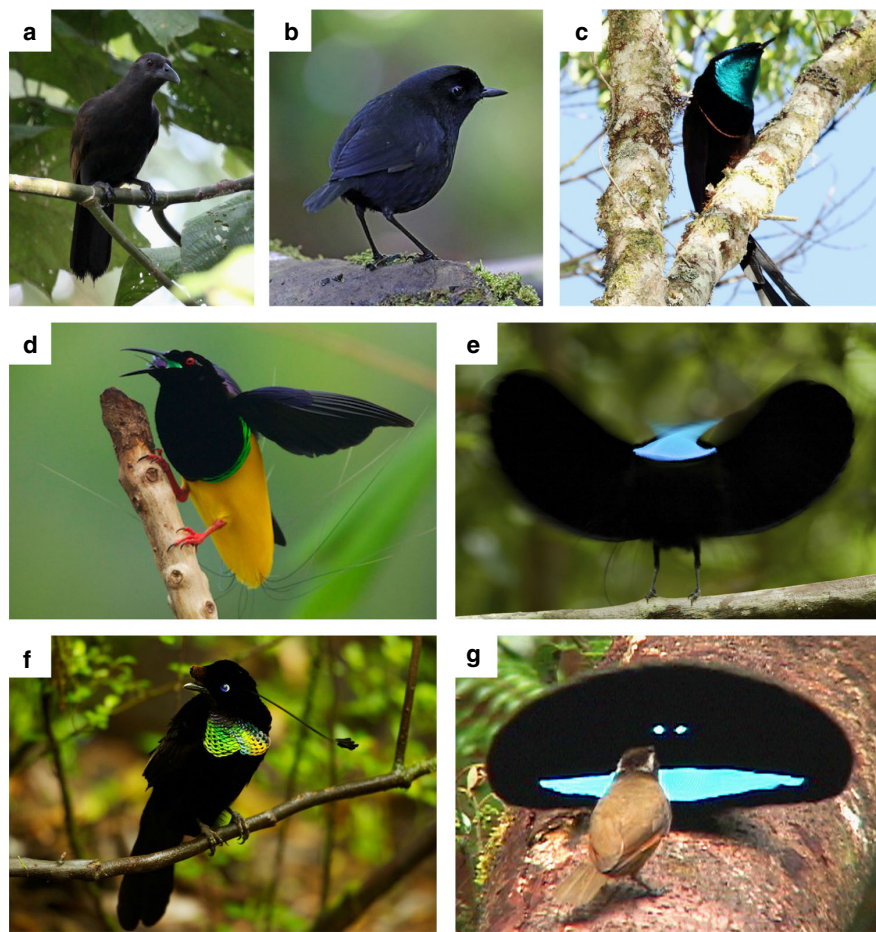


Fig. 1 Six species of birds of paradise and one close relative. **a, b** Species with normal black plumage patches. **c–g** Species with super black plumage patches. **a** Paradise-crow *Lycocorax pyrrhopterus*. **b** Lesser Melampitta *Melampitta lugubris*, a Papuan corvoid closely related to birds of paradise. **c** Princess Stephanie's Astrapia *Astrapia stephaniae*. **d** Twelve-wired Birds-of-Paradise *Seleucidis melanoleucus*. **e** Paradise Riflebird *Ptiloris paradiseus* during courtship display. **f** Wahnes' Parotia *Parotia wahnesi*. **g** Superb Bird-of-Paradise *Lophorina superba* during courtship display with female (brown plumage). Photo credits: **a** @Hanom Bashari/Burung Indonesia; **b** Daniel López-Velasco; **c** Trans Niugini Tours; **d–f** Tim Laman; **g** Ed Scholes

cause multiple scattering of light⁵. Even shiny metal surfaces can appear black if they have the appropriate surface microstructure^{11–13}. The tilted barbule arrays in super black bird of paradise feathers had intra-barbule cavities that were ~200–400-μm deep and ~5–30-μm wide, with smaller cavities along the barbule margins at a < 5-μm scale (Fig. 3b and Supplementary Figs. 4–6). Remarkably, the super black feathers retained their velvety black appearance even after sputter coating with gold for SEM, whereas the normal black feathers appeared gold (Fig. 3c, d). This direct, experimental evidence shows that super black feathers structurally absorb light to create their profoundly dark appearance.

Light-scattering simulations. To directly quantify the effects of barbule surface microstructure on light absorption in feathers, we used virtual ray-tracing simulations to model the interaction of light with 3D nanoscale tomographic models of normal black and super black feathers (Supplementary Fig. 8). Ray-tracing simulations calculate the path and radiant power of light rays as they interact with a 3D model. Each time a simulated light ray intersects the feather surface (a scattering event), a portion of its radiant power is reflected from the surface, and the remaining

portion is transmitted into the material where it can be absorbed. Our simulations assumed no surface roughness and 100% absorption of transmitted light. These assumptions restricted light scattering to the specular direction and allowed us to control for any variation in pigmentation, internal structure, or surface roughness that might be present in the real feathers. Thus, the ray-tracing experiments isolated the effects of external feather microstructure on light scattering to characterize structural absorption among feathers with different barbule morphologies.

First, we conducted ray-tracing simulations that modeled the normal directional reflectance spectrophotometry measurements. Our simulations confirmed that feather barbule microstructure causes multiple scattering of light (Fig. 4a and Supplementary Table 1). The percentage of light rays that scattered at least twice varied among feathers from 33 to 95%, documenting the contribution of barbule morphology to light-scattering behavior (Fig. 4b and Supplementary Table 1). Super black feathers with modified barbule arrays caused more multiple scattering, and had greater simulated structural absorption, than normal black feathers (Fig. 4b and Supplementary Table 1). Furthermore, we found a significant negative relationship between measured normal, directional reflectance and the percentage of simulated

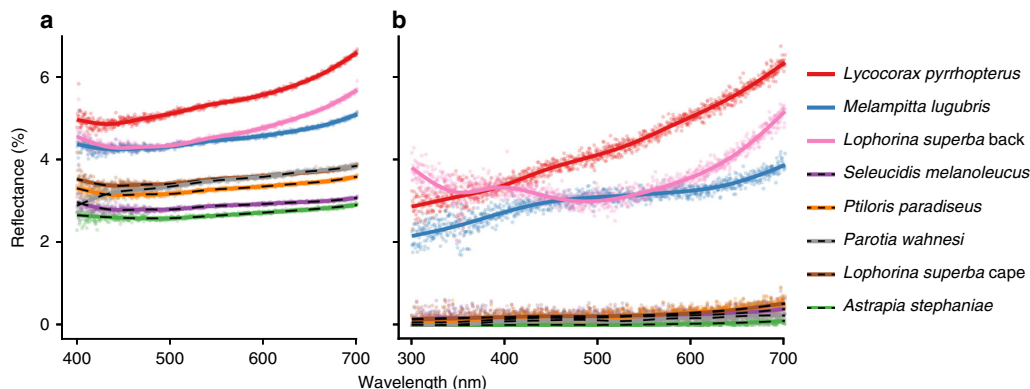


Fig. 2 Reflectance spectra of black and super black plumages. **a** Total integrated (diffuse and specular) reflectance. **b** Normal, directional reflectance. Dotted lines are super black plumages. See Supplementary Figs. 1 and 2 for detailed spectra for each species

light rays that scattered at least twice (Fig. 4c; linear regression: $R^2 = 0.68$, slope = -0.063 , SE = 0.021, and $P < 0.05$). These results demonstrate that the modified barbule arrays of super black feathers increase multiple scattering of light, and contribute to a darker appearance (i.e., lower reflectance) through increased structural absorption, relative to the typical barbule morphology of normal black feathers.

Next, we configured ray-tracing simulations with several different idealized lighting conditions to investigate how appearance varies with viewing direction and illumination. Total integrated reflectance measurements of super black feathers were only 50% lower than for normal black feathers (Fig. 2), indicating specular reflectance from other angles. Furthermore, the curved, laminar barbules of the super black feathers angle toward the distal tip of the feather, rather than projecting up perpendicular to the plane of the feather vane. This titled barbule orientation could produce directional variation in structural absorption, and thus reflectance³. To investigate, we calculated the simulated directional reflectance for four different lighting setups: (i) omnidirectional light, (ii) directional light tilted $+45^\circ$ toward the proximal end of the feather, (iii) directional light at 0° normal to the feather (as above), and (iv) directional light tilted at -45° toward the distal end of the feather (see Methods for details). The omni-directional illumination (setup i) is comparable to light in an open environment on a cloudy day, whereas the directional illuminations (setups ii–iv) are comparable to light in a closed environment, such as the forest floor, with breaks in the canopy that constrain incident light to a narrow angular range²⁰.

Normal black and super black feathers differed markedly in their directional reflectance. Normal black feathers reflected light in a manner consistent with classical glossy surface reflection theory²¹: the majority of energy was reflected in directions roughly equal and opposite to that of the directional incident light (Fig. 5a and Supplementary Fig. 9a, b). Thus, the darkest viewing quadrant varied with the angle of illumination for normal black feathers (Supplementary Table 2). In contrast, super black feathers always reflected the majority of energy toward the proximal viewing quadrant, regardless of the angle of illumination (Fig. 5b and Supplementary Fig. 9c–f). Super black feathers were the darkest when viewed from the distal viewing angle (Supplementary Table 2), which corresponds to looking into the openings of the deep cavities between barbule tips (Fig. 5b and Supplementary Fig. 9).

Discussion

Our findings demonstrate that super black bird of paradise feathers structurally absorb up to 99.95% of directly incident light, and that variation in external surface microstructure can contribute to observed differences in visual appearance of bird plumage. The vertically tilted barbule arrays of super black bird of paradise feathers create deep, curved cavities. This morphology is distinct from the longitudinal ridges of butterfly scales¹¹ and the vertical cones of snake scales¹³, substantially expanding the diversity of structurally absorbing biological materials in nature.

The extreme directional reflectance bias in super black feathers is congruent with field observations of bird of paradise courtship behavior²². Males of many species perform displays that maintain a specific directional orientation between their ornaments and the viewing females¹⁷ (Fig. 1g). We hypothesize that the tilted barbule arrays function in coordination with the behavioral repertoire to ensure that females view super black plumage patches at their darkest orientation.

Interestingly, in both butterflies and birds of paradise, super black patches are always adjacent to bright, highly saturated, and structural colors. For example, *Lophorina* has a super black plumage display cape surrounding its intensely brilliant blue patches, but normal black plumage on the back that is not featured during display (Fig. 1g and Supplementary Figs. 1c, h and 2c, h). We hypothesize that structurally absorbing super black patches evolve because they exaggerate the perceived brilliance of adjacent color patches through a sensory/cognitive bias inherent in the vertebrate mechanism of color correction. Vertebrates use specular highlights, or white reflectance from object surfaces, within the visual field to correct for the spectrum and quantity of ambient light²³. We propose that structurally absorbing super black patches (i) eliminate specular reflectances around the brilliant color patch, (ii) lower the observers perceived estimate of the quantity of ambient light upon that portion of the visual scene, and thus (iii) disrupt the perceiver's capacity to estimate the brilliance of the color patch. If the brain perceives that more light is coming from a patch than it estimates is ambient upon it, the patch will appear to be self-luminous or to float in space^{24–27}. Perceptual experiments demonstrate this bias in the color correction mechanisms of goldfish (which are tetrachromats like birds) and humans²⁸.

Displays of some bird of paradise, like male *Lophorina*, produce exactly this self-luminous effect on human observers and in videos and photographs (Fig. 1g), and we predict that these plumages produce similar perceptual effects on avian observers. Theoretically, white balancing (i.e., von Kries correction) involves dividing the signal stimulus from each cone type by that cone

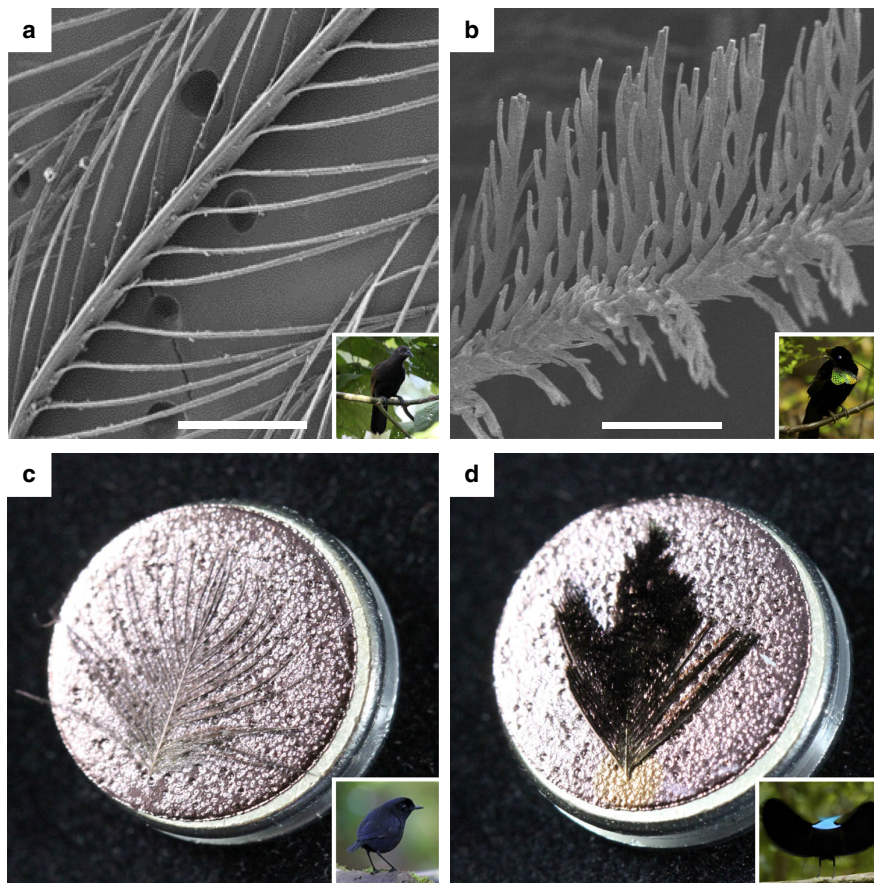


Fig. 3 Examples of normal and super black feather microstructure. **a** SEM micrograph of *Lycocorax pyrrhopterus* normal black feather with typical barbule morphology; scale bar, 200 μm . **b** SEM micrograph of *Parotia wahnesi* super black feather with modified barbule arrays; scale bar, 50 μm . **c** Gold sputter-coated normal black breast feather of *Melampitta lugubris* appears gold. **d** Gold sputter-coated super black breast feather of *Ptiloris paradiseus* retains a black appearance indicating structural absorption. SEM stubs are 12.8 mm in diameter. See Fig. 1 for inset photo credits

type's response to the spectrum of an adjacent "white" point—usually a specular highlight²⁹. Reducing the value of the denominator in this correction to zero would effectively eliminate the individual's capacity for color correction.

Further research is required to understand the role of multiple scattering among barbs and barbules of multiple feathers in structural absorption by the entire plumage, and on the color correction mechanisms of birds. However, it is clear that structural absorption should be considered along with pigments, structural coloration, and specular reflection, as an important component in determining the visual appearance of organisms. Biological examples of structural absorption have in at least one case inspired the fabrication of new biomimetic materials¹⁵, and the feather structures described herein may have similar direct applications.

Methods

Specimens. Five bird species with profoundly black plumage and two species with normal black plumage were identified by visual observation of museum study skins from the Yale Peabody Museum (YPM), Harvard Museum of Comparative Zoology (MCZ), American Museum of Natural History (AMNH), and the University of Kansas Biodiversity Institute (KU). Details of the specimens and plumage patches studied are summarized in Supplementary Table 1. To the human observer, super black plumage had a strongly matte appearance with so little specular reflectance that it was difficult to focus on the surface of the plumage and distinguish individual feathers. The species with normal black plumage lacked any conspicuous glossy specular highlights. Individual contour feathers were sampled

from museum skins for scanning electron microscopy (SEM) and synchrotron-radiation X-ray microtomography (nano-CT). We could not obtain SEM of *Lophorina superba* back feathers or CT scans for *Lophorina superba* back and display cape feathers due to availability of material. Visual inspection of the *Lophorina* back plumage using a light microscope confirmed that the barbules have normal morphology, without the modified barbule arrays present in super black feathers.

Spectrophotometry. Light reflectance and absorbance by the plumage can be influenced by the specific orientation of the feathers in the plumage and also by the interaction of light scattered by multiple feathers. The optical properties of the intact plumage cannot be reconstructed reliably by plucking feathers and then laying them (singly or together) on a different surface. Therefore, reflectance spectra of super black and normal black plumage patches were recorded directly from the plumage of prepared museum skins.

Total integrated (diffuse and specular) reflectance spectra were measured with an Ocean Optics USB2000 spectrophotometer and ISP-REF integrating sphere using a Spectralon white standard (Ocean Optics, Dunedin, FL). The light source provided diffuse light from all directions and the gloss trap was closed to collect both specular and diffuse reflectance. To ensure repeatable measures of reflectance from these profoundly black samples, we averaged 10 scans for each output file, and used an integration time of 40 μs . For each patch, we measured three spectra from three different positions within the patch and averaged them to produce a single spectrum for the patch. Two specimens per species were measured for all species except for *Astrapia stephaniae* and *Parotia wahnesi*, for which only one specimen was measured due to availability of material.

Directional reflectance spectra were measured with an Ocean Optics USB2000 spectrophotometer and Ocean Optics DH-2000Bal deuterium–halogen light source (Ocean Optics, Dunedin, FL, USA). The geometry of the directional reflectance measurements placed the detector at 0° normal to the plumage, which

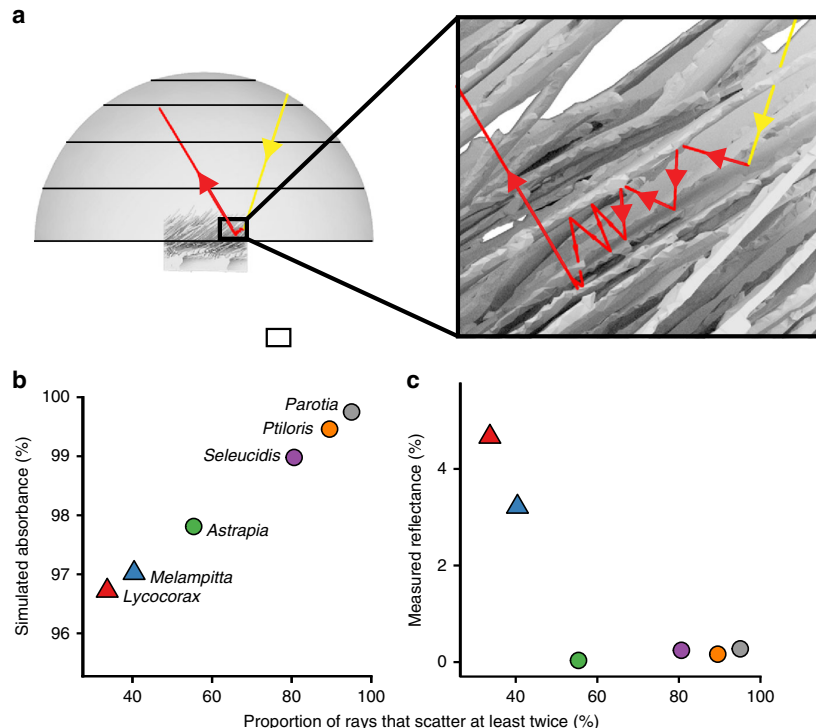


Fig. 4 Ray-tracing simulations. **a** Simulation from FRED showing the trace of a ray that scatters multiple times between barbules of a super black feather. **b** Substantial variation in frequency of multiple scattering events among species predicts variation in structural absorption. **c** Measured reflectance is significantly negatively correlated with the proportion of reflected rays that scattered at least twice (linear regression: $R^2 = 0.68$, slope = -0.063 , SE = 0.021, and $P < 0.05$)

would be the specular direction for typically flat materials. A bifurcated illumination/detection optical fiber was held in an anodized aluminum block ~6 mm above and perpendicular to the plumage. A ~3-mm-diameter circle of light illuminated the plumage. Reflectance between 300 and 700 nm was recorded to obtain the species spectra for the patch. Measures of super black plumage reflectance were quite low and noisy, and signal processing was required. Negative values were converted to 0, and five spectra from each individual were averaged to produce an average spectrum for the patch. Loess smoothing was applied to produce a reflectance spectrum curve (Supplementary Fig. 2).

The light source in our integrating sphere lacked near-ultraviolet light (300–400 nm), but the directional reflectance measures confirmed that none of these patches produced UV reflectance features. Reflectance, %R, was calculated as the area under the measured reflectance spectrum between 400 and 700 nm using Riemann sums and was normalized by the number of wavelength bins measured and 100% reflectance of the white standard.

SEM. For SEM, feathers were mounted on stubs using carbon-adhesive tabs, coated with ~15 nm of gold, and viewed and micrographed using an ISI SS40 SEM operating at 10 kV. For *Parotia wahnesi*, *Ptiloris paradiseus* (Fig. 3d), and *Melampitta lugubris* (Fig. 3c) feathers were coated with 5 nm of gold, and then viewed and photographed using a SEM-4 FESEM Ultra55 operating at 5 kV.

Nano-CT. For nano-CT, one black contour feather from each species was washed and then soaked in an aqueous solution of Lugol's solution—1% (wt/v) iodine metal (I_2) + 2% potassium iodide (KI) in water—for 2–3 weeks to improve X-ray contrast³⁰. Feathers were scanned at beamline 2-BM at the Advanced Photon Source facility at U.S. Department of Energy's Argonne National Laboratory, Argonne, IL. Feathers were mounted to a post using modeling clay and surrounded by a Kapton tube to reduce sample motion. Feathers were aligned in the beam to scan a portion of the distal tip that is exposed in the plumage. Scans were made with an exposure time of 30 ms at 24.9 keV to acquire 1500 projections as the sample rotated 180° at $3^\circ s^{-1}$. Data sets were reconstructed as TIFF image stacks using the TomoPy Python package (<https://tomopy.readthedocs.io>) in Linux on a Dell Precision T7610 workstation with two Intel Xeon processors yielding 16 cores, 192-GB RAM, and NVIDIA Quadro K6000 with 12-GB VRAM. The isotropic voxel dimensions of the image stacks were 0.65 μm and the field of view of each data set was ~1.5 mm^3 .

3D polygon models. The external surface of each feather was segmented in VGStudioMAX 2.0 (Volume Graphics) and a 3D polygonal mesh comprising a geometric model of the external surface was extracted using the QuickMesh setting and exported as an OBJ file. To optimize the ray-tracing simulations, each polygonal model was cropped to a 500- μm by 500- μm swatch of the feather vane and then the triangle count was further reduced using the decimate feature (tolerance set to 325 nm) in Geomagic Wrap (3D Systems). Finally, we used the Mesh Doctor feature in Geomagic Wrap to make the surface model manifold, i.e., "water tight." This last step was necessary to repair any defects in the polygonal mesh through which simulated rays could artificially enter and become trapped inside the feather during ray-tracing simulations.

Ray-tracing simulations. The directional reflectance, transmittance, and absorbance of super black and normal black plumage patches were analyzed by numerical ray trace simulations using the software package FRED³¹ (Photon Engineering LLC). Simulations employing two types of illumination were conducted for each feather: (1) omni-directional and (2) directional.

The "omni-directional" setup was configured with a hemispherical light source, a hemispherical reflectance detector, and a hemispherical transmittance detector. Into this setup, we imported a 3D polygonal mesh of each feather. Feathers were placed at the center of all three hemispheres and oriented with their vanes in plane with the base of the hemispheres and perpendicular to their poles. The upper or obverse feather surface was oriented toward the light source and reflectance hemisphere; the lower or reverse feather surface was oriented toward the transmittance hemisphere. One million rays of random wavelength between 300 and 700 nm were emitted from random positions on the hemispherical source and propagated in random directions constrained by a square plane with a side length of 330 μm centered on the feather (corresponding to 66% of the width of the feather swatch).

The "directional" setup was configured as a scale model of the directional reflectance spectrophotometry setup. Directional reflectance simulations were conducted for each feather sample under three different light source orientations: (i) tilted +45° toward the proximal end of the feather, (ii) 0° normal to the feather, and (iii) tilted -45° toward the distal end of the feather. While the plumage was illuminated by a 3-mm-diameter spot in the spectrophotometry experiments, the illumination spot in the simulations was scaled from 11% to 330 μm (corresponding to 66% of the 500- μm width of the feather swatch). The width of the light source representing the bare optical fiber bundle and its distance above the

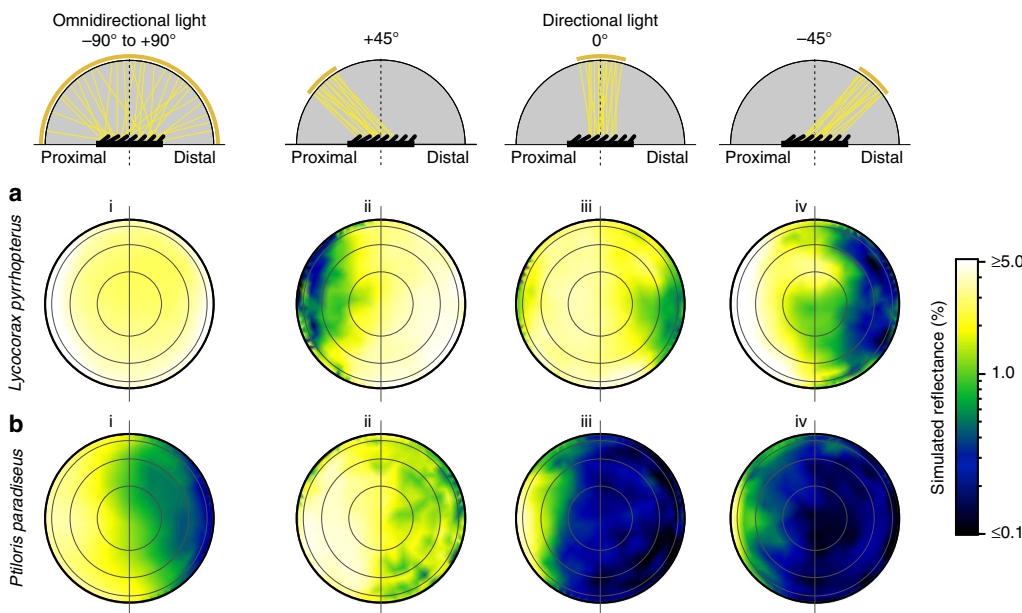


Fig. 5 The impact of viewing direction and illumination on the appearance of feathers. **a** Normal black *Lycocorax* back feather. **b** Super black *Ptiloris* breast feather with modified barbule arrays. Directional reflectance from ray-tracing simulations is plotted as a log-scale color gradient on orthogonal projections of the reflectance hemisphere under four different lighting conditions (i–iv). Concentric rings represent 22.5° , 45° , 67.5° , and 90° . Horizontal line separates proximal and distal viewing quadrants. Schematics show a cross-sectional view of the optical setup of each illumination. Reflectance hemisphere in gray, feather in black. Concentric gold band indicates the angle of light source, yellow lines show the path of incident light (subsequent path of reflected light not shown). For normal black *Lycocorax*, the darkest viewing quadrant varies with the direction of incident light (compare ii with iv), whereas super black *Ptiloris* shows a strong directional bias in which the distal viewing quadrant is the darkest under all lighting conditions. See Supplementary Fig. 9 for additional species

feather swatch were also scaled at 11% to ensure that the size of the solid angle illuminating the plumage patch in the simulations matched that in the spectrophotometry measurements. One million rays of random wavelength between 300 and 700 nm were positioned on a grid spanning the light source. A circular aperture was used to cull rays from the square source, thereby shaping the source to match that of the spectrophotometer probe. Ultimately, 785,398 rays were emitted by the circular source in random directions within an angular range of 28° , thereby illuminating the 330- μm -diameter spot centered on the feather.

In both “omni-directional” and “directional” simulations, each ray had one of three possible fates. (1) No interaction, where the ray passes through gaps in the feather vane without ever striking the surface of the feather and ultimately terminates when it intersects the transmittance hemisphere. (2) “Transmitted,” where the ray strikes the surface of the feather one or more times until it ultimately exits the underside or reverse surface of the feather vane and terminates on the transmittance hemisphere. (3) “Reflected,” where the ray strikes the surface of the feather one or more times until it ultimately exits the topside or obverse surface of the feather vane and terminates on the reflectance hemisphere. For the scope of this study, we only consider the subset of incident rays that are “reflected” (fate 3). Rays that terminate on the transmittance hemisphere (fates 1 and 2), represent more complex interactions between multiple overlapping feathers in the plumage and/or the skin that we do not consider here.

We simplified the ray-tracing simulations of the feather surface and controlled for potential differences in surface roughness between the real feathers by excluding surface scattering caused by surface roughness (reflections in nonspecular directions) from the simulation. We traced rays using the surface normals of the bare polygon mesh of the feather, treating each polygon in the mesh as a smooth surface. Since no BRDF model was applied to the surface, all radiant power was directed in the specular direction. Thus, each time a ray struck the surface of the feather (a simplified “scattering” event), it bifurcated into one and only one component ray that reflected from the surface of the feather, and one and only one component ray that transmitted into the feather. The direction of the reflected ray was computed based on the law of reflection ($\theta_i = \theta_r$), and Fresnel equations yielded the fraction of the incident radiant power reflected as a function of the incident angle and the ratio of the index of refraction of air (1.0) and feather keratin (1.56). To investigate the effects of surface microstructure independent of any potential differences in melanin or internal nanostructure between the real feathers, we assumed that rays transmitted into the feather were entirely absorbed before exiting the feather. Thus, any difference in calculated absorption between simulated feathers is caused by variations in the orientation of the feather surface and differences in the number of multiple scattering events.

The ray-tracing simulation proceeded as follows: first, rays with equal amounts of radiant power were emitted from the light source and propagated in the direction of the feather. Then, rays repeatedly intersected the surfaces of the feather vane and reflected from those surfaces in the specular direction until they exited the volume of space occupied by the feather vane and terminated on a hemisphere. For each ray, the simulation recorded the number of light ray-surface intersections, the hemisphere of and spherical coordinates of the termination point, and the ending radiant power. For each ray, absorbance was calculated from the difference between the starting and ending radiant power. For comparison with the directional reflectance spectrophotometry measurements, total absorbance under 0° normal directional illumination was calculated as the sum of reflected light rays that terminated within an angular range of 27° . Percent multiple scattering was calculated as the percentage of this set of rays that scattered two or more times off of the surface of the feather.

To determine how reflectance varies based on the angle incident light and viewing directions, we calculated the locally averaged reflectance at different viewing directions with a nonparametric kernel regression fit using the kreg function with default settings from the R package gplm. The kernel density estimate and regression fits were evaluated at 400 points, representing different viewing directions that were uniformly distributed over the reflectance hemisphere, and the results were plotted as a log-scale color gradient on orthogonal projections of the hemisphere using the persp3d function from the R package rgl.

We used linear regression to estimate correlation between the proportion of rays that scattered at least twice and the actual measured reflectance for the 0° normal directional light ray-tracing setup; we report R^2 , slope, standard error of the slope, and P value.

Data availability. The data that support the findings of this study are available from the corresponding author on request.

Received: 11 May 2017 Accepted: 3 November 2017

Published online: 09 January 2018

References

- Hill, G. E. & McGraw, K. J. *Bird Coloration: Function and Evolution*. Vol. 2 (Harvard University Press, Cambridge, 2006).

2. Shawkey, M. D. & D'Alba, L. Interactions between colour-producing mechanisms and their effects on the integumentary colour palette. *Philos. Trans. R. Soc. B* **372**, 20160536 (2017).
3. Harvey, T. A., Bostwick, K. S. & Marschner, S. Directional reflectance and milli-scale feather morphology of the African Emerald Cuckoo *Chrysococcyx Cupreus*. *J. R. Soc. Interface* **10**, 20130391 (2013).
4. Liu, X. et al. Black silicon: fabrication methods, properties and solar energy applications. *Energy Environ. Sci.* **7**, 3223–3263 (2014).
5. Tao, H. et al. Formation of strong light-trapping nano-and microscale structures on a spherical metal surface by femtosecond laser filament. *Appl. Phys. Lett.* **100**, 201111 (2012).
6. Vorobyev, A. Y., Topkov, A. N., Gurin, O. V., Svirch, V. A. & Guo, C. Enhanced absorption of metals over ultrabroad electromagnetic spectrum. *Appl. Phys. Lett.* **95**, 121106 (2009).
7. Sher, M.-J. et al. Mid-infrared absorptance of silicon hyperdoped with chalcogen via fs-laser irradiation. *J. Appl. Phys.* **113**, 63520 (2013).
8. Brown, R. J. C., Brewer, P. J. & Milton, M. J. T. The physical and chemical properties of electroless nickel-phosphorus alloys and low reflectance nickel-phosphorus black surfaces. *J. Mater. Chem.* **12**, 2749–2754 (2002).
9. Crouch, C. H. et al. Comparison of structure and properties of femtosecond and nanosecond laser-structured silicon. *Appl. Phys. Lett.* **84**, 1850–1852 (2004).
10. Vukusic, P., Sambles, J. R. & Lawrence, C. R. Structurally assisted blackness in butterfly scales. *Proc. R. Soc. Lond. Ser. B Biol. Sci.* **271**, S237–S239 (2004).
11. Zhao, Q. et al. Art of blackness in butterfly wings as natural solar collector. *Soft Matter* **7**, 11433–11439 (2011).
12. Han, Z. et al. An ingenious super light trapping surface templated from butterfly wing scales. *Nanoscale Res. Lett.* **10**, 344 (2015).
13. Spinner, M., Kovalev, A., Gorb, S. N. & Westhoff, G. Snake velvet black: hierarchical micro- and nanostructure enhances dark colouration in *Bitis rhinoceros*. *Sci. Rep.* **3**, 1846 (2013).
14. Panagiotopoulos, N. T. et al. Nanocomposite catalysts producing durable, super-black carbon nanotube systems: applications in solar thermal harvesting. *ACS Nano* **6**, 10475–10485 (2012).
15. Zhao, Q. et al. Super black and ultrathin amorphous carbon film inspired by anti-reflection architecture in butterfly wing. *Carbon N. Y.* **49**, 877–883 (2011).
16. Hill, G. E. & McGraw, K. J. *Bird Coloration: Mechanisms and Measurements*. Vol. 1 (Harvard University Press, Cambridge, 2006).
17. Laman, T. & Scholes, E. *Birds of Paradise: Revealing the World's Most Extraordinary Birds* (National Geographic Books, Washington, DC, 2012).
18. Maia, R., D'Alba, L. & Shawkey, M. D. What makes a feather shine? A nanostructural basis for glossy black colours in feathers. *Proc. Biol. Sci.* **278**, 1973–1980 (2011).
19. McGraw, K. J., Mackillop, E. A., Dale, J. & Hauber, M. E. Different colors reveal different information: how nutritional stress affects the expression of melanin- and structurally based ornamental plumage. *J. Exp. Biol.* **205**, 3747–3755 (2002).
20. Endler, J. A. The color of light in forests and its implications. *Ecol. Monogr.* **63**, 1–27 (1993).
21. Willmott, F. M. in *Optical Properties of Polymers* (ed. Meeten, G. H.) 265–334 (Elsevier Applied Science Publishers, London, 1986).
22. Bostwick, K. S., Harvey, T. A. & Scholes, E. in *The Extended Specimen: Emerging Frontiers in Collections-Based Ornithological Research* (ed. Webster, M. S.) (CRC Press, Boca Raton, 2017).
23. Brainard, D. H., Wandell, B. A. & Chichilnisky, E.-J. Color constancy: from physics to appearance. *Curr. Dir. Psychol. Sci.* **2**, 165–170 (1993).
24. Speigle, J. M. & Brainard, D. H. Luminosity thresholds: effects of test chromaticity and ambient illumination. *JOSA A* **13**, 436–451 (1996).
25. Kreezer, G. Luminous appearances. *J. Gen. Psychol.* **4**, 247–281 (1930).
26. Hering, E. Der raumsinn und die bewegungen des auges. *Hermann L. Handbuch der Physiol. III (tl. I)* (1879).
27. Hunt, R. W. G. An improved predictor of colourfulness in a model of colour vision. *Color Res. Appl.* **19**, 23–26 (1994).
28. Neumeyer, C., Dorr, S., Fritsch, J. & Kardelky, C. Colour constancy in goldfish and man: influence of surround size and lightness. *Percept. Lond.* **31**, 171–188 (2002).
29. West, G. & Brill, M. H. Necessary and sufficient conditions for von Kries chromatic adaptation to give color constancy. *J. Math. Biol.* **15**, 249–258 (1982).
30. Metscher, B. D. MicroCT for developmental biology: a versatile tool for high-contrast 3D imaging at histological resolutions. *Dev. Dyn.* **238**, 632–640 (2009).
31. Harvey, J. E., Irvin, R. G. & Pfisterer, R. N. Modeling physical optics phenomena by complex ray tracing. *Opt. Eng.* **54**, 35105 (2015).

Acknowledgements

Xianghui Xiao and the 2-BM beamline group provided assistance with CT scanning and analysis at the APS facility, Argonne National Lab. Jeremiah Trimble and Kate Eldridge assisted with collections usage. The research has been improved by discussions with David Brainard, David Shoehalter, Kristof Zyskowski, David Haig, James Harvey, Ryan Irvin, and members of the Prum Lab. Ed Scholes, Tim Laman, Trans Niugini Tours, Hanom Bashari, and Daniel López kindly gave permission to reproduce photos of birds of paradise (Fig. 1). Andrew Farris assisted with kernal regressions for the directional reflectance plots. This research was funded by the W. R. Coe Fund of Yale University, by a Sigma XI student research fellowship to D.E.M., and by a Mind, Brain, and Behavior Graduate Student Award to D.E.M. D.E.M. was supported by the Department of Defense (DoD) through the National Defense Science and Engineering Graduate Fellowship (NDSEG) Program. D.E.M. was also supported by a Theodore H. Ashford Graduate Fellowship in the Sciences. Tomography data collections at the Advanced Photon Source beamline 2-BM, Argonne National Laboratory were supported by the U.S. Department of Energy Office of Science (Proposal ID 41887). T.J.F. was supported by a NSF Postdoctoral Fellowship in Biology (#1523857). Richard Pfisterer of Photon Engineering graciously licensed FRED to T.A.H. for this research. This work was performed in part at the Harvard University Center for Nanoscale Systems (CNS), a member of the National Nanotechnology Coordinated Infrastructure Network (NNCI), which is supported by the National Science Foundation under NSF ECCS award no. 1541959.

Author contributions

All authors conceived the research design, analyzed the data, and wrote the paper jointly. D.E.M. and R.O.P. performed the spectrophotometry, and D.E.M. conducted the SEM experiments. T.A.H. performed the ray-tracing experiments. T.A.H., T.F., and R.O.P. performed CT scans and analyzed ray-tracing experiments. D.E.M., T.A.H., and T.F. prepared the figures.

Additional information

Supplementary Information accompanies this paper at <https://doi.org/10.1038/s41467-017-02088-w>.

Competing interests: The authors declare no competing financial interests.

Reprints and permission information is available online at <http://npg.nature.com/reprintsandpermissions/>

Publisher's note: Springer Nature remains neutral with regard to jurisdictional claims in published maps and institutional affiliations.



Open Access This article is licensed under a Creative Commons Attribution 4.0 International License, which permits use, sharing, adaptation, distribution and reproduction in any medium or format, as long as you give appropriate credit to the original author(s) and the source, provide a link to the Creative Commons license, and indicate if changes were made. The images or other third party material in this article are included in the article's Creative Commons license, unless indicated otherwise in a credit line to the material. If material is not included in the article's Creative Commons license and your intended use is not permitted by statutory regulation or exceeds the permitted use, you will need to obtain permission directly from the copyright holder. To view a copy of this license, visit <http://creativecommons.org/licenses/by/4.0/>.

© The Author(s) 2017

We take to the breeze, we go as we please.

E. B. White, *Charlotte's Web*



Super Black in Colorful Peacock Spiders

REPRINTED FROM: McCoy, D.E., McCoy, V.E., Mandsberg, N.K., Shneidman, A.V., Aizenberg, J., Prum, R.O. and Haig, D., 2019. Structurally assisted super black in colourful peacock spiders. *Proceedings of the Royal Society B*, 286(1902), p.20190589.

ARTICLE AND SUPPLEMENT AVAILABLE AT: <http://dx.doi.org/10.1098/rspb.2019.0589>





Cite this article: McCoy DE, McCoy VE, Mandsberg NK, Shneidman AV, Aizenberg J, Prum RO, Haig D. 2019 Structurally assisted super black in colourful peacock spiders. *Proc. R. Soc. B* **286**: 20190589. <http://dx.doi.org/10.1098/rspb.2019.0589>

Received: 12 March 2019

Accepted: 23 April 2019

Subject Category:

Evolution

Subject Areas:

evolution, biomaterials

Keywords:

microlens arrays, structural colour, peacock spiders, sexual selection

Author for correspondence:

Dakota E. McCoy

e-mail: dakotamccoy@g.harvard.edu

Electronic supplementary material is available online at <https://dx.doi.org/10.6084/m9.figshare.c.4486193>.

Structurally assisted super black in colourful peacock spiders

Dakota E. McCoy¹, Victoria E. McCoy², Nikolaj K. Mandsberg^{3,4}, Anna V. Shneidman⁴, Joanna Aizenberg^{4,5,6}, Richard O. Prum⁷ and David Haig¹

¹Department of Organismic and Evolutionary Biology, Harvard University, 26 Oxford Street, Cambridge, MA 02138, USA

²Steinmann-Institut für Geologie, Mineralogie und Paläontologie, Universität Bonn, Nussallee 8, 53115 Bonn, Germany

³Department of Health Technology, Technical University of Denmark, 2800 Kongens Lyngby, Denmark

⁴John A. Paulson School of Engineering and Applied Sciences, Harvard University, 9 Oxford Street, Cambridge, MA 02138, USA

⁵Department of Chemistry and Chemical Biology, Harvard University, 12 Oxford Street, Cambridge, MA, USA

⁶Kavli Institute for Bionano Science and Technology, Harvard University, 29 Oxford Street, Cambridge, MA, USA

⁷Department of Ecology and Evolutionary Biology, and Peabody Museum of Natural History, Yale University, New Haven, CT 06511, USA

DEM, 0000-0001-8383-8084; VEM, 0000-0002-5655-0381; NKM, 0000-0003-3285-3887; AVS, 0000-0001-6064-5378; JA, 0000-0002-2343-8705; DH, 0000-0001-7377-1605

Male peacock spiders (*Maratus*, Salticidae) compete to attract female mates using elaborate, sexually selected displays. They evolved both brilliant colour and velvety black. Here, we use scanning electron microscopy, hyperspectral imaging and finite-difference time-domain optical modelling to investigate the deep black surfaces of peacock spiders. We found that super black regions reflect less than 0.5% of light (for a 30° collection angle) in *Maratus speciosus* (0.44%) and *Maratus karrie* (0.35%) owing to microscale structures. Both species evolved unusually high, tightly packed cuticular bumps (microlens arrays), and *M. karrie* has an additional dense covering of black brush-like scales atop the cuticle. Our optical models show that the radius and height of spider microlenses achieve a balance between (i) decreased surface reflectance and (ii) enhanced melanin absorption (through multiple scattering, diffraction out of the acceptance cone of female eyes and increased path length of light through absorbing melanin pigments). The birds of paradise (Paradisaeidae), ecological analogues of peacock spiders, also evolved super black near bright colour patches. Super black locally eliminates white specular highlights, reference points used to calibrate colour perception, making nearby colours appear brighter, even luminous, to vertebrates. We propose that this pre-existing, qualitative sensory experience—‘sensory bias’—is also found in spiders, leading to the convergent evolution of super black for mating displays in jumping spiders.

1. Background

Colour plays a number of roles in inter- or intra-specific visual signalling, including camouflage, mimicry, warning coloration and social signalling [1]. Some of the most elaborate colour displays have evolved because of sexual selection by mate choice [2–5], exemplified by the peacock spiders (*Maratus*, Salticidae [6]), which are subject to unusually intense sexual selection [7]. Among males, competition to be preferred by females and secure mating opportunities has produced innovative visual traits at multiple size scales [6,8–11]. Investigating these stimulating visual displays can (i) reveal novel colour-producing mechanisms [10,12], (ii) inform our understanding of animals’ visual ecology and sensory experiences [8,13], and (iii) guide the design of human-made devices for colour production and other forms of light manipulation [12].

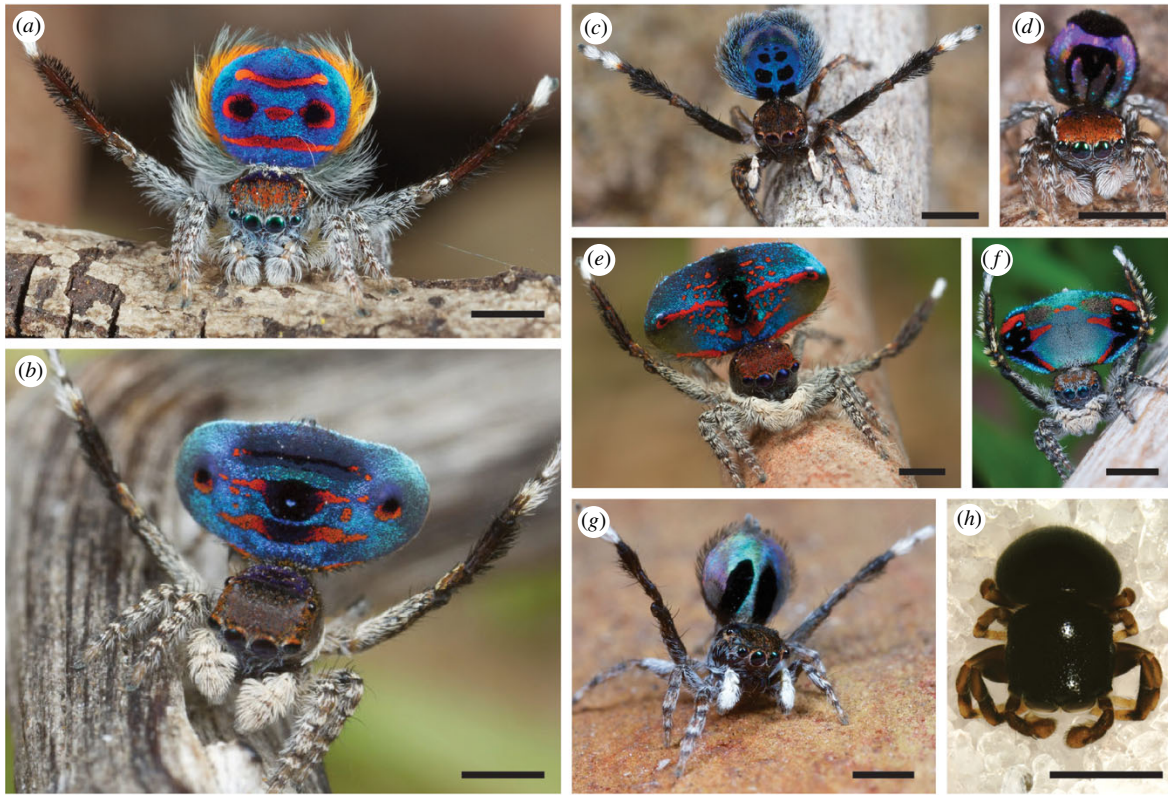


Figure 1. Deep black patches alongside brilliant colours in peacock spiders (*a–g*), and a closely related shiny black spider (*h*). (*a*) *Maratus speciosus*, (*b*) *Maratus karrie*, (*c*) *Maratus nigromaculatus*, (*d*) *Maratus robinsoni*, (*e*) *Maratus hortorum*, (*f*) *Maratus avibus*, (*g*) *Maratus chrysomelas* and (*h*) *Cylistella* sp. Scale bars are all 1 mm; for (*a–g*), they are estimated based on species-typical size. Scale bars are taken from: (*a,b*) specimen measurements herein, (*c*) [20,21], (*d*) [20], (*e*) [22], (*f*) [23], (*g*) [24] and (*h*) Facundo Martín Labarque. Pictures are courtesy of (*a–g*) Jürgen Otto and (*h*) Facundo Martín Labarque and may not be reproduced.

The highly visual, polygynous jumping spiders (Salticidae) have elaborate displays of bright colours and behaviours [6,14]. Particularly, male jumping spiders of the genus *Maratus*, known as peacock spiders, have splendidly coloured abdomens which they erect and wave side-to-side during mating displays to females [6,8,9]. Structural colours in peacock spiders are produced by plate-like blue scales (modified setae) with a dual thin film structure [10] or rainbow scales with two-dimensional diffraction gratings atop a convex three-dimensional microstructure [12]. Brush-like scales produce cream, yellow or red colours through pigments in combination with structural effects [10,14]. Other brush-like black scales contain melanins [12,15]. There is strong mate choice by female peacock spiders for strikingly bright and bold colour patterns; jumping spiders have acute colour vision [16,17] and colourful male ornaments are the direct targets of female choice [7,18,19]. Furthermore, female peacock spiders are extremely choosy and usually mate only once [6]. Therefore, males are under powerful selective pressure to fulfil female preferences.

Intriguingly, males of many species of peacock spiders have dark, velvety black patches adjacent to bright colour patches (figure 1). This is reminiscent of the super black plumage near bright colours in the birds of paradise (Paradisaeidae), which are also subject to intense sexual selection [25] and have evolved extraordinarily elaborate mating displays [26–30]. Many male birds of paradise evolved deep velvet, ‘super black’ plumages near bright colour [26,28,30,31]; super black is produced by multiple scattering

among barbule microstructures which greatly enhances the efficiency of melanin absorption [31]. More generally, super black is defined as structural or structurally assisted absorption with significantly reduced specular reflectance compared to that of a flat (unstructured) surface of the same material [31–33]. In nature, anti-reflection (whether in combination with pigmentary absorption or not) has evolved in moth eyes to reduce glare [34], in transparent aquatic animals to evade detection [35], in glasswing butterflies to avoid avian predators [36], in velvet black spots on a viper to merge into shadows on the forest floor [37] and more—and frequently has inspired anti-reflective engineered materials (e.g. [38]).

Super black coloration is extremely low reflectance (e.g. less than 0.5% directional reflectance in birds of paradise), approaching the darkest human-made materials available [39–41]; this raises the question of why such an intricate, extreme trait evolved. In birds of paradise, super black may have evolved through sensory bias [31], whereby a trait stimulates pre-existing sensory/cognitive biases and preferences in females [4,42,43]. Specifically, in a variety of vertebrates, super black surfaces impede natural mechanisms of colour correction by removing white specular highlights that are used as white-balancing reference points, causing nearby colours to appear brighter—even luminescent [44–46]. Are the velvety black patches in peacock spiders a convergent example of structurally assisted super black for colour emphasis? If so, this implies (i) a widespread sensory bias intrinsic to colour vision in distantly related species, and (ii) a significant role for sensory bias at the extremes of competitive sexual selection.

Here, we characterize the spectral reflectance and surface microstructures of the black areas in two brilliant and boldly patterned species of peacock spiders, *Maratus speciosus* (figure 1a) and *Maratus karrie* (figure 1b). We use hyperspectral analysis, scanning electron microscopy (SEM) and finite-difference time-domain (FDTD) modelling of the interaction between the structures and incident electromagnetic field. We determine that they use super black, structurally assisted absorption in their displays, which are much less reflective than the normal black cuticle of a closely related normal black spider (*Cylistella* sp., which has no bright colours), and comparable in reflectance to super black bird of paradise plumages. Moreover, we observe a new, distinct type of microstructure in super black spiders different than those previously described in birds of paradise. *Maratus* has brush-like scales similar to the bird of paradise feathers, but also has novel anti-reflective microlens arrays. Based on FDTD modelling, we propose a mechanism for the reduced reflectance and increased light absorption. We further demonstrate that the spiders' microstructural features are roughly at an optimum for the microstructures to achieve minimal reflectance and maximal absorption in the melanin layer.

2. Methods

(a) Specimen details

All spider specimens were obtained from the Harvard Museum of Comparative Zoology Invertebrate Zoology collections, and both bird specimens are from the Yale Peabody Museum of Natural History Ornithological Collections. Note that multiple individual specimens are identified by a single specimen number because they are curated in lots of approximately 3–10 individuals from the same locality and collection date in a single jar.

(b) Scanning electron microscopy

Spiders were dried, mounted and sputter-coated with 10 nm of Pt/Pd to prepare for SEM. SEM images were taken on an FESEM Ultra55, and measurements were taken from these images using IMAGEJ. The location of SEM images on the specimens is indicated in the electronic supplementary material, figure S1.

(c) Hyperspectral imaging

To record reflectance spectra for these spiders, standard spectroscopy could not be used owing to their small size (approx. 2–5 mm in diameter, with even smaller velvety black regions). Therefore, we used a form of microspectrophotometry which captures an image where every pixel encodes a reflectance spectrum between wavelengths 420 and 1000 nm, normalized by a mirror standard (Thorlabs Inc.). We used a Horiba and Cyto-viva Model XploRA hyperspectral microscope with MICROMANAGER and ENVI software (issue 4.8). The light source was a DC-950 Fiber-Lite (Colan-Jenner Industries). We used a 50× microscope objective (numerical aperture 0.5) and exposure time of 1000 ms for the super black regions. The mirror standard was too reflective for this exposure time, so we used exposure 100 ms and multiplied all values by 10 (we could perform a linear transformation because the charged-coupled device is a linear detector for the intensities employed). To control for background noise from our instruments, we normalized all measurements by the lamp spectrum; to ensure there was no background noise from ambient conditions, we turned off the light source and took a hyperspectral measurement.

From the resulting hyperspectral images, we averaged 10 reflectance spectra from points that were in focus on the image

(limited owing to the curvature of spider bodies). To calculate total %-reflectance, we integrated a loess (locally estimated scatterplot smoothing) curve from wavelengths 420–700 and divided the result by the integral of a perfect mirror reflectance standard with reflectance = 100% for the studied 280 nm wavelength span. We performed this analysis with all three species of spiders and with one species from the bird of paradise (Paradisaeidae), which were previously characterized [31], in order to validate the procedure.

We ensured that the black patches did not reflect in the ultraviolet range through multispectral imaging of one male specimen of each species and a female *M. speciosus* (electronic supplementary material, figure S2).

Specimens stored in ethanol may have changes in colour owing to pigment leaching; before hyperspectral imaging, we allowed the spiders to dry for 60 s in air (surface drying of *Maratus* restores the original colour [20]). Further, we were quantitatively analysing the 'darkness' of a region; if melanin had been leached, our measurements of the 'darkness' of a region are an underestimation, implying that the super black effect is even more pronounced in live peacock spiders.

(d) Optical modelling

FDTD simulations were performed using the commercially available software LUMERICAL FDTD, which employs the standard Yee cell method [47] to calculate the spatio-temporal electromagnetic field distribution resulting from an initial pulse launched into the simulation domain. Each real microlens (figure 2a) has a super-ellipsoidal shape (figure 2b–d), described by the following function (equation (2.1)), with characteristic structure size, R_0 , height, h_0 , elongation, e_0 , and shape N (where $N = 2$ corresponds to an ellipsoid and $N = 1$ is near-pyramidal in the x -direction)

$$z(x,y) = R_0 h_0 \left[1 - \left| \frac{x}{R_0} \right|^N - \left| \frac{y}{R_0 e_0} \right|^2 \right]^{\frac{1}{\sqrt{2N}}}. \quad (2.1)$$

The structures were discretized such that at least 50 mesh elements per half-width were used in each Cartesian direction, with a maximum mesh element size of 30 nm. For the air region outside of the structure, the built-in mesh of 2 was used in the z -direction.

In calculating reflectance, three collection angles are of interest: (i) 30° to match the microscope set-up, (ii) 90° to obtain the total reflected light, and (iii) 12°, an estimate of the collection angle of female eyes approximately 0.85 mm from end-to-end facing an approximately 2.1 mm male abdomen sitting approximately 7 mm away (figure 2e,f). Although female peacock spider eyes have an impressive field of view of 58° [48], only rays reflected or emitted from the male's abdomen that intersect her eyes are relevant to our work.

For this work, a plane wave was normally incident (z -direction) on an infinite array of microstructures in the (x,y) -plane. The simulation domain was bounded in the z -direction by perfectly matched layers (PMLs) while symmetry and anti-symmetry boundary conditions were used in the x and y directions, depending on which polarization was chosen for the incident light. All presented results are averages of two simulations with orthogonal polarization. Frequency domain field monitors were placed above and below the structure to collect the reflected and transmitted light, respectively. A hexagonal packing was chosen in order to emulate the predominant packing observed in the SEMs of the two studied spider species.

The electromagnetic pulse spanned the wavelength range of approximately 350–750 nm (in order to ensure an appreciable field strength in the range of interest, 400–700 nm). PML boundaries and monitors were spaced a distance of at least $\lambda_{\max}/2$ apart from each other and from the structure. The simulation was terminated with an auto shutoff level of 10^{-4} . The built-in

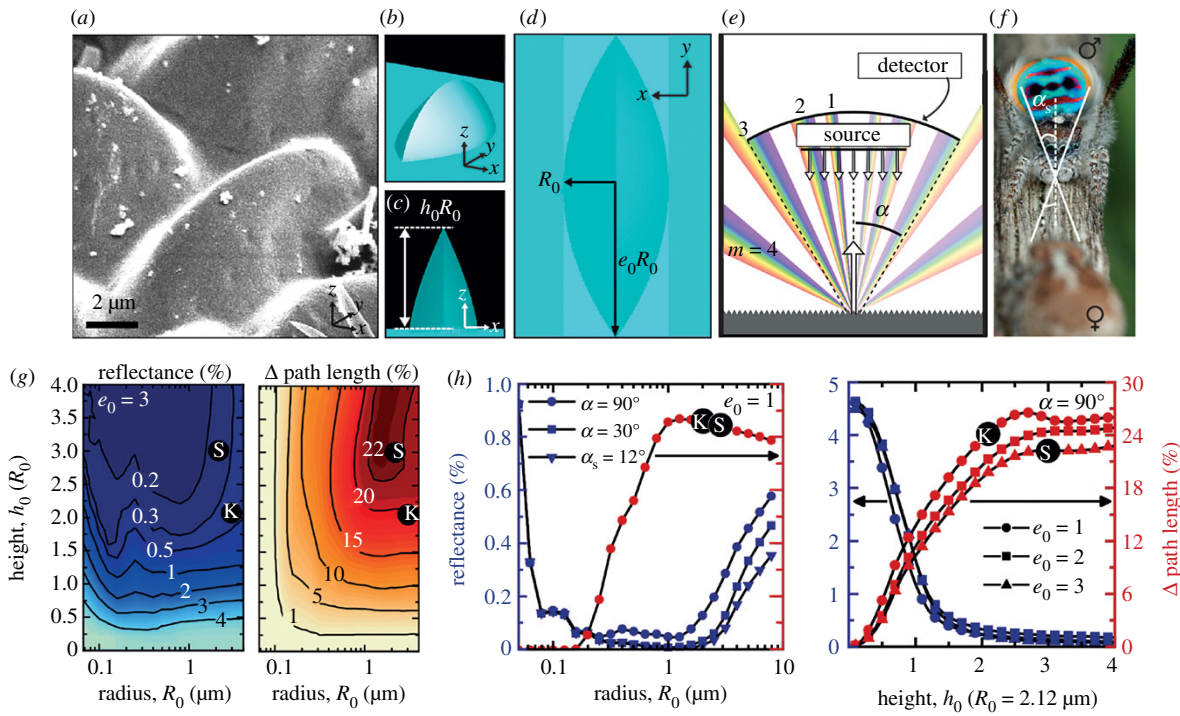


Figure 2. FDTD simulations confirm that spider-like microlens arrays cause path length increase and decrease specular reflectance. (a) SEM micrograph of a group of microlenses of *M. speciosus* in a super black region. (b) Perspective view of single microlens in the simulation of an infinite hexagonal array. (c) xz perspective and (d) top views of the single microlens, including definitions of the geometrical parameters used in the simulation. (e) Schematic of grating-like behaviour (showing orders $m = 0$ through to 4) of the periodic microstructure, with definition of collection angle α , where only reflected angles lesser than α are collected in the experimental reflectance measurement as well as by the female spider. (f) Photograph of male (top)–female (bottom) interaction, with an estimate of the collection angle, α , for female spiders, which is determined by considering male abdomen width, female eyes centre-to-centre distance, and courtship distance. The male abdomen is approximately 2.1 mm wide. Photo courtesy of Jürgen Otto and may not be reproduced. (g) Contour maps showing the dependence of reflectance (left) and change in path length (right) on the microlens length scales: radius, R_0 , and height, h_0 , for lens elongation $e_0 = 3$ and collection angle, $\alpha = 90^\circ$. 'S' and 'K' approximate the height and radius for *M. speciosus* and *M. karrie*, respectively. (h) Reflectance (left axis, blue curves) and change in path length (right axis, red curves) for different α (left plot) and e_0 (right plot) and as a function of R_0 (with $e_0 = 1$, left plot) and h_0 (where $\alpha = 90^\circ$, right plot).

grating projection function was used to decompose the fields collected by the monitors into sets of planar waves travelling in different directions, θ . For the reflection, these directions are equivalent to the diffraction angle, where angles larger than the acceptance angle (either defined by the choice of microscopy objective or position of the spiders during courtship) were filtered out. For the transmission, the travelling angles were used to calculate the increase in path length compared to a flat surface, which would not refract normally incident light; the increase in path length is thus given by $\Delta \text{path length} = 1/\cos\theta - 1$. The results are presented for wavelengths linearly sampled in steps of 10 nm from the 400–700 nm wavelength span.

The value used in simulations for the refractive index of spider cuticle ranges from 1.5 to 1.63, commonly inferred by identifying a liquid of known refractive index which matches that of the cuticle [9,49,50], thus eliminating structural colours upon immersion. More precise measures of refractive index, for example, Jamin-Lebedoff interference microscopy, find comparable values for butterfly chitin [51], a material related to spider cuticle [48]. We assume that the imaginary component of the refractive index is equivalent to 0, following what was assumed for unpigmented chitin in butterfly wings in [51]. This may contribute to a small overestimation of reflectance, which is preferable to an underestimation because we are here studying the degree to which spider cuticle can be low reflectance. Here, following [10], we use the value of $n = 1.55$ (except where we study the effects of varying n in simulation), which is validated by a close match between calculation and measurement (electronic supplementary material, equation S1, see Results).

In peacock spiders, black colour is produced by melanin packaged in spherical pigment granules called melanosomes [15]. In the species studied herein, we identified melanosomes in a dense, disorganized, clumped layer beneath the cuticle (electronic supplementary material, figure S3, 'Mel' in figure 4), of the same size and location as melanosomes identified in Hsiung's work on related species [9,15]. For this analysis, we focus on the microstructures but do not specifically model the melanin absorption (see the electronic supplementary material, Methods).

3. Results

Using hyperspectral imaging, we find that the velvety black areas reflect only 0.44% of incident light in *M. speciosus*, and 0.35% in *M. karrie* (figures 1a,b and 3; electronic supplementary material, figure S1 and table S1, collection angle is 30°), which is similar to values for human-made anti-reflective surfaces [39–41]. These super black patches in *M. speciosus* and *M. karrie* are darker than the normal black cuticle in a closely related, all-black jumping spider (Salticidae) *Cylistella* sp. (4.61% reflectance, figure 3a) and brown/black cuticle in *Maratus* (electronic supplementary material, table S1). Super black reflectance in the peacock spiders is comparable to directional reflectance of super black plumage in birds of paradise (figure 3a); the bird of paradise measured herein—*Drepanornis bruijnii*, the pale-billed sicklebill—had super black feathers with 0.17% reflectance adjacent to

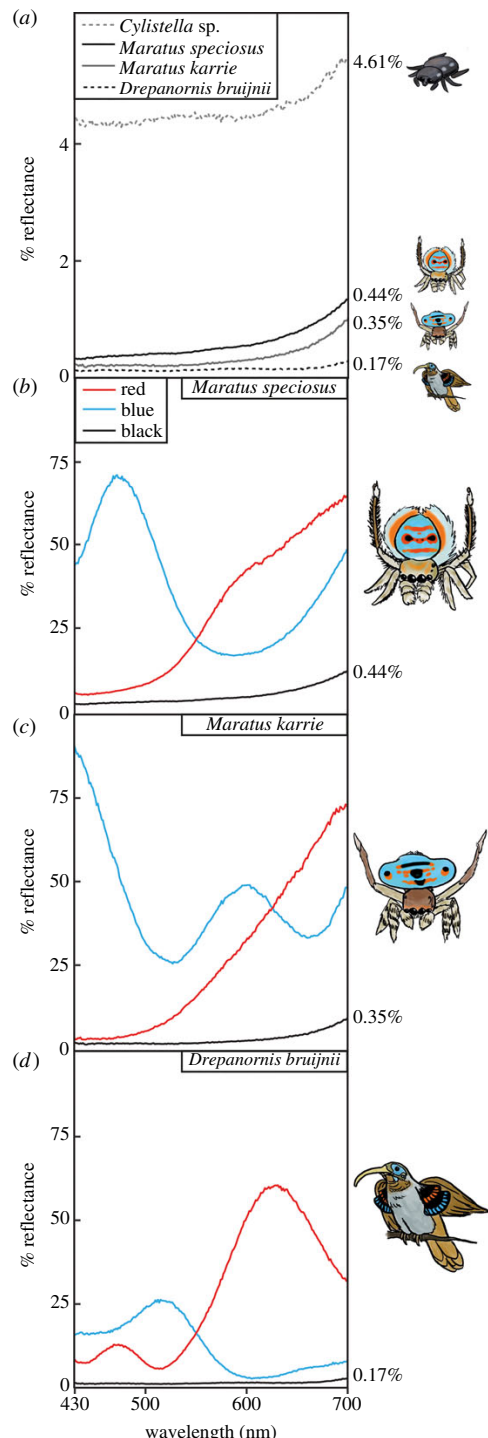


Figure 3. Spectral reflectance measurements using a 30° angle of collection. (a) Reflectance curves for typical black spider *Cylistella* sp., super black cuticle in *M. speciosus*, super black cuticle plus super black brush-like scales in *M. karrie* and super black display feathers from bird of paradise *D. bruijnii*. Numbers to the right of the graph represent total per cent reflectance compared to a mirror standard (area under the reflectance curve divided by area under a 100% reflectance curve). (b) Reflectance curves for red scales, blue scales and super black regions of *M. speciosus*. (c) Reflectance curves for red scales, blue scales and super black regions of *M. karrie*. (d) Reflectance curves for red feather tip, blue feather tip and super black feathers of *D. bruijnii*. All measurements were performed with the same hyperspectral imaging set-up, with $50\times$ microscope objective (numerical aperture 0.5). Artwork credit Kay Xia. (Online version in colour.)

bright red and blue, while other birds of paradise from [31] range from 0.05 to 0.31%.

Using SEM imaging, we identify two types of microstructure present in super black regions of these peacock spiders: cuticular microlens arrays in both and black brush-like scales with many tapering protrusions in *M. karrie* (figure 4). Typical salticid cuticle is smooth and relatively flat and unstructured [48,52] (figure 4a,b; electronic supplementary material, figure S4), but the cuticle in super black regions of *Maratus* is patterned by microlens arrays with tall, tightly packed, regularly spaced bumps, resembling loose rows of protruding discs or cones ('MLA' in figure 4c–f). The bumps are approximately $6\ \mu\text{m}$ tall in both species, but they are more disc-like in *M. speciosus* and more conical in *M. karrie* (electronic supplementary material, tables S2 and S3). The microlens arrays in super black regions differ from: (i) the irregular and low-relief cuticle in dark brown *Maratus* females, (ii) the flat cuticle in non-display regions of males (figure 4a,b), and (iii) the smooth unstructured cuticle in the all-black, closely related Salticid spider *Cylistella* (electronic supplementary material, figure S4). In some male *Maratus*, beneath colourful scales, there is relatively flat cuticle patterned with small bumps (electronic supplementary material, figure S5), which ranges in colour from normal black to weak, dark blue [10]. Super black cuticle bumps are significantly taller than this regular bumpy cuticle by 3–4 μm (electronic supplementary material, tables S2 and S3). In human-made materials, taller microlenses are more anti-reflective [53]; therefore, these simple, relatively flat blue or black cuticular bumps may become super black when the bumps increase in height.

Both the microlens arrays and the brush-like scales decrease specular reflectance and enhance melanin-based absorption. The brush-like scales achieve a reflectance of only 0.77% alone (measurement of isolated super black brush-like scale on pale black background; electronic supplementary material, table S1 and figure S5B). We hypothesize that the brush-like scales multiply scatter light between the spiny projections (figure 4g, no. 1); at each scattering event, a portion of the light is transmitted into the scale where it is absorbed by melanin pigments, while the remaining portion of the light is reflected at the air–cuticle interface. Rather than being reflected away from the surface of the spider, most of these reflected waves will subsequently encounter another spiny scale projection, where the process is repeated. Thus, multiple scattering causes iterative, near-complete absorption. Super black surface features with many spiny projections have been modelled previously [31], and for two jumping spider genera (*Phidippus* and *Platycryptus*, Salticidae), Hill [54] observed that the shape of dark-pigmented scales 'minimizes surface glare, thus placing a premium on the interaction of incident light with pigment within the scale' [54, p. 200]. Therefore, we focused our simulations on the microlenses.

Simulations of light propagation by the surface structures alone accurately model the experimental reflectance for (i) the two peacock spiders (circles labelled S and K on the plots; figure 2h) and for (ii) the normal black, unstructured cuticle of *Cylistella* sp. (figure 3; we predicted approx. 4.6% reflectance, consistent with electronic supplementary material, equation S1).

Our numerical simulations confirm that the microlens array surface features decrease specular reflectance (figure 2; electronic supplementary material, figures S6–S8).

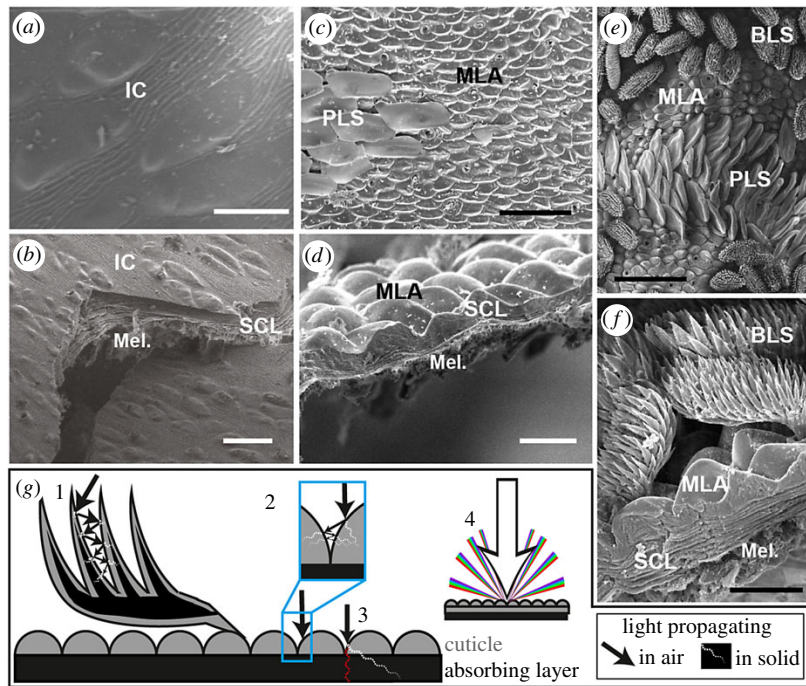


Figure 4. Super black regions in peacock spiders have distinct microstructures compared to normal black regions. (a,b) SEMs of the brown region of *M. speciosus*, showing the (a) surface and (b) cross-section. (c,d) SEMs of super black region in *M. speciosus*, showing the (c) surface and (d) cross-section. (e,f) SEMs of super black region in *M. karrie*, showing the (e) surface and (f) cross-section; BLS, brush-like scales; MLA, microlens array; PLS, blue plate-like scales; IC, irregular cuticle; SLC, striated cuticle layers; Mel., absorbing layer of melanin pigment granules. (g) Diagram of the proposed structurally assisted absorption mechanisms by peacock spider microstructures: 1, multiple scattering between spiny projections and iterative absorption as light propagates through cuticle and into the absorbing layer at each scattering event (dotted white line); 2, multiple scattering between bumps and iterative absorption as light propagates through cuticle and into the absorbing layer at each scattering event (dotted white line); 3, increased path length through melanin layers for enhanced absorption (dotted white line) compared with a flat surface (dotted red line); and 4, diffraction of light owing to periodic microlens array, such that less light enters the visual cone of the female spider. Scale bars: (a) 30 µm, (b) 10 µm, (c) 30 µm, (d) 10 µm, (e) 50 µm and (f) 10 µm. The location of SEM images on specimen is indicated in the electronic supplementary material, figure S1.

We describe three optical mechanisms. First, we show that less light is reflected away from the spider's body at the air–cuticle interface; instead, we propose that light is multiply scattered between adjacent lenses, causing iterative absorption (figure 4g, no. 2) and a decrease in total surface reflectance. For a flat cuticle surface, reflected light waves scatter back from the surface of the spider causing a brighter appearance. For the cuticular microlens array, reflected light waves frequently encounter another microlens, where some portion of the light is transmitted and absorbed. Through repeated scattering at the air–cuticle interface, less light overall is reflected away from the spider and more light is absorbed as it propagates through the cuticle and absorbing layer (figure 4g, dotted white lines). In this manner, the super black regions have less specular reflectance, and less total reflectance, than a comparable flat surface.

Second, our simulations document that the microlens arrays augment light absorption by increasing the path length of light interacting with pigment (figures 2g,h and 3g, no. 3). The microlens arrays of both *M. karrie* and *M. speciosus* increase the transmitted light path length by 20% compared to an unstructured cuticular surface (figure 2). Such an increase in path length enhances the interaction between the incident light and homogeneous absorbing layer beneath the lens. This would allow the spiders to employ a thinner absorbing layer compared to the thickness required to achieve the same absorption with an unstructured

surface. While the melanin granules contribute to scattering as well as absorption, our calculations based on [55] suggest that the relative importance of scattering is low and thus, the path length increase is indeed important for the mechanism of super black (see the electronic supplementary material, Methods).

Third, the microlens arrays reduce specular reflectance by diffracting light out of the viewing cone of a female's eyes (figures 2e and 3g, no. 4). While the feature size (lens diameter approx. 5–10 µm) is large compared to the wavelength of light, it is still small enough to redirect light into diffraction orders off of normal reflection, thus reducing the portion of light that can enter the acceptance angle of an onlooker's eyes or objective lens (figure 2e). This is consistent with observations in measurements of human-made anti-reflective coatings with 2 µm periodicity [53].

Finally, through simulations, we studied how variations in parameters—size, shape, arrangement, refractive index, etc.—could affect the super black phenomenon. Importantly, by sweeping the dimensions of the microlens in simulation, we find that the size and shape of the microlens arrays in the peacock spiders are a balanced optimum between two anti-reflective optical effects: (i) decreased surface reflectance (through diffraction and multiple scattering) and (ii) increased pigmentary absorption (path length increase through the pigmentary layer). Larger microlenses are less efficient at decreasing surface reflectance but more efficient

at increasing transmitted light path length (figure 2g,h). A radius of approximately 2 µm and height of two to three times that radius (approx. 4–6 µm, plotted in figure 2h as a function of radius), as observed in these spiders, sits at an optimum trade-off between these two physical effects (figure 2g,h). Radius and height are most important; variation in refractive index from 1.5 to 1.65 (electronic supplementary material, figure S6), shape N from ellipsoid to pyramidal (electronic supplementary material, figure S7) and packing system (the arrangement of microlenses from a top-down view) whether hexagonal versus rectangular (electronic supplementary material, figure S8) had comparably small effects.

To compare the effect of nanostructures versus microstructures, we simulated microlenses with radii ranging from 0.01 to 10 µm. Nanostructures are more effective, i.e. produce lower reflectance, over a wide-angle range (90°), but they do not necessarily perform better when a smaller collection angle is employed, as evident in figure 2g,h.

4. Discussion

Peacock spiders have structurally enhanced, anti-reflective, super black coloration. Brilliantly coloured peacock spiders *M. speciosus* and *M. karrie* produce super black colour owing to microlens arrays on the cuticle (and in *M. karrie*, an overlaying forest of black brush-like scales) above a dense absorbing layer of pigment.

The microlenses of super black cuticle in peacock spiders bear a striking resemblance to anti-reflective surface ornamentation that enhances absorption and reduces specular reflectance in other organisms—including flower petals [56–59], tropical shade plant leaves [60], light-sensitive brittlestar arms [61] and ommatidia in moth eyes [62]. For example, in flowers, conical cells focus incident light and scatter reflected or re-emitted light [63] to produce a velvety coloured appearance and enhance light absorption by the pigment. Applying flower-inspired structures to solar cells (flower power) significantly increased efficiency [64,65]. Flowers and plants evolved simple structures to efficiently harvest light (i) omnidirectionally and (ii) across the visible spectrum (broadband anti-reflection), so they are useful inspiration for broadband and omnidirectional light harvesting [65]. In flowers, as the ratio between microlens height and diameter increases from 0.1 to 0.4, reflection losses drop precipitously [65]. We observe the same pattern in spider microlenses, for which ensembles of taller microlenses are more anti-reflective (figure 2h).

Our models show that microlens arrays in spiders behave similarly to engineered microlenses, which are widespread for anti-reflective applications [53,66,67]. The active layer in solar cells is analogous to the dense absorbing layer of melanin beneath the cuticle in *Maratus* spiders (figure 4; electronic supplementary material, figure S3, [15]). Engineers added a microlens array to the light-facing side of a solar cell in order to increase the light absorption efficiency compared to the flat surface by up to 10%; the microlens array reduces optical losses through diffraction and light focusing to increase the path length of light in the active layer [53]. The microlenses in peacock spiders are differently shaped than these engineered microlenses, so it would be informative to simulate optical losses for a solar cell with a spider-inspired ellipsoidal microlens array.

Archetypal anti-reflective surfaces typically have nanosstructured features (e.g. moth eyes [34], the glasswing butterfly [36] and black silicon for solar cells [39]), but super black features in peacock spiders and birds of paradise primarily have microstructures. Through our simulations, we investigated the relative performance of microlens arrays ranging in radius from 0.01 to 10 µm. Nanostructures clearly provide a lower reflectance over a wide collection angle (90°), but they lose their advantage at smaller collection angles (figure 2g,h). During their mating displays, spiders and birds have control over the angle at which they are seen by their potential mate by repositioning their body [11,13,29,31,68]. Thus, males can restrict the collection angle relevant to female eyes; they must be super black only over the viewing cone of a female (estimated herein at 12°; see Methods). On the other hand, in the case of a moth eye, the key evolutionary driving pressure is collecting as much light as possible from all directions to see in low light conditions (as well as to reduce glare in all directions to hide from predators); this gave rise to nanostructures which provide low angle anti-reflection in all directions.

In most organisms, melanin pigments produce normal black colour with white, specular highlights (e.g. glossy hair). By contrast, structural super black in peacock spiders—as well as birds [31], butterflies [69], snakes [37] and human-made materials [32]—creates a featureless black surface with no highlights. Generally, super black seems always adjacent to bright colour in peacock spiders (herein, adjacent to red and blue: figures 1 and 3b–d) and birds of paradise [31]. The convergent evolution of structurally absorbing black coloration for colourful sexual display by both birds of paradise and now peacock spiders suggests that broadband, featureless black surfaces play an important sensory role in colourful displays for distantly related, but ecologically similar, species.

We hypothesize that super black evolved in peacock spiders and birds of paradise convergently through a shared sensory bias intrinsic to colour perception. According to sensory bias theory, an adaptive feature of the sensory or cognitive system may give rise to a novel or inherently stimulating perceptual experience in the context of social or sexual signalling [70]. Here, we suggest that colour vision in spiders, as in vertebrates, has the adaptive feature for colour correction which gives rise to an intrinsic sensory bias stimulated by super black near brilliant colour. Vertebrates use specular highlights, or gleams from object surfaces, to estimate the magnitude and spectrum of the ambient light illuminating the visual scene, and ‘white balance’ their colour perceptions based on this information [46]. Super black essentially eliminates specular reference points. In vertebrates (specifically humans and goldfish), anti-reflective black surfaces impede the observer’s ability to adjust for the amount of ambient light [44,45,71], causing colourful patches to appear self-luminous or popping above the plane of the image. This perceptual illusion is similar to the well-studied Adelson’s checker-shadow [72], in which the context around a grey square greatly influences our perception of its brightness. Furthermore, anti-reflective surface features have been shown to enhance the brilliance and saturation of pigmentary colours in snapdragons (*Antirrhinum majus* [57]) and plastic polymers [73]. Super black surrounding or adjacent to bright colour would have the same chromatic effect. Therefore, we hypothesize that the adaptive trait of colour correction also produces an

intrinsic sensory/cognitive bias; males in extreme competition for mating may be able to produce impossibly bright colours by stimulating this intrinsic bias through super black.

In both birds and spiders, sexual selection has apparently led to the evolution of a convergent optical, often angle-dependent, illusion—the use of super black structurally assisted absorption to enhance the perceived brilliance of adjacent colours. Super black reveals a fundamental, and broadly distributed, sensory bias.

Data accessibility. Data available from the Dryad Digital Repository: <https://doi.org/10.5061/dryad.m9n940m> [74].

Authors' contributions. All authors conceived the research plan. D.E.M. and V.E.M. performed and analysed the hyperspectral and SEM measurements, under the direction of R.O.P. and D.H. N.K.M. and A.V.S. performed the optical modelling, under the direction of J.A. All authors jointly wrote the paper.

Competing interests. We declare no competing interests.

Funding. This work was supported in part by the National Science Foundation (NSF) Materials Research Science and Engineering Centers (MRSEC) at Harvard University under award no. DMR 14-20570, and this work was performed in part at the Center for Nanoscale Systems (CNS), a member of the National

Nanotechnology Coordinated Infrastructure Network (NNCI), which is supported by the National Science Foundation under NSF award no. 1541959. CNS is part of Harvard University. V.E.M. is supported by a DFG grant (RU 665/13-1, project number 396637283). D.E.M. conducted this research with Government support under and awarded by DoD, Air Force Office of Scientific Research, National Defense Science and Engineering Graduate (NDSEG) Fellowship, 32 CFR 168a. D.E.M. is also supported by a Theodore H. Ashford Graduate Fellowship in the Sciences, and by a Mind, Brain, and Behavior Graduate Student Award. A.V.S. and N.K.M. are supported by the Kavli Institute for Bionano Science and Technology at Harvard. N.K.M. is supported by the Fulbright, Danmark-Amerika Fondet, Weibel Scientific, Augustinus Fonden and an Excellence PhD Scholarship from DTU Nanotech.

Acknowledgements. We are very grateful to Laura Leibensperger, Arthur McClelland, Richard Childers, Carolyn Marks, Amos Meeks, Mary Salcedo, Tom McCoy and Mara Laslo for assistance with imaging, specimen preparation and analysis. We thank Jürgen Otto and Facundo Martín Labarque for providing beautiful photos of spiders. Sam Church and Seth Donoughe provided helpful comments on the manuscript. We greatly appreciate Victoria Hwang and Ming Xiao for their insights on scattering in the mela-nosome-containing layer and providing the calculations of scattering and absorption lengths. We thank Kay Xia for illustrations of the study species.

References

- Cuthill IC *et al.* 2017 The biology of color. *Science* **357**, eaan0221. ([doi:10.1126/science.aan0221](https://doi.org/10.1126/science.aan0221))
- Zahavi A. 1975 Mate selection—a selection for a handicap. *J. Theor. Biol.* **53**, 205–214. ([doi:10.1016/0022-5193\(75\)90111-3](https://doi.org/10.1016/0022-5193(75)90111-3))
- Prum RO. 2012 Aesthetic evolution by mate choice: Darwin's really dangerous idea. *Phil. Trans. R. Soc. B* **367**, 2253–2265.
- Dawkins MS, Guilford T. 1996 Sensory bias and the adaptiveness of female choice. *Am. Nat.* **148**, 937–942. ([doi:10.1086/285964](https://doi.org/10.1086/285964))
- Hill GE. 1991 Plumage coloration is a sexually selected indicator of male quality. *Nature* **350**, 337–339. ([doi:10.1038/350337a0](https://doi.org/10.1038/350337a0))
- Girard MB, Endler JA. 2014 Peacock spiders. *Curr. Biol.* **24**, R588–R590. ([doi:10.1016/j.cub.2014.05.026](https://doi.org/10.1016/j.cub.2014.05.026))
- Masta SE, Maddison WP. 2002 Sexual selection driving diversification in jumping spiders. *Proc. Natl Acad. Sci. USA* **99**, 4442–4447. ([doi:10.1073/pnas.072493099](https://doi.org/10.1073/pnas.072493099))
- Hill DE, Otto JC. 2011 Visual display by male *Maratus pavonis* (Dunn 1947) and *Maratus splendens* (Rainbow 1896) (Araneae: Salticidae: Euophryinae). *Peckhamia* **89**, 1–41.
- Hsiung B-K, Justyn NM, Blackledge TA, Shawkey MD. 2017 Spiders have rich pigmentary and structural colour palettes. *J. Exp. Biol.* **220**, 1975–1983. ([doi:10.1242/jeb.156083](https://doi.org/10.1242/jeb.156083))
- Stavenga DG, Otto JC, Wilts BD. 2016 Splendid coloration of the peacock spider *Maratus splendens*. *J. R. Soc. Interface* **13**, 20160437. ([doi:10.1098/rsif.2016.0437](https://doi.org/10.1098/rsif.2016.0437))
- Otto JC, Hill DE. 2013 A new peacock spider from Australia displays three 'sapphire gems' on a field of gold (Araneae: Salticidae: Euophryinae: *Maratus* Karsch 1878). *Peckhamia* **105**, 1–8. ([doi:10.11646/zootaxa.4564.1.3](https://doi.org/10.11646/zootaxa.4564.1.3))
- Hsiung B-K *et al.* 2017 Rainbow peacock spiders inspire miniature super-iridescent optics. *Nat. Commun.* **8**, 2278. ([doi:10.1038/s41467-017-02451-x](https://doi.org/10.1038/s41467-017-02451-x))
- Girard MB, Kasumovic MM, Elias DO. 2011 Multi-modal courtship in the peacock spider, *Maratus volans* (OP-Cambridge, 1874). *PLoS ONE* **6**, e25390. ([doi:10.1371/journal.pone.0025390](https://doi.org/10.1371/journal.pone.0025390))
- Foelix RF, Erb B, Hill DE. 2013 Structural colors in spiders. In *Spider ecophysiology* (ed. W Nentwig), pp. 333–347. Berlin, Germany: Springer.
- Hsiung B-K, Blackledge TA, Shawkey MD. 2015 Spiders do have melanin after all. *J. Exp. Biol.* **218**, 3632–3635. ([doi:10.1242/jeb.128801](https://doi.org/10.1242/jeb.128801))
- Zurek DB, Cronin TW, Taylor LA, Byrne K, Sullivan MLG, Morehouse NI. 2015 Spectral filtering enables trichromatic vision in colorful jumping spiders. *Curr. Biol.* **25**, R403–R404. ([doi:10.1016/j.cub.2015.03.033](https://doi.org/10.1016/j.cub.2015.03.033))
- Nakamura T, Yamashita S. 2000 Learning and discrimination of colored papers in jumping spiders (Araneae, Salticidae). *J. Comp. Physiol. A* **186**, 897–901. ([doi:10.1007/s003590000143](https://doi.org/10.1007/s003590000143))
- Taylor LA, McGraw KJ. 2013 Male ornamental coloration improves courtship success in a jumping spider, but only in the sun. *Behav. Ecol.* **24**, 955–967. ([doi:10.1093/beheco/art011](https://doi.org/10.1093/beheco/art011))
- Lim MLM, Li J, Li D. 2008 Effect of UV-reflecting markings on female mate-choice decisions in *Cosmophasis umbratica*, a jumping spider from Singapore. *Behav. Ecol.* **19**, 61–66. ([doi:10.1093/beheco/arm100](https://doi.org/10.1093/beheco/arm100))
- Otto JC, Hill DE. 2012 Notes on *Maratus* Karsch 1878 and related jumping spiders from Australia, with five new species (Araneae: Salticidae: Euophryinae). *Peckhamia* **103**, 1–81. ([doi:10.11646/zootaxa.4564.1.3](https://doi.org/10.11646/zootaxa.4564.1.3))
- Keyserling E. 1882 Die Arachniden Australiens. *Nunberg* **1**, 1325–1420.
- Waldock JM. 2014 Two new species of peacock spider of the *Maratus mungaich* species-group (Araneae: Salticidae) from south-western Australia. *Rec. West. Aust. Museum* **29**, 149–158. ([doi:10.18195/issn.0312-3162.29\(2\).2014.149-158](https://doi.org/10.18195/issn.0312-3162.29(2).2014.149-158))
- Otto JC, Hill DE. 2014 Spiders of the mungaich group from Western Australia (Araneae: Salticidae: Euophryinae: Maratus), with one new species from Cape Arid. *Peckhamia* **112**, 1–35.
- Waldock JM. 2002 Redescription of *Lycidas chrysomelas* (Simon) (Araneae: Salticidae). *Rec. Aust. MUSEUM* **21**, 227–234. ([doi:10.18195/issn.0312-3162.21\(3\).2002.227-234](https://doi.org/10.18195/issn.0312-3162.21(3).2002.227-234))
- Irestedt M, Jönsson KA, Fjeldså J, Christidis L, Ericson PGP. 2009 An unexpectedly long history of sexual selection in birds of paradise. *BMC Evol. Biol.* **9**, 235. ([doi:10.1186/1471-2148-9-235](https://doi.org/10.1186/1471-2148-9-235))
- Wilts BD, Michielsen K, De Raedt H, Stavenga DG. 2014 Sparkling feather reflections of a bird-of-paradise explained by finite-difference time-domain modeling. *Proc. Natl Acad. Sci. USA* **111**, 4363–4368. ([doi:10.1073/pnas.1323611111](https://doi.org/10.1073/pnas.1323611111))
- Stavenga DG, Leertouwer HL, Marshall NJ, Osorio D. 2011 Dramatic colour changes in a bird of paradise caused by uniquely structured breast feather barbules. *Proc. R. Soc. B* **278**, 2098–2104. ([doi:10.1098/rspb.2010.2293](https://doi.org/10.1098/rspb.2010.2293))
- Scholes E, Laman TG. 2018 Distinctive courtship phenotype of the Vogelkop superb bird-of-paradise *Lophorina niedda* Mayr, 1930 confirms new species status. *PeerJ* **6**, e4621. ([doi:10.7717/peerj.4621](https://doi.org/10.7717/peerj.4621))

29. Frith DW, Frith CW. 1988 Courtship display and mating of the superb bird of paradise *Lophorina superba*. *Emu* **88**, 183–188. (doi:10.1071/MU9880183)
30. Laman T, Scholes E. 2012 *Birds of paradise: revealing the world's most extraordinary birds*. Washington, DC: National Geographic Books.
31. McCoy DE, Feo T, Harvey TA, Prum RO. 2018 Structural absorption by barbule microstructures of super black bird of paradise feathers. *Nat. Commun.* **9**, 1. (doi:10.1038/s41467-017-02088-w)
32. Panagiotopoulos NT, Diamanti EK, Koutsokeras LE, Baikousi M, Kordatos E, Matikas TE, Gournis D, Patsalas P. 2012 Nanocomposite catalysts producing durable, super-black carbon nanotube systems: applications in solar thermal harvesting. *ACS Nano* **6**, 10 475–10 485. (doi:10.1021/nn304531k)
33. Zhao Q, Fan T, Ding J, Zhang D, Guo Q, Kamada M. 2011 Super black and ultrathin amorphous carbon film inspired by anti-reflection architecture in butterfly wing. *Carbon N. Y.* **49**, 877–883. (doi:10.1016/j.carbon.2010.10.048)
34. Boden SA, Bagnall DM. 2012 Moth-eye antireflective structures. In *Encyclopedia of nanotechnology* (ed. B Bhushan), pp. 1–11. Dordrecht, The Netherlands: Springer.
35. Johnsen S. 2001 Hidden in plain sight: the ecology and physiology of organismal transparency. *Biol. Bull.* **201**, 301–318. (doi:10.2307/1543609)
36. Siddique RH, Gomard G, Hölscher H. 2015 The role of random nanostructures for the omnidirectional anti-reflection properties of the glasswing butterfly. *Nat. Commun.* **6**, 6909. (doi:10.1038/ncomms7909)
37. Spinner M, Kovalev A, Gorb SN, Westhoff G. 2013 Snake velvet black: hierarchical micro- and nanostructure enhances dark colouration in *Bitis rhinoceros*. *Sci. Rep.* **3**, 1846. (doi:10.1038/srep01846)
38. Tan G, Lee J-H, Lan Y-H, Wei M-K, Peng L-H, Cheng I-C, Wu S-T. 2017 Broadband antireflection film with moth-eye-like structure for flexible display applications. *Optica* **4**, 678–683. (doi:10.1364/OPTICA.4.000678)
39. Liu X, Coxon PR, Peters M, Hoex B, Cole JM, Fray DJ. 2014 Black silicon: fabrication methods, properties and solar energy applications. *Energy Environ. Sci.* **7**, 3223–3263. (doi:10.1039/C4EE01152J)
40. NanoLab Inc. 2017 Carbon nanotubes information sheet. NanoLab. See <https://sep.yimg.com/ty/cdn/nanolab2000/20170302-SDS-NT-NT.pdf> (accessed on 13 July 2018).
41. Surrey NanoSystems Limited. 2018 Vantablack. See <https://www.surreynanosystems.com/vantablack> (accessed on 13 July 2018).
42. Guilford T, Dawkins MS. 1991 Receiver psychology and the evolution of animal signals. *Anim. Behav.* **42**, 1–14. (doi:10.1016/S0003-3472(05)80600-1)
43. Ryan MJ. 1990 Sexual selection, sensory systems and sensory exploitation. *Oxford Surv. Evol. Biol.* **7**, 157–195.
44. Kreezer G. 1930 Luminous appearances. *J. Gen. Psychol.* **4**, 247–281. (doi:10.1080/00221309.1930.9918313)
45. Speigle JM, Brainard DH. 1996 Luminosity thresholds: effects of test chromaticity and ambient illumination. *J. Opt. Soc. Am. A* **13**, 436–451. (doi:10.1364/JOSAA.13.000436)
46. Brainard DH, Wandell BA, Chichilnisky E-J. 1993 Color constancy: from physics to appearance. *Curr. Dir. Psychol. Sci.* **2**, 165–170. (doi:10.1111/1467-8721.ep10769003)
47. Taflove A, Hagness SC. 2005 *Computational electromagnetics: the finite-difference time-domain method*. Norwood, UK: Artech House.
48. Foelix RF. 1983 Biology of spiders. *Insect Syst. Evol.* **14**, 16. (doi:10.1163/187631283X00371)
49. Hsiung BK, Deheyn DD, Shawkey MD, Blackledge TA. 2015 Blue reflectance in tarantulas is evolutionarily conserved despite nanostructural diversity. *Sci. Adv.* **1**, e1500709. (doi:10.1126/sciadv.1500709)
50. Parker AR, Hegedus Z. 2003 Diffractive optics in spiders. *J. Opt. A: Pure Appl. Opt.* **5**, S111–S116. (doi:10.1088/1464-4258/5/4/364)
51. Leertouwer HL, Wilts BD, Stavenga DG. 2011 Refractive index and dispersion of butterfly chitin and bird keratin measured by polarizing interference microscopy. *Opt. Express* **19**, 24 061–24 066. (doi:10.1364/OE.19.024061)
52. Gorb SN. (ed.) 2009 *Functional surfaces in biology: little structures with big effects*, vol 1. Dordrecht, The Netherlands: Springer.
53. Chen Y *et al.* 2015 Reducing optical losses in organic solar cells using microlens arrays: theoretical and experimental investigation of microlens dimensions. *Phys. Chem. Chem. Phys.* **17**, 3723–3730. (doi:10.1039/c4cp05221h)
54. Hill DE. 1979 The scales of salticid spiders. *Zool. J. Linn. Soc.* **65**, 193–218. (doi:10.1111/j.1096-3642.1979.tb01091.x)
55. Xiao M, Li Y, Allen MC, Deheyn DD, Yue X, Zhao J, Gianneschi NC, Shawkey MD, Dhinojwala A. 2015 Bio-inspired structural colors produced via self-assembly of synthetic melanin nanoparticles. *ACS Nano* **9**, 5454–5460. (doi:10.1021/acsnano.5b01298)
56. Gikas D, Argiropoulos A, Rhizopoulou S. 2015 Epidermal focusing of light and modelling of reflectance in floral-petals with conically shaped epidermal cells. *Flora Morphol. Distrib. Funct. Ecol. Plants* **212**, 38–45. (doi:10.1016/j.flora.2015.02.005)
57. Gorton HL, Vogelmann TC. 1996 Effects of epidermal cell shape and pigmentation on optical properties of *Antirrhinum* petals at visible and ultraviolet wavelengths. *Plant Physiol.* **112**, 879–888. (doi:10.1104/pp.112.3.879)
58. Wilts BD, Rudall PJ, Moyroud E, Gregory T, Ogawa Y, Vignolini S, Steiner U, Glover BJ. 2018 Ultrastructure and optics of the prism-like petal epidermal cells of *Echscholzia californica* (California poppy). *New Phytol.* **219**, 1124–1133. (doi:10.1111/nph.15229)
59. Bailes EJ, Glover BJ. 2018 Intraspecific variation in the petal epidermal cell morphology of *Vicia faba* L. (Fabaceae). *Flora* **244**, 29–36. (doi:10.1016/j.flora.2018.06.005)
60. Bone RA, Lee DW, Norman JM. 1985 Epidermal cells functioning as lenses in leaves of tropical rain-forest shade plants. *Appl. Opt.* **24**, 1408–1412. (doi:10.1364/AO.24.001408)
61. Aizenberg J, Tkachenko A, Weiner S, Addadi L, Hendler G. 2001 Calcitic microlenses as part of the photoreceptor system in brittlestars. *Nature* **412**, 819–822. (doi:10.1038/35090573)
62. Land MF. 1997 Microlens arrays in the animal kingdom. *Pure Appl. Opt. J. Eur. Opt. Soc. Part A* **6**, 599–602. (doi:10.1088/0963-9659/6/6/002)
63. Kay QON, Daoud HS, Stirton CH. 1981 Pigment distribution, light reflection and cell structure in petals. *Bot. J. Linn. Soc.* **83**, 57–83. (doi:10.1111/j.1095-8339.1981.tb00129.x)
64. Schmager R, Fritz B, Hüning R, Ding K, Lemmer U, Richards BS, Gomard G, Paetzold UW. 2017 Texture of the viola flower for light harvesting in photovoltaics. *ACS Photonics* **4**, 2687–2692. (doi:10.1021/acsphtronics.7b01153)
65. Hüning R *et al.* 2016 Flower power: exploiting plants' epidermal structures for enhanced light harvesting in thin-film solar cells. *Adv. Opt. Mater.* **4**, 1487–1493. (doi:10.1002/adom.201600046)
66. Chen Y, Elshobaki M, Ye Z, Park J-MM, Noack MA, Ho K-MM, Chaudhary S. 2013 Microlens array induced light absorption enhancement in polymer solar cells. *Phys. Chem. Chem. Phys.* **15**, 4297–4302. (doi:10.1039/c3cp50297j)
67. Peer A, Biswas R, Park J-M, Shinar R, Shinar J. 2017 Light management in perovskite solar cells and organic LEDs with microlens arrays. *Opt. Express* **25**, 10 704–10 709. (doi:10.1364/OE.25.010704)
68. Echeverri SA, Morehouse NI, Zurek DB. 2017 Control of signaling alignment during the dynamic courtship display of a jumping spider. *Behav. Ecol.* **28**, 1445–1453. (doi:10.1093/beheco/arx107)
69. Vukusic P, Sambles JR, Lawrence CR. 2004 Structurally assisted blackness in butterfly scales. *Proc. R. Soc. Lond. B* **271**, S237–S239.
70. Ryan MJ, Cummings ME. 2013 Perceptual biases and mate choice. *Annu. Rev. Ecol. Evol. Syst.* **44**, 437–459. (doi:10.1146/annurev-ecolsys-110512-135901)
71. Neumeyer C, Dorr S, Fritsch J, Kardelky C. 2002 Colour constancy in goldfish and man: influence of surround size and lightness. *Perception* **31**, 171–188. (doi:10.1088/p05sp)
72. Adelson EH. 2000 Lightness perception and lightness illusions. In *The new cognitive neurosciences*, 2nd edn (ed. M Gazzaniga), pp. 339–351. Cambridge, MA: MIT Press.
73. Clausen JS, Christiansen AB, Kristensen A, Mortensen NA. 2013 Enhancing the chroma of pigmented polymers using antireflective surface structures. *Appl. Opt.* **52**, 7832–7837. (doi:10.1364/AO.52.007832)
74. McCoy DE, McCoy VE, Mardsberg NK, Shneidman AV, Aizenberg J, Prum RO, Haig D. 2019 Data from: Structurally assisted super black in colourful peacock spiders. Dryad Digital Repository. (<https://doi.org/10.5061/dryad.m9n940m>)

From the distance of the moon, Earth was four times the size of a full moon seen from Earth. It was a brilliant jewel in the black velvet sky.

Buzz Aldrin



Super Black Evolved Convergently in 15

Brilliant Bird Families

REPRINTED FROM: McCoy, D.E. and Prum, R.O., 2019. Convergent evolution of super black plumage near bright color in 15 bird families. *Journal of Experimental Biology*, 222(18).

ARTICLE AND SUPPLEMENT AVAILABLE AT: <https://doi.org/10.1242/jeb.208140>



RESEARCH ARTICLE

Convergent evolution of super black plumage near bright color in 15 bird families

Dakota E. McCoy^{1,*} and Richard O. Prum²

ABSTRACT

We examined extremely low-reflectance, velvety black plumage patches in 32 bird species from 15 families and five orders and compared them with 22 closely related control species with normal black plumage. We used scanning electron microscopy to investigate microscopic feather anatomy, and applied spectrophotometry and hyperspectral imaging to measure plumage reflectance. Super black plumages are significantly darker and have more broadband low reflectance than normal black plumages, and they have evolved convergently in 15 avian families. Super black feather barbules quantitatively differ in microstructure from normal black feathers. Microstructural variation is significantly correlated with reflectance: tightly packed, strap-shaped barbules have lower reflectance. We assigned these super black feathers to five heuristic classes of microstructure, each of which has evolved multiple times independently. All classes have minimal exposed horizontal surface area and 3D micrometer-scale cavities greater in width and depth than wavelengths of light. In many species, barbule morphology varied between the super black exposed tip of a feather and its (i) concealed base or (ii) iridescently colored spot. We propose that super black plumages reduce reflectance, and flatten reflectance spectra, through multiple light scattering between the vertically oriented surfaces of microscale cavities, contributing to near-complete absorption of light by melanin. All super black plumage patches identified occur adjacent to brilliant colored patches. Super black plumage lacks all white specular reflections (reference points used to calibrate color perception), thus exaggerating the perceived brightness of nearby colors. We hypothesize that this sensory bias is an unavoidable by-product of color correction in variable light environments.

KEY WORDS: Color correction, Anti-reflection, Reflectance, Sexual selection, Structural absorption, Sensory bias

INTRODUCTION

The physics, chemistry, social function and evolutionary history of avian plumage coloration have been intensively studied, resulting in a deep understanding of the great diversity in the form and function of avian plumage coloration (Hill and McGraw, 2006). For example, birds-of-paradise have evolved sparkling, multicolored, three-dimensional microscopic reflectors (Stavenga et al., 2011; Wilts

et al., 2014), an array of elaborate courtship dances (Scholes, 2008; Scholes and Laman, 2018) and spreadable capes of velvet black feathers (Frith and Frith, 1988; McCoy et al., 2018; Scholes and Laman, 2018). Integumentary colors are generally categorized as pigmentary – produced by chemical pigments with specific absorption spectra – or structural – produced by nanoscale features that constructively or destructively interfere with different wavelengths of light. Granules of the pigment melanin, which have a high refractive index, can contribute to structural colors by their packaging and arrangement within the feather (Prum, 2006; Stavenga et al., 2015). This is frequently studied at the nanoscale.

However, microscale morphological features at a larger size scale than wavelengths of light can also impact plumage appearance. Barb and barbule shape, smoothness and orientation can produce glossy features in a diversity of birds (Harvey et al., 2013; Iskandar et al., 2016; Shawkey and D'Alba, 2017). Recently, we have demonstrated that microscale optical cavities in the surface of birds-of-paradise feathers create structurally assisted light absorption – or super black – through multiple scattering (McCoy et al., 2018). As in profoundly black technologies, such as Vantablack™ and carbon nanotube forests, multiple scattering and absorption interact to generate a deep black appearance (Liu et al., 2014). This ‘super black’ appears to interact with the perceptual mechanisms of the observer to create a distinct sensory experience: an optical illusion that enhances nearby color (Kreezer, 1930; Brainard et al., 1993; Speigle and Brainard, 1996).

Super black plumages in birds-of-paradise (McCoy et al., 2018), super black cuticle in peacock spiders (McCoy et al., 2019) and super black scales in various butterflies (Vukusic et al., 2004) eliminate specular reflections, or white highlights. In all three cases, these super black patches are found adjacent to bright, saturated color patches. Vertebrates use specular highlights to white-balance their visual perceptions and control for variations in the amount and color of ambient light in the visual scene. By reducing specular reflections from super black patches, the adjacent colors in birds-of-paradise, peacock spiders and butterflies may appear brighter or even self-luminous (Brainard et al., 1993; Speigle and Brainard, 1996; Neumeyer et al., 2002; McCoy et al., 2018). This general phenomenon has been confirmed psychologically in humans and goldfish (Neumeyer et al., 2002).

Here, we investigated deep black feathers from 32 species of birds (Fig. 1). We demonstrate that super black plumage has independently evolved in at least 15 different avian families – from eiders (Anatidae) and guans (Cracidae) to hummingbirds (Trochilidae), fairywrens (Maluridae) and fairy-bluebirds (Irenidae). The diverse taxonomic distribution of super black plumage in birds raises important new physical, anatomical and evolutionary questions. How do these feather morphologies absorb ambient light so effectively? How do sexual and social selection for plumage patch brilliance select on the morphology of adjacent black feathers to minimize plumage reflectance?

¹Department of Organismic and Evolutionary Biology, Harvard University, Cambridge, MA 02138, USA. ²Department of Ecology and Evolutionary Biology, and Peabody Museum of Natural History, Yale University, New Haven, CT 06520, USA.

*Author for correspondence (dakotamccoy@g.harvard.edu)

 D.E.M., 0000-0001-8383-8084

Received 4 June 2019; Accepted 15 August 2019



Fig. 1. Representative species with profoundly dark, super black plumage patches. (A) *Somateria spectabilis*. (B) *Balearica pavonina*. (C) *Oreophanus derbianus*. (D) *Lafresnaya lafresnayi*. (E) *Boissonneaua jardini*. (F) *Philepitta castanea*. (G) *Laniarius corona velutinus*. (H) *Malurus melanotis*. (I) *Sericulus chrysocephalus*. (J) *Lophorina superba*. (K) *Crypsirina temia*. (L) *Lamprotornis superbus*. (M) *Irena puella*. (N) *Sericossypha albocristata*. (O) *Tangara chilensis*. (P) *Cyanerpes cyaneus*. Photo credits: (A) Ron Knight (CC BY 2.0); (B) Michael Möller (CC BY-SA 2.0 DE); (C) Yinan Chen; (D) Ralph Paonessa; (E) Gaston Cassus; (F) Werner Suter; (G) Photo © 2011 Justin Black/justinblackphoto.com; (H) Greg Miles (CC BY-SA 2.0); (I) Rob Drummond; (J) Ed Scholes; (K) Michael Gillam (CC BY 2.0); (L) Robert Winslow; (M) Bob Barbour, www.BobBarbour.Photoshelter.com; (N) Lou Hegedus; (O) Shane Torgerson; (P) Alexander Ramirez. Photos may not be reproduced without permission from the photographers.

In this study, we investigated the reflectance and morphological structure of super black plumages – defined as having less than 2% directional reflectance at normal incidence, with broadband low reflectance – across Aves. Using spectrophotometry and scanning

electron microscopy (SEM), we compared profoundly black patches with normal black plumages from closely related, phylogenetic control species. The profoundly black plumages are significantly darker than normal black plumages. Further, we identified five

anatomical classes of super black barbule morphology, each of which evolved independently in multiple families. A phylogenetic PCA identifies two features which primarily separate super black feathers from normal black feathers: interbarbule distance and strap-shaped (rather than cylindrical) barbules, which are angled perpendicularly to the feather vane. Both features reduce exposed horizontal surface area and provide vertical surfaces that multiply scatter reflected light among feather barbules. We propose that each morphological class functions through structurally assisted absorption to reduce reflectance, as has previously been demonstrated for many manmade materials (Brown et al., 2002; Zhao et al., 2011a; Panagiotopoulos et al., 2012; Liu et al., 2014), birds-of-paradise (McCoy et al., 2018), peacock spiders (McCoy et al., 2019), butterflies (Vukusic et al., 2004), the West African Gaboon viper (Spinner et al., 2013) and a stick insect (Maurer et al., 2017). Structurally assisted absorption, hereafter ‘structural absorption’, occurs when micro- or nano-structures scatter or diffract light to enhance absorption by a material (Brown et al., 2002; Crouch et al., 2004; Vorobyev et al., 2009; Tao et al., 2012; Liu et al., 2014; McCoy et al., 2019).

In all avian species tested, profoundly black plumage was located adjacent to brilliantly colored plumage patches or fleshy ornaments. We hypothesize that super black plumages have evolved through sensory bias, owing to fundamental features of the cognitive color correction mechanisms in the vertebrate visual system, which exaggerate the perceived brilliance of adjacent colors. The massively convergent evolution of super black plumages in association with bright, saturated color patches in many avian lineages provides further evidence for this generalized sensory bias in color perception.

MATERIALS AND METHODS

Specimens

We selected 32 bird species with profoundly black plumage from 15 families and five orders, and 22 closely related species with normal black plumage for the study (Dataset 1). The species were identified by visual observation of museum study skins from the Yale Peabody Museum (YPM), the Harvard Museum of Comparative Zoology (MCZ) and the American Museum of Natural History (AMNH; Dataset 1). To the human eye, super black plumage patches are strongly velvet with minimal specular reflectance, such that it is difficult to focus on the surface of the plumage. The species with normal black plumage lacked any conspicuous glossy specular highlights, but the surface of the feathers is easily perceived. Individual contour feathers were sampled from museum skins for scanning electron microscopy (SEM). Three species had both super black and normal black patches in the same plumage: *Oreophasis derbianus*, *Lophorina superba* and *Coeligena torquata* (Dataset 1).

Spectrophotometry (reflectance)

Reflectance spectra were recorded directly from plumage patches on prepared museum skins. Directional reflectance spectra between 300 and 700 nm were measured perpendicular to the plumage with an Ocean Optics USB2000 spectrophotometer with a bifurcated probe and Ocean Optics DH-2000Bal deuterium-halogen light source. Spectralon (Ocean Optics) was used as a white standard. Negative values recorded for some measures of super black plumage were converted to 0, and three spectra from each patch (different locations within the patch) were averaged to produce an average spectrum for the patch (five for birds-of-paradise; McCoy et al., 2018). Two specimens per species were measured for all species except seven for which only one specimen was available

(Dataset 1). To produce final reflectance curves (Fig. S1), we averaged values from both specimens. Reflectance was calculated as the area under the measured reflectance spectrum by integrating the LOESS (locally estimated scatterplot smoothing) curve between 300 and 700 nm, then dividing that value by the integral of a 100% reflectance curve (the white standard).

Many species retain a profoundly black appearance after gold coating for SEM, which demonstrates a structural component to the black color. In order to quantify how dark these feathers were after being coated in gold (i.e. to quantify the structural contribution), we used hyperspectral imaging for two species, *Drepanornis bruijnii* and *Lamprotorornis splendidus*. Specifically, we used a form of microspectrophotometry that captures an image where every pixel encodes a reflectance spectrum between wavelengths 420 and 1000 nm, normalized by a mirror standard (Thorlabs Inc.). We used a Horiba and Cytoviva Model XploRA Hyperspectral Microscope with MicroManager and ENVI software (issue 4.8). The light source was a DC-950 Fiber-Lite (Colan-Jenner Industries). We used a 50× microscope objective (numerical aperture 0.5) and exposure time of 1000 ms for the super black regions. The mirror standard was too reflective for this exposure time, so we used an exposure of 100 ms and multiplied all values by 10 (we could perform a linear transformation because the charged coupled device is a linear detector for the intensities employed). To control for background noise from our instruments, we normalized all measurements by the lamp spectrum; to ensure there was no background noise from ambient conditions, we turned off the light source and took a hyperspectral measurement. From the resulting hyperspectral images, we averaged 10 reflectance spectra. To calculate total percent reflectance, we integrated a LOESS curve from wavelengths 420–700 nm and divided the result by the integral of a perfect mirror reflectance standard with reflectance=100% for the studied 280 nm wavelength span.

Lastly, we calculated the ‘flatness’ of the reflectance spectra of super black and normal black birds, by fitting a linear model to the reflectance spectra, and recording the slope. In this manner, we can compare the rise in reflectance over the avian visual spectrum between normal and super black plumages.

To create phylogenetically independent comparisons of reflectance and slope between super black feathers and normal black feathers, we paired super black species with a closely related normal black bird, a phylogenetic ‘control’ species from within the same, or nearest, family (see Dataset 1). Because super black plumage is not a homologous character shared among multiple bird families (see below), each such comparison constitutes a phylogenetically independent comparison (*sensu* Felsenstein, 1985). We then performed a paired two-sided *t*-test in R version 3.4.3 with these phylogenetically controlled species pairs, randomly selecting one super black and one control species per family group. We repeated this procedure with 100 random selections of control and test pairs to check for robustness and ensure that our random choice of control and test birds did not impact results.

Scanning electron microscopy (microstructure)

For SEM, feathers were mounted on stubs using carbon adhesive tabs, coated with ~15 nm of gold or platinum/palladium, and viewed and micrographed using an ISI SS40 SEM operating at 10 kV or an SEM-4 FESEM Ultra55 operating at 5 kV. All SEM figures are available from the corresponding author upon request.

To quantify feather microstructure, we measured nine barbule features on each species (we took 10 measurements for each feature in ImageJ and averaged them). These are 2D measurements of a 2D representation of a 3D structure, but they nonetheless are a useful

start to understanding qualitative categories of barbule microstructure. The two species categorized as ‘brushy barb’ (*O. derbianus* and *Somateria fischeri*) were excluded from the phylogenetic PCA analysis because they do not have barbules.

Variables included: (1) barb/barbule angle, the angle between the barbules and the central barb; (2) barbule length, the full length of the barbule, following the path of the barbule free-hand; (3) barbule thickness, the thickness of the barbule viewed from the side (i.e. thinnest point); (4) barbule width, the width of the barbule viewed head-on (i.e. widest point); (5) central barb width, the width of the central barb viewed top-down; (6) degree of barbule curvature, where a circle was fit to the curviest portion of each barbule (in many cases, the entire barbule curved smoothly) and the diameter of curvature was recorded, the arc length of the curved portion was also recorded, and from this the degree of curvature was calculated; (7) inter-barbule distance, the distance between two adjacent barbules on one side of a feather; (8) length of marginal spikes, the length of spikes, approximated by a straight line running from tip of spike along the center of the spike to marginal edge of the barbule; and (9) strappiness, barbule width divided by thickness.

Phylogenetic analyses

To perform robust phylogenetic analyses (Jetz et al., 2012, 2014; Rubolini et al., 2015), we downloaded 100 trees from birdtree.org, including all species measured herein and in Stoddard and Prum (2011).

For phylogenetically controlled principal component analysis (phyloPCA) of feather microstructural characters, we scaled and centered all data before the analysis and then used function phyl.pca in the R package phytools (Revell, 2012). For the method of correlation, we used lambda, and the PCA mode was set to ‘cov’ (covariance).

We performed a phylogenetic generalized least squares (PGLS) model to test for correlations between feather microstructure and percent reflectance. We used the PCA PC1 scores, which captured 33.3% of the variance in feather microstructure. We used PGLS (Grafen, 1989; Martins and Hansen, 1997) with a Brownian motion model to account for phylogeny. We repeated this analysis for 100 phylogenetic trees (first calculating PC1, then fitting a PGLS model) and recorded estimates, 95% confidence intervals and *P*-values for all. PGLS is required rather than a non-phylogenetic method even though we are using phylogenetic PCA scores (Revell, 2009).

We reconstructed the evolutionary history of black plumage reflectance for a large sample of avian species, both those measured herein and those measured in the eumelanin spectral archive (Stoddard and Prum, 2011). We removed species with reflectance >10% from Stoddard and Prum (2011). We performed the reconstruction with the contMap function in phytools v. 0.6-44 (Revell, 2012, 2013), which uses maximum likelihood to estimate states at internal nodes and interpolate these states along internal branches (Felsenstein, 1985). We performed this analysis on a consensus tree, obtained through the function consensus.edges in the library phytools in R.

RESULTS

Reflectance

We compared super black plumages – which are all, except for one, adjacent to saturated color patches (Fig. 1) – with normal black plumages. Super black plumages were profoundly darker, with flatter reflectance curves, than normal black plumages (Figs 2 and 3). Reflectance of the super black plumages ranged from 0.045% (*Astrapia stephaniae*) to 1.97% (*Malurus albocapulatus*) and

averaged 0.94%. For the control black birds, reflectance ranged from 2.32% to 6.26% and averaged 4.02%.

Super black plumages reflected significantly less light than did normal black plumages of phylogenetic control species for reflectance with 90 deg incident light (paired *t*-tests: $P<0.0005$; 95% CI=−0.038, −0.025; Figs 2 and 3A, Fig. S1). Statistics are presented for one randomly chosen control and super black bird per family. We repeated the test procedure 100 times with randomly selected pairs of super black and control species for families with multiple samples of either, and found significant results irrespective of which super black and control birds were chosen in each family (average *P*-value=8.25×10^{−8}, average 95% CI=−0.039, −0.026; for distributions of *P*-values and confidence intervals, see Fig. S2A,B).

As predicted, reflectance spectra of super black bird plumages were nearly flat compared with normal black plumages, whereas reflectance spectra of normal black plumages showed pronounced upward slopes at longer wavelengths (Figs 2 and 3C, Fig. S1). Surface structure can enhance the absorption efficiency of melanin by multiply scattering light among 3D elements of the feather. With each scattering event, some proportion of incident light is transmitted and absorbed (Brown et al., 2002; Crouch et al., 2004; Vorobyev et al., 2009; Tao et al., 2012; Liu et al., 2014). By iterative absorption, these plumages achieve a super black, broadband appearance.

For reflectance spectra, control birds had slopes ranging from 0.24 to 10 with a mean of 5.3% μm^{−1}, while super black birds ranged from 0.16 to 3.5 with a mean of 1.1% μm^{−1}. The slopes of super black reflectance spectra were significantly lower (i.e. the spectra were flatter) than those of normal black plumages (paired *t*-tests: $P<0.0005$; 95% CI=−6.0, −3.4; Fig. 3C,D). Statistics are presented for one randomly chosen control and super black bird per family. We repeated the test procedure 100 times with randomly selected pairs of super black and control species for families with multiple samples of either, and found significant results irrespective of which super black and control birds were chosen in each family (average *P*-value=2.0×10^{−5}, average 95% CI=−5.6, −2.8; for distributions of *P*-values and confidence intervals, see Fig. S2C,D).

In many cases, as predicted by iterative absorption, super black plumages had reflectance curves with a spectral shape similar to that of normal black plumage reflectance curves of their closest relative divided by a factor of 3–12 (depending on the species). This proportionality factor differs substantially between families, for example, ranging from ~3–4 in Trochilidae and Pipridae to ~8 in Gruidae and ~10–12 in Cnemophilidae and Paradisaeidae. Intriguingly, for several taxa, the super black curves do not show a proportional rise in reflectance (i.e. super black curves appear substantially flatter even when divided by an appropriate proportionality factor). These taxa are *Malurus* spp., some birds-of-paradise (Paradisaeidae), *Irena puella* and *Nettapus auritus*. All except *Malurus* spp. have curved array barbules, the most efficient microstructural enhancers of absorption reported here.

Black plumages measured herein were combined with a previous study of 134 black, eumelanin pigmented plumage patches from 53 species of birds (Stoddard and Prum, 2011) to achieve representation among 40 total avian families (Fig. 3B,D). An ancestral state reconstruction illustrates that the ancestral state of black plumage reflectance is highly likely to be ≥4% reflectance (Fig. 4). We document at least 15 independent evolutionary origins of super black plumage in 15 families. Super black, defined as less than 2% reflectance, evolved from ancestral states of 3–5% reflectance.

To show how dark and broadband low reflection these plumages are in the larger context of bird plumage diversity, we also plotted

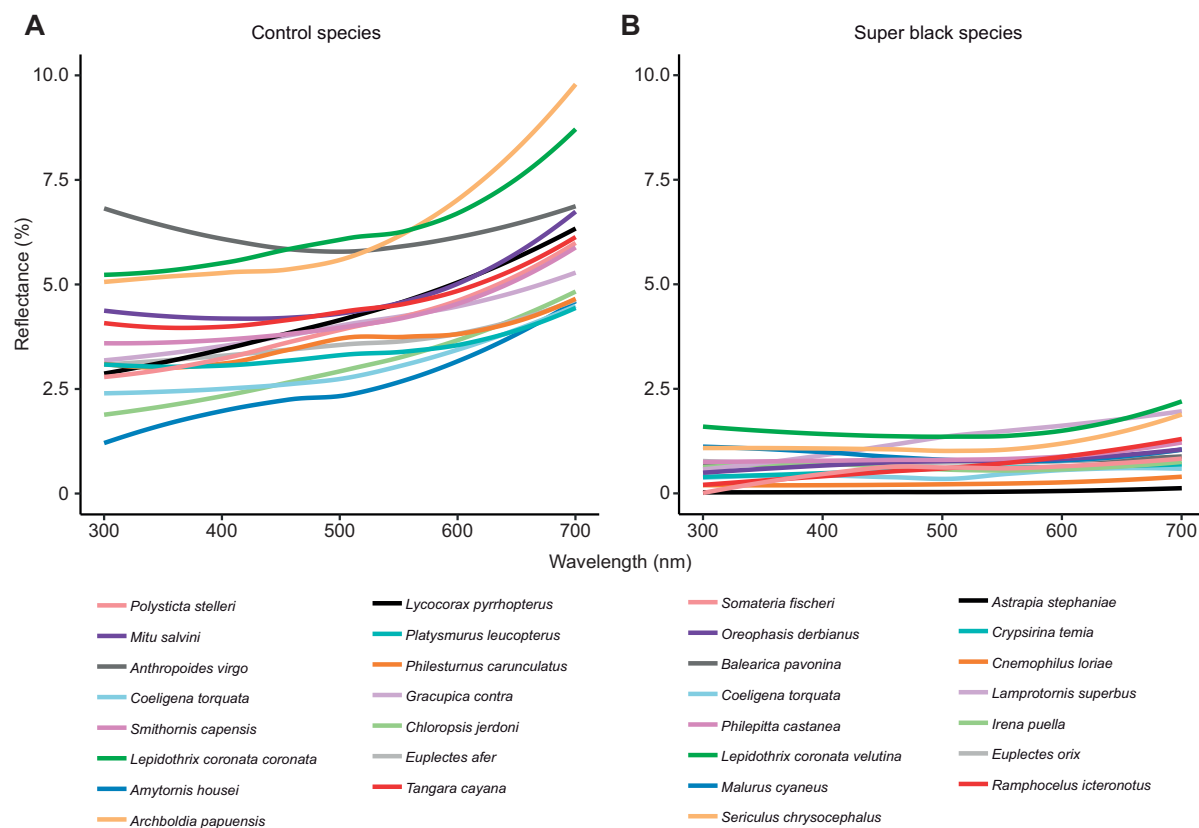


Fig. 2. Super black plumage has low, broadband reflectance. (A) Control species with normal black plumage. (B) Sample species with super black plumage (structurally assisted absorption). Here, we plot $n=30$ example species; plumage patch locations and percent reflectance for all species are in Dataset 1; all reflectance curves are in Fig. S1.

the total reflectance and slope of the reflectance spectrum from the Stoddard and Prum (2011) dataset (Fig. 3B,D) after eliminating patches from this previous sample that had more than 10% reflectance. Of the remaining 120 plumage patches, the mean reflectance was 3.95%, and the mean reflectance spectrum slope was $4.0\% \mu\text{m}^{-1}$ (values comparable to those of the normal, control black birds chosen in this study).

We observed that every instance but one of super black plumage was associated with a brilliant and highly chromatic plumage color patch (Dataset 1), or a fleshy patch, horn or caruncle (*Somateria spectabilis*, *O. derbianus*, *Balearica pavonina*, *Philepitta castanea*). Control species with normal black plumage had few colorful patches (Dataset 1). White patches, however, were observed in multiple control species, but only one of the super black species had an adjacent white patch (Dataset 1; see Discussion, Super black occurs near brilliant color in visual displays).

Remarkably, some super black feathers still appear profoundly black even after being coated in ~ 15 nm gold for SEM. We measured the reflectances of two feathers that appeared black even with a gold coating, an upper wing covert from *L. splendidus* and a pectoral plume from *D. bruijnii*, using a microscope equipped with hyperspectral imaging. Typically, feathers coated in gold appear gold; indeed, the bright, structurally colored regions of the gold-coated *D. bruijnii* feather reflected between 10 and 20% of light across all wavelengths (Fig. S3). In contrast, in both

cases, reflectance of the gold coated super black region was $<0.5\%$ across all measured wavelengths – two orders of magnitude lower (Fig. S3). These data provide strong physical evidence for structural absorption.

Feather morphology

Our evaluation of SEMs of feathers from super black plumage patches from 15 different families revealed multiple qualitative differences of barbule morphology that we classified heuristically in five classes (Fig. 5). Each of these barbule types has evolved in at least two families separately (Fig. 4). Furthermore, we made quantitative measurements of SEMs from all feathers and documented clustering by morphological group (Fig. 6A).

SEMs of normal black plumage patches revealed uniform barbule structure and cluster together in the phylogenetic PCA (Fig. 6A, Figs S4–S6): the barbules are simple, undifferentiated and generally oriented horizontally (the only exception being *Tangara cayana*, for which barbules demonstrate some vertical angling; Fig. S6D). Very little variation in barbule morphology was observed between the exposed distal and more basal portions of the feather vane or an individual barb.

In contrast, super black feathers cluster separately from the normal black feathers on the phylogenetic PCA (Fig. 6A); they produce multiple scattering and enhanced melanin absorption through a variety of three-dimensional surface structures (Fig. 5,

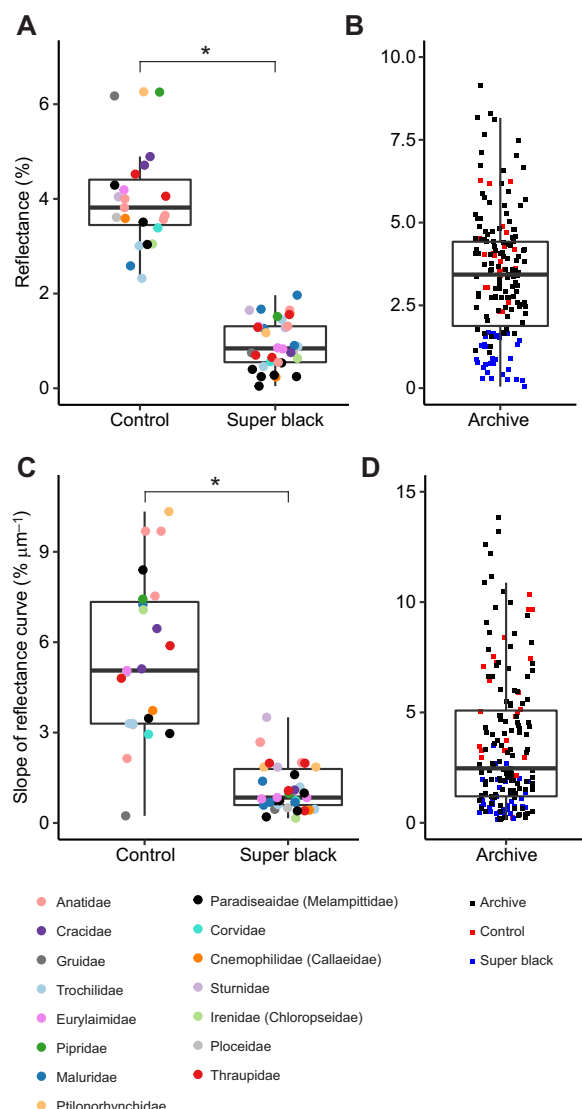


Fig. 3. Super black plumage is significantly darker, with a flatter reflectance curve, than normal black plumage. (A) Percent reflectance, 90 deg incident light, for $n=55$ control and super black birds; $P<0.0005$; 95% CI= -0.040 , -0.023 . (B) Percent reflectance, 90 deg incident light, from an archive of $n=120$ black plumage patches from 53 bird species (Stoddard and Prum, 2011) with all control (green) and super black species (purple) plotted. (C) Slope of linear model of the reflectance spectra for $n=55$ control and super black birds; $P<0.0005$; 95% CI= -6.0 , -3.4 . The outlier among control bird slopes (dark grey dot) is *Anthropoides virgo* (Gruidae), which has a U-shaped reflectance curve (i.e. slope of linear fit is near 0) but still reflects 5–7% of light; see Fig. 2A. (D) Slope of linear models of reflectance curves from an archive of $n=120$ black plumage patches from 53 bird species (Stoddard and Prum, 2011) with all control (green) and super black species (purple) plotted. Statistics are presented for one randomly chosen control and super black bird per family; details in Materials and Methods. All P -values and confidence intervals from the 100 repetitions are plotted in Fig. S2A–D.

Figs S4–S6). We identified five qualitative categories of super black plumages: (1) curved arrays, (2) dihedral straps, (3) dense straps, (4) sparse straps and (5) brushy barbs.

Curved arrays (dense, curved, upright array of barbules)

Eleven species from five families showed densely packed barbules that curve vertically above the plane of the feather vane at variable angles (Fig. 5A,B). Species with this morphology are six birds-of-paradise, *Ptiloris paradiseus*, *A. stephaniae*, *Seleucidis melanoleucus*, *Parotia wahnesi*, *D. bruijnii* and *L. superba* (Paradiseidae; all but *D. bruijnii* previously reported in McCoy et al., 2018); the Asian fairy-bluebird, *I. puella* (Irenidae); two starlings, *Lamprotornis superbus* and *L. splendidus* (Sturnidae); the duck *Nettapus auratus* (Anatidae); and the velvet satinbird, *Cnemophilus loriae* (Cnemophilidae) (Figs 5A,B, 6A, 7A). These structures form a disorganized array of curved, planar structures sticking up from the barb ramus like a semi-cylindrical bottle brush. The barbules of the birds-of-paradise, *C. loriae* and *I. puella* have spikes and protrusions along their margins, like serrations on leaves. The starlings *L. superbus* and *L. splendidus* have largely smooth, undifferentiated barbule margins; occasionally, some marginal spikes and protrusions are visible (Fig. 5A). The curvature of the barbule surfaces creates complex microcavities between barbules, in which straight-line paths out of the bottom of the cavity are limited or nonexistent. We note that *N. auratus* and *C. loriae* combine this barbule morphology in a dihedral organization (see below).

Dihedral straps (dense, strap-shaped, dihedral barbules)

Six species from five families have densely packed, strap-shaped barbules that angle upwards toward the upper (obverse) surface of the feather vane on either side of the ramus to form a dihedrally shaped vanule, or ‘valley’, toward the tip of each ramus (Figs 5C,D, 6A, 7B). These species with dihedral morphology are the crane *B. pavonina* (Gruidae); the bowerbirds *Sericulus chrysocephalus* and *S. bakeri* (Ptilonorhynchidae); and the tanager *Ramphocelus icteronotus* (Thraupidae). The barbules are simple and rectangular in cross-section, with minimal change in barbule shape from base to tip. The barbules are quite straight (*S. chrysocephalus*) or only slightly curved (*R. icteronotus*), and oriented parallel to one another. Barbules extend from the rami in neat rows at a constant angle without radial dissymmetry. The barb itself is extremely oblong, shaped like a razor rather than a cylinder, with a minimum of horizontally exposed surface area. The duck *N. auratus* (Anatidae) and the velvet satinbird, *C. loriae* (Cnemophilidae), combine the dihedral organization with curved barbule surfaces and complex protrusions on the barbule margins (see above).

Dense straps (dense, bundled, strap-like or hair-like barbules)

Eight species from five families have densely spaced, strap-like barbules with generally simple margins that curve only slightly upwards, most notably toward the end of each ramus where the barbules appear ‘bundled’ or ‘hairlike’ (Figs 5E,F, 6A, 7C). The strap-shaped barbules are oriented with their narrow margins facing outward (obverse) and their broad surfaces facing one another, in the plane of the vane. Species with these feathers are the broadbill *P. castanea* (Eurylaimidae); two fairywrens, *Malurus cyaneus* and *M. melanocephalus* (Maluridae); the treepie *Crypsirina temia* (Corvidae); the bishop *Euplectes orix* (Ploceidae); and three tanagers, *Cyanerpes cyaneus*, *Sericossypha albocristata* and *Tangara chilensis* (Thraupidae). The barbules are not oriented in neat rows, like they are in the ‘dihedral strap’ species, but appear more chaotic (like branches of pine trees). However, the barbules are similarly simple and rectangular in structure.

Sparse straps (sparse, strap-shaped barbules)

Six species from four families have vertically oriented, strap-shaped barbules (i.e. higher than they are wide) with a minimum of



Fig. 4. Super black plumage has evolved independently in at least 15 avian families. An ancestral state reconstruction of reflectance is presented on a consensus phylogenetic tree to illustrate the multiple parallel evolutions of super black in 15 avian families. Reflectance data from this paper were combined with data from Stoddard and Prum (2011). Families are listed on the right, and families with at least one evolution of super black are written in black rather than grey with an accompanying silhouette. *Lepidothrix coronata* refers to subspecies *velutina*; subspecies *coronata* is not included here. *Drepanornis bruijnii* had no available phylogenetic data and is not included. Silhouette credits (from Phylopic.org): Cracidae: uncredited, copyright free; Anatidae: Maija Karala; Gruidae: Lauren Anderson; Trochilidae, Ptilonorhynchidae, Paradisaeidae: Ferran Sayol; Corvidae: L. Shyamal; Maluridae: Michael Scroggie; Sturnidae: Maxime Dahirel. We generated silhouettes for Pipridae, Eurylaimidae, Cnemophilidae, Ploceidae, Irenidae and Thraupidae.

broad, horizontally exposed surfaces (Figs 5G,H, 6A, 7D). Species with the sparse strap morphology are the duck *Somateria spectabilis* (Anatidae), the hummingbirds *C. torquata* (nape), *Boissonneaua jardini* and *Lafresnaya lafresnayi* (Trochilidae), the manakin *Lepidothrix coronata velutina* (Pipridae) and the Australasian wren *M. alboscapulatus* (Maluridae). The flat

surfaces of the barbules are slightly twisted near the base (thus exposing some horizontal surface), but at the tip almost no surface is horizontally exposed. These barbules are not densely packed near each other on the ramus; however, observations of the specimens suggest that the feathers themselves are densely packed.

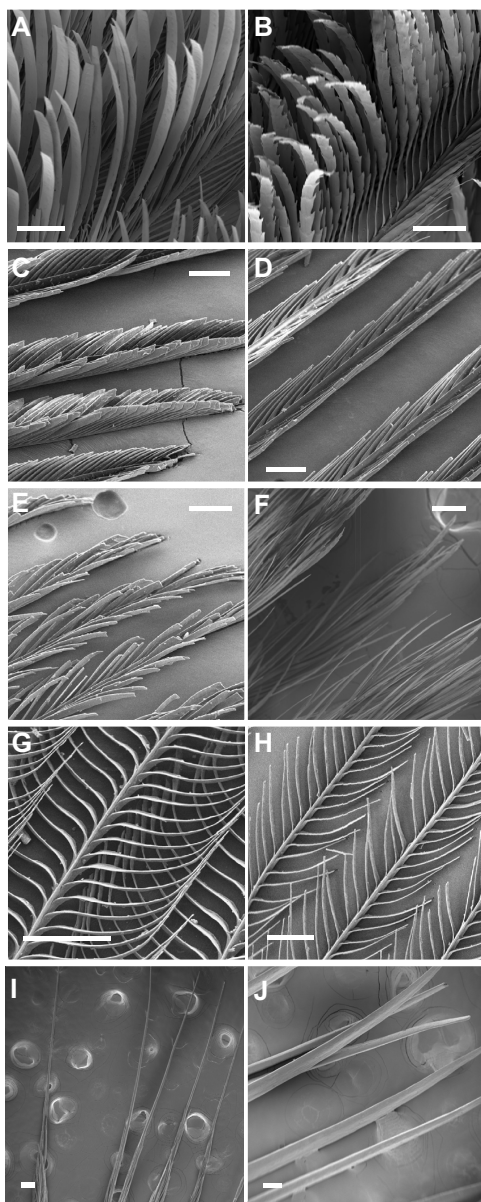


Fig. 5. Birds evolved five morphological categories of super black feathers with structurally assisted absorption. We observed five qualitative categories of feathers (for quantitative analysis, see Fig. 6) based on barbule morphology: (A,B) curved arrays, (C,D) dihedral straps, (E,F) dense straps, (G,H) sparse straps and (I,J) brushy barbs. (A) *Lamprotornis superbus* black spot on wing covert; (B) *Drepanornis bruijnii* black spot on pectoral plume; (C) *Ramphocelus icteronotus* back; (D) *Sericulus chrysocephalus* back; (E) *Tangara chilensis* back; (F) *Malurus cyaneus* upper back; (G) *Boissonneaua jardini*; (H) *Somateria spectabilis* rim around bill; (I) *Oreophasis derbianus* forecrown; (J) *Somateria fischeri* facial ring. Scale bars are 100 µm.

Brushy barbs (no barbules at tip, narrow tapered barbs)

Black feathers from the horned guan, *O. derbianus*, forecrown and the duck *S. fischeri* eyering are very tiny, erect and completely lack barbules at the tip (Figs 5I,J, 6A, 7E, Fig. S4A,B). The barbs are

long and tapering. This very simple morphology suggests that scattering interactions among multiple feathers play an important role in structural absorption in these plumages.

Phylogenetic PCA

The phylogenetic PCA supported three distinct feather groups primarily along PC1: control feathers at one end, curved array super black feathers at the other end, and all other super black feathers in between. PC1 was correlated with (i) the extent to which barbules are strap-shaped versus cylindrical and (ii) the distance between barbules (Fig. 6A, Dataset 2). These are two proxies for exposed horizontal surface area. The most strap-shaped and most tightly packed barbules are curved arrays, while at the other end are the control feathers. In between is a cluster of feathers with strap-shaped barbules that we divide into dihedral, dense and sparse based on additional qualitative characteristics that were not distinguished by the PCA. Brushy barb feathers were not included in the PCA because they have no barbules.

Morphology and reflectance variation among feather classes

PC1, a measure of feather microstructure, is significantly correlated with reflectance (PGLS; for one tree, estimate=−0.30, 95% CI=−0.47, −0.14, $P<0.005$; Fig. 6B; P -values and confidence intervals for the same analysis conducted over 100 trees are presented in Fig. S2E,F; results were significant in each case). In other words, feathers with more strap-shaped (rather than cylindrical) barbules, and with more tightly packed barbules, are darker. This analysis was conducted without the brushy barb class feathers, which do not have barbules.

The five morphological classes varied substantially in their absorption efficiency (Fig. 6B). The darkest two classes were curved array and brushy barbs, with mean reflectances of 0.58% and 0.62%, respectively. The other three morphological classes had mean reflectance values closer to 1%: dihedral strap (0.88%), dense strap (1.03%) and sparse strap (mean 1.25%). We ranked these barbule classes and ‘normal’ class from 1 to 6, with 1 through 5 being those five super black morphologies and 6 being the control feathers, and applied a tie-corrected Spearman’s rank correlation in R (version 3.4.3 2017). We found Spearman’s rho=0.85, $P<0.0005$ (this result was robust when we applied Kendall’s tau-B as well).

Within-feather variation in morphology

In most species, it was also possible to identify barbule morphologies associated with light absorption by comparing barbules at the exposed distal tips of the feather vane with those nearer the bases of the feather vane (McCoy et al., 2018), because the exposed tips of the vanes contribute to the plumage appearance while the bases of the vanes are concealed within the plumage by other, overlying contour feathers.

Philepitta castanea provides an interesting exception. At the end of the breeding season, male *P. castanea* have a single, annual, prebasic molt that produces a plumage with a scaly appearance of contour feathers with yellow-green distal tips and black bases (Prum and Razafindrantsita, 1997). Over the non-breeding season, the green tips gradually wear off to reveal a distinctive, super black male breeding aspect, which gives the velvet asity its common name. The green tips of the freshly molted male contour feathers have carotenoid pigments and relatively sparse barbules that form a flat, horizontal vanule. However, toward the bases of these feathers, the melanin pigmented barbules, which will be fully exposed after feather wear during the breeding season, are much denser and exhibit the prominent dihedral vanules.

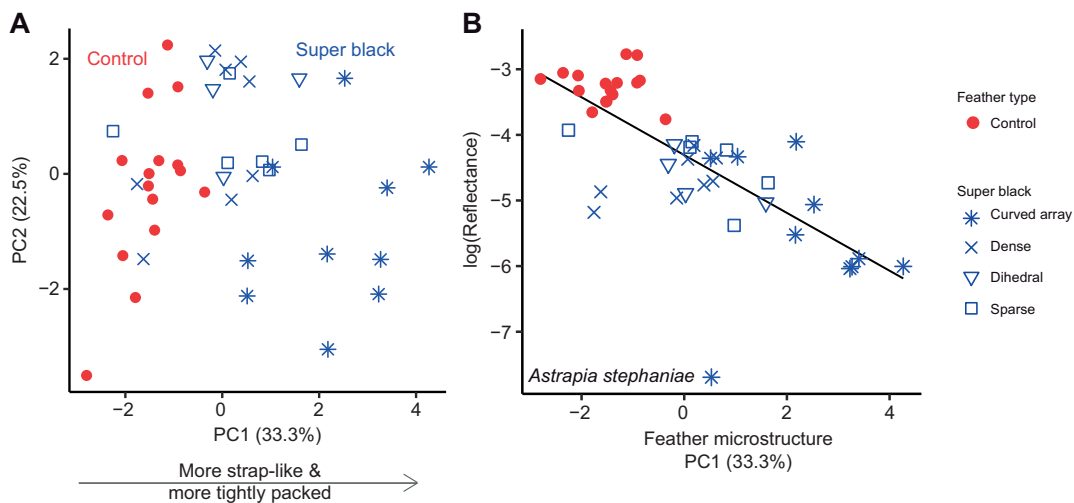


Fig. 6. Feather barbule microstructure is significantly correlated with reflectance. We included $n=53$ species; brushy barb feathers are not included here, because they have no barbules. (A) A phylogenetic PCA reveals that feathers cluster into discrete morphological groups based on microstructural measurements (for PCA loadings and PCA scores by species, see Dataset 2); PC1 scores were determined primarily by how much exposed surface area was present on the feathers (how strap-shaped barbules were and inter-barbule distance), while PC2 was largely determined by barb/barbule angle and degree of curvature. The two species categorized as ‘brushy barb’ (*Oreophasis derbianus* and *Somateria fischeri*) were excluded from the phylogenetic PCA analysis because they do not have barbules. (B) PC1, a measure of feather microstructure, is significantly correlated with log(reflectance) (PGLS; for one tree, estimate = -0.30, 95% CI = -0.46, -0.14, $P < 0.005$; Fig. 6B; P -values and confidence intervals for same analysis conducted over 100 trees are presented in Fig. S2E,F). We repeated the phylogenetic PCA and the PGLS model over 100 trees; P -values and confidence intervals for all analyses are presented in Fig. S2E,F.

In three species, barbule morphology varied significantly within a single feather between areas of structural black and vivid structurally color, which are produced by arrays of melanosomes within the barbules (Fig. 8). *Lamprotornis superbus* and *L. splendidus* have black spots on their wing covert feathers that are surrounded by iridescent blue. *Drepanornis bruijnii* has black pectoral plumes tipped with structural red or blue. In all three species, barbules within the iridescent portions of the vane were flat, smooth, straps lying horizontal in the plane of the feather, but in the super black areas, the barbules curved conspicuously upwards and gained some jagged tips to their margins (Fig. 8).

DISCUSSION

Super black plumage evolved convergently in 15 avian families

Here, we describe the convergent evolution of super black plumage in 15 families of birds from five orders (Figs 1 and 4). These species have less than 2% reflectance of directly incident light. Super black is defined as a structural or structurally assisted black surface with (i) significantly reduced specular reflectance and (ii) a flatter reflectance curve (broadband low-reflectance) compared with that expected from a flat surface of the same material (Zhao et al., 2011a; Panagiotopoulos et al., 2012; McCoy et al., 2018). The super black plumages described here are significantly

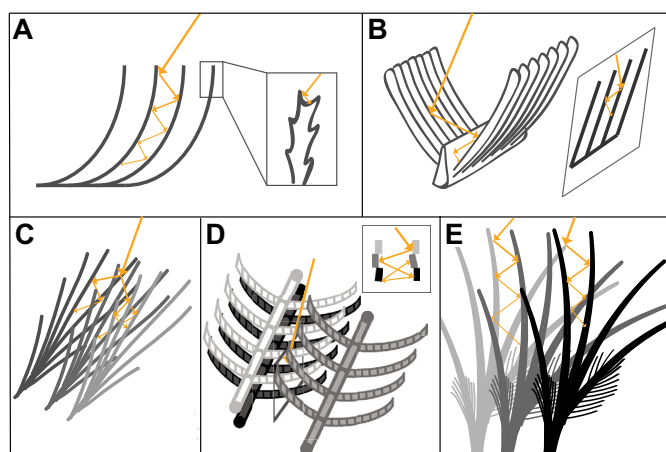


Fig. 7. Schematic models of structural absorption for each of five feather morphology classes. (A) Curved array feathers multiply scatter light between deep curved cavities between barbules; inset: jagged barbule margins on some curved array feathers may enhance multiple scattering. (B) Dihedral strap feathers multiply scatter light between the V-shaped barbule arrays and within deep cavities between adjacent barbules. (C) Dense strap feathers form a chaotic array with minimally exposed horizontal surface area, which multiply scatters light. (D) Sparse strap feathers apparently form deep cavities among feathers that produce multi-feather (black, gray, white) scattering. Inset: cross-section of light being multiply scattered between different feathers. (E) Brushy barb feathers multiply scatter light between vertically oriented, simple barbs of multiple densely packed feathers which project vertically from the bird skin.

darker—with significantly flatter reflectance curves (broadband low-reflectance)—than plumages of closely related normal black species (Figs 2 and 3). Melanin pigments absorb shorter wavelengths of light more efficiently, resulting in higher reflectance in the red than the ultraviolet (Meredith and Sarna, 2006). Typically, reflectance curves of black plumage slope upward (Fig. 2A). In contrast, structurally assisted absorption causes plumages to have not only lower overall reflectance but also more uniform reflectance (McCoy et al., 2018). In all cases, the super black plumages described here reflect <2% of light and have a broadband, flat reflectance curve compared with normal black plumages.

In previous work, we analyzed unusual feather microstructures in male bird-of-paradise plumages, which profoundly diminish plumage reflectance through multiple scattering and iterative absorption (McCoy et al., 2018). Likewise, brush-like scales and cuticle microlens arrays in elaborate, brilliantly colored male peacock spiders diminish reflectance and enhance absorption (McCoy et al., 2019). Here, we find that sexual and social selection for profoundly black plumage appearance have resulted in the evolution of five qualitative classes of barbule morphologies: (1) curved arrays, (2) dihedral straps, (3) dense straps, (4) sparse straps and (5) brushy barbs (Figs 5 and 6). Each class of super black feather morphology evolved more than once in multiple avian families (Fig. 4). Quantitative measures of categories 1–4 show that super black feathers are darker if their barbules have cavities in which light is multiply scattered, that is, tightly packed strap-shaped barbules (Fig. 6). We hypothesize that super black evolved through sexual selection because it makes nearby colors (Fig. 1) appear

brighter, or even glowing, to observers (Kreezer, 1930; Brainard et al., 1993; Speigle and Brainard, 1996; see Discussion, Super black may enhance nearby color owing to sensory bias).

Microstructures enhance absorption through multiple scattering

Surface structure can collaborate with melanin pigmentation to produce structurally-assisted absorption; with each scattering event, some proportion of incident light is transmitted into the material where it will be absorbed by melanin pigments (Brown et al., 2002; Crouch et al., 2004; Vorobyev et al., 2009; Tao et al., 2012; Liu et al., 2014). Multiple scattering among three-dimensional microscopic surface features much greater in width than wavelengths of visible light thus enhances absorption (Tao et al., 2012). Eumelanin (the pigment molecule in many black bird feathers) has a broadband absorption spectrum (Riesz et al., 2006), with slightly lower absorption at higher wavelengths (Fig. 2). Multiple scattering enhances the absorption efficiency of eumelanin, contributing to lower reflectance and a flatter reflectance curve (Figs 2 and 3). Microscale rough surface features create a velvety, diffuse appearance devoid of specular reflections (Maurer et al., 2017).

Particular structural features of super black feathers minimize exposed horizontal surface area in the viewing direction of an observing individual, but have laminar surfaces oriented vertically to maximize multiple scattering (McCoy et al., 2018). Thus multiple scattering causes iterative melanin-based absorption. These barbule arrays are similar to arrays of razor blades (or other flat objects) that collect stray light ('beam dumps'; Cadj et al., 1987; Den Hartog

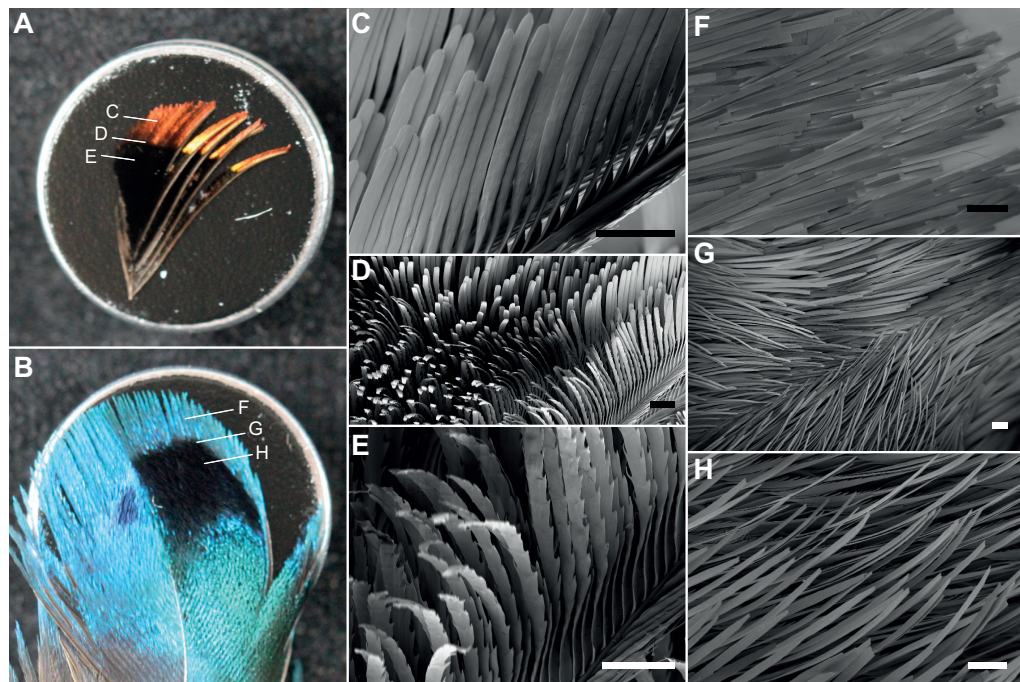


Fig. 8. Barbule morphology varies by color within single feathers in multiple species. Variation in barbule orientation within a single feather of (A,C–E) *Drepanornis bruijnii* (Paradisaeidae) and (B,F–H) *Lamprotornis splendidus* (Sturnidae). (A) *Drepanornis bruijnii* feather mounted on SEM stub. (B) *Lamprotornis splendidus* feather mounted on SEM stub. (C–E) SEM images of *D. bruijnii* corresponding to the letters in A, demonstrating the change in barbule shape and orientation from super black to structurally colored, copper regions. (F–H) SEM images of *L. splendidus* corresponding to the letters in B, demonstrating the change in barbule shape and orientation from super black to copper regions. Diameter of SEM stubs is 12.7 mm; all scale bars are 100 µm.

and Cekic, 1994). Here, quantitative measurements of feather microstructures and a phylogenetic PCA demonstrate that super black feathers separate from normal black feathers owing to (i) how strap-like, rather than cylindrical, the barbules are, and (ii) how tightly packed the barbules are (major components of PC1; Fig. 6A; Dataset S2). The laminar surfaces of strap-like barbules, when they are oriented perpendicularly to the plane of a bird's body, scatter light between the surfaces, causing iterative absorption by melanin. Indeed, PC1 is significantly correlated with reflectance (Fig. 6B,C), supporting this mechanistic conclusion about how super black feathers decrease reflectance through structural effects.

The feathers in the curved array, dihedral strap and dense strap classes enhance absorption through multiple scattering among the barbules of the same barbs (Fig. 7A–C). In contrast, feathers in the sparse strap and brushy barb categories appear to enhance light absorption through multiple scattering among the barbule and ramus surfaces of multiple feathers (Fig. 7D,E). In super black patches of *S. fischeri* and *O. derbianus*, each of these simple brushy feathers is very small, and sticks up vertically from the skin. Together, these arrays of brushy feathers appear to function like the curved arrays of barbules within individual barbs of birds-of-paradise, starlings and fairy-bluebirds (Fig. 7E). Further testing of the hypothesis of multiple scattering among feathers will require examining the 3D structure of microcavities within the intact plumages of the sparse strap and brushy barb type black patches.

The five morphological classes show significant variation in their absorption efficiency, with curved array class feathers having the lowest reflectance – particularly the appropriately named velvet satinbird, *C. loriae*, the Asian fairy-bluebird *I. puella* and the birds-of-paradise – followed by the simple brushy barbs of *S. fischeri* and *O. derbianus*, dihedral strap, dense strap, simple strap and the controls (Spearman's tie-corrected rank correlation, $P<0.0005$). Variations among the independently evolved morphological classes has produced corresponding variation in structural absorption efficiency (Fig. 6A–C). The micro-scale cavities in the curved array barbules are deeper than cavities formed by the other morphological categories, which may make for a more effective light trap.

As predicted by iterative absorption, the spectral shape of many super black reflectance curves resembles the shape of normal black reflectance curves divided by a factor of ~3–12. Intriguingly, the exceptions to this rule are primarily species with curved array barbules [some birds-of-paradise (Paradisaeidae), the fairy bluebird, *I. puella*, and the duck *N. auritus*], for which the reflectance curves are flatter than normal black reflectance curves of close relative even when divided by an appropriate proportionality factor. Curved array barbules are the most efficient microstructural enhancers of absorption reported here, and further research could focus specifically on microstructural correlates of broadband absorption. Detailed optical simulations would be useful to further explore structural absorption in birds.

Super black occurs near brilliant color in visual displays

All but one of these super black plumage patches are found adjacent to brightly colored plumage patches or fleshy ornaments (Fig. 1, Dataset 1; see discussion of the one exception, *M. alboscipulatus*, below). Super black can frame color, as in *L. superba* (Fig. 1J) and *I. puella* (Fig. 1M), but sometimes super black occurs as small patches inside a colorful scene, as in *S. spectabilis* (Fig. 1A) and *L. superbus* (Fig. 1L). Brilliantly colored peacock spiders also have super black patches within a colorful abdomen (McCoy et al., 2019). Small patches of super black inside colorful plumage look like black

holes – dimensionless, profound holes occurring on another plane than the colorful surroundings.

As in birds, the super black wing scales of *Papilio ulysses*, *Troides aeacus* and *Parides sesostris* (Papilionidae) are immediately adjacent to brilliant structurally colored blue, pigmentary yellow and structural green patches, respectively (Vukusic et al., 2004; Zhao et al., 2011b; Wilts et al., 2012). The super black structures of these butterflies may be aposematic signals that have evolved through the sensory biases of avian predators (or they may, too, operate in mate choice). In peacock spiders, the super black cuticle and scales of *Maratus speciosus* and *Maratus karrie* are adjacent to brilliant blue and red patches, and are prominently featured during extended mating displays (Otto and Hill, 2012, 2014).

Most of the normal black, control species lacked vivid color patches, but the few exceptions are instructive. For example, like most other subspecies, *Lepidothrix coronata coronata* has a vivid blue crown with normal black body plumage. But the Central American subspecies, *L. c. velutina*, combines super black body plumage with a similar blue crown (Fig. 1D). Thus, super black body plumage evolved uniquely in *L. c. velutina* after the origin of the vividly blue crown and normal black plumage in the common ancestor of *Lepidothrix coronata*, as the sensory bias hypothesis predicts. A parallel evolutionary pattern is also exhibited by the manakin *Masius chrysopterus pax* compared with other subspecies.

One bird has super black plumage without adjacent colorful patches: *M. alboscipulatus* has super black body plumage combined with white epaulets. However, we found that super black plumage is shared by, and primitive to, all *Malurus* species, and likely evolved in the most recent common ancestor of the genus in combination with brilliant structural blue coloration (Fig. 2). Thus, *M. alboscipulatus* – the brightest super black bird in our sample – has retained super black plumage despite having lost saturated blue feathers and evolved bright white patches.

Super black may enhance nearby color owing to sensory bias

We propose that super black is an optical illusion for color emphasis. Super black in visual display is found adjacent to bright colors (see Discussion, Super black occurs near brilliant color in visual displays). We hypothesize that, as in birds-of-paradise (McCoy et al., 2018) and brilliantly colored peacock spiders (McCoy et al., 2019), super black plumage patches enhance the perceived brilliance of adjacent patches of saturated colors owing to a sensory/cognitive bias intrinsic to color vision in variable light environments. Vertebrates use white, specular highlights across the visual scene to estimate, and control for, variation in ambient light intensity and spectral composition (Brainard et al., 1993). In this manner, the observer creates color perceptions that do not fluctuate freely with variation in ambient light conditions. Dark black surfaces eliminate the specular highlights that provide local information about the quantity of ambient light illuminating the visual scene. When a colored surface is reflecting more light than the observer estimates is ambient on it, then the surfaces may appear 'self-luminous' – i.e. as if emitting their own light – or appear to 'pop' out from the surface (Hering, 1879; Kreezer, 1930; Brainard et al., 1993; Speigle and Brainard, 1996). Super black will not make adjacent white surfaces appear brighter because white surfaces themselves provide visual information about the magnitude and quality of ambient illumination (Hering, 1879; Kreezer, 1930; Speigle and Brainard, 1996).

Evidence of the use of specular reflections for color correction has been found in goldfish and humans (Speigle and Brainard,

1996; Neumeyer et al., 2002; Bach and Poloschek, 2006). Thus, we hypothesize that this neural mechanism for color correction evolved in the most recent common ancestor of all bony vertebrates, and created an enduring, systemic sensory/cognitive bias that has influenced the evolution of ornamental sexual and social signals within birds. Sensory and cognitive biases have been proposed to influence signal perception owing to an observer's underlying sensory physiology or cognitive mechanisms (Ryan, 1990; Ryan and Rand, 1990; Endler and Basolo, 1998; Rosenthal and Evans, 1998; Basolo, 2002). Super black plumage adjacent to bright color appears to be an example of evolution by sensory bias. Recently, we have shown that some peacock spiders (*Maratus* sp.) have also evolved super black near brilliant color patches used in sexual displays (McCoy et al., 2019). Although mechanistically dissimilar from that of vertebrates (Zurek et al., 2015), color vision in peacock spiders may share the same color correction mechanism, leading to this sensory bias.

We do not yet have experimental confirmation of the effect of super black on mechanisms of color correction in birds. It is important to note, however, that the discovery of massively parallel evolution of super black plumage patches adjacent to brilliant, saturated colors that function in communication is, by itself, evidence of a sensory/cognitive bias in multiple independent lineages of birds. Further research is required to investigate this mechanistic basis behind this bias.

Acknowledgements

We thank the Yale Peabody Museum of Natural History, the American Museum of Natural History and the Harvard Museum of Comparative Zoology for research use of ornithological specimens. We are grateful to Kristof Zyskowski, Jeremiah Trimble, Kate Eldridge and Arthur McClelland for help selecting and imaging specimens. David Haig provided useful feedback.

Competing interests

The authors declare no competing or financial interests.

Author contributions

Conceptualization: D.E.M., R.O.P.; Methodology: D.E.M., R.O.P.; Software: D.E.M.; Validation: D.E.M., R.O.P.; Formal analysis: D.E.M.; Investigation: D.E.M.; Resources: D.E.M., R.O.P.; Data curation: D.E.M., R.O.P.; Writing - original draft: D.E.M., R.O.P.; Writing - review & editing: D.E.M., R.O.P.; Visualization: D.E.M., R.O.P.; Supervision: R.O.P.; Project administration: R.O.P.; Funding acquisition: D.E.M., R.O.P.

Funding

This work was performed in part at the Harvard University Center for Nanoscale Systems (CNS), a member of the National Nanotechnology Coordinated Infrastructure Network (NNCI), which is supported by the National Science Foundation under NSF ECCS award no. 1541959. D.E.M.'s research is conducted with Government support under and awarded by the Department of Defense, Army Research Office, National Defense Science and Engineering Graduate (NDSEG) Fellowship, 32 CFR 168a. D.E.M. is also supported by a Theodore H. Ashford Graduate Fellowship. The research was supported by the William Robertson Coe Fund of Yale University.

Supplementary information

Supplementary information available online at <http://jeb.biologists.org/lookup/doi/10.1242/jeb.208140.supplemental>

References

- Bach, M. and Poloschek, C. M. (2006). Optical illusions. *Adv. Clin. Neurosci. Rehabil.* **6**, 20-21.
- Basolo, A. L. (2002). Congruence between the sexes in preexisting receiver responses. *Behav. Ecol.* **13**, 832-837. doi:10.1093/beheco/13.6.832
- Brainard, D. H., Wandell, B. A. and Chichilnisky, E.-J. (1993). Color constancy: from physics to appearance. *Curr. Dir. Psychol. Sci.* **2**, 165-170. doi:10.1111/1467-8721.ep10769003
- Brown, R. J. C., Brewer, P. J. and Milton, M. J. T. (2002). The physical and chemical properties of electroless nickel-phosphorus alloys and low reflectance nickel-phosphorus black surfaces. *J. Mater. Chem.* **12**, 2749-2754. doi:10.1039/B204483H
- Cadj, F. M., Cheever, D. R., Klicker, K. A. and Stover, J. C. (1987). Comparison of scatter data from various beam dumps. In *Current Developments in Optical Engineering II* (ed. R. E. Fischer, W. J. Smith), pp. 21-25. International Society for Optics and Photonics.
- Crouch, C. H., Carey, J. E., Warrender, J. M., Aziz, M. J., Mazur, E. and Génin, F. Y. (2004). Comparison of structure and properties of femtosecond and nanosecond laser-structured silicon. *Appl. Phys. Lett.* **84**, 1850-1852. doi:10.1063/1.1667004
- Den Hartog, D. J. and Cekic, M. (1994). A simple, high-performance Thomson-scattering diagnostic for high-temperature plasma research. *Meas. Sci. Technol.* **5**, 1115. doi:10.1088/0957-0233/5/9/013
- Endler, J. A. and Basolo, A. L. (1998). Sensory ecology, receiver biases and sexual selection. *Trends Ecol. Evol.* **13**, 415-420. doi:10.1016/S0169-5347(98)01471-2
- Felsenstein, J. (1985). Phylogenies and the comparative method. *Am. Nat.* **125**, 1-15. doi:10.1086/284325
- Frith, D. W. and Frith, C. W. (1988). Courtship display and mating of the superb bird of paradise *Lophornis superbus*. *Emu* **88**, 183-188. doi:10.1071/MU9880183
- Grafen, A. (1989). The phylogenetic regression. *Philos. Trans. R. Soc. B* **326**, 119-157. doi:10.1098/rstb.1989.0106
- Harvey, T. A., Bostwick, K. S. and Marschner, S. (2013). Directional reflectance and milli-scale feather morphology of the African emerald cuckoo, *Chrysococcyx cupreus*. *J. R. Soc. Interface* **10**, 20130391. doi:10.1098/rsif.2013.0391
- Hering, E. (1879). Der Rauminn und Die Bewegungen Des Auges. *Handbuch der Physiologie* (ed. L. Hermann). Leipzig: FCW Vogel.
- Hill, G. E. and McGraw, K. J. (2006). *Bird Coloration: Function and Evolution*. Cambridge: Harvard University Press.
- Iskandar, J.-P., Eliason, C. M., Astrop, T., Igic, B., Maia, R. and Shawkey, M. D. (2016). Morphological basis of glossy red plumage colours. *Biol. J. Linn. Soc.* **119**, 477-487. doi:10.1111/bij.12810
- Jetz, W., Thomas, G. H., Joy, J. B., Hartmann, K. and Mooers, A. O. (2012). The global diversity of birds in space and time. *Nature* **491**, 444-448. doi:10.1038/nature11631
- Jetz, W., Thomas, G. H., Joy, J. B., Redding, D. W., Hartmann, K. and Mooers, A. O. (2014). Global distribution and conservation of evolutionary distinctness in birds. *Curr. Biol.* **24**, 919-930. doi:10.1016/j.cub.2014.03.011
- Kreezer, G. (1930). Luminous appearances. *J. Gen. Psychol.* **4**, 247-281. doi:10.1080/00221309.1930.9918313
- Liu, X., Coxon, P. R., Peters, M., Hoex, B., Cole, J. M. and Fray, D. J. (2014). Black silicon: fabrication methods, properties and solar energy applications. *Energy Environ. Sci.* **7**, 3223-3263. doi:10.1039/C4EE01152J
- Martins, E. P. and Hansen, T. F. (1997). Phylogenies and the comparative method: a general approach to incorporating phylogenetic information into the analysis of interspecific data. *Am. Nat.* **149**, 646-667. doi:10.1086/286013
- Maurer, D. L., Kohl, T. and Gebhardt, M. J. (2017). Cuticular microstructures turn specular black into matt black in a stick insect. *Arthropod. Struct. Dev.* **46**, 147-155. doi:10.1016/j.asd.2016.11.006
- McCoy, D. E., Feo, T., Harvey, T. A. and Prum, R. O. (2018). Structural absorption by barbule microstructures of super black bird of paradise feathers. *Nat. Commun.* **9**, 1-8. doi:10.1038/s41467-017-02088-w
- McCoy, D. E., McCoy, V. E., Mandsberg, N. K., Shneidman, A. V., Aizenberg, J., Prum, R. O. and Haig, D. (2019). Structurally assisted super black in colourful peacock spiders. *Proc. R. Soc. B* **286**, 20190589. doi:10.1098/rspb.2019.0589
- Meredith, P. and Sarna, T. (2006). The physical and chemical properties of emelanin. *Pigment Cell Res.* **19**, 572-594. doi:10.1111/j.1600-0749.2006.00345.x
- Neumeyer, C., Dör, S., Fritsch, J. and Kardelky, C. (2002). Colour constancy in goldfish and man: influence of surround size and lightness. *Perception* **31**, 171-188. doi:10.1088/p05sp
- Otto, J. C. and Hill, D. E. (2012). Notes on *Maratus* Karsch 1878 and related jumping spiders from Australia, with five new species (Araneae: Salticidae: Euophryinae). *Peckhamia* **103**, 1-81. doi:10.11646/zootaxa.4564.1.3
- Otto, J. C. and Hill, D. E. (2014). Spiders of the mungajah group from Western Australia (Araneae: Salticidae: Euophryinae: Maratus), with one new species from Cape Arid. *Peckhamia* **112**, 1-35. doi:10.18195/issn.0312-3162.29(2).2014.149-158
- Panagiotopoulos, N. T., Diamanti, E. K., Koutsokeras, L. E., Baikousi, M., Kordatos, E., Matikas, T. E., Gournis, D. and Patsalas, P. (2012). Nanocomposite catalysts producing durable, super-black carbon nanotube systems: applications in solar thermal harvesting. *ACS Nano* **6**, 10475-10485. doi:10.1021/nn304531k
- Prum, R. O. (2006). Anatomy, physics, and evolution of avian structural colors. In: *Bird Coloration. Vol. 1: Mechanisms and Measurements* (ed. G. E. Hill, K. J. McGraw), pp. 295-353. Harvard University Press.
- Prum, R. O. and Razafindrantsita, V. R. (1997). Lek behavior and natural history of the velvet asity (*Philepitta castanea*: Eurylaimidae). *Wilson Bull.* **109**, 371-392.
- Revell, L. J. (2009). Size-correction and principal components for interspecific comparative studies. *Evolution* **63**, 3258-3268. doi:10.1111/j.1558-5646.2009.00804.x
- Revell, L. J. (2012). phytols: an R package for phylogenetic comparative biology (and other things). *Methods Ecol. Evol.* **3**, 217-223. doi:10.1111/j.2041-210X.2011.00169.x

- Revell, L. J.** (2013). Two new graphical methods for mapping trait evolution on phylogenies. *Methods Ecol. Evol.* **4**, 754–759. doi:10.1111/2041-210X.12066
- Riesz, J., Gilmore, J. and Meredith, P.** (2006). Quantitative scattering of melanin solutions. *Biophys. J.* **90**, 4137–4144. doi:10.1529/biophysj.105.075713
- Rosenthal, G. G. and Evans, C. S.** (1998). Female preference for swords in *Xiphophorus helleri* reflects a bias for large apparent size. *Proc. Natl. Acad. Sci. USA* **95**, 4431–4436. doi:10.1073/pnas.95.8.4431
- Rubolini, D., Liker, A., Garamszegi, L. Z., Møller, A. P. and Saino, N.** (2015). Using the BirdTree.org website to obtain robust phylogenies for avian comparative studies: a primer. *Curr. Zool.* **61**, 959–965. doi:10.1093/czoolo/61.6.959
- Ryan, M. J.** (1990). Sexual selection, sensory systems and sensory exploitation. *Oxford Surv. Evol. Biol.* **7**, 157–195.
- Ryan, M. J. and Rand, A. S.** (1990). The sensory basis of sexual selection for complex calls in the túngara frog, *Physalaemus pustulosus* (sexual selection for sensory exploitation). *Evolution* **44**, 305–314. doi:10.1111/j.1558-5646.1990.tb05200.x
- Scholes, E.** (2008). Structure and composition of the courtship phenotype in the bird of paradise *Parotia lawesii* (Aves: Paradisaeidae). *Zoology* **111**, 260–278. doi:10.1016/j.zool.2007.07.012
- Scholes, E. and Laman, T. G.** (2018). Distinctive courtship phenotype of the Vogelkop superb bird-of-paradise, *Lophorina niedda* Mayr, 1930 confirms new species status. *PeerJ* **6**, e4621. doi:10.7717/peerj.4621
- Shawkey, M. D. and D'Alba, L.** (2017). Interactions between colour-producing mechanisms and their effects on the integumentary colour palette. *Philos. Trans. R. Soc. B* **372**, 20160536. doi:10.1098/rstb.2016.0536
- Speigle, J. M. and Brainard, D. H.** (1996). Luminosity thresholds: effects of test chromaticity and ambient illumination. *JOSA A* **13**, 436–451. doi:10.1364/JOSAA.13.000436
- Spinner, M., Kovalev, A., Gorb, S. N. and Westhoff, G.** (2013). Snake velvet black: hierarchical micro- and nanostructure enhances dark colouration in *Bitis rhinoceros*. *Sci. Rep.* **3**, 1846. doi:10.1038/srep01846
- Stavenga, D. G., Leertouwer, H. L., Marshall, N. J. and Osorio, D.** (2011). Dramatic colour changes in a bird of paradise caused by uniquely structured breast feather barbules. *Proc. R. Soc. B Biol. Sci.* **278**, 2098–2104. doi:10.1098/rspb.2010.2293
- Stavenga, D. G., Leertouwer, H. L., Osorio, D. C. and Wilts, B. D.** (2015). High refractive index of melanin in shiny occipital feathers of a bird of paradise. *Light Sci. Appl.* **4**, e243. doi:10.1038/lsci.2015.16
- Stoddard, M. C. and Prum, R. O.** (2011). How colorful are birds? Evolution of the avian plumage color gamut. *Behav. Ecol.* **22**, 1042–1052. doi:10.1093/beheco/arr088
- Tao, H., Lin, J., Hao, Z., Gao, X., Song, X., Sun, C. and Tan, X.** (2012). Formation of strong light-trapping nano- and microscale structures on a spherical metal surface by femtosecond laser filament. *Appl. Phys. Lett.* **100**, 201111. doi:10.1063/1.4719108
- Vorobyev, A. Y., Topkov, A. N., Gurin, O. V., Svirch, V. A. and Guo, C.** (2009). Enhanced absorption of metals over ultrabroad electromagnetic spectrum. *Appl. Phys. Lett.* **95**, 121106. doi:10.1063/1.3227668
- Vukusic, P., Sambles, J. R. and Lawrence, C. R.** (2004). Structurally assisted blackness in butterfly scales. *Proc. R. Soc. London. Ser. B Biol. Sci.* **271**, S237–S239. doi:10.1098/rsbl.2003.0150
- Wilts, B. D., Michielsen, K., De Raedt, H. and Stavenga, D. G.** (2012). Iridescence and spectral filtering of the gyroid-type photonic crystals in *Parides sesostris* wing scales. *Interface Focus* **2**, 681–687. doi:10.1098/rsfs.2011.0082
- Wilts, B. D., Michielsen, K., De Raedt, H. and Stavenga, D. G.** (2014). Sparkling feather reflections of a bird-of-paradise explained by finite-difference time-domain modeling. *Proc. Natl. Acad. Sci. USA* **111**, 4363–4368. doi:10.1073/pnas.1323611111
- Zhao, Q., Fan, T., Ding, J., Zhang, D., Guo, Q. and Kamada, M.** (2011a). Super black and ultrathin amorphous carbon film inspired by anti-reflection architecture in butterfly wing. *Carbon N. Y.* **49**, 877–883. doi:10.1016/j.carbon.2010.10.048
- Zhao, Q., Guo, X., Fan, T., Ding, J., Zhang, D. and Guo, Q.** (2011b). Art of blackness in butterfly wings as natural solar collector. *Soft Mat.* **7**, 11433–11439. doi:10.1039/c1sm06167d
- Zurek, D. B., Cronin, T. W., Taylor, L. A., Byrne, K., Sullivan, M. L. G. and Morehouse, N. I.** (2015). Spectral filtering enables trichromatic vision in colorful jumping spiders. *Curr. Biol.* **25**, R403–R404. doi:10.1016/j.cub.2015.03.033

Aristotle giveth the Cause, vainely, why the Feathers of Birds are of more lively Colours, than the Haires of Beasts. ... He saith, It is, because Birds are more in the Beames of the Sunne, than Beasts; But that is manifestly untrue; For Cattle are more in the Sun than Birds, that live commonly in the Woods, or in some Covert. The true Cause is, that the Excrementious Moisture of living Creatures, which maketh as well the Feathers in Birds, as the Haires in Beasts, passeth in Birds through a finer and more delicate Strainer, than it doth in Beastes: For Feathers passe through Quills; and Haire through Skin.

Francis Bacon, *Sylva sylvarum*



4

Microstructures Amplify Carotenoid Plumage Signals in Tanagers

REPRINTED FROM: McCoy, D.E., Shultz, A.J., Vidoudez, C., van der Heide, E., Dall, J., Trauger, S.A. and Haig, D., 2020. Microstructures amplify carotenoid plumage signals in colorful tanagers. *bioRxiv*, p.799783.

ARTICLE AND SUPPLEMENT AVAILABLE AT: : <https://doi.org/10.1101/799783>

Microstructures amplify carotenoid plumage signals in tanagers

1 **Authors:** Dakota E. McCoy^{1*}, Allison J. Shultz^{1,2,3,4}, Charles Vidoudez⁵, Emma van der Heide¹,
 2 Jacqueline E. Dall⁴, Sunia A. Trauger⁵, David Haig¹

3

1. Department of Organismic and Evolutionary Biology, Harvard University, 26 Oxford Street,
 Cambridge, MA 02138

2. Informatics Group, Harvard University, 38 Oxford Street, Cambridge, MA 02138

3. Museum of Comparative Zoology, Harvard University, 26 Oxford Street, Cambridge, MA 02138

4. Ornithology Department, Natural History Museum of Los Angeles County, 900 Exposition Blvd, Los
 Angeles, CA 90007

5. Harvard Center for Mass Spectrometry, Harvard University, 52 Oxford Street (B2), Cambridge, MA
 02138

* corresponding author: dakotamccoy@g.harvard.edu

4 **Abstract:**

5 Brilliantly-colored birds are a model system for research into evolution and sexual selection. Red, orange,
 6 and yellow carotenoid-colored plumages have been considered honest signals of condition; however, sex
 7 differences in feather pigments and microstructures are not well understood. Here, we show that
 8 microstructures, rather than carotenoid pigments, seem to be a major driver of male-female color
 9 differences in the social, sexually-dimorphic tanager genus *Ramphocelus*. We comprehensively quantified
 10 feather (i) color (using spectrophotometry), (ii) pigments (using liquid chromatography–mass spectrometry
 11 (LC-MS)), and (iii) microstructures (using scanning electron microscopy (SEM) and finite-difference time-
 12 domain (FDTD) optical modeling). Males have significantly more saturated color patches than females.
 13 However, our exploratory analysis of pigments suggested that males and females have concordant
 14 carotenoid pigment profiles across all species (MCMC glmm female:male ratio = 0.95). Male, but not
 15 female, feathers have elaborate microstructures which amplify color appearance. Oblong, expanded feather
 16 barbs in males enhance color saturation (for the same amount of pigment) by increasing the transmission
 17 of optical power through the feather. Dihedral barbules (vertically-angled, strap-shaped barbules) in males
 18 reduce total reflectance to generate “super black” and “velvet red” plumage. Melanin in females explains
 19 some, but not all, of the male-female plumage differences. Together, our results suggest that a widely cited
 20 index of honesty—carotenoid pigments—cannot fully explain male appearance. We propose that males are
 21 selected to evolve amplifiers of honest signals—in this case, microstructures that enhance appearance —
 22 that are not necessarily themselves linked to quality.

23

24 **Keywords:** sexual selection, honest signaling, Goodhart’s law, carotenoid pigments, microstructure,
 25 LCMS, FDTD

26

27 **Introduction**

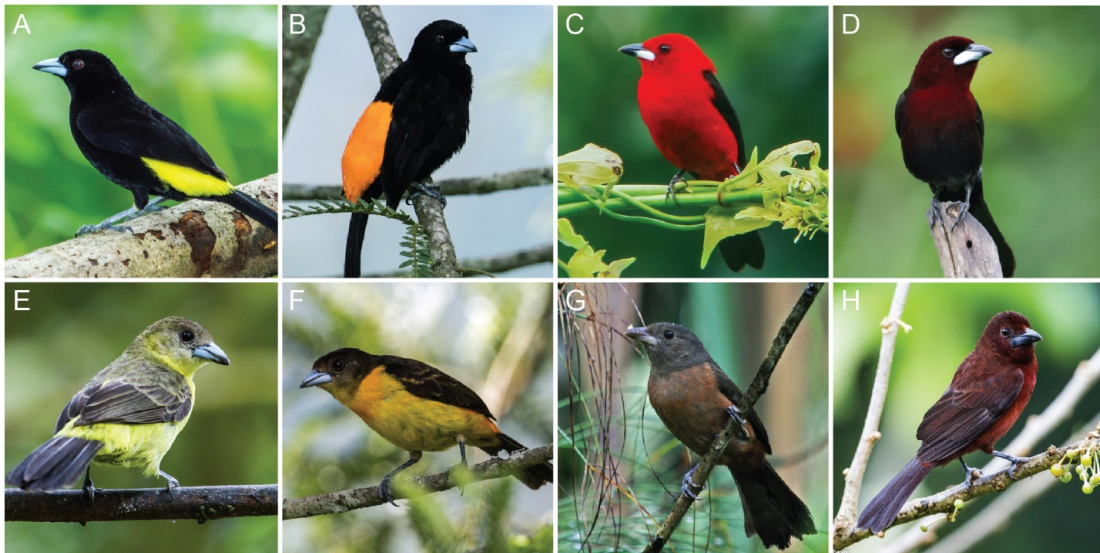
28 Why are so many birds colorful? To investigate this evolutionary “why,” we study both the physical
 29 mechanisms of color (pigments and structures) and the evolutionary mechanisms which favor colorful
 30 signals over time (selective forces). If we can fully understand the physical basis of traits, we may gain
 31 insights into their evolutionary history.

32 Three overlapping selective pressures shape the evolution of colorful mating displays. First,
 33 coloration may facilitate species identification, essential to avoid sterile hybrids and wasted mating efforts
 34 ¹. Second, colorful ornaments may reflect aesthetic preferences in the choosing sex ², perhaps shaped by a
 35 Fisherian runaway process ³ or by selection on another domain such as foraging—termed “sensory bias”⁴.
 36 Third, and most commonly researched, color may indicate individual quality (“honest signaling theory”),
 37 either as (i) an index of health ^{5–9} or (ii) as a costly signal (e.g., due to parasite load ¹⁰, general handicap ¹¹,
 38 or social costs ^{12–18}).

39 Honest signaling theory is the most prominent explanation for colorful bird plumages, and red,
 40 orange, and yellow carotenoid-colored birds are a “textbook example of an honest signal” ⁶. Carotenoids
 41 must be eaten by vertebrates rather than synthesized and may be scarce in nature. Carotenoids are correlated
 42 with some (but not all) individual quality measures ^{5,6,19}, and may be an index of proper metabolic function
 43 rather than a costly signal ²⁰ (see research on finches *Taeniopygia guttata* ⁷, crossbills *Loxia curvirostra* ⁸,
 44 and house finches *Haemorhous mexicanus* ²¹).

45 Carotenoid-colored birds are used widely to research sexual selection and honest signaling, but the
 46 full physical basis of color in males compared to females is not yet understood (i.e., pigmentary and
 47 structural differences). It is useful to note that nanostructures and pigments are generally well understood
 48 in bird coloration ²² but microstructures are less well studied. Several studies show that microstructures are
 49 important in bird color; microstructures (i) make carotenoid-based colors glossy or matte ²³, (ii) create green
 50 mirrors in the African Emerald Cuckoo *Chrysococcyx cupreus* ²⁴, (iii) enhance melanin to generate super
 51 black appearance in 15 families of birds ^{25,26}, and (iv) differ between male and female fairy wrens *Malurus*
 52 spp. ²⁷. Outside of birds, many organisms use microstructures to enhance the impact of pigments: flowers
 53 use conical epidermal cells to make richer petal colors ^{28–31} and microstructures contribute to super black
 54 color in peacock spiders ³², stick insects ³³, and snakes ³⁴. To what extent may microstructures, rather than
 55 pigments, explain color differences between carotenoid-colored male and female birds? The answer may
 56 help us determine which selective forces favor colorful ornaments.

57 Here, we explore the physical basis of carotenoid color in male versus female birds, and thus draw
 58 inferences about the evolutionary selective pressures which favor colorful signals. We focus on the social,
 59 sexually dimorphic *Ramphocelus* tanagers, a useful clade for questions of visual signaling ^{35,36} and mating
 60 behavior ^{37–39}. These tanagers have carotenoid-based coloration ranging from bright yellow to dark matte
 61 red in males, while females are relatively duller (Figure 1). Using scanning electron microscopy (SEM),
 62 finite-difference time-domain (FDTD) optical modeling, pigment extraction, liquid chromatography–mass
 63 spectrometry (LC-MS), spectrophotometry, and digital light microscopy, we document the physical and
 64 chemical basis of feather color in both males and females. From these exploratory analyses, we make
 65 inferences about the dynamics of mate choice over evolutionary time. We find preliminary evidence that
 66 microstructures enhance carotenoid-based signals in males.
 67



68

69 **Figure 1. Male *Ramphocelus* tanagers (top row) have more striking carotenoid-based coloration**
70 **than females (bottom row).** A. *R. flammigerus icteronotus* male with vivid yellow and deep black
71 plumage. B. *R. flammigerus icteronotus* female. C. *R. flammigerus* male with vivid orange and deep black
72 plumage. D. *R. flammigerus* female. E. *R. bresilius* male with bright red plumage. F. *R. bresilius* female.
73 G. *R. carbo* male with velvet red and deep black plumage. H. *R. carbo* female. All photos are credit Nick
74 Athanas - www.antpitta.com.

75

76 Material and Methods

77

78 Specimens

79 *Ramphocelus* tanager specimens were selected from the Ornithology Collection at the Harvard
80 Museum of Comparative Zoology (MCZ; specimen numbers are listed in Table S1). We selected N=20
81 total intact male and female specimens, one from each species in the genus *Ramphocelus* plus one
82 subspecies with visually divergent plumage that had full species status in the past⁴⁰: Crimson-collared
83 tanager, *Ramphocelus sanguinolentus*; Masked crimson tanager, *Ramphocelus nigrogularis*; Crimson-
84 backed tanager, *Ramphocelus dimidiatus*; Huallaga tanager, *Ramphocelus melanogaster*; Silver-beaked
85 tanager, *Ramphocelus carbo*; Brazilian tanager, *Ramphocelus bresilius*; Passerini's tanager, *Ramphocelus*
86 *passerinii*; Cherrie's tanager, *Ramphocelus costaricensis*; Flame-rumped tanager, *Ramphocelus*
87 *flammigerus*; Lemon-rumped tanager, *Ramphocelus flammigerus icteronotus*. Taxonomy is according to
88 the Clements Checklist v.2017⁴¹. We selected only one individual per species because we were primarily
89 focused on interspecific variation, but we confirmed the repeatability of pigment extractions using 3
90 individuals per species for two species (see below). Colorfastness of carotenoids varies tremendously
91 between bird species, with some species such as *Cardinalis* (Cardinalidae; closely related to the
92 *Ramphocelus* tanagers) retaining their color in darkness “almost indefinitely”⁴². To ensure that collection
93 methods, preparation, handling, and age of the specimen did not bias our results, we selected males and
94 females within a species from the same collecting trips (specimen details in Table S1; information about
95 specimens available from Harvard Museum of Comparative Zoology MCZBase). Age of the specimen had
96 no discernible effect on carotenoid presence.

97 We designate *R. flammigerus*, *R. f. icteronotus*, *R. passerinii*, and *R. costaricensis* to be the
98 “rumped” tanagers because they form a clade with vivid color restricted to the rump. We designate the

99 clade of tanagers with color on their whole body to be the “whole body” clade (*Ramphocelus nigrogularis*,
 100 *Ramphocelus dimidiatus*, *Ramphocelus melanogaster*, *Ramphocelus carbo*, *Ramphocelus bresilius*). *R.*
 101 *sanguinolentis* is the sister to all others.

102

103 **Spectrophotometry**

104 We performed spectrophotometry using an OceanOptics PX2 with a pulsed xenon light source, and
 105 OceanOptics USB4000, and an OceanOptics Spectralon White Standard. We used an integration time of
 106 100 ms, averaged 5 scans, and set a boxcar width of 5. We measured three replicates per plumage patch for
 107 each of N=20 individuals (male and female from 10 species). The replicates were averaged for plotting and
 108 for statistical comparisons (Figure 2). For each specimen, we measured the bird at 7 locations: crown, back,
 109 rump, dorsal tail, throat, breast, and belly. Using an OceanOptics reflectance probe holder, we measured
 110 reflectance for 90° incident light and for 45° incident light. These two angles of incidence allow us to
 111 determine the directionality and structural absorption potential of the plumage patches.

112 We wished to compare saturation of colorful regions and brightness of black regions between males
 113 and females. Brightness depends on total reflected light; therefore, we calculated brightness as the integral
 114 of the area under the reflectance curve between 300 and 700 nm divided by 400. Saturation depends on the
 115 steepness and narrowness of a color peak⁴³; therefore, we calculated an index of saturation by modifying
 116 typical full width at half maximum calculations⁴⁴. Specifically, we calculated the maximum reflectance,
 117 divided that value by two, and calculated the leftwards width of the reflectance curve between the maximum
 118 and half-maximum reflectance values. To compare darkness of black regions, we selected the body region
 119 of each male and female bird that was darkest (usually backs; see Figure 2). To compare saturation of
 120 colorful regions, we selected the body region of each male and female bird that had the highest reflectance
 121 (usually rumps; see Figure 2).

122

123 **Carotenoid Identification (Mass Spectrometry)**

124 We prepared feathers for pigment extraction using a simple mechanical procedure. First, we washed
 125 all feathers in hexane and allowed them to air dry. Next, we trimmed off the entirety of colored portions of
 126 barbs and barbules from three feathers. We carefully weighed them, then placed these barbules with 0.3
 127 mL methanol in a screw cap micro tube in the presence of 10 ceramic beads (2mm). We subjected these
 128 tubes to bead beating in a FastPrep FP120 for three cycles, each for 45 seconds at level 6.0. We centrifuged
 129 the resulting mixture in an Eppendorf centrifuge 5417R for 5 minutes at 3000 RCF, then transferred the
 130 supernatant (ensuring that no carotenoid-based color remained in the tube) and dried it under a stream of
 131 nitrogen. All samples were kept at -80 °C until analysis. The samples were resuspended in 100 µL of
 132 acetonitrile:methanol (1:1) and transferred to micro inserts in amber glass vials; immediately after
 133 resuspension, the samples were analyzed.

134 Initially, we took 9 feathers per species (three feathers from each of three specimens for two
 135 species) to ensure that we had enough material; for all additional species we took 3 feathers from a single
 136 patch on a single individual, which proved sufficient. In order to ensure that results were repeatable between
 137 individuals of a single species, we extracted pigments from two additional individuals for each of two
 138 species—*R. flammigerus* and *R. flammigerus icteronotus*. The pigment profiles were significantly
 139 correlated (Figure S3, Linear regression output for *R. flammigerus*: slope = 0.88, SE = 0.066, R² = 0.87, p
 140 < 0.0005. Linear regression output for *R. f. icteronotus*: slope = 0.96, SE = 0.054, R² = 0.92, p < 0.0005),
 141 indicating that our extraction and characterization procedure was repeatable across individuals of a species.
 142 See Statistics section for details. Excluding the repeated measures of *R. flammigerus* and *R. flammigerus*
 143 *icteronotus*, we extracted pigments from N=32 plumage regions in males and females, from 3 feathers per
 144 plumage region. To select which feathers to use for carotenoid extractions, we plotted all reflectance spectra
 145 for the following regions of each bird -- crown, back, rump, tail, throat, breast, stomach – and observed that
 146 rump was nearly always the most saturated region (complete data in Supplemental Data). To avoid
 147 confounding our dataset of structures and pigments with many different body regions, which may have
 148 differently shaped feathers, we thus selected rump feathers for pigment extraction from every bird where
 149 the rump was a saturated color (versus a brown or a black). For the dark-colored species *R. melanogaster*

150 and *R. carbo*, the rump was not a saturated color- therefore we selected the colorful patches of these birds,
 151 which were: male *R. melanogaster* throat and upper throat; female *R. melanogaster* throat and chest; male
 152 *R. carbo* breast; female *R. carbo* crown. In addition, we wanted to investigate variation in bright, specular
 153 red versus matte, dark red within single birds. We already had this contrast from *R. melanogaster* and thus
 154 also sampled rump and throat from *R. dimidiatus* male and female. Finally, we were curious about the
 155 females with both orange and yellow coloration, so in addition to rump, we sampled throat from *R.*
 156 *costaricensis* and breast from *R. flammigerus*.

157 We acquired pigment standards for 8-apo carotenal, Canthaxanthin, Astaxanthin (Sigma Aldrich),
 158 Lycopene (Santa Cruz Biotechnology), and Alloxanthin (ChromaDex). Carotenoid contents were analyzed
 159 using an Ultimate 3000 LC coupled with a Q-Exactive Plus hybrid quadrupole-orbitrap mass spectrometer
 160 (Thermo Fisher Scientific). The LC was fitted with a Kinetex C18 (2.6 μ m, 100 \AA , 150 mm x 2.1 mm,
 161 Phenomenex) column and the mobile phases used were MA: Acetonitrile:Methanol 85:15 and MB: 2-
 162 propanol. The gradient elution started with 4 min of 5% MB, then to 100% MB in 11 min, followed by 4
 163 min at 100% MB, 1 min to get back to 5% MA and 4 min re-equilibration at 5% MB. The flow was kept
 164 constant at 0.185 mL min⁻¹, and 10 μ L of samples were injected. Electrospray ionization was used in
 165 positive ion mode. The mass spectrometer was operated at 70,000 resolving power, scanning the m/z 150-
 166 1500 range, with data-dependent (top 5) MS/MS scan at 17500 resolution, 1 m/z isolation and fragmentation
 167 at stepped normalized collision energy 15, 35, and 55. The data were first manually analyzed to identify
 168 peaks of ions with accurate masses corresponding to potential carotenoids within a 5ppm mass accuracy
 169 threshold. The potential carotenoids included both known molecules, and those with a similar molecular
 170 formula based on their accurate mass and mass defect. MS/MS fragmentation spectra were then compared
 171 with the standards available or to MS/MS database entries within METLIN (-metlin.scripps.edu) to assign
 172 identity when standards were available or putative identity based on fragmentation pattern similarity.
 173 Lastly, peaks corresponding to carotenoids or carotenoids-candidates were integrated using Quan Browser
 174 (Xcalibur, Thermo Fisher Scientific). Pigments were grouped into “families”, based on their accurate mass
 175 and relation to standards and fragmentation similarities.

176 LCMS allowed us to precisely characterize which molecules comprised the plumage carotenoids
 177 across all species in the genus *Ramphocelus*, but it is important to note that this is an exploratory analysis.
 178 LCMS is useful to explore trends in sex differences across species, but the signal strengths of different
 179 carotenoid molecules cannot be directly compared. As one measure to control for this, we incorporated
 180 pigment family as a random effect in our statistical models (see below). Also, we focused on free
 181 carotenoids rather than considering carotenoid esters (see⁴⁵; see Limitations).

182 We assessed feathers for melanin presence using digital light microscopy and, following⁴⁶, by
 183 analyzing parameters of the reflectance curves (Supplementary Methods, Equation S1).

184 **SEM & Feather Microstructure**

185 In preparation for SEM, we mounted a single feather from each specimen (N=20 feathers) on a pin
 186 using a carbon adhesive tab. We sputter-coated the feathers with ~12 nm of Pt/Pd at a current of 40 mA.
 187 We performed scanning electron microscopy on an FESEM Ultra55.

188 Using ImageJ, we made multiple measurements on each SEM image, including maximum barb
 189 width, top-down barb width (barb width when viewing the feather from directly above), barbule width,
 190 inter-barbule distance, barb-barbule angle, and barbule length. We also coded feathers according to whether
 191 the barbules were strap shaped or cylindrical, and whether the barbules emerged from the plane of the
 192 feather (i.e., had “3-D” structure).

193 **Optical Modelling: Finite-Difference Time-Domain Simulations of (i) Angled Barbules and (ii) Oblong, 194 Expanded Barb**

195 To approximate the optical effect of the observed microstructures, we performed finite-difference
 196 time-domain (FDTD) simulations using the commercially available software Lumerical FDTD. FDTD is a
 197 versatile method for simulating the interaction of light with objects by computationally solving Maxwell’s
 198 equations. FDTD simulations calculate the spatio-temporal electromagnetic field distribution that results

when an initial pulse of light is launched onto, and interacts with, simulation objects within a bounded measurement domain—the “Yee cell” method⁴⁷.

For each simulation, our general setup was as follows. A plane wave of light (ranging from 400-700nm) was normally incident (y-direction) on an idealized feather cross-section in the x-y plane. We performed 2D simulations without incorporating pigment because (i) we wished to isolate the effect of structure in a simple, interpretable manner and (ii) the mathematical characterization of carotenoid absorption is not well understood when multiple pigments are mixed in a feather, as is the case here (but future work focusing on absorption spectra could use the Kramers-Kronig relationship to characterize the refractive indices of each pigment⁴⁸). The simulation domain was bounded at the horizontal edges of the y plane by perfectly matched layers (which are artificial absorbing layers) and at the vertical edges by periodic boundary conditions (which repeat the unit of our single-feather simulation at both edges to simulate a feather plumage composed of many side-by-side feathers). Frequency domain field monitors were placed above and below the structure to collect the reflected and transmitted light, respectively. We used a mesh size of $0.025 \times 0.025 \mu\text{m}^2$.

We conducted two sets of simulations for two apparently important microstructural features, as determined by the PCA described below: (i) angled barbules (hypothesized to decrease reflectance) and (ii) oblong and expanded barb (hypothesized to increase saturation).

(i) Angled Barbules. We hypothesized that angled barbules caused lower total reflectance. Therefore, for our optical models of angled barbules, we assessed total reflectance based on structure alone without considering the contribution of melanin. That is, we calculated the quantitative decrease in feather reflectance from angled barbule structure alone. To focus only on the impact of surface reflections and light’s path through the feather after surface diffraction, we extended the bottom feather surface to beyond the bottom vertical perfectly-matched layer boundary in the y-plane. This was a measure to eliminate reflections from the underside of the feather because in life, feathers are arranged in complex stacks in a plumage, which we did not simulate; feathers are flush with other feathers (i.e., the bottom of a feather would be a feather-feather interface, not a feather-air interface). For these simulations of angled barbules, we simulated a feather with hemispherical barb (radius $12.5 \mu\text{m}$) and barbules $80 \mu\text{m}$ long varying in angle from 0 to 80° . We present the average and standard deviation reflectance for 15 barbule angles (15 simulations).

(i) Oblong, Expanded Barb. We hypothesized that more oblong, expanded bars cause more saturated colors. We could not measure color saturation directly, because carotenoid absorption is not well characterized for the molecules of interest (but see XXX). Therefore, for this exploratory analysis we measured a proxy of color saturation: optical power transmission through the barb, a measure of how much light energy passes through an area. The greater the total optical power transmission through pigment (i.e., light passing through the pigment), the greater the light-pigment interactions. For example, when flowers use conical cells to focus light onto pigment, increasing the optical power transmission therethrough, the resulting color is more saturated²⁹. The barb is carotenoid-pigmented in *Ramphocelus* tanagers (Figure S5B-G) and other carotenoid-colored birds⁴², often with carotenoids scattered throughout the keratin substrate⁴⁹. Therefore by calculating increase in power transmission through the barb, we can approximate the structural enhancement of pigmentary color due to barb size and shape in males. For our simulations of the male-typical barb versus female-typical barb, we simulated an average female feather barb based on our measurements: $22.2 \mu\text{m}$ tall by $18.9 \mu\text{m}$ wide—and an average male feather barb: $39.8 \mu\text{m}$ by $27.7 \mu\text{m}$.

For the oblong, expanded barb simulations, we implemented four strategies test the robustness of our results. First, we measured optical power transmission through an entire feather, including the feather bottom (feather-air interface). Second, because in life feathers are packed into a plumage with no bottom feather-air interface, we simulated a feather truncated at its base, excluding structural effects of the feather bottom. Third, in life feathers often contain vacuoles, so we simulated male and female feathers with a $10\mu\text{m}$ -diameter circular air vacuole in the center. Fourth, for all simulations we calculated the total optical power transmission through four $7.5 \times 7.5 \mu\text{m}^2$ square regions of the barb: (i) center, (ii) side, offset $15 \mu\text{m}$ in the X direction, (iii) 45° angle, offset $10 \mu\text{m}$ in both X and Y directions, and (iv) top, offset $20 \mu\text{m}$ in the Y direction. We performed a one-way paired t-test, using the R function t.test (alternative = “less”), of our

252 11 total power transmission measurements to check whether males do indeed have higher power
 253 transmission than females (the total of 11 measurements comes from four measurements (barb center, side,
 254 top, 45° angle) for each of three simulations, minus the barb center for the vacuole simulation). We present
 255 total optical power transmission for all 11 measurements of male and female feathers, as well as results of
 256 the t-test, in Table S6, and in Figure 6 we plot power transmission for 700nm light (results were similar for
 257 other wavelengths of light) from one simulation (entire feather, no vacuole).

258

259 **Phylogeny**

260 Several recent studies have examined the phylogeny of *Ramphocelus* tanagers^{50–52}. Unfortunately
 261 Burns and Racicot (2009) and Burns et al. (2014) did not include *R. f. icteronotus*, and Hackett (1996) did
 262 not include *R. melanogaster* or *R. dimidiatus*, but the two studies combined had *cytochrome b* (cyt b)
 263 sequences available for all species. To construct a phylogeny, we downloaded cyt b sequences from
 264 NCBI for all *Ramphocelus* species, and six outgroups from the Tachyphoninae clade (*Tachyphonus*
 265 *coronatus*, *T. rufus*, *T. phoenicius*, *Eucometis penicillata*, *Lanio fulvus*, and *T. luctuosus*). NCBI accession
 266 numbers are available in Table S2. We aligned the sequences with MAFFT v. 7.313⁵³, and constructed
 267 the best-scoring maximum likelihood phylogeny with Raxml v. 8.2.10 using the GTRCAT model with
 268 100 bootstrap replicates^{54,55}. The resulting phylogeny confirmed the relationships found by previous
 269 studies, and so we extracted the monophyletic *Ramphocelus* clade for use in downstream analyses (Figure
 270 3).

271

272 **Statistics**

273 To compare saturation and feather brightness in males and females, we performed phylogenetically
 274 controlled two-sample t-tests in R, using `phyl.pairedttest` from package `phytools` v. 0.6-44^{56,57}. For these
 275 tests each of the three replicates per species and sex were averaged (Figure 2).

276

277 To assess the correlation between male and female carotenoid pigment profiles across species while
 278 controlling for the influence of phylogeny, we fit generalized linear mixed models using the `MCMCglmm`
 279 package in R⁵⁸. Such models can include phylogenetic effects and use Markov chain Monte Carlo sampling
 280^{59–61}. Phylogenetic effects and pigment family were included as random variables. It was necessary to
 281 include pigment family, because our carotenoid quantification method—LCMS—measures signal
 282 intensity, not amount, and different types of carotenoids cannot be directly compared. For the results
 283 reported herein, we specified the prior [`list(R = list(V = 1, nu = 0.002), G = list(G1 = list(V = 1, nu = 0.002),`
 284 `G1 = list(V = 1, nu = 0.002)))`]; we also ran models with medium and high belief priors to ensure that model
 285 outcomes were insensitive to prior parameterization. We used 1,000,000 iterations, a burn-in period of
 286 100,000, and a sampling interval of 500. We assessed graphical diagnoses of model performance (plotting
 287 `model_name$Sol` and `model_name$VCV`), ensured that levels of autocorrelation were below 0.1 using
 288 `autocorr(model_name$VCV)`, ensured that each model generated effective sample sizes of ~1000, and
 289 assessed phylogenetic signal by calculating `lambda`^{59–61}. Additionally, we ran two sensitivity models: (i)
 290 excluding the pigment apo-8-carotenal (found only in male *R. passerini*), and (ii) without the random effect
 291 of pigment family to check whether pigment family exerted a strong influence on model performance.
 292 Finally, because the isomers observed herein may not be relevant to phenotype, we ran all models again
 293 after summing all pigment isomer signals within a pigment family. To assess whether model outcome was
 294 sensitive to these decisions, we compared posterior means and Deviance Information Criteria, or DICs. As
 295 a further sensitivity test, and to investigate each pigment separately, we performed a phylogenetic paired t-
 296 test to check for differences between male and female pigment presence for each pigment family using the
 297 function `phyl.pairedttest` in package `phytools`⁵⁷.

298

299 To derive a quantitative estimate of the relationship between male and female carotenoid pigment
 300 profiles, we used the function `predict` in the `MCMCglmm` package in R⁵⁸, randomly subsampling our
 301 data frame of male pigment values to predict female pigment values 100 times. During each sub-sampling
 iteration, we summed the model-predicted female values and divided them by the real male values to
 generate an estimate of female:male pigment ratio. We subsampled 50 data points for two all-isomer models

302 and 20 data points for two summed-isomer models, and repeated each procedure 100 times, therefore
 303 producing 400 total estimates.

304 We performed principal component analyses (PCAs) on microstructure in males and females, using
 305 both standard and phylogenetic PCA methods in the software program R, version 3.4.3. We log transformed
 306 and centered all data. For standard PCAs we used function `prcomp` in R, both centering and scaling the data
 307 on feather microstructure (Table S3). PC1 and PC2 were extracted and used for visualizations; PC1 was
 308 used to assess correlations between males and females.

309 For phylogenetic PCAs of feather microstructure, we used function `phylo.pca` in the R package
 310 `phytools`⁵⁷, with a lambda method of correlation, and PCA mode “cov” (covariance).

311 To assess whether male feather microstructure was correlated with plumage saturation, we
 312 performed a phylogenetic generalized least squares model (PGLS;^{62,63}) using function `gls` from package
 313 `nlme`⁶⁴. Specifically, we tested whether saturation correlated with PC2, which captured barbule width and
 314 oblong-ness.

315 We tested for correlations between the proportions of carotenoids detected (carotenoid signal, as
 316 peak area) in two replicates each of two species, *R. flammigerus* and *R. f. icteronotus*. First, for each
 317 individual, we normalized the signal for each carotenoid to account for variation in overall amounts of
 318 carotenoid detected (versus proportion) by dividing the signal of each carotenoid by the sample weight and
 319 then by the maximum signal detected for that individual. We then tested for a correlation between the two
 320 individuals of each species separately with a linear model. We performed the same procedure to test for
 321 correlations between the upper and lower throat of male *R. melanogaster* and the throat and rump of male
 322 *R. dimidiatus*.

323 We also tested for correlations between male and female feather structure using the PCA scores,
 324 which captured a large proportion of the variance. For microstructure, we tested PC1 and PC2, and used
 325 phylogenetic generalized least squares (PGLS;^{62,63}) with a Brownian motion model to account for
 326 phylogeny. We could not use PGLS for multiple patches when measured, so we randomly selected one
 327 patch for each species. Analyses using the alternative patch were qualitatively similar, but not presented
 328 here. Results are robust to alternative phylogeny transformations (Brownian motion model, Ornstein-
 329 Uhlenbeck model). Note that these PC scores were taken from the non-phylogenetic microstructure PCA,
 330 and thus are directly comparable between males and females (both of which were included in the PCA).

331 Finally, we reconstructed the evolutionary history of carotenoid evolution for each pigment family
 332 for males and females. Because there might have been slight variations in isoform for different species, we
 333 decided to focus on carotenoid families as the most biologically meaningful variables. First, for each
 334 pigment family, we summed all isoforms for males and females, and log-transformed them (base 10). We
 335 removed any species that were missing data for both males and female for that family. We did the
 336 reconstruction with the `contMap` function in `phytools` v. 0.6-44^{56,57}, which uses maximum likelihood to
 337 estimate states at internal nodes and interpolate these states along internal branches⁶⁵.

338 **Results**

339

340 ***Male Ramphocelus tanagers have significantly more saturated colors and darker blacks than females.***

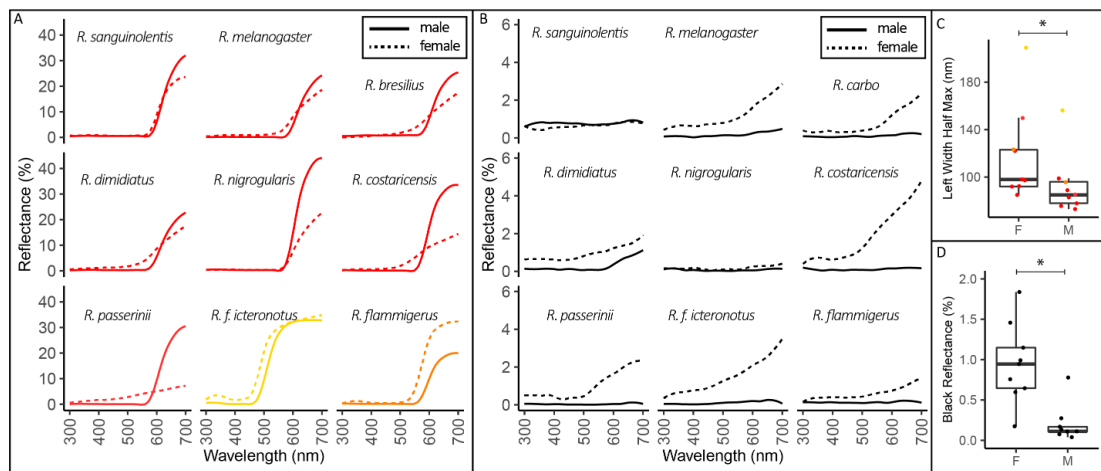
341 Spectrophotometry revealed a wide range of yellows, oranges, and reds in males and females,
 342 adjacent to blacks (Figure 2, complete results in Supplementary Data). Vivid, highly saturated color patches
 343 in males typically reflected almost no light for short wavelengths before sloping sharply upwards to reflect
 344 long wavelengths in the yellow-orange-red space (Figure 2A). In contrast, females of most species had
 345 colorful patches with a relatively more gradual upward slope, a greater-than-0 reflectance over a broad
 346 range of wavelengths, and a relatively lower peak reflectance (Figure 2A). Males from multiple species had
 347 extremely low-reflectance black plumage, with broadband flat reflectance below 0.5%, in areas adjacent to
 348 bright color patches (Figure 2B). Females had typical black plumage reflectances, with a slight increase in
 349 reflectance at higher wavelengths (Figure 2B).

350 Males had significantly more saturated color than females (phylogenetic two-sample paired t-test;
 351 p-value = 0.0072, 95% CI: [13.0, 38.1]) based on a measure of saturation, leftwards width at half maximum
 352 reflectance (Figure 2C). That is, they had narrower peaks. Males had significantly darker black regions than
 353 females (phylogenetic two-sample paired t-test; p-value = 0.0066, 95% CI: [0.38, 1.11]), where darkness
 354 was measured as total integrated reflectance under the curve (Figure 2D).

355 Many males also had unusual “velvet red” coloration, which we define as plumages red in hue that
 356 reflect < 5% of incident light and are matte (absent specular reflections, similarly to super black plumages;
 357 Supplementary Data) in a manner similar to the super black plumages in other species (Figure 2B). One
 358 species, *R. carbo*, has velvet red color on its whole body.

359 In general, many of the colored feathers were strong directional reflectors, such that reflected light
 360 differed in quantity (percent total reflectance) from 90° incident light to 45° incident light (Supplementary
 361 Data). For example, the velvet red patches on *R. carbo* increased their reflectance from ~0-1% to roughly
 362 5-7% when the angle of light incidence changed from 90° to 45°. This characteristic, reflecting more light
 363 at a lower angle of incidence, is a hallmark of feathers with microstructures that impact absorbance and
 364 reflection²⁵.

365



366

367 **Figure 2. Male Ramphocelus tanagers have significantly more saturated colors and darker blacks than females.**
 368 Spectrophotometry results for 90° incident light. **A:** Males (solid lines) have brighter and more saturated colors for all
 369 species except *R. flammigerus* and *R. f. icteronotus*. We included the body region of each male and female with the
 370 max reflectance, which was rump for all species except male *R. sanguinolentis* (crown), male *R. bresilius* (crown),
 371 female *R. bresilius* (stomach), female *R. dimidiatus* (stomach), female *R. costaricensis* (breast), and female *R.*
 372 *passerinii* (throat). We excluded *R. carbo* from this plot, because it is dark red rather than brilliant; N = 9. **B:** Males
 373 (solid lines) have a darker black color, with a flatter reflectance curves, on their backs compared to females (dashed
 374 lines) for all species except *R. sanguinolentis*. We measured the black back of each species except *R. dimidiatus*, for
 375 which we measured the black throat. We excluded *R. bresilius*, which is all red except for its tail and wings; N = 9.
 376 **C:** For a measure of saturation, leftwards width at half maximum reflectance, males had significantly more saturated
 377 color than females (phylogenetic two-sample paired t-test; p-value = 0.0072, 95% CI: [13.0, 38.1]). Narrower peaks
 378 (i.e., smaller value for left width at half maximum reflectance), indicate a more saturated color. **D:** For a measure of
 379 darkness, total integrated reflectance under the curve, males had significantly darker black regions than females
 380 (phylogenetic two-sample paired t-test; p-value = 0.0066, 95% CI: [0.38, 1.11]). Complete spectrophotometry results
 381 are in Supplemental Data 1. Integration time was 100 ms, and each line in the spectra (A-B) and point in the boxplots
 382 (C-D) represents the average of three replicates within the same plumage patch.

383 ***Across species, males and females have significantly correlated carotenoid profiles with a mean
384 female:male ratio of 0.95.***

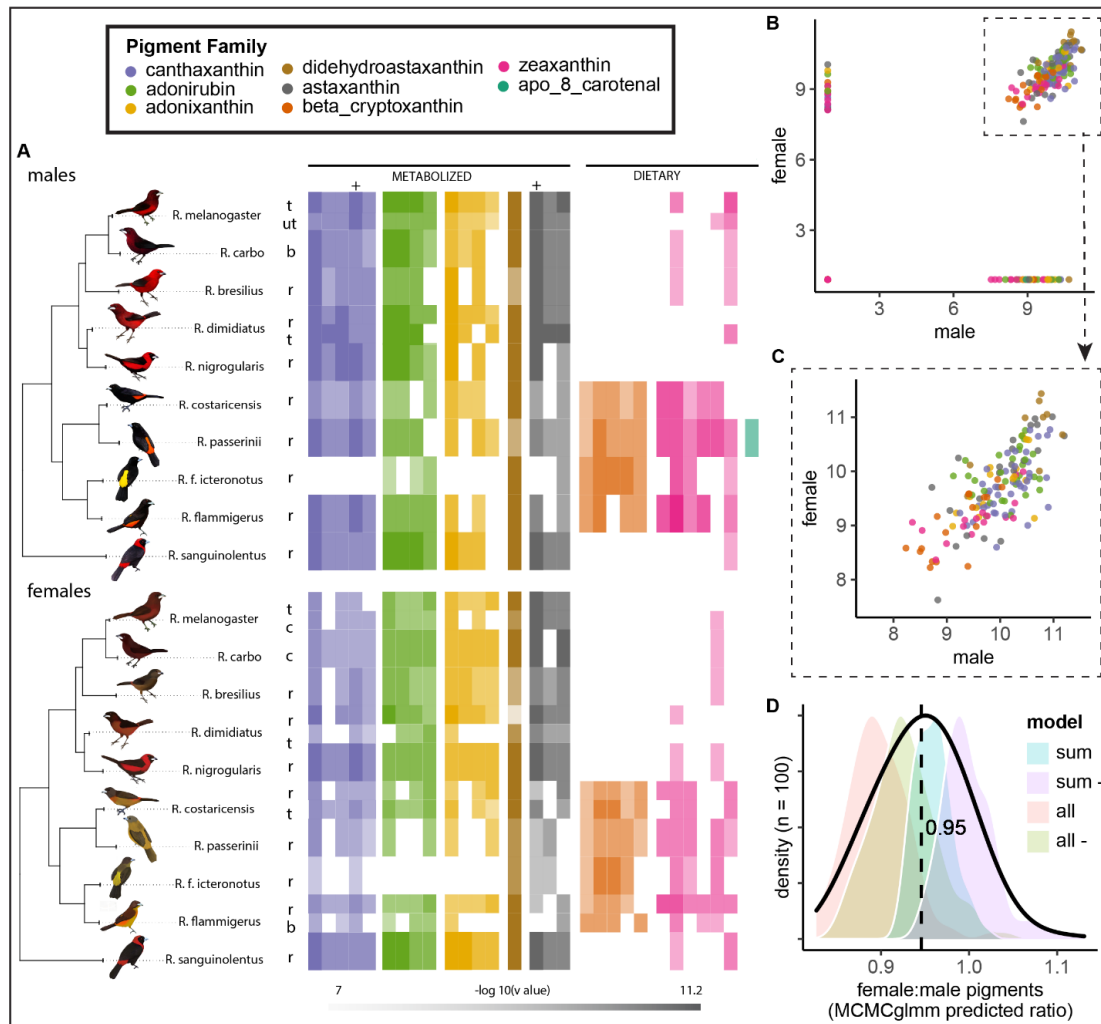
385 Through these exploratory analyses, we identified 29 distinct molecules that matched the
386 absorption spectra of carotenoids. These fell into 8 groups by monoisotopic molecular mass, with 1-6
387 different molecules in each pigment group, which we refer to as pigment families (Table S4). We mapped
388 the relative abundances of all described molecules onto a tree for both males and females (Figure 3A),
389 performed ancestral state reconstructions for each pigment family (Figure S1), and mapped all identified
390 pigments onto a metabolic network that shows how different molecules can be modified within the body
391 (Figure S2).

392 Five of the molecules matched our purchased pigment standards and could be conclusively
393 identified. For the remaining pigments, the molecule's identity was inferred based on accurate mass,
394 retention time, MS/MS spectra, and pigments commonly found in bird feathers as described in the literature.
395 For example, it is difficult to distinguish between the two dietary carotenoids lutein and zeaxanthin. Using
396 the metabolic networks presented in Morrison and Badyaev (2016) and LaFountain et al. (2015), we identify
397 the molecules with the accurate mass 568.43 as zeaxanthin because none of the common avian derivates
398 from lutein were found in any of our samples, while many derivates of zeaxanthin (and related metabolites)
399 were found. If some or all of the detected molecules with this mass were lutein, it would not change the
400 conclusions herein, because both are dietary pigments.

401 We found that dietary pigments zeaxanthin, β -cryptoxanthin, and apo-8-carotenal were found
402 primarily in the rumped tanager clade (Figure 3A, blue stars in Figure S2) while the whole-body tanagers
403 and *R. sanguinolentis* had primarily metabolized carotenoids. The “rumped” tanager clade had less
404 metabolized pigments than the “whole-body” clade and *R. sanguinolentis* (Figure 3A). This was affirmed
405 through ancestral state reconstructions (Figure S1). These mappings also showed qualitative concordance
406 between male and female pigment profiles within a species, and qualitative concordance between pigment
407 profiles of different regions within a bird (Figure 3).

408 To assess the relationship between male and female carotenoid pigments, we conducted exploratory
409 MCMCglmm analyses (but see Limitations). Female carotenoid pigment scores were correlated
410 significantly with male for MCMCglmm models including all pigment isomers (Figure 3A-C) and
411 including summed pigment signals within a family (Figure S4); (MCMCglmm model included pigment
412 family and phylogeny as random effects; main model: for fixed effect male pigment as a predictor of
413 female pigment, posterior mean = 0.55, 95% CI = [0.4434, 0.67], $N_{\text{effective}} = 1800$, $p < 0.001$, DIC =
414 1578.2; summed isomers model (Figure S4): posterior mean = 0.74, 95% CI = [0.52, 0.96], $N_{\text{effective}} =$
415 1800, $p < 0.001$, DIC = 377.9). Models were insensitive to prior parameterization, autocorrelation was
416 near <0.1 for all ⁵⁹, and model results also did not change when we excluded pigment family as a random
417 effect (suggesting pigment family is not exerting a strong influence). When we ran the model with
418 summed pigment isomers, the DIC was significantly lower (DIC=337.9 vs 1578.2), but those values
419 cannot be directly quantitatively compared. For both all-isomer and summed-isomer models, the DIC
420 improved significantly when we excluded apo-8-carotenal from the model, likely because this pigment
421 was present only in male *R. passerini*. Phylogenetic signal (calculated as lambda) was 0.039, suggesting
422 a very low influence of phylogenetic structure on the data. When we predicted female:male pigment ratios
423 using our top four models (Figure 3D), we found a mean value of 0.95. This suggests that male and
424 female pigment profiles are highly similar. The plots of the raw data (Figure 3A-C; Figure S4 for summed
425 data plots) qualitatively support our quantitative conclusions based on MCMCglmm models: male and
426 female tanagers have concordant pigment profiles. However, it is critical to note that we measured signal
427 intensity—not pigment amount, directly—and therefore these results should be treated as exploratory
428 findings across species (rather than precise findings within species).

429 As a simple sensitivity test, we performed a phylogenetic paired t test to investigate male versus
430 female values for each pigment separately; we found no significant differences between males and
431 females, supporting the results in the MCMCglmm.



432
433
434
435
436
437
438
439
440
441
442
443
444
445
446
447
448

Figure 3: Across species, males and females have significantly correlated carotenoid profiles with a mean female:male ratio of 0.95. **A.** Relative log-transformed presence of pigments across birds for males ($N_{\text{species}} = 10$, $N_{\text{patches}} = 12$) and females ($N_{\text{species}} = 10$, $N_{\text{patches}} = 14$). Color saturation indicates normalized signal strength of a given pigment molecule within a bird, where pale is least and rich is most. Relative intensity comparison can therefore only be made within each molecule (column). Some comparisons are possible within each family, because response factors of isomers are expected to be similar. Because standards were not available for all molecules, some molecules were identified based on accurate mass, retention time, MS/MS spectra, and the literature (see Table S4). **B-C.** Male versus female carotenoid pigments; each point represents the signal strength (a proxy for presence and amount) of a given pigment in both a male and female of one species. All values are log-transformed and normalized. Male and female pigment profiles are significantly correlated (MCMCglmm model including pigment family and phylogeny as random effects; for fixed effect male pigment as a predictor of female pigment, posterior mean = 0.55, 95% CI = [0.4434, 0.67], $N_{\text{effective}} = 1800$, $p < 0.001$, DIC = 1578.2; when pigments were summed by family (Figure S4, posterior mean = 0.74, 95% CI = [0.52, 0.96], $N_{\text{effective}} = 1800$, $p < 0.001$, DIC = 377.9). **C.** Zoom in on male versus female carotenoid pigments as shown in **B** but, for visualization, restricted to points where male and female values were both greater-than-0. **D.** MCMCglmm model predictions for the ratio between male and female pigment levels; mean ratio was 0.95. Models included were all (all isomers), all- (all isomers minus apo-

449 8-carotenal), sum (summed isomers within pigment families), and sum- (summed isomers within pigment families
 450 minus apo-8-carotenal). Abbreviations: t: throat; ut: upper throat; r: rump; b: breast; c: chest. Artwork in male
 451 silhouettes credit Gabriel Ugueto; female silhouettes are modified by Allison Shultz from original art by Gabriel
 452 Ugueto.

453

454 ***Some plumages incorporate melanin, particularly in females***

455 In some cases, male and female birds differed perceptibly in not only saturation but also brightness
 456 and hue, which (unlike most changes in saturation) could be explained by melanin⁶⁸. We found indirect
 457 evidence of melanin in regions from 8 females and 2 males (Figure S5A; by analyzing reflectance curves)
 458 and direct microscopy evidence of melanin in five of six colorful females and one of six colorful males
 459 (Figure S5B-G). Taken together, these exploratory results suggest that melanin pigments play a role in any
 460 unexplained differences in *brightness* or *hue* between male and female feathers.

461

462 ***Males, but not females, have diverse and elaborate feather microstructure***

463 Female *Ramphocelus* tanager feathers were mostly of standard microstructural appearance²⁶. That
 464 is, feather microstructure usually looks the same as feather macrostructure, with simple cylindrical barbules
 465 extending from the central cylindrical barb, all in a single plane (Figure 4A, Table 1, Table S3). The only
 466 female to exhibit broad variation was *R. sanguinolentis* (Table 1, Figure S8, Table S3). Female *R.*
 467 *sanguinolentis* in fact had microstructural characteristics more typical of male feathers: angled, strap-
 468 shaped barbules, and an oblong expanded barb.

469 In contrast, male *Ramphocelus* tanagers exhibited wide variation in feather microstructure (Figure
 470 4, Table 1, Table S3, Figure S8), including widely expanded barbs, oblong barbs, strap-shaped barbules
 471 (rather than cylindrical), and angled barbules that projected from the plane of the feather (Figure 4E, Table
 472 1). Among the angled barbules, we observed a dihedral morphology in super black and velvet red feathers
 473 as described previously for super black plumages of *R. flammigerus*²⁶. Two of these unusual male
 474 morphological traits, which we assess through optical simulations, deserve special mention (Figure 4):

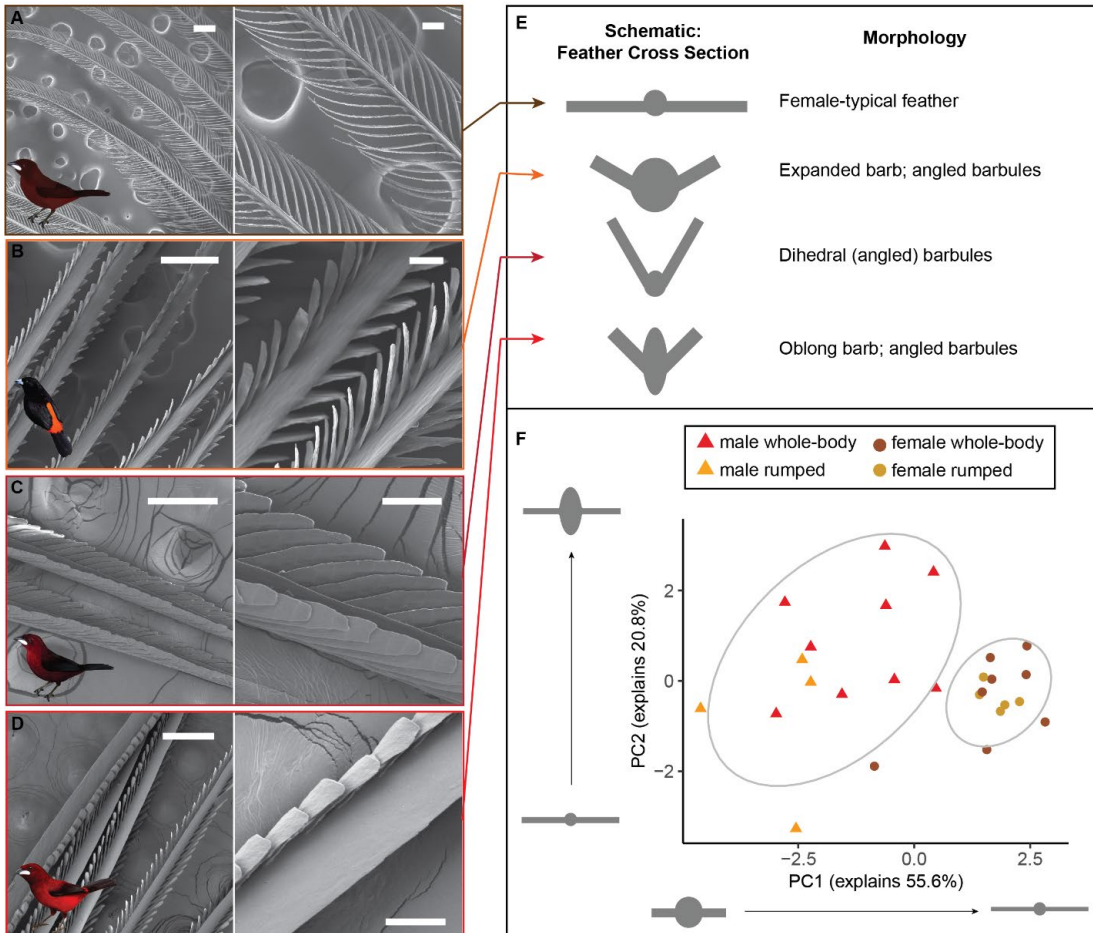
475 *Dihedral*. In the dark red crown of *R. carbo*, feathers have densely packed, strap-shaped barbules
 476 pointing upwards out of the plane of the feather to form a dihedral structure, while the central barb was
 477 shaped like a razor or narrow triangular prism (Figure 4C). *Ramphocelus dimidiatus* shared the dihedral
 478 morphology present in *R. carbo* in its upper throat feathers, which are a velvet red color (Figure S8). Both
 479 are reminiscent of the structurally absorbing “super black” feather morphology present in *Ramphocelus*
 480 *flammigerus* (McCoy and Prum 2019). Similar morphology, to a lesser degree, was observed in *R.*
 481 *melanogaster* velvet red throat feathers and in red feathers of both male and female *R. sanguinolentis*
 482 (Figure S8G,J). To the human eye, dihedral feather structure generates a velvety appearance.

483 *Expanded barb*. Multiple species had expanded barbs, including the broad and roughly cylindrical
 484 barbs of the rump feathers of *R. flammigerus* (e.g., Figure 4B,D, *R. nigrogularis*, and *R. passerinii*). These
 485 feathers also had flatter, strap-shaped barbules shorter in length than that of females but wider in width.
 486 Additionally, the rump and body feathers of *R. dimidiatus* are vivid red feathers with strong specular
 487 reflections; these feathers have a more extremely expanded central barb with a featureless surface (Figure
 488 4D). They also have upward-slanting, densely packed, strap-shaped barbules (Figure 4D). Together, this
 489 generates (to the human eye) strong specular reflection at an angle, so that the bird shows flashes of white
 490 reflection when rotated in the hand.

491 A PCA of feather microstructure measurements demonstrated that males and female cluster
 492 separately and are not correlated (Figure 4F; PC1 55.6%, PC2 20.8%; PGLS with microstructure PC1
 493 scores: coefficient = -0.023, SE = 0.17, p= 0.90); a phylogenetic PCA was not possible to compare males
 494 and females, because such analyses can consider only one value per species, but we performed sex-specific
 495 phylogenetic PCAs of one patch per species and observed some clustering by clade for males (whole-body
 496 versus rumped, Figure S6) and that females cluster tightly with the exception of outliers *R. sanguinolentis*
 497 and *R. bresilius*, both of which are females with wider-than-median barbs (Table 1). *R. sanguinolentis* is
 498 also the female with the most male-like scores in the regular PCA (Figure 4F). Barb width, barbule width,

499 barb oblongness, and interbarbule distance were primary axes along which males and females separated
 500 (Table S5). No species-specific or region-specific (e.g., rump feather versus chest feather) clustering was
 501 observed in these microstructural measurements (Figure S6). In particular, it was important that we
 502 observed no region-specific variation in microstructure (i.e., rump feathers from one species did not cluster
 503 with rump feathers from other species).

504



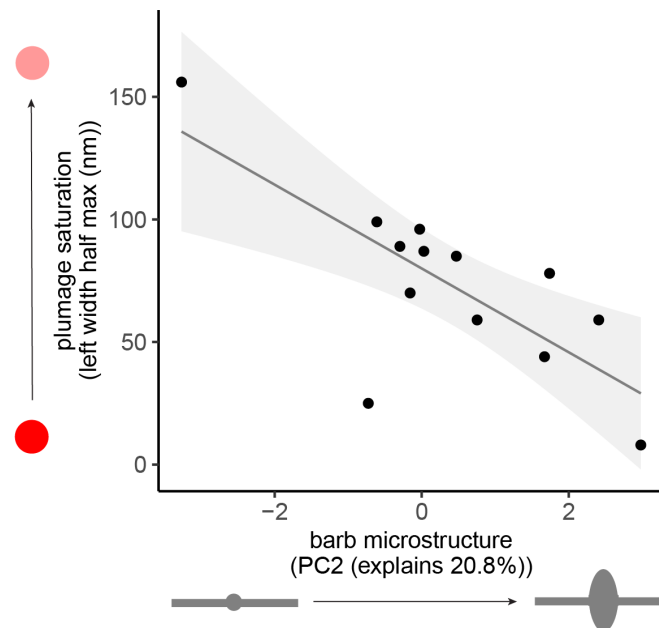
505
 506 **Figure 4: Males, but not females, have diverse and elaborate feather microstructure.** A. Female *R. carbo* red
 507 chest feather with typical simple morphology. B: Male *R. passerinii* bright orange rump feather with expanded barb
 508 and strap-shaped barbules. C. Male *R. carbo* velvet red back feather with dihedral barbules. D: Male *R. dimidiatus*
 509 shiny red rump feather with expanded, oblong barb and strap-shaped barbules. Scale bars in left column are 200 μm ;
 510 scale bars in right column (B, D, F, H) are 50 μm . Artwork in inset silhouettes credit Gabriel Ugueto. E. Schematic
 511 illustrations of idealized cross-sections of each feather type in A-D. F. PCA of log-transformed centered
 512 microstructural measurements for all patches from all males and all females, showing that males separate from
 513 females. Male and female microstructures are not correlated (PGLS with microstructure PC1 scores: coefficient = -
 514 0.023, SE = 0.17, p= 0.90). This PCA does not consider differences in three-dimensional structure, including dihedral
 515 barbule morphology; see Table 1.

516

517 **Male barb microstructure correlates significantly with plumage saturation**

518 To test whether microstructures may influence plumage appearance, we used a phylogenetic
 519 generalized least squares model to assess whether male microstructure PC scores (Figure 4) correlate with
 520 to plumage saturation (Figure 2). We found that PC2 was a significant correlate of plumage saturation,
 521 whereby more oblong and wider barbules were associated with more saturated plumage.

522
523



524
525
526
527
528
529

Figure 5: Male barb microstructure correlates significantly with plumage saturation. Wider, more oblong male barbs are correlated with more saturated plumage, as measured through left-width half-maximum of reflectance curve (see Figure 2). We performed a PGLS with microstructure PC2 and PC1 scores as independent variables, and with plumage saturation as dependent variable (PC2 coefficient = 20.8, SE 6.79, $p < 0.025$; PC1 coefficient = 12.6, SE=7.49; $p = 0.1361$).

530
531
532

Optical simulations suggest that male-typical microstructures can enhance (i) blackness and (ii) color saturation

533 Using 2D finite-difference time-domain (FDTD) simulations of idealized feather cross-sections,
 534 we isolated the effect of two male-typical structure on reflectance: dihedral barbules and expanded, oblong
 535 barb. We selected these two features because they were associated with (i) male-female differences in color
 536 appearance within a species and (ii) within-bird color changes from bright, saturated red to dark, matte
 537 velvet red (Figure S7).

538 We found that “dihedral” barbules²⁶, projecting out of the plane of the feather and associated with
 539 super blacks and velvet reds in our study species, contribute to a lower reflectance (Figure 6A). Total
 540 reflectance based on light-keratin interactions alone, without considering the contribution of melanin or
 541 carotenoids, drops from ~4% to 0.5% as barbules increase in angle from 0° to 80°. That is, the dihedral
 542 feather morphology in super black regions of these tanagers are made blacker in part due to structure.
 543 Likewise, the velvet red feathers in *R. carbo* and *R. dimidiatus* are made darker and more matte by melanin
 544 pigments in combination with dihedral barbule microstructure.

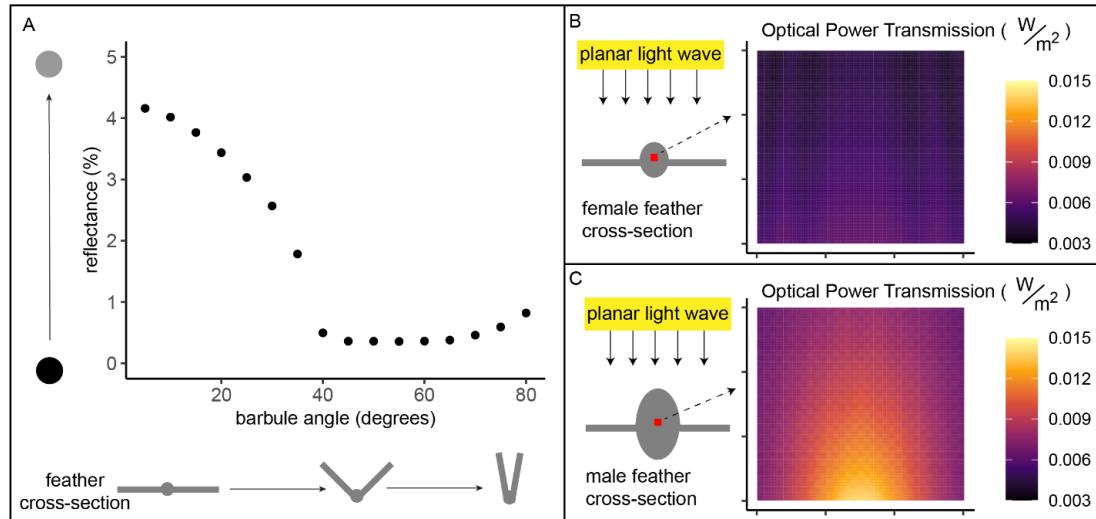
545 Further, we found that male-typical expanded feather barbs, which are wider than female barbs in
 546 80% of species and more oblong than female barbs in 60% of our species (Table 1), substantially enhance

optical power flow through the pigmented portion of the feather (Figure 6B-C). In other words, this male-typical barb shape focuses light to cause greater light-pigment interactions, even though females and males across species have the same amount and types of pigment (Figure 3). Therefore, the structure may contribute to a richer, more saturated color in the same manner as flower petals' conical epidermal cells²⁸. Interestingly, oblong and wide male barbs focus light more in particular regions within the feather barb (although they also increase optical power transmission generally across the whole barb, akin to flower petals²⁹). Because the male-typical feathers focus light more on particular regions, it may be the case that pigments are not distributed evenly within the feather barb; further work with cross-sectional data is needed to investigate this idea.

We predicted that the ~30-45° angled barbules of many males, paired with an expanded barb, would further enhance color saturation, akin to angled flower petals causing a more saturated color⁶⁹; simulations showed that the angled barbs contributed negligibly compared to the very large effect of an expanded barb. Across all sensitivity simulations (whole-feather, truncated feather, and feather with vacuole) and locations within the feather barb (side, top, and 45° angle) males had greater optical power transmission (Table S6; one-way paired t-test, $p = 0.0021$, mean of difference = -125.9, 95% CI = [-Inf, -64.2]).

It is important to note that these simulations represent idealized feather cross-sections, not real cross-sectional data. Our simulations provide proof-of-concept that expanded, oblong barbs in males focus light differently than simple barbs in females, enhancing color saturation; our simulation results are further buttressed by the observation that microstructural measurements are significantly correlated with color saturation (Figure 5). However, further work to identify the specific locations of pigment, vacuoles, and internal nanostructures is needed to fully characterize these feathers.

568



569

570

Figure 6: Optical simulations show that male-typical microstructures can (i) enhance blackness and (ii) increase color saturation. All simulations are finite-difference time-domain (FDTD) simulations on 2D idealized feather cross-sections, simulating structural effects only without accounting for pigmentary absorption. **A:** A male-typical black feather, with angled barbules, has structurally enhanced blackness compared to a female-typical feather with flat barbules. As the barbule angle increases out of the plane of the feather, percent reflectance arising from the keratin structure alone decreases from 4% to 0.5%. We did not simulate absorption effects of melanin, but instead we isolated the effect of structure alone. **B:** For a female-typical colored feather, the amount of light passing through the pigmented barb (optical power transmission through red square) totals 452.4 W/m². **C:** For a male-typical colored feather, an oblong, expanded central barb increases the amount of light passing through the pigmented barb (optical power transmission through red square; totaling 788.1 W/m²). This enhanced power transmission enhances

581 pigmentary activity for the same amount of incident light. For A, each dot is the average of 3 simulations (and an
 582 error bar is plotted although not visible because all standard deviations were < 0.035). For B-C, optical power
 583 transmission is shown for 700nm light, at the center of a barb, and for a single simulation, but males have greater
 584 optical power transmission than females over all wavelengths, four different locations within the feather barb, and
 585 three simulation types (see methods; Table S6; one-way paired t-test, p = 0.0021, mean of difference = -125.9, 95%
 586 CI = [-Inf, -64.2]).

587

588

589 ***Spectral curve-fitting suggests that male-female color differences result from both (i) melanin in***
 590 ***females and (ii) microstructures in males***

591 We used curve-fitting as a preliminary test of whether (i) melanin in females and/or (ii) the
 592 optical impacts of male microstructures, as identified by our FDTD simulations (Figure 6), could explain
 593 male-female color differences (details in Supplemental Methods).

594 We found that both melanin and microstructures were required to explain male-female
 595 differences in colorful red and orange plumage (Figure 7A-C). For both *R. dimidiatus* and *R. bresilius*,
 596 curve simulating “female minus melanin plus expanded barb” matched well with the observed reflectance
 597 spectra of male rumps (Hausdorff distances for male versus simulated female-melanin+structure were 0.7
 598 (*R. bresilius*; compared to 7.5 before manipulation) and 1.9 (*R. dimidiatus*; compared to 10.8 before
 599 manipulation). However, for *R. passerinii*, the simulated curve (dashed black line Figure 7C) was a poor
 600 match.

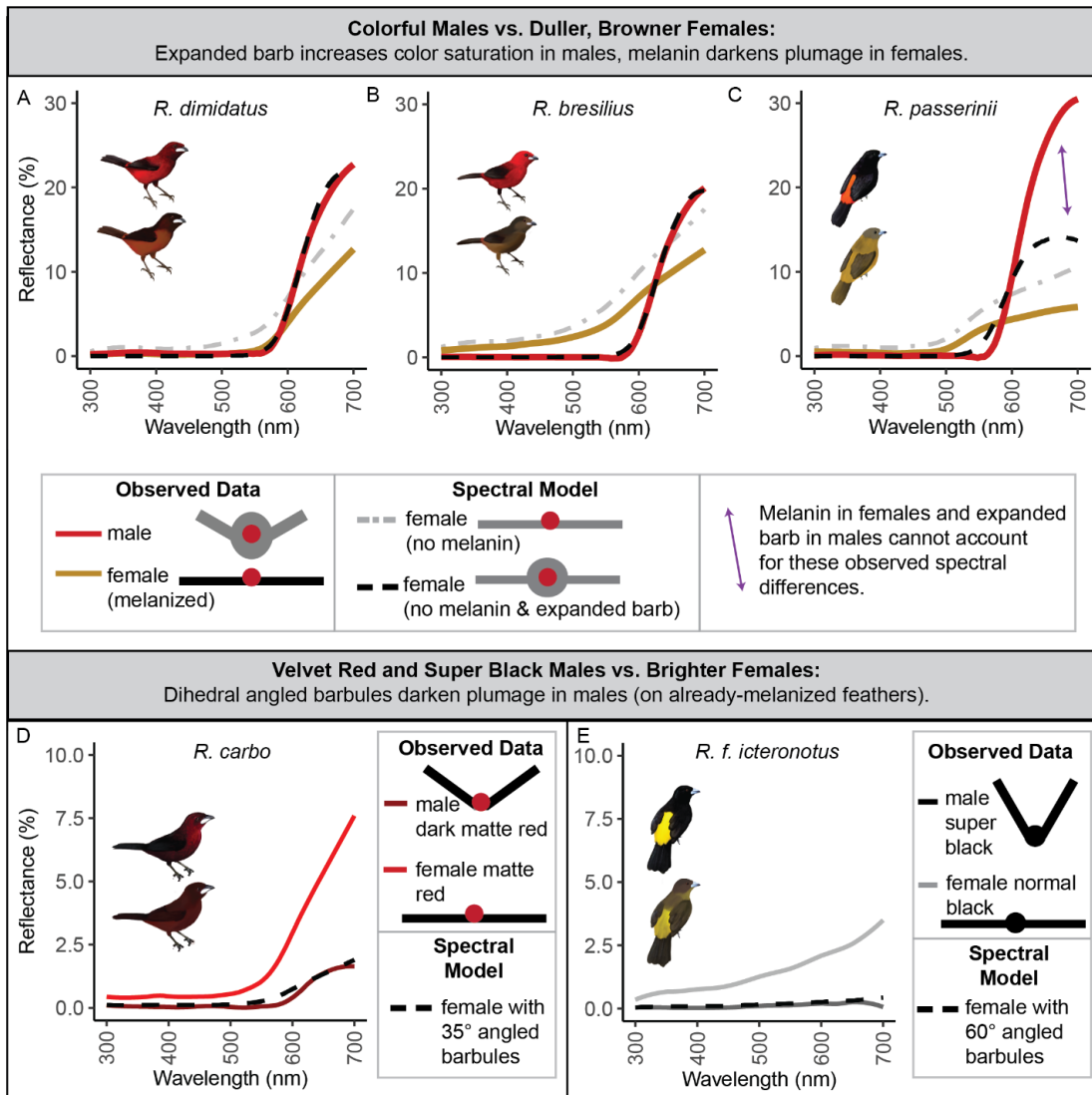
601 We found that microstructure alone—angled barbules—was sufficient to explain differences
 602 between (i) velvet red male, and brighter red female, plumages and (ii) super black male and normal black
 603 female plumages (Figure 7D). For velvet red male *R. carbo* plumage, the corresponding female
 604 reflectance spectra divided by 4 matches closely to the male (Hausdorff distance 0.4), corresponding to
 605 barbules at an angle of ~35° (Figure 6A). Likewise, for super black male *R. f. icteronotus*, female
 606 plumage divided by 8 matches well to the super black male (Hausdorff distance 0.05), which corresponds
 607 to barbules at an angle of ~60° (Figure 6A).

608

609 ***Velvet red (versus bright red) within a bird arises from microstructure and melanin, not change in***
 610 ***carotenoids.***

611 To better assess the relative contribution of microstructure and pigment, we compared within-bird
 612 pigment profiles of shiny saturated red patches versus dark velvet red patches for both *R. melanogaster* and
 613 *R. dimidiatus* (Figure S7). For each bird, these two patches had significantly correlated pigment profiles at
 614 equal levels for *R. melanogaster* and with slightly more pigment in the bright red region for *R. dimidiatus*
 615 (Figure S7A,E; Regression output for *R. melanogaster*: slope = 0.99, SE = 0.051, R² = 0.93, p < 0.0005.
 616 Regression output for *R. dimidiatus*: slope = 0.76, SE = 0.061, R² = 0.85, p < 0.0005.) However, the SEM
 617 photos revealed large differences in feather microstructure between dark and bright patches (Figure
 618 S7B,C,F,G). Expanded barbs were associated with bright saturated color while vertically-angled or dihedral
 619 barbules were associated with velvet red color. Importantly, digital light microscopy showed melanized
 620 barbules in the velvet red feathers of *R. dimidiatus*, suggesting that melanin is present in velvet red
 621 plumages.

622



623

624

625
626
627
628
629
630
631
632
633
634
635
636
637

Figure 7: Curve-fitting with reflectance spectra suggests that male-female color differences are attributable to (i) melanin in females and (ii) microstructures in males. We manipulated real reflectance spectra of females to assess the role of melanin and microstructures in male-female differences (Supplementary Methods). We compared A-C colorful, saturated males to duller, browner female and D-E velvet red and super black males to relatively brighter females. **A.** Reflectance spectra of a female *R. dimidiatus* rump (orange line), minus the effect of melanin (grey dashed line), and plus the predicted saturation increase due to an oblong expanded barb (dashed black line) matches well with observed reflectance spectra of a male *R. dimidiatus* rump (red line). Sigmoid curve parameters are $a_{\text{female}}=0.02$, $a_{\text{male}} = 0.06$, $b = 620$, $c = 22$. **B.** Reflectance spectra of a female *R. bresilius* rump (orange line), minus the effect of melanin (grey dashed line), and plus the predicted saturation increase due to an expanded barb (dashed black line) matches well with observed reflectance spectra of a male *R. bresilius* rump (red line). Parameters are $a_{\text{female}}=0.02$, $a_{\text{male}} = 0.06$, $b = 630$, $c = 20$. **C.** Reflectance spectra of a female *R. passerinii* rump (orange line), minus the effect of melanin (grey dashed line), and plus the predicted saturation increase of an expanded barb (dashed black line), is a poor match (purple arrow) for the observed reflectance spectra of a male *R. passerinii* rump

638 (red line). Parameters are $a_{\text{female}}=0.02$, $a_{\text{male}} = 0.06$, $b = 590$, $c = 14$. **D.** Reflectance spectra of female *R. carbo* dark
 639 red breast (red line), divided by 4 to indicate structural contribution of dihedral barbules at a $\sim 35^\circ$ angle (dashed
 640 black line), matches well to observed reflectance spectra of *R. carbo* dark matte red breast (dark red line). **E.**
 641 Reflectance spectra of female *R. f. icteronotus* black back (grey line), divided by 8 to indicate structural contribution
 642 of dihedral barbules at a $\sim 60^\circ$ angle (dashed black line), matches well to observed reflectance spectra of male *R. f.*
 643 *icteronotus* super black back (black line). Divisors for each barbule angle can be found in Figure 6A. Artwork in
 644 male silhouettes credit Gabriel Ugueto; female silhouettes are modified by Allison Shultz from original art by
 645 Gabriel Ugueto. For information about melanin presence, see Supplementary Information.
 646

647 Discussion

648

649 *Summary*

650 Why are so many birds colorful? Our study directly addressed a proximate, physical “why” by
 651 showing that microstructures significantly enhance the red, orange, and yellow colors in male carotenoid
 652 plumages. Across species, colorful male and significantly drabber female *Ramphocelus* (Figures 1-2) have
 653 significantly correlated carotenoid pigment profiles at a female:male ratio of 0.95 (Figure 3). However,
 654 unusual microstructures in male (but not female) feathers augment male appearance in two ways (Figures
 655 4-7). First, wider, more oblong barbs in males create a more vivid, saturated color from structure alone
 656 without requiring more pigment. Second, dihedral barbules in male feathers produce (i) “velvet red”
 657 feathers adjacent to brilliantly reflective beaks and (ii) “super black” near colorful patches. We observe that
 658 structures contribute significantly to color signal appearance in males, rather than pigment alone.

659 But why are so many birds colorful? A deeper evolutionary “why” asks for the history of selective
 660 forces that produce colorful patterns and ornaments. Carotenoid-based coloration has often been invoked
 661 as a “textbook”⁶ or “classic”⁷⁰ example of honest signaling, thought to be costly or indicative of metabolic
 662 function^{6-8,20,71}. We propose that carotenoid coloration may have originated as an honest indicator, but
 663 males have been selected to amplify their appearance by microstructural enhancers that are not themselves
 664 necessarily linked to quality. We do not suggest that signals have no indicator value, but rather that diverse
 665 microstructures in males suggest an evolutionary arms race between female preference and male appearance
 666⁷². We discuss this “proxy treadmill” interpretation, and other possibilities, below.

667

668 *Pigments: males and females have concordant carotenoids*

669 Unexpectedly, males and females across species had significantly correlated carotenoid profiles in
 670 feathers with a female:male ratio of 0.95 (Figure 3; MCMC glmm). Because our LCMS method does not
 671 allow direct comparisons between different pigments, we confirmed that male and female pigments do not
 672 differ significantly using a within-pigment-family phylogenetic paired t-test. These results are exploratory,
 673 across-species, findings (rather than precise within-species quantifications). See further discussion in
 674 Limitations section below.

675 If carotenoids were present in feathers as an honest (because costly) signal, it would be surprising
 676 to see the same levels in females (the choosing sex) as in males (the displaying sex). It is difficult to argue
 677 that the presence of carotenoids in feathers is costly, is favored in males because it is costly, but females
 678 who gain no benefit therefrom have been unable to exclude carotenoids from their feathers (and indeed
 679 deposit melanin to dampen the color; Figure S4). However, it is still possible that carotenoids are an index
 680 of metabolic function or that sexual selection is acting on both males and females.

681 It is worth dedicating a few sentences to the significance of dietary versus metabolized carotenoids.
 682 Carotenoids are consumed in a yellow (dietary) form and then metabolized within vertebrate bodies to
 683 become redder in color; red, not yellow, carotenoids seem to drive correlations between male appearance
 684 and health⁶. Oddly, it appears that *R. f. icteronotus* and *R. flammigerus* evolved to use dietary carotenoids
 685 (yellow & orange) from a likely ancestral state of metabolized (red) carotenoids (Figure 3, Figure S1;⁵¹).
 686 Yellow-to-red transitions, but not red-to-yellow, are common in model clades (fringillid finches⁷³; new
 687 world blackbirds⁷⁴). The possible reversion from red to yellow and orange documented herein is rare and

688 worth further study; perhaps *Ramphocelus* males were not selected to display metabolically indicative or
 689 costly traits. In a hybrid zone, Morales-Rozo and colleagues demonstrate that the yellow *R. f. icteronotus*
 690 outcompetes the orange *R. flammigerus* in areas where both male phenotypes occur (i.e., where females
 691 have a choice; ⁷⁵). Perhaps females prefer a less-elaborate, less-costly trait—as predicted by Hill (1994)
 692 for an arbitrary rather than honest signal. Further research should be done on the behavioural ecology of
 693 these fascinating tanagers to clarify female preferences and social interactions.
 694

695 **Structures: microstructures amplify plumage appearance in males**

696 Feathers in *Ramphocelus* males, but not females, vary remarkably in microscopic structure (Table
 697 1, Figure 4, Figure S8). Taken together, our data (Figure 5), optical simulations (Figure 6, Figure XXX),
 698 and post-hoc curve fitting (Figure 7) suggest that microstructures cause males to have more saturated colors
 699 than females, darker blacks than females, and—in some species—striking velvet red coloration.

700 Oblong, expanded barbs in males increase the optical power transmitted through the pigmented
 701 barb (Figure 6B-C): more light interacts with the same amount of pigment to generate a more saturated,
 702 vivid color (Figures 1-2). This is analogous to conical epidermal cells in flower petals, which enhance light
 703 transmission through the whole petal but enhance it to a greater degree in the pigmented region ²⁹. Further
 704 cross-sectional studies of feather pigment location—and potentially impactful nanostructures (XXX)—
 705 would be invaluable.

706 Upward-angled barbs in a dihedral arrangement reduce total reflectance from a plumage (Figure
 707 6A) to make super black color (if paired with melanin) or velvet red color (if paired with carotenoids; see
 708 *R. carbo* Figure 1D with velvet red adjacent to a brilliant silver beak). Super black color is an optical
 709 illusion which enhances the perceived brilliance of adjacent colors ^{25,26,32,76–78}, thereby potentially
 710 amplifying male appearance. The velvet red color in *Ramphocelus* tanagers calls to mind mourning cloak
 711 butterflies *Nymphalis antiopa*. It is intriguing to speculate that the structures causing super black in
 712 butterflies ⁷⁹ also underly this velvet red color in *Nymphalis* when combined with red (rather than black)
 713 pigment.

714 Research on microstructural variation in colorful displays, including sex differences, is expanding
 715 rapidly ^{23,25–27,80}. To gain more insight into evolutionary dynamics, we require a complete understanding of
 716 the physical basis of color. This means accounting for the optical effects of microstructure in addition to
 717 the traditionally studied pigments and nanostructure ⁸¹.

718 **The proxy treadmill: honest signals can be gamed, causing trait elaboration**

719 Why did male feathers evolve elaborate microstructures? If female choice is a significant driver of
 720 male plumage, then males will be selected to produce female-preferred signals whether this is by changes
 721 to the chemical composition or microstructure of their feathers. From this perspective, the evolutionary
 722 dynamics of female preferences and male traits has aspects of an arms race between the conflicting interests
 723 of the sexes ^{72,82–86}. Females establish tests of quality and males are selected to pass these tests whether by
 724 ‘honest’ displays or ‘gaming’ the test. Rather than eating and metabolizing more carotenoids to honestly
 725 signal a more saturated red ^{5–9} males could use microstructural amplifiers to make their plumage appear a
 726 more saturated red. Following substantial past work ^{72,82–85,87,88}, we suggest that males, under intense
 727 selection to satisfy testing criteria by choosy females, evolve “amplifiers” to honest signals (in this case,
 728 microstructures that enhance light-pigment interactions).

729 Perhaps red carotenoid-based colors were favored by female selection as an index of physiological
 730 health, but selection on males to deliver a saturated red signal by whatever means gradually diluted the
 731 information about male quality ⁸². As males exaggerate their appearance, females are selected to develop
 732 additional quality tests to separate the wheat from the chaff (e.g., females may prefer even more saturated
 733 feathers or new, additional ornaments). Because females cannot unilaterally abandon a prior quality test
 734 without dooming their sons to being unattractive, male ornaments may pile atop one another, potentially
 735 causing extreme and elaborate signals. This is the proxy treadmill⁷²: signal traits become exaggerated as
 736

737 proxies of quality are continuously modified or replaced (because examinees are under strong selective
 738 pressure to inflate their apparent quality, thus devaluing any given proxy).

739 Males of many taxa find ways to amplify their carotenoid signals. Male guppies (*Poecilia*
 740 *reticulata*) have orange carotenoid-colored spots for sexual display. Recall that carotenoids must be eaten
 741 and metabolized rather than synthesized *de novo*, a commonly-cited reason supporting the idea that
 742 carotenoids are honest signals. Guppies synthesize (*de novo*) red pteridine pigments (drosopterins) similar
 743 in hue to carotenoids and include these pigments in their red spots. The authors suggest that male guppies
 744 use drosopterin pigments “in a manner that dilutes, but does not eliminate, the indicator value of carotenoid
 745 coloration”⁷⁰. Greater flamingos (*Phoenicopterus roseus*), a classic example of carotenoid-colored birds,
 746 amplify their plumage color by “applying cosmetics”: they secrete carotenoid-colored preen oils to coat
 747 their feathers, and do so more often during display times⁸⁹.

748 Beyond carotenoids, direct evidence for deceptive elements to honest signaling have been reported
 749 in many invertebrates^{90–92} and a few vertebrates^{93–95}. Beyond mate choice, the analogous arena of embryo
 750 selection shows evidence of the proxy treadmill⁷². During human pregnancy, embryos “audition” for the
 751 role of a lifetime⁹⁶ and must pass signaling “checkpoints” to be carried to term⁹⁷. One measure of embryo
 752 quality, the signaling hormone chorionic gonadotropin, has seen an extreme inflation over evolutionary
 753 time with no clear functional significance⁷²—reminiscent of the elaborate microstructures that underpin
 754 male *Ramphocelus* color. Goodhart’s Law in economics and the analogous Campbell’s Law describe this
 755 well-observed phenomenon: “when a measure becomes a target, it ceases to be a good measure”⁹⁸.

756 In addition to our proposal—the proxy treadmill—sexual selection is complex and many selective
 757 forces likely interact to influence coloration, including predation risk^{16,99}, intra-sex aggression^{12–14,17},
 758 honest signaling via the structures themselves^{100–103}, arbitrary preferences², and species recognition¹.

759 *Limitations and Conclusion*

760 We would like to note limitations of this exploratory study which should be addressed in detailed
 761 follow-up work. First, we have data from only one male and one female of each of ten species; future work
 762 could include data from many males and many females per species in order to conduct detailed within-
 763 species comparisons. Second, we do not report cross-sectional data for our feathers, which could be
 764 achieved through transmission electron microscopy for detailed future work on optics. Third, we used a
 765 mechanical extraction procedure for the carotenoids, and it would be useful to conduct follow-up tests
 766 comparing this extraction procedure to pyridine extraction¹⁰⁴. Fourth, we used LCMS to identify
 767 carotenoids with signal strength as a proxy for amount. The signal strengths cannot be compared directly
 768 between pigment families because carotenoids ionize differently depending on the molecular structure.
 769 Therefore, follow-up work could employ more tradition UV-Vis quantification. Finally, we did not look
 770 for carotenoid esters, which can comprise a portion of feather pigments⁴⁵; therefore future work could
 771 benefit from UV-Vis-MS analyses.

772 Few studies quantify plumage signals in both males and females, but a comparative approach can
 773 advance our understanding of evolution³⁶. More broadly, signals cannot be pigeonholed as purely honest,
 774 purely deceptive, or purely arising from one selective force. Individuals struggle to satisfy many competing
 775 selective pressures which vary over time and space, from avoiding predators to finding a mate. Nature is
 776 red in tooth, claw, and male tanager feathers.

777

778 **Author Contributions:** All authors conceived the research design. DEM and EH performed all pigment
 779 extractions, SEM work, and spectrophotometry. CV and ST designed and implemented the LC-MS
 780 procedure for carotenoid characterization. DEM performed the optical simulations and spectral
 781 manipulations. DEM and AJS performed MCMCglmm modelling. AJS constructed the phylogeny and
 782 performed all regressions. AJS and JED performed the digital light microscopy. DH provided conceptual
 783 groundwork. All authors jointly wrote the paper.

785 **Acknowledgements:**
 786 We are very grateful to Jeremiah Trimble and Kate Eldridge for their help with the ornithological
 787 collections. Special thanks to Dan Utter and Professor Colleen Cavanaugh for their methodological
 788 assistance and use of their lab equipment. Thank you to Sofia Prado-Irwin and Dan Utter for helpful
 789 comments on the manuscript. We also thank three reviewers for their thoughtful feedback. Thank you to
 790 Gabriel Ugueto for the outstanding artwork, and to Nick Athanas – antpitta.com – for the beautiful
 791 photos. This work was performed in part at the Harvard University Center for Nanoscale Systems (CNS),
 792 a member of the National Nanotechnology Coordinated Infrastructure Network (NNCI), which is
 793 supported by the National Science Foundation under NSF ECCS award no. 1541959. DEM’s research is
 794 conducted with Government support under and awarded by DoD, Air Force Office of Scientific Research,
 795 National Defense Science and Engineering Graduate (NDSEG) Fellowship, 32 CFR 168a, and DEM and
 796 AJS were supported by research funds from the Harvard University Department of Organismic and
 797 Evolutionary Biology (OEB).

798
 799 **Conflict of Interest Statement:** The authors declare no conflicts of interest.
 800
 801 **Data Availability:** All data is included as supplemental information. Source data are provided with this
 802 paper. We provide source data for Figures 2-7 and supplemental Figures S1-S6.
 803
 804 **Code Availability:** All code is included as supplemental information.

805 **Supplemental Data:**
 806
 807 Supplemental Information PDF (tables and figures)
 808
 809 Additional Supplemental Files, in zipped Supplemental_Files folder:
 810 **Data Files:** pigment_names.csv , Carotenoid_Pigments_Ramphocelus.csv,
 811 Microstructure_SEM_Measurements_Ramphocelus.csv, Spectrophotometry_Ramphocelus.xlsx,
 812 **R Code Files:** carotenoid_analyses.R, spectrophotometry_analyses.R,
 813 microstructure_analyses.R)
 814 **Lumerical Code Files:** Dihedral_Barbules_Angle_Sweep.lsf,
 815 Expanded_Feather_Barb_Female_vs_Male.lsf
 816 **Phylogenetic Trees:** ramphocelus_rooted_ingrouponly.tree,
 817 ramphocelus_rooted_ingrouponly_ultrametric.tree

818
 819 **References**
 820
 821 1. Hill, G. E. Sexiness, Individual Condition, and Species Identity: The Information Signaled by
 822 Ornaments and Assessed by Choosing Females. *Evol. Biol.* **42**, 251–259 (2015).
 823 2. Prum, R. O. Aesthetic evolution by mate choice: Darwin’s really dangerous idea. *Philos. Trans. R.*
 824 *Soc. B Biol. Sci.* **367**, 2253–2265 (2012).
 825 3. Fisher, R. A. *The genetical theory of natural selection: a complete variorum edition.* (Oxford
 826 University Press, 1999).
 827 4. Dawkins, M. S. & Guilford, T. Sensory bias and the adaptiveness of female choice. *Am. Nat.* 937–
 828 942 (1996).
 829 5. Simons, M. J. P., Cohen, A. A. & Verhulst, S. What does carotenoid-dependent coloration tell?
 830 Plasma carotenoid level signals immunocompetence and oxidative stress state in birds-a meta-
 831 analysis. *PLoS One* **7**, (2012).
 832 6. Weaver, R. J., Santos, E. S. A., Tucker, A. M., Wilson, A. E. & Hill, G. E. Carotenoid metabolism
 833 strengthens the link between feather coloration and individual quality. *Nat. Commun.* **9**, 73 (2018).

- 834 7. Cantarero, A. & Alonso-Alvarez, C. Mitochondria-targeted molecules determine the redness of the
835 zebra finch bill. *Biol. Lett.* (2017) doi:10.1098/rsbl.2017.0455.
- 836 8. Cantarero, A. *et al.* A mitochondria-targeted antioxidant affects the carotenoid-based plumage of
837 red crossbills. *bioRxiv* 839670 (2019).
- 838 9. Hill, G. E. *et al.* Plumage redness signals mitochondrial function in the house finch. *Proc. R. Soc.
839 B Biol. Sci.* (2019) doi:10.1098/rspb.2019.1354.
- 840 10. Folstad, I. & Karter, A. J. Parasites, Bright Males, and the Immunocompetence Handicap. *Am.
841 Nat.* **139**, 603–622 (1992).
- 842 11. Zahavi, A. Mate selection—a selection for a handicap. *J. Theor. Biol.* **53**, 205–214 (1975).
- 843 12. Tibbetts, E. A. & Dale, J. A socially enforced signal of quality in a paper wasp. *Nature* (2004)
844 doi:10.1038/nature02949.
- 845 13. Tibbetts, E. A. The evolution of honest communication: Integrating social and physiological costs
846 of ornamentation. in *Integrative and Comparative Biology* (2014). doi:10.1093/icb/icu083.
- 847 14. Chaine, A. S., Roth, A. M., Shizuka, D. & Lyon, B. E. Experimental confirmation that avian
848 plumage traits function as multiple status signals in winter contests. *Anim. Behav.* (2013)
849 doi:10.1016/j.anbehav.2013.05.034.
- 850 15. Endler, J. A. A Predator’s View of Animal Color Patterns. in *Evolutionary Biology* (1978).
851 doi:10.1007/978-1-4615-6956-5_5.
- 852 16. McQueen, A. *et al.* Evolutionary drivers of seasonal plumage colours: colour change by moult
853 correlates with sexual selection, predation risk and seasonality across passerines. *Ecology Letters*
854 (2019) doi:10.1111/ele.13375.
- 855 17. Leitão, A. V., Hall, M. L., Delhey, K. & Mulder, R. A. Female and male plumage colour signals
856 aggression in a dichromatic tropical songbird. *Anim. Behav.* **150**, 285–301 (2019).
- 857 18. Webster, M. S., Ligon, R. A. & Leighton, G. M. Social costs are an underappreciated force for
858 honest signalling in animal aggregations. *Anim. Behav.* (2018) doi:10.1016/j.anbehav.2017.12.006.
- 859 19. Koch, R. E. *et al.* No evidence that carotenoid pigments boost either immune or antioxidant
860 defenses in a songbird. *Nat. Commun.* **9**, 491 (2018).
- 861 20. Weaver, R. J., Koch, R. E. & Hill, G. E. What maintains signal honesty in animal colour displays
862 used in mate choice? *Phil. Trans. R. Soc. B* **372**, 20160343 (2017).
- 863 21. Hill, G. E. & Montgomerie, R. Plumage colour signals nutritional condition in the house finch.
864 *Proc. R. Soc. B Biol. Sci.* **258**, 47–52 (1994).
- 865 22. Hill, G. E. & McGraw, K. J. *Bird coloration: mechanisms and measurements*. vol. 1 (Harvard
866 University Press, 2006).
- 867 23. Iskandar, J.-P. *et al.* Morphological basis of glossy red plumage colours. *Biol. J. Linn. Soc.* **119**,
868 477–487 (2016).
- 869 24. Harvey, T. A., Bostwick, K. S. & Marschner, S. Directional reflectance and milli-scale feather
870 morphology of the African Emerald Cuckoo, *Chrysococcyx cupreus*. *J. R. Soc. Interface* **10**,
871 20130391 (2013).
- 872 25. McCoy, D. E., Feo, T., Harvey, T. A. & Prum, R. O. Structural absorption by barbule
873 microstructures of super black bird of paradise feathers. *Nat. Commun.* **9**, 1–8 (2018).
- 874 26. McCoy, D. E. & Prum, R. O. Convergent evolution of super black plumage near bright color in 15
875 bird families. *J. Exp. Biol.* **222**, jeb208140 (2019).
- 876 27. Enbody, E. D., Lantz, S. M. & Karubian, J. Production of plumage ornaments among males and
877 females of two closely related tropical passerine bird species. *Ecol. Evol.* **7**, 4024–4034 (2017).
- 878 28. Gkikas, D., Argiropoulos, A. & Rhizopoulou, S. Epidermal focusing of light and modelling of
879 reflectance in floral-petals with conically shaped epidermal cells. *Flora Morphol. Distrib. Funct.
Ecol. Plants* **212**, 38–45 (2015).
- 880 29. Gorton, H. L. & Vogelmann, T. C. Effects of epidermal cell shape and pigmentation on optical
881 properties of Antirrhinum petals at visible and ultraviolet wavelengths. *Plant Physiol.* **112**, 879–
883 888 (1996).
- 884 30. Wilts, B. D. *et al.* Ultrastructure and optics of the prism-like petal epidermal cells of *Eschscholzia*

- 885 californica (California poppy). *New Phytol.* **219**, 1124–1133 (2018).
- 886 31. Kay, Q. O. N., Daoud, H. S. & Stirton, C. H. Pigment distribution, light reflection and cell
887 structure in petals. *Bot. J. Linn. Soc.* **83**, 57–83 (1981).
- 888 32. McCoy, D. E. *et al.* Structurally assisted super black in colourful peacock spiders. *Proc. R. Soc. B*
889 **286**, 20190589 (2019).
- 890 33. Maurer, D. L., Kohl, T. & Gebhardt, M. J. Cuticular microstructures turn specular black into matt
891 black in a stick insect. *Arthropod Struct. Dev.* **46**, 147–155 (2017).
- 892 34. Spinner, M., Kovalev, A., Gorb, S. N. & Westhoff, G. Snake velvet black: hierarchical micro- and
893 nanostructure enhances dark colouration in *Bitis rhinoceros*. *Sci. Rep.* **3**, 1846 (2013).
- 894 35. Burns, K. J. & Shultz, A. J. Widespread cryptic dichromatism and ultraviolet reflectance in the
895 largest radiation of Neotropical songbirds: implications of accounting for avian vision in the study
896 of plumage evolution. *Auk* **129**, 211–221 (2012).
- 897 36. Shultz, A. J. & Burns, K. J. The role of sexual and natural selection in shaping patterns of sexual
898 dichromatism in the largest family of songbirds (Aves: Thraupidae). *Evolution (N. Y.)*. (2017).
- 899 37. Krueger, T. R., Williams, D. A. & Searcy, W. A. The genetic mating system of a tropical tanager.
900 *Condor* **110**, 559–562 (2008).
- 901 38. Harris, E. Breeding, Husbandry and Management of Tanager Species. *AFA Watchb.* **14**, 20–27
902 (1987).
- 903 39. Moynihan, M. Display Patterns of Tropical American" Nine-Primaried" Songbirds II. Some
904 Species of Ramphocelus. *Auk* **79**, 655–686 (1962).
- 905 40. Griscom, L. Notes on imaginary species of Ramphocelus. *Auk* **49**, 199–203 (1932).
- 906 41. Clements, J. F. *et al.* The eBird/Clements checklist of birds of the world: v2017.
907 <http://www.birds.cornell.edu/clementschecklist/download/> (2017).
- 908 42. Hudon, J. Considerations in the Conservation of Feathers and Hair , Particularly their Pigments. in
909 *CAC/ACCR 31st Annual Conference, Jasper* (2005).
- 910 43. Endler, J. A. On the measurement and classification of colour in studies of animal colour patterns.
911 *Biol. J. Linn. Soc.* **41**, 315–352 (1990).
- 912 44. Eliason, C. M., Maia, R. & Shawkey, M. D. Modular color evolution facilitated by a complex
913 nanostructure in birds. *Evolution (N. Y.)* **69**, 357–367 (2015).
- 914 45. García-de Blas, E., Mateo, R., Viñuela, J. & Alonso-Álvarez, C. Identification of carotenoid
915 pigments and their fatty acid esters in an avian integument combining HPLC-DAD and LC-MS
916 analyses. *J. Chromatogr. B Anal. Technol. Biomed. Life Sci.* (2011)
917 doi:10.1016/j.jchromb.2010.12.019.
- 918 46. Toral, G. M., Figuerola, J. & Negro, J. J. Multiple ways to become red: Pigment identification in
919 red feathers using spectrometry. *Comp. Biochem. Physiol. - B Biochem. Mol. Biol.* (2008)
920 doi:10.1016/j.cbpb.2008.02.006.
- 921 47. Taflove, A. & Hagness, S. C. Computational electromagnetics: the finite-difference time-domain
922 method. *Artech House, Norwood* (2005).
- 923 48. Sai, T., Saba, M., Dufresne, E. R., Steiner, U. & Wilts, B. D. Designing refractive index fluids
924 using the Kramers–Kronig relations. *Faraday Discuss.* **223**, 136–144 (2020).
- 925 49. Shawkey, M. D. & Hill, G. E. Carotenoids need structural colours to shine. *Biol. Lett.* **1**, 121–124
926 (2005).
- 927 50. Burns, K. J. *et al.* Phylogenetics and diversification of tanagers (Passeriformes: Thraupidae), the
928 largest radiation of Neotropical songbirds. *Mol. Phylogenet. Evol.* **75**, 41–77 (2014).
- 929 51. Burns, K. J. & Racicot, R. A. Molecular Phylogenetics of a Clade of Lowland Tanagers:
930 Implications for Avian Participation in the Great American Interchange. *Auk* **126**, 635–648 (2009).
- 931 52. Hackett, S. J. Molecular phylogenetics and biogeography of tanagers in the genus Ramphocelus
932 (Aves). *Mol. Phylogenet. Evol.* **5**, 368–382 (1996).
- 933 53. Katoh, K. & Standley, D. M. MAFFT multiple sequence alignment software version 7:
934 Improvements in performance and usability. *Mol. Biol. Evol.* **30**, 772–780 (2013).
- 935 54. Stamatakis, A. RAxML-VI-HPC: Maximum likelihood-based phylogenetic analyses with

- 936 thousands of taxa and mixed models. *Bioinformatics* **22**, 2688–2690 (2006).
- 937 55. Stamatakis, A. RAxML version 8: A tool for phylogenetic analysis and post-analysis of large
938 phylogenies. *Bioinformatics* **30**, 1312–1313 (2014).
- 939 56. Revell, L. J. Two new graphical methods for mapping trait evolution on phylogenies. *Methods*
940 *Ecol. Evol.* **4**, 754–759 (2013).
- 941 57. Revell, L. J. phytools: An R package for phylogenetic comparative biology (and other things).
942 *Methods Ecol. Evol.* **3**, 217–223 (2012).
- 943 58. Hadfield, J. D. MCMC methods for multi-response generalized linear mixed models: the
944 MCMCglmm R package. *J. Stat. Softw.* **33**, 1–22 (2010).
- 945 59. Hadfield, J. D. MCMCglmm course notes. See <http://cran.r-project.org/web/packages/MCMCglmm/vignettes/CourseNotes.pdf> (2012).
- 946 60. Wilson, A. J. *et al.* An ecologist's guide to the animal model. *J. Anim. Ecol.* **79**, 13–26 (2010).
- 947 61. de Villemereuil, P. & Nakagawa, S. General quantitative genetic methods for comparative
948 biology. in *Modern phylogenetic comparative methods and their application in evolutionary*
949 *biology* 287–303 (Springer, 2014).
- 950 62. Grafen, A. The phylogenetic regression. *Phil. Trans. R. Soc. B* **326**, 119–157 (1989).
- 951 63. Martins, E. P. & Hansen, T. F. Phylogenies and the comparative method: a general approach to
952 incorporating phylogenetic information into the analysis of interspecific data. *Am. Nat.* **149**, 646–
953 667 (1997).
- 954 64. Pinheiro, J., Bates, D., DebRoy, S. & Sarkar, D. nlme: Linear and Nonlinear Mixed Effects
955 Models. *R Dev. Core Team* (2007) doi:Doi 10.1038/Ncb1288.
- 956 65. Felsenstein, J. Phylogenies and the Comparative Method. *Am. Nat.* **125**, 1–15 (1985).
- 957 66. Morrison, E. S. & Badyaev, A. V. Structuring evolution: biochemical networks and metabolic
958 diversification in birds. *BMC Evol. Biol.* **16**, 168 (2016).
- 959 67. LaFountain, A. M., Prum, R. O. & Frank, H. A. Diversity, physiology, and evolution of avian
960 plumage carotenoids and the role of carotenoid–protein interactions in plumage color appearance.
961 *Arch. Biochem. Biophys.* **572**, 201–212 (2015).
- 962 68. Gilbert, P. U. P. A. & Haeberli, W. Experiments on subtractive color mixing with a
963 spectrophotometer. *Am. J. Phys.* (2007) doi:10.1119/1.2431654.
- 964 69. Eckert, M. P. & Carter, G. A. Flowers produce variations in color saturation by arranging petals at
965 oblique and varying angles. *JOSA A* **17**, 825–830 (2000).
- 966 70. Grether, G. F., Hudon, J. & Endler, J. A. Carotenoid scarcity, synthetic pteridine pigments and the
967 evolution of sexual coloration in guppies (*Poecilia reticulata*). *Proc. R. Soc. B Biol. Sci.* (2001)
968 doi:10.1098/rspb.2001.1624.
- 969 71. Koch, R. E. *et al.* Testing the resource trade-off hypothesis for carotenoid-based signal honesty
970 using genetic variants of the domestic canary. *J. Exp. Biol.* **222**, jeb188102 (2019).
- 971 72. McCoy, D. E. & Haig, D. Embryo Selection and Mate Choice: Can 'Honest Signals' Be Trusted?
972 *Trends Ecol. Evol.* (2020).
- 973 73. Ligon, R. A., Simpson, R. K., Mason, N. A., Hill, G. E. & McGraw, K. J. Evolutionary innovation
974 and diversification of carotenoid-based pigmentation in finches. *Evolution (N. Y.)* **70**, 2839–2852
975 (2016).
- 976 74. Friedman, N. R., Kiere, L. M. & Omland, K. E. Convergent gains of red carotenoid-based
977 coloration in the new world blackbirds. *Auk* **128**, 1–10 (2011).
- 978 75. Morales-Rozo, A., Tenorio, E. A., Carling, M. D. & Cadena, C. D. Origin and cross-century
979 dynamics of an avian hybrid zone. *BMC Evol. Biol.* **17**, 257 (2017).
- 980 76. Speigle, J. M. & Brainard, D. H. Luminosity thresholds: Effects of test chromaticity and ambient
981 illumination. *JOSA A* **13**, 436–451 (1996).
- 982 77. Brainard, D. H., Wandell, B. A. & Chichilnisky, E.-J. Color constancy: from physics to
983 appearance. *Curr. Dir. Psychol. Sci.* 165–170 (1993).
- 984 78. Kreezer, G. Luminous appearances. *J. Gen. Psychol.* **4**, 247–281 (1930).
- 985 79. Vukusic, P., Sambles, J. R. & Lawrence, C. R. Structurally assisted blackness in butterfly scales.
- 986

- 987 80. *Proc. R. Soc. London. Ser. B Biol. Sci.* **271**, S237–S239 (2004).
- 988 80. Lee, E., Aoyama, M. & Sugita, S. Microstructure of the feather in Japanese Jungle Crows (*Corvus*
989 macrorhynchos) with distinguishing gender differences. *Anat. Sci. Int.* **84**, 141–147 (2009).
- 990 81. Burns, K. J., McGraw, K. J., Shultz, A. J., Stoddard, M. C. & Thomas, D. B. Advanced methods
991 for studying pigments and coloration using avian specimens. in *The Extended Specimen: Emerging*
992 *Frontiers in Collections-Based Ornithological Research* (CRC press, 2017).
993 doi:10.1201/9781315120454.
- 994 82. Hill, G. E. Trait elaboration via adaptive mate choice: sexual conflict in the evolution of signals of
995 male quality. *Ethol. Ecol. Evol.* **6**, 351–370 (1994).
- 996 83. Burk, T. Acoustic signals, arms races and the costs of honest signalling. *Florida Entomol.* **71**, 400
997 (1988).
- 998 84. Krebs, J. R. & Dawkins, R. Animal signals: mindreading and manipulation. in *Behavioural*
999 *Ecology: an evolutionary approach* 380–402 (Blackwell Scientific Publication, 1984).
- 1000 85. Dawkins, R. & Krebs, J. R. Animal signals: information or manipulation. in *Behavioural ecology:*
1001 *An evolutionary approach* vol. 2 282–309 (1978).
- 1002 86. Funk, D. H. & Tallamy, D. W. Courtship role reversal and deceptive signals in the long-tailed
1003 dance fly, *Rhamphomyia longicauda*. *Anim. Behav.* **59**, 411–421 (2000).
- 1004 87. Dawkins, M. S. & Guilford, T. The corruption of honest signalling. *Anim. Behav.* **41**, 865–873
1005 (1991).
- 1006 88. Parker, G. A. Sexual conflict over mating and fertilization: an overview. *Philos. Trans. R. Soc.*
1007 *London B Biol. Sci.* **361**, 235–259 (2006).
- 1008 89. Amat, J. A. et al. Greater flamingos *Phoenicopterus roseus* use uropygial secretions as make-up.
1009 *Behav. Ecol. Sociobiol.* (2011) doi:10.1007/s00265-010-1068-z.
- 1010 90. Christy, J. H. & Rittschof, D. Deception in visual and chemical communication in crustaceans. in
1011 *Chemical communication in crustaceans* 313–333 (Springer, 2010).
- 1012 91. Wilson, R. S., Angilletta Jr, M. J., James, R. S., Navas, C. & Seebacher, F. Dishonest signals of
1013 strength in male slender crayfish (*Cherax dispar*) during agonistic encounters. *Am. Nat.* **170**, 284–
1014 291 (2007).
- 1015 92. Ghislandi, P. G., Beyer, M., Velado, P. & Tuni, C. Silk wrapping of nuptial gifts aids cheating
1016 behaviour in male spiders. *Behav. Ecol.* **28**, 744–749 (2017).
- 1017 93. Bro-Jørgensen, J. & Pangle, W. M. Male Topi Antelopes Alarm Snort Deceptively to Retain
1018 Females for Mating. *Am. Nat.* **176**, E33–E39 (2010).
- 1019 94. Summers, K. Sexual conflict and deception in poison frogs. *Curr. Zool.* **60**, 37–42 (2014).
- 1020 95. Candolin, U. The relationship between signal quality and physical condition : is sexual signalling
1021 honest in the three-spined stickleback ? 1261–1267 (1999).
- 1022 96. Forsdyke, D. R. When few survive to tell the tale: thymus and gonad as auditioning organs:
1023 historical overview. *Theory Biosci.* 1–10 (2019).
- 1024 97. Ewington, L. J., Tewary, S. & Brosens, J. J. New insights into the mechanisms underlying
1025 recurrent pregnancy loss. *Journal of Obstetrics and Gynaecology Research* (2019)
1026 doi:10.1111/jog.13837.
- 1027 98. Strathern, M. ‘Improving ratings’: audit in the British University system. *Eur. Rev.* **5**, 305–321
1028 (1997).
- 1029 99. Endler, J. A. Natural and sexual selection on color patterns in poeciliid fishes. in *Evolutionary*
1030 *ecology of neotropical freshwater fishes* 95–111 (Springer, 1984).
- 1031 100. Shawkey, M. D., Pillai, S. R., Hill, G. E., Siefferman, L. M. & Roberts, S. R. Bacteria as an agent
1032 for change in structural plumage color: correlational and experimental evidence. *Am. Nat.* **169**,
1033 S112–S121 (2007).
- 1034 101. Hill, G. E., Doucet, S. M. & Buchholz, R. The effect of coccidial infection on iridescent plumage
1035 coloration in wild turkeys. *Anim. Behav.* **69**, 387–394 (2005).
- 1036 102. Keyser, A. J. & Hill, G. E. Structurally based plumage coloration is an honest signal of quality in
1037 male blue grosbeaks. *Behav. Ecol.* **11**, 202–209 (2000).

- 1038 103. White, T. E. Structural colours reflect individual quality: a meta-analysis. *bioRxiv* (2020).
- 1039 104. McGraw, K. J., Hudon, J., Hill, G. E. & Parker, R. S. A simple and inexpensive chemical test for
1040 behavioral ecologists to determine the presence of carotenoid pigments in animal tissues. *Behav.*
1041 *Ecol. Sociobiol.* **57**, 391–397 (2005).
- 1042
- 1043
- 1044

1045

1046 **Tables**

1047

1048

1049 **Table 1: Males, but not females, have diverse and elaborate feather microstructure.** Male
 1050 *Ramphocelus* tanagers have many atypical microstructural features compared to females. “3D barbules”
 1051 refers to whether or not barbules extended upwards from the plane of the feather; “strap-shaped barbules”
 1052 refers to whether barbules were flattened rather than classically cylindrical; “oblong barb” refers to
 1053 whether bars were taller than they were wide (numerical threshold: > median (max barb width)/(top-
 1054 down barb width)); wide barb refers to whether the barb was expanded (numerical threshold: > median
 1055 barb width value). Complete numerical measurements can be found in Table S3.

1056

species	sex	region	angled barbules	strap-shaped barbules	oblong barb	expanded barb
<i>R. bresilius</i>	f	rump	--	--	--	yes
<i>R. carbo</i>	f	chest	--	--	yes	--
<i>R. costaricensis</i>	f	throat	--	--	--	--
<i>R. dimidiatus</i>	f	rump	--	--	--	--
<i>R. dimidiatus</i>	f	throat	--	--	yes	--
<i>R. flammigerus</i>	f	breast	--	--	--	--
<i>R. flammigerus</i>	f	rump	--	yes	--	--
<i>R. f. icteronotus</i>	f	rump	--	yes	--	--
<i>R. melanogaster</i>	f	chest	--	--	--	--
<i>R. melanogaster</i>	f	throat	--	yes	--	--
<i>R. nigrogularis</i>	f	rump	--	--	yes	--
<i>R. passerinii</i>	f	rump	--	--	yes	--
<i>R. sanguinolentis</i>	f	rump	yes	yes	yes	yes
<i>R. bresilius</i>	m	rump	yes	yes	yes	--
<i>R. carbo</i>	m	back	yes	yes	yes	yes
<i>R. carbo</i>	m	breast	yes	yes	yes	yes
<i>R. costaricensis</i>	m	rump	yes	yes	--	yes
<i>R. dimidiatus</i>	m	throat	yes	yes	--	yes
<i>R. dimidiatus</i>	m	rump	yes	yes	yes	yes
<i>R. flammigerus</i>	m	rump	yes	yes	--	yes
<i>R. f. icteronotus</i>	m	rump	yes	yes	yes	--
		upper				
<i>R. melanogaster</i>	m	throat	yes	yes	yes	yes
		lower				
<i>R. melanogaster</i>	m	throat	yes	yes	yes	yes
<i>R. nigrogularis</i>	m	rump	yes	yes	--	yes
<i>R. passerinii</i>	m	rump	yes	--	--	yes
<i>R. sanguinolentis</i>	m	rump	yes	yes	yes	yes

When a measure becomes a target, it ceases to be a good measure.

Marilyn Strathern



Embryo Selection & Mate Choice: Can 'Honest Signals' Be Trusted?

REPRINTED FROM: McCoy, D.E. and Haig, D., 2020. Embryo Selection and Mate Choice: Can Honest Signals Be Trusted?. *Trends in Ecology & Evolution*, 35(4), pp.308-318.

ARTICLE AND SUPPLEMENT AVAILABLE AT: <https://doi.org/10.1016/j.tree.2019.12.002>



Opinion

Embryo Selection and Mate Choice: Can 'Honest Signals' Be Trusted?

Dakota E. McCoy^{1,*,@} and David Haig¹

When a measure becomes a target, it often ceases to be a good measure – an effect familiar from the declining usefulness of standardized testing in schools. This economic principle also applies to mate choice and, perhaps surprisingly, pregnancy. Just as females screen potential mates under many metrics, human mothers unconsciously screen embryos for quality. ‘Examinees’ are under intense selection to improve test performance by exaggerating formerly ‘honest’ signals of quality. Examiners must change their screening criteria to maintain useful information (but cannot abandon old criteria unilaterally). By the resulting ‘proxy treadmill’, new honest indicators arise while old degraded indicators linger, resulting in trait elaboration and exaggeration. Hormone signals during pregnancy show extreme evolutionary escalation (akin to elaborate mating displays).

If the Stakes Are High, Measurement Is Hard

High-stakes testing is meant to measure performance in many contexts, but it also causes systemic, and unwanted behavior change. Often the things tested are easily measured proxies (e.g., standardized test scores at a middle school) for more difficult-to-measure attributes (e.g., how well the middle school teachers educate their pupils). Teachers ‘teach to the test’ rather than improving students’ reading skills [1]. Poorly performing students are sometimes encouraged to stay home [2,3]. In a different context, test scores for university admissions are intended to provide objective measures of intellectual quality but come to also measure economic means as some families can afford expensive test-preparation courses that are unavailable to poorer families. Such tests convey some useful information but are distorted by confounding factors. When high stakes depend on an ‘objective’ measure, the measure may cease to provide reliable information because behavior changes to satisfy testing criteria, thus degrading the correlation between the proxies and the attributes that are the real target of evaluation. In economics and the social sciences, this is variously known as **Goodhart’s law** (see [Glossary](#)) [4] or **Campbell’s law** [5], succinctly phrased as ‘When a measure becomes a target it ceases to be a good measure’ [6]. In fields ranging from health care to academic publishing, many metrics become less correlated with quality over time ([Box 1](#)).

In economic and social contexts, Campbell’s law predicts that simple indicators of quality can be corrupted; this may cause an arms race between the evaluating system and the agents being evaluated. As a result, both the indicator and the test become more complicated. For example, as Twitter bots spread to exploit automated measurements of impact, bot-detection algorithms must race to identify honest indicators of ‘human-ness’ [7]. As bots find ways to deceive each new indicator, both the algorithm and the bot are encumbered by the continued detection and production, respectively, of ‘human-ness’ indicators. The bot cannot afford to abandon old, degraded indicators of human-ness or it will be caught; the algorithm cannot afford to dally without finding new indicators of humanness or it will never catch the new and improved bots. The same

Highlights

Mate choice by honest signaling is a classic explanation for elaborate traits in nature. Many researchers have: (i) observed deceptive signaling, and (ii) wondered how honest signals relate to trait elaboration.

Honest signaling is analogous to high-stakes testing. Quality is hard to measure directly, so proxies (tests) are used. High-stakes testing causes ‘teaching to the test’ without improving educational outcomes.

Embryo choice is another high-stakes test. Mothers select healthy embryos and terminate sub-par embryos automatically. Embryos are selected to pass maternal tests without improving their quality. The resulting arms race causes extreme and elaborate signals during pregnancy.

We can better understand elaborate traits in nature if we interpret mate selection, and embryo choice, as a dynamic give-and-take between two parties with conflicting fitness interests.

¹Department of Organismic and Evolutionary Biology, Harvard University, Cambridge, MA 02138, USA

*Correspondence:
dakotamccoy@g.harvard.edu
 (D.E. McCoy).
 @Twitter: [@WildlifeMcCoy](#)



Box 1. When a Measure Becomes a Target, It Ceases to Be a Good Measure

In public schools in the USA, high-stakes testing has many unintended consequences. Teachers in Chicago guided poorly performing students away from subjects that counted towards performance ratings [2,3] and test scores in Texas skyrocketed after implementation of high-stakes testing but actual skills (e.g., reading) did not improve and ethnic performance gaps remained or even widened [1]. Educational outcomes are hard to measure, so we rely on test scores as a proxy of quality. Educational proxies degrade given sufficient incentive, as do proxies in many other fields [69]. Medicine is not immune to signal degradation. When hospitals were rated based on how long patients had to wait, emergency departments refused to admit patients from waiting ambulances until they could be seen, prompting ambulance companies to purchase makeshift tents to store patients in limbo [70]. In academic publishing, metrics such as impact factor over time become less informative of quality and depend heavily on field [71]. Likewise, researchers subset data or collect data selectively to achieve a significant P value, a practice known as ' P hacking' [72]. We want nutritional labels to convey food health, but food manufacturers game this system by labeling foods 'low-fat' but adding extra sugar [73]. These disparate examples show that metrics meant to improve performance often can be gamed. As metrics are gamed, regulatory agencies must establish more detailed and elaborate regulations, the result of an arms race resulting from high-stakes testing.

logic may explain why US tax law, an arena wherein people and corporations have strong incentives to deceive, is so cumbersome and elaborate. In contexts where honesty matters to the receiver but deception enriches the signaler, both the signal and the receiving apparatus become more elaborate over time.

Campbell's law also applies to high-stakes examinations in biology. Mate choice and embryo selection are, respectively, indirect and direct means of selecting fit offspring. In both arenas, many candidates compete for few slots. Candidates' intrinsic quality can be assessed through information that correlates with fitness (termed an **honest signal** in the domain of mate choice). But selection favors candidates who can exaggerate their own apparent quality. Indeed, in the well-studied domain of mate choice, substantial theoretical work [8–13] and many experimental results (Box 2) show that deception is widespread and suggest that antagonistic coevolution between the sexes may cause elaborate display traits. Signaling can find means to reduce the cost of, or invest disproportionately in, formerly honest signals – including by evolving enhancers to the signal. In response, receivers can raise the necessary signal threshold or adopt new, additional standards. By the '**proxy treadmill**', receivers seek honesty and signalers seek to deceive, but receivers cannot unilaterally abandon a prior trait preference (e.g., if a female selects a male who does not conform to majority preference, her sons will be disadvantaged in the mating market).

We argue that the conflict of interest between examiners and examinees of lower quality promotes instability, escalation, and elaboration (of both signal and test). We hope to provide three useful contributions. First, the proxy treadmill arises from fundamental principles and should be expected in studies of honest signals. While it is uncontroversial that deception is widespread in mate choice, the idea of trait elaboration via arms races is not well-embedded in the field. In any study of honest signaling, we suggest that researchers should expect that the pressure to deceive begets pressure to evaluate better (causing signal elaboration). Second, research on deception in mate choice provides the framework to interpret the biology of human pregnancy: pregnancy is a high-stakes test of embryo quality. Just as males find deceptive means to enhance their apparent fitness to choosy females, we argue that embryos have evolved illusions of health and fitness as well as tools to coerce maternal bodies into continuing, rather than terminating, a pregnancy. Third, massive signal elaboration in embryo selection supports the theory of the proxy treadmill in other biological domains (such as mate choice). Mate choice is a complicated and controversial field involving multiple sensory systems, a chaotic environment, and competing (nonexclusive) selective pressures. Embryo selection occurs in a comparatively constrained environment, the maternal body, and operates primarily via hormone signals for which the genetics are understood.

Glossary

Aesthetic residue: display trait which is no longer indicative of quality but is nonetheless retained in signaler-displayer examinations because it would be costly to abandon.

Campbell's law: a principle in social sciences that states that quantitative proxies, or metrics, meant to measure complicated phenomena are subject to corruption when the indicator is used for decision-making. 'When a measure becomes a target it ceases to be a good measure.'

Chorionic gonadotropin (CG): hormone produced by the placenta that is molecularly and functionally related to maternally derived luteinizing hormone; it maintains pregnancy by stimulating the corpus luteum to produce progesterone. It has evolved independently in equids and primates.

Honest signal: display trait thought to correlate with intrinsic quality (health or fitness) of the display, thus giving valid information to the observer.

Goodhart's law: another name for Campbell's law.

Luteinizing hormone (LH): hormone produced by the maternal pituitary that is required to maintain a pregnancy (it stimulates the corpus luteum to produce progesterone).

Parent–offspring conflict: an evolutionary theory based on differences between parents and offspring over the optimal investment a parent should give to a single offspring. This leads to many evolved signatures of conflict, such as genomic arms races.

Proxy treadmill: a proposed phenomenon by which signal traits become exaggerated as proxies of quality are continuously modified or replaced (because examinees are under strong selective pressure to inflate their apparent quality, thus devaluing any given proxy).

Elaborate mating displays demanded by the choosing sex, and elaborate hormone signals required for an embryo to be carried to term, are analogous to cumbersome regulations intended to detect bad behavior in many socio-economic arenas.

Choosing a Partner: The Displaying Sex Has Incentives to ‘Cheat’, but Some Forces Resist

In mate choice, members of one sex, usually females, assess the performance of the other sex in a mating display. Multiple selective pressures interact to shape female preference and favor particular male traits, including sensory bias (pre-existing preference for particular traits [14,15]), arbitrary aesthetic preferences [16–20], and the need to identify members of one’s own species [21]; however, the most common explanation is that females use display traits to select a healthy and fit male ('honest signaling'). Under honest signaling theory, signals may indicate quality by incurring a cost [22–24] or by being causally linked to important physiological processes ('index' [25,26]).

Honest signals in mate choice are analogous to high-stakes tests: one sex uses proxies of quality to select mates of the opposite sex. Decades of research on mate choice have shown that signaling between two parties with conflicting interests is subject to deception [11,12,27–31] (Box 2). Signals evolve to manipulate or persuade receivers in a manner favorable to the sender, not merely to inform. The fundamental conflict of interest between chosen and choosing sexes [32] may cause an arms race where displayers exaggerate their appearance without improving their quality [11–13,33]. In sexual selection, the choosing sex (hereafter ‘females’) is selected to elicit honest information about displayers (hereafter ‘males’), but males are selected to evolve deceptive strategies to appear higher-quality than they are. Low-quality males have a larger incentive to exaggerate. Deceptive enhancers may sweep through a population, reducing the value of that signal and raising the bar on how high-quality males must appear in order to mate [8,12,13,33–35].

Even as a signal becomes less valuable as an honest indicator, a female retains the preference for this signal because to unilaterally abandon her preference for a particular trait may disadvantage her sons (who, lacking that trait, would appear undesirable to the majority of females in the population). However, females are still selected to extract quality signals and will thus either adopt a more stringent version of the same test and/or adopt new tests of quality. In this manner signaling traits become more elaborate, as females demand new indicators of quality while retaining old, degraded indicators as **aesthetic residue** (for further discussion see following section). ‘Honest’ signaling is thus susceptible to bluffing displayers, which are widespread, and animals frequently evolve enhancers to their displays, associated traits with no obvious ‘honest’ content themselves that make the entire display more elaborate (Box 2). Deception in mate selection may be widespread [12] but frequently hidden because it is selected to be undetectable [36]. It likely is no coincidence that most deceptive signals have been described in small animals easy to observe, manipulate, and test.

Despite the pressure to deceive, many signals in nature are reliable. Some deceptive mating displays do not imply that signals convey no useful information. Many studies demonstrate correlations between display signal and quality. What selective forces resist the deterioration of honest assessment? First, certain tests of quality are challenging to manipulate. Index signals, which are tied to uncheatable physical processes rather than invoking a cost themselves, may be resistant to manipulation [8]. Courtship displays that are selected to reveal vigor are more challenging to fake if they operate on multiple physical modalities (i.e., singing, drumming, moving one’s whole body, and more). Finally, Campbell’s and Goodhart’s laws predict that honest assessment is possible as long as the examiner stays one step ahead of the examinee. Examiners

can escalate the level of signal required, or add new required signals of quality, while retaining old signals as ‘aesthetic residue’. We argue below that pregnancy is another clear case where signals between two individuals (mother and embryo) become more elaborate due to a conflict of interest. Mate choice is complex (due to the interaction of brains, sensory systems, and complex behaviors) but it should be subject to this same general phenomenon.

The Proxy Treadmill: New Honest Signals Evolve and Degraded Signals Linger

Observable proxies are chosen because they correlate with more difficult-to-observe qualities. However, this correlation tends to weaken because the proxy becomes a direct target of selection for test-taking ability. This can be thought of as ‘sensory manipulation’ of the examiner by the examinee. If examiners are to continue to select higher-quality examinees, they must seek new proxies that are better correlates of desired qualities. However, there is a conservative force, recognized by Fisher, that prevents a simple replacement of the degraded proxy by a better proxy [20]. This is the ‘desirability’ of the examiner’s offspring when they become examinees. A degraded proxy remains ‘sexy’ because an examiner who

Box 2. Examples of Signal Elaboration Caused by Deception in Mate Choice

Deception and subterfuge abound in mate choice. When male fiddler crabs *Uca annulipes* lose their large display claw (Figure 1A), 44% grow a large, but fragile, replacement ([36]; see also [74,75]). Male Trinidadian guppies *Poecilia reticulata* (Figure 1B) prefer to display near relatively unattractive males to make themselves look better [76]. Further examples show that deception may cause trait elaboration.

Female long-tailed dance flies, *Rhamphomyia longicauda*, compete for protein-rich nuptial gifts from males (for which females exchange copulations). They fly in leks to attract male attention, and males prefer females that have distended abdomens [77]. Distended abdomens have been interpreted as an honest signal of egg development and thus of female mate quality. However, just before the lek, females swallow large quantities of air to inflate pouches on their abdomen and then further wrap their legs around the abdomen, creating an apparently huge abdomen, which completely masks egg development (Figure 1C, [77]). In a related pouch-less species, *Rhamphomyia sociabilis*, abdomen size is indeed an honest correlate of egg development. This suggests that females evolved to deceive males after males were selected to prefer females at a later stage of egg development. Selection for deception caused elaboration.

Male nursery web spiders *Pisaura mirabilis* gather nuptial gifts to buy mating opportunities; these are nutritious substances often wrapped in silk. The ‘worth’ of male gifts varies, from nutritious prey to inedible popped red balloon [78,79]. It is thought that the gifts or the silk itself are honest signals of quality [78]. However, males offered deceptive, worthless gifts in 58% of field trials and 85% of laboratory trials [34]. Further, (i) worthless gifts were not connected to poor body condition; (ii) cheaters who offer worthless gifts in fact gain body mass; and (iii) males adaptively wrap more silk around worthless gifts, to conceal worthlessness and prolong female feeding time to allow mating [34]. The authors describe this as ‘an antagonistic arms race between males under selection to deceive and females under selection to evolve resistance to deception’ [34]. The arms race causes more elaborate male gifts.

Many male mammals are thought to scent-mark with urine to honestly convey their reproductive status, social rank [80], and, based on mark height, body size [81]. Indeed, dwarf mongooses (*Helogale parvula* [82]) spend longer investigating scent-marks that are higher from the ground. However, some individuals paint a larger-than-life portrait of themselves. Undersized male dwarf mongooses scent-mark higher than expected and, in fact, dwarf mongooses typically hand-stand to scent-mark (Figure 1D, [82,83]). Small dogs (*Canis familiaris*) raise their leg at a higher angle than large dogs, thus exaggerating their relative mark height [84]. Males who could hand-stand and leg-cock could deceptively over-represent their own height; once these traits swept through the population, scent-marks would again honestly convey body size. The signal became more elaborate over evolutionary time.

In sea lamprey (*Petromyzon marinus*), the pheromone 3-keto petromyzonol sulfate (3kPZS) originated as a nonsexual, larvally produced migratory cue and was coopted by deceptive males to attract females [85]. This ‘sensory trap’ [86] could be reclaimed as an honest signal [87], whereby females assess male body size and condition via pheromone production [88]. Once 3kPZS became a proxy, selection favored males who could ‘dramatically upregulate the 3kPZS biosynthetic pathway’, causing males to have an ‘up to 8000-fold increase’ of production in their livers [89]. Further, small males have disproportionately larger livers and greater 3kPZS production [88], a potentially deceptive overinvestment. In response, female reception adaptively shifted to avoid costly confusion between larvally produced and sexually produced 3kPZS [89]. An originally deceptive signal was reclaimed as honest, was further corrupted, and promoted receiver adaptation to better discriminate.



Trends In Ecology & Evolution

Figure I. Examples of Deceptive Signaling in Mate Choice. (A) When male fiddler crabs *Uca annulipes* lose their large claw (used for signaling and fighting), they regrow a huge but brittle claw. (Photo credit Rujuta Vinod; license CC BY-SA 4.0). (B) Female (bottom) and male (top) Trinidadian guppies (*Poecilia reticulata*); males preferentially display near comparatively unattractive males. (Photo credit Amy E. Deacon, Hideyasu Shimadzu, Maria Dornelas, Indar W. Ramnarine, and Anne E. Magurran; license CC BY 4.0). (C) A female long-tailed dance fly (*Rhamphomyia longicauda*) inflates sacs on her abdomen to appear as if she has well-developed eggs, a trait favored by observing males. (Photo credit Dave Funk.) (D) Male dwarf mongooses that are undersized scent-mark higher than expected and many individuals handstand. (Photo credit Lynda Sharpe.)

unilaterally drops the proxy will have sons who lose out in the mating market because of the established preferences of other females. Princeton University's attempt to halt grade inflation is a useful analogy [37]. Amidst steadily increasing university grade point averages, Princeton University implemented grade deflation in 2004 but abandoned this policy in 2014 when no peer institutions followed suit [38]. Critics pointed out that low grades could harm students applying for jobs and that some students (perhaps concerned about their grades) chose to attend other schools [37], placing Princeton at a competitive disadvantage in university rankings. Unilateral changes by examiners invoke a serious selective cost.

This is the proxy treadmill. Proxies are initially adopted because they convey reliable information about male quality: females who adopt a reliable proxy are winners, as are the high-quality males they choose. But high-stakes examinations unwittingly select for males that appear better than their objective quality. Because 'dissemblers' are rewarded, high-quality males who do not dissemble lose their advantage. Females who adopt entirely new examinations in response place their own sons at a selective disadvantage because they will be evaluated by the established criteria of other females. Therefore, old preferences are retained as aesthetic residue while new preferences are established to test quality. In this manner, 'looking good on paper' can sweep through a population, placing selective

pressure on females to update their discriminatory abilities by adoption of new proxies while retaining older criteria as purely aesthetic preferences. This dynamic can potentially favor an extraordinary elaboration of desirable traits.

Imagine that female birds assess males based on how red their feathers are (redness, resulting from metabolized carotenoid pigments, is considered an honest index of metabolic function [25,26]). If some males evolve structural components to the feather that enhance redness by 25%, females can simply raise their preference bar by 25% to preserve an honest signal. Alternatively, females can develop a new test – say, the vigor of a male's display dance – in addition to the redness test. While redness is no longer a reliable signal of quality, the female preference for redness may remain as aesthetic residue, while males now must also dance vigorously. As traits become more exaggerated or multiple traits stack together to resist signal erosion, sexually selected traits may become more elaborate. (We note that the proxy treadmill is not the only mechanism by which traits become more elaborate; for example, an animal's fundamental sensory ecology can shape diversification [14]).

Honest signaling is not an equilibrium state because the information conveyed by signals is corrupted over time as males find ways to inflate their own appearance of quality (but see [Outstanding Questions](#)). But females are under constant selection to find new sources of useful information, whether this can be extracted from deceptive signals, or by adding new criteria of selection. This idea has long been described (e.g., [11,13,29,33]), but has not fully been adopted by researchers of sexual selection who investigate honest signals. This may be because sexual selection is extremely complex; mate choice involves multisensory perception in chaotic environments. It is challenging to document trait costs, assess whether honest signalers have higher fitness, and reconstruct the evolutionary history of traits, required to demonstrate the proxy treadmill in operation. A comparatively more constrained area of signaling, *in utero* embryo choice, provides a useful analogy.

Choosing a Child: Signal Elaboration by the Proxy Treadmill during Human Pregnancy

One rationale for 'honest signaling' or 'good genes' models of mate choice is that females select males based on the expected quality of their genetic contribution to offspring. This is indirect selection of offspring: a high-quality male may father some low-quality offspring because of the vagaries of genetic recombination and epistatic interactions between maternal and paternal genomes. A more direct way to improve the quality of offspring would be to examine offspring themselves before major commitment of resources [39]. Mothers, in species with postzygotic provisioning of offspring, are incentivized to terminate investment in subpar offspring early and redirect resources to better quality offspring [40,41]. The earlier a choice can be made, the greater the savings. Thus, the most intense period of mortality in human life-history occurs during the first month after conception: at least 22% of human embryos [42], perhaps more than 70% [43], are eliminated. Embryos audition for the role of a lifetime before unforgiving judges.

We focus on one criterion of maternal choice: the hormonal output of early embryos. Hormone signaling between embryo and mother is analogous to mating displays between males and females. Embryonic signaling is, in some ways, more evolutionarily tractable than sexual signaling. We understand the genetic underpinnings of many hormone signals and signaling occurs within the maternal body rather than in complex external environments. As such, embryo choice is a useful analogy to mate choice. Equally, substantial work on mate choice [11–13,33] underpins our investigation of pregnancy as a high-stakes examination.

Embryonic hormones may provide useful information about embryo quality, but this system has escalated via an intergenerational arms race due to differing evolutionary interests of mothers and embryos [44,45]. Researchers study this conflict of interest between mothers and embryos under the theoretical umbrella of **parent-offspring conflict**. Mothers are selected to gestate only high-quality offspring, but embryos are selected to exaggerate their perceived quality [46]. Akin to males exaggerating their appearance in front of choosy females, embryos hijack systems of maternal control and evolve amplified hormonal signals. As remarked by Roberts [47], under this high-stakes testing regime, the embryo represents its own interests ‘possibly even to the point of relaying misleading information regarding its own fitness and potential. The trophoblast-maternal interface thus represents a battleground that has shaped remarkable rates of evolutionary change’ [47].

Progesterone is essential for the maintenance of mammalian pregnancy. The ancestral source of progesterone was the corpus luteum formed from the ruptured follicle at ovulation. By 7 weeks of gestation, the human placenta becomes a sufficient source of progesterone to obviate the need for luteal progesterone [48]. However, prior to this ‘luteoplacental shift’, pregnancies miscarry if the corpus luteum is removed or ceases to produce progesterone. The corpus luteum initially produces progesterone in response to **luteinizing hormone (LH)** produced by the maternal pituitary, but the quantity of LH required to maintain the corpus luteum rapidly increases, resulting in menstruation (shedding the endometrial lining) 2 weeks after ovulation. Many early-stage human embryos are terminated through the process of menstruation, after they have embedded, at the regular menstrual time or after a slightly delayed period.

Early embryos of simian primates [49] and equids [50] have independently evolved a placental version of LH, **chorionic gonadotropin (CG)**, that is secreted into the maternal circulation to maintain progesterone production by the corpus luteum, thus preventing loss of the pregnancy (Figure 1A). The rapid increase of the LH requirement to maintain pregnancy is not observed in mammalian groups that do not produce CGs and is much greater than the ancestral levels of LH necessary to maintain progesterone production. Embryonic secretion of CGs can be conjectured to have originated as a simple form of ‘cheating’ in which embryos forged a statement they had passed uterine quality control and submitted it to the corpus luteum, rendering null and void whatever prior testing procedures had existed, akin to a student forging ‘A+’ on their report card [44].

However, even initially dishonest signals can be reclaimed as honest signals of quality. CG is a glycoprotein that reveals basic competences in protein synthesis and glycosylation [55]. The maternal evolutionary response was to rapidly increase LH requirements after ovulation and use levels of CG as a proxy of embryo quality. Embryos that produced abundant CG were healthier than embryos that produced lesser amounts. Tiny embryos came to be assessed on their relative prowess in production of CG and must now produce ‘heroic concentrations’ of CG [56] to avoid being terminated at menstruation. The extreme levels of CG produced by human embryos are the outcome of a long history of ‘grade inflation’: of selection on embryos to perform better at maternal examinations, regardless of their intrinsic quality, and of corresponding escalation of the ‘passing grade’ to maintain quality control.

While in theory CG could remain honest, as an index of protein synthesis and glycosylation, embryos have found deceptive means to increase CG concentrations regardless of their quality. Primate embryos evolved at least two initially ‘dishonest’ test-taking strategies: duplications of β CG genes and extended half-lives of CG (Figure 1B,C). There are six copies of β CG in each haploid human genome and three in rhesus macaques [49]. Before an increased number of gene copies became fixed in an ancestral population, embryos with more gene copies had

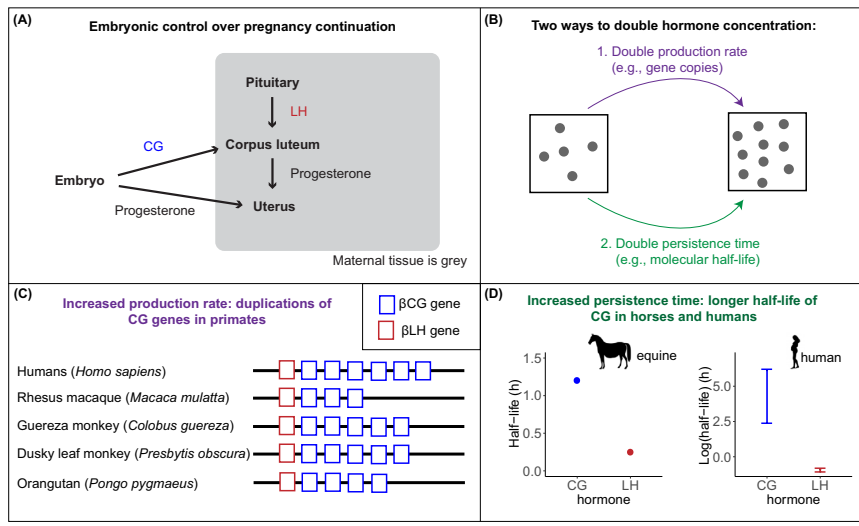


Figure 1. Hormone Signaling during Pregnancy Reflects an Evolutionary Arms Race between Embryos and Mothers, Causing Elaborate Signals. (A) In most mammals, pregnant females produce luteinizing hormone (LH) in their anterior pituitary, which causes the corpus luteum to produce progesterone (thus maintaining the endometrial lining rather than shedding it and the embryo). By withdrawing LH, she could terminate a pregnancy. But over evolutionary time, embryos seized control by producing a biochemical analog of LH, chorionic gonadotropin (CG), thus allowing pregnancies to continue even if the maternal body reduces or withdraws all LH. Embryos also became an independent source of progesterone. (B) The standing concentration of a hormone within the maternal body can be increased in two ways: (1) by increasing the production rate (e.g., through gene duplications); and (2) by increasing the persistence time (e.g., the molecular half-life). (C) Primates have had many gene duplications of β CG from an ancestral β LH gene [49]. (D) CG convergently evolved a much longer half-life in both equines and humans [51–54], allowing it to remain in circulation longer. Silhouette credits: horse (Openclipart, uncredited, public domain); woman (publicdomainpictures.net, credit Tanya Hall, public domain).

an ‘unfair’ advantage relative to embryos with fewer gene copies. Second, CG has evolved to have a much longer half-life than ancestral LH [51,57]. The half-life of LH is around 21–25 minutes, while that of hCG varies from 11 to 462 hours [51–53] because of a C terminal peptide of β CG that is absent in β LH [58–63]. An extended half-life increases the effective concentration of a hormone for the same rate of production. Therefore, the novel, longer-lived C terminal peptide would initially have given an ‘unfair’ advantage to embryos that possessed the peptide relative to those that retained the ancestral CG with a much shorter half-life. A similar C terminal peptide that extends half-life has evolved independently for the CG-LH of horses [50]. The half-life of equine CG is further extended relative to equine LH by differential glycosylation. As a result, equine LH is removed from circulation 5.7 times more rapidly than equine CG (when equine LH and equine CG were injected into horse liver and kidney, 75% of CG but only 25% of LH remained in circulation after 30 minutes [54]; Figure 1D).

In summary, to pass maternal tests embryos found shortcuts that were decoupled from their intrinsic quality. The predicted maternal countermeasure, in evolutionary time, was to adjust upward the amount of CG required to maintain pregnancy which, in turn, favored increased embryonic production of CG. The predicted, and observed, outcome of this coevolution of proxy and test is an escalation to high levels of production of placental hormones with decreasing maternal responsiveness [45]. This coevolutionary arms race explains the ‘bewildering’ lack of coherence in placental structure and physiology across mammals [47].

Concluding Remarks: Why Are Placentas Like Birds-of-Paradise?

Placentas must achieve a simple task: passing goods between mother and fetus. It should be a piece of cake. But placentas are wildly diverse across mammals, ‘evolving and experimenting at a disturbingly rapid pace’ [47], reminiscent of the bizarre diversity of birds-of-paradise [64]. Pregnancy in placental mammals is a case of antagonistic coevolution between signaler and receiver. The sensory onslaughts of placental hormones in embryo choice, and fantastic ornaments in mate choice, are outcomes of arms races between examiners and examinees in the context of high-stakes testing.

Elaborate mating displays and hormone signals during pregnancy are analogous to burdensome socio-economic evaluations and regulations: in all cases, a fundamental conflict of interest promotes rapid escalation and elaboration between examiners and examinees. Many researchers of mate choice have described this arms race, but the framework has not been widely adopted. Researchers investigating honest signals should expect, and look for, deception and arms races. Embryo selection, described herein, supports the theory that one source of rapid elaboration and escalation in evolutionary biology is the proxy treadmill.

In addition, embryo–maternal relations are not typically considered to be conflictual, nor even are hormones produced during pregnancy typically considered as signals between two individuals with differing evolutionary interests. Research on mate choice provides a strong framework to interpret pregnancy as a high-stakes testing bed for embryos, rife with manipulation and deception.

The proxy treadmill framework offers several predictions. We predict that in lineages where placental hormones have evolved to manipulate maternal physiology (e.g., placental CG as a mimic of maternal LH to extend pregnancy and prevent termination), maternal receptors will demonstrate rapid evolution of the binding sites to resist embryonic manipulation. Likewise, we hypothesize that females who judge males on the quality of sensory displays will have evolved heightened sensory perception over relevant domains (e.g., discriminating yellow wavelengths if males have a yellow color display). We suggest that in lineages where the stakes are particularly high (e.g., mating success rates are very low), the choosing sex will come to rely on multiple independent quality signals as predicted by Campbell [5] in the socio-economic context. We also predict that enhancers should frequently evolve to ‘honest’ signals (those with some well-understood physiological link to quality). For example, carotenoid-colored feathers should be accompanied by structural modifications that enhance the color. Finally, we predict that illusions will tend to evolve in quality signaling pathways, such as placental hormones that mimic maternal hormones or optical illusions [90,91] in visual displays.

We suggest that Campbell’s law applies to biology in many additional contexts related to embryo choice. For example, some marsupials give birth to more young than the pouch contains nipples, causing a high-stakes race to the teat. Northern quoll *Dasyurus hallucatus* have eight teats but up to 17 neonates immediately after the birth scramble; in one case, all losers in the race for a teat had disappeared 12 hours after birth [65]. Do marsupial neonates show Campbellian adaptations to this high-stakes test? Plants, too, frequently initiate many more seeds than will ultimately come to maturity [66]. The Australian plants *Banksia* spp. are a particularly dramatic example: in *Banksia elegans*, fewer than one in a thousand zygotes develop into a provisioned seed [67]. Is this a (very) high-stakes quality test? Indeed, in the related *Banksia spinulosa*, researchers found that the parent plant was selectively aborting lower-quality embryos (i.e., aborting self-fertilized embryos, which are inferior to outcrossed embryos [68]).

Outstanding Questions

How prevalent are deceptive signals in surveys of wild animal populations?

What sorts of signals are more resistant to deception?

Do successful tests maintain value by eliminating the bottom of the distribution or by discriminating at the top?

Are preferred signals with a long history in a clade ('basal' signals) more likely to be: (i) inherently honest and resistant to deception; or (ii) aesthetic residue (not condition-dependent), having uncoupled from true quality long ago by the proxy treadmill?

Do species with more exaggerated signaling traits also have more numerous signals of quality (in both mate choice and embryo selection)?

Both mate choice and embryo choice are selective sieves determining whose genes persist and whose disappear. The stakes could not be higher. And as every poker player will tell you, when the stakes are high, you cannot trust anyone.

Acknowledgments

We are very grateful to two anonymous reviewers for their feedback. We would like to thank John Christy for particularly useful feedback, including suggesting the terminology ‘aesthetic residue’ and suggesting multiple specific predictions and outstanding questions. We are grateful to Arvid Ågren, Pavitra Muralidhar, Carl Veller, and Inbar Mayaan for comments on the manuscript. D.E.M.’s research is conducted with Government support under and awarded by DoD, Air Force Office of Scientific Research, National Defense Science and Engineering Graduate (NDSEG) Fellowship, 32 CFR 168a. D.E.M. is also supported by a Theodore H. Ashford Graduate Fellowship.

References

- Goldstein, H. (2004) Education for all: the globalization of learning targets. *Comp. Educ.* 40, 7–14
- Jacob, B. (2005) Accountability, incentives and behavior: evidence from school reform in Chicago. *J. Public Econ.* 89, 761–796
- Macfadyen, L.P. et al. (2014) Embracing big data in complex educational systems: the learning analytics imperative and the policy challenge. *Res. Pract. Assess.* 9, 17–28
- Goodhart, C.A.E. (1983) *Monetary Theory and Practice: The UK-Experience*. Macmillan International Higher Education
- Campbell, D.T. (1979) Assessing the impact of planned social change. *Eval. Program Plann.* 2, 67–90
- Strathern, M. (1997) ‘Improving ratings’: audit in the British University system. *Eur. Rev.* 5, 305–321
- Hausein, S. et al. (2016) Tweets as impact indicators: examining the implications of automated “bot” accounts on Twitter. *J. Assoc. Inf. Sci. Technol.* 67, 232–238
- Maynard-Smith, J. and Harper, D. (2003) *Animal Signals*. Oxford University Press
- Johnstone, R.A. and Grafen, A. (1993) Dishonesty and the handicap principle. *Anim. Behav.* 46, 759–764
- Guilford, T. and Dawkins, M.S. (1991) Receiver psychology and the evolution of animal signals. *Anim. Behav.* 42, 1–14
- Krebs, J.R. and Dawkins, R. (1984) Animal signals: mindreading and manipulation. In *Behavioural Ecology: An Evolutionary Approach* (Krebs, J.R. and Davies, N., eds), pp. 380–402, Blackwell Scientific Publication
- Dawkins, M.S. and Guilford, T. (1991) The corruption of honest signalling. *Anim. Behav.* 41, 865–873
- Hill, G.E. (1994) Trait elaboration via adaptive mate choice: sexual conflict in the evolution of signals of male quality. *Ethol. Ecol. Evol.* 6, 351–370
- Endler, J.A. and Basolo, A.L. (1998) Sensory ecology, receiver biases and sexual selection. *Trends Ecol. Evol.* 13, 415–420
- Dawkins, M.S. and Guilford, T. (1996) Sensory bias and the adaptiveness of female choice. *Am. Nat.* 148, 937–942
- Prum, R.O. (2012) Aesthetic evolution by mate choice: Darwin’s really dangerous idea. *Philos. Trans. R. Soc. B Biol. Sci.* 367, 2253–2265
- Lande, R. (1981) Models of speciation by sexual selection on polygenic traits. *Proc. Natl. Acad. Sci. U. S. A.* 78, 3721–3725
- Kirkpatrick, M. (2006) Sexual selection and the evolution of female choice. *Evolution (N. Y.)* 36, 1–12
- Kirkpatrick, M. and Ryan, M.J. (1991) The evolution of mating preferences and the paradox of the lek. *Nature* 350, 33–38
- Fisher, R.A. (1999) *The Genetical Theory of Natural Selection: A Complete Variorum Edition*. Oxford University Press
- Hill, G.E. (2015) Sexiness, individual condition, and species identity: the information signaled by ornaments and assessed by choosing females. *Evol. Biol.* 42, 251–259
- Zahavi, A. (1975) Mate selection—a selection for a handicap. *J. Theor. Biol.* 53, 205–214
- Walker-Bolton, A.D. and Parga, J.A. (2017) “Slink flirting” in ring-tailed lemurs (*Lemur catta*): male olfactory displays to females as honest, costly signals. *Am. J. Primatol.* 79, e22724
- Olson, V.A. and Owens, I.P.F. (1998) Costly sexual signals: are carotenoids rare, risky or required? *Trends Ecol. Evol.* 13, 510–514
- Weaver, R.J. et al. (2018) Carotenoid metabolism strengthens the link between feather coloration and individual quality. *Nat. Commun.* 9, 73
- Weaver, R.J. et al. (2017) What maintains signal honesty in animal colour displays used in mate choice? *Philos. Trans. R. Soc. B Biol. Sci.* 372, 20160343
- Fisher, R.A. (1915) The evolution of sexual preference. *Eugen. Rev.* 7, 184–192
- Williams, G.C. (1966) Natural selection, the costs of reproduction, and a refinement of Lack’s principle. *Am. Nat.* 100, 687–690
- Dawkins, R. and Krebs, J.R. (1978) Animal signals: information or manipulation. In *Behavioural Ecology: An Evolutionary Approach* (Krebs, J.R. and Davies, N., eds), pp. 282–309, Blackwell Scientific Publication
- Wickler, W. (1965) Mimicry and the evolution of animal communication. *Nature* 208, 519
- Wickler, W. (1968) *Mimicry in Plants and Animals*. Weidenfeld & Nicolson
- Parker, G.A. (2006) Sexual conflict over mating and fertilization: an overview. *Philos. Trans. R. Soc. London B Biol. Sci.* 361, 235–259
- Burk, T. (1988) Acoustic signals, arms races and the costs of honest signalling. *Florida Entomol.* 71, 400
- Ghislandi, P.G. et al. (2017) Silk wrapping of nuptial gifts aids cheating behaviour in male spiders. *Behav. Ecol.* 28, 744–749
- Burk, T. (1981) Signaling and sex in acalyptate flies. *Florida Entomol.* 64, 30–43
- Backwell, P.R.Y. et al. (2000) Dishonest signalling in a fiddler crab. *Proc. R. Soc. London B Biol. Sci.* 267, 719–724
- Fineftter-Rosenbluh, I. and Levinson, M. (2015) What is wrong with grade inflation (if anything)? *Philos. Inq. Educ.* 23, 3–21
- Stroebe, W. (2016) Why good teaching evaluations may reward bad teaching: on grade inflation and other unintended consequences of student evaluations. *Perspect. Psychol. Sci.* 11, 800–816
- Macklon, N.S. and Brosens, J.J. (2014) The human endometrium as a sensor of embryo quality. *Biol. Reprod.* 91, 1–8
- Buchholz, J.T. (1922) Developmental selection in vascular plants. *Bot. Gaz.* 73, 249–286
- Haig, D. (1990) Brood reduction and optimal parental investment when offspring differ in quality. *Am. Nat.* 136, 550–556
- Wilcox, A.J. et al. (1988) Incidence of early loss of pregnancy. *N. Engl. J. Med.* 319, 189–194
- Roberts, C.J. and Lowe, C.R. (1975) Where have all the conceptions gone? In *Problems of Birth Defects* (Persaud, T.V.N., ed), pp. 148–150, Springer
- Haig, D. (1993) Genetic conflicts in human pregnancy. *Q. Rev. Biol.* 68, 495–532
- Haig, D. (1996) Altercation of generations: genetic conflicts of pregnancy. *Am. J. Reprod. Immunol.* 35, 226–232
- Haig, D. (2019) Cooperation and conflict in human pregnancy. *Curr. Biol.* 29, R455–R458
- Roberts, R.M. (1996) Interferon- α and pregnancy. *J. Interf. Cytokine Res.* 16, 271–273
- Csapo, A.I. et al. (1972) The significance of the human corpus luteum in pregnancy maintenance. I. Preliminary studies. *Am. J. Obstet. Gynecol.* 112, 1061–1067
- Maston, G.A. and Ruvolo, M. (2002) Chorionic gonadotropin has a recent origin within primates and an evolutionary history of selection. *Mol. Biol. Evol.* 19, 320–335

50. Sherman, G.B. *et al.* (1992) A single gene encodes the beta-subunits of equine luteinizing hormone and chorionic gonadotropin. *Mol. Endocrinol.* 6, 951–959
51. Casarini, L. *et al.* (2018) Two hormones for one receptor: evolution, biochemistry, actions, and pathophysiology of LH and hCG. *Endocr. Rev.* 39, 549–592
52. Cole, L.A. (2012) HCG, five independent molecules. *Clin. Chim. Acta* 413, 48–65
53. Yen, S.S. *et al.* (1968) Disappearance rates of endogenous luteinizing hormone and chorionic gonadotropin in man. *J. Clin. Endocrinol. Metab.* 28, 1763–1767
54. Smith, P.L. *et al.* (1993) Equine lutropin and chorionic gonadotropin bear oligosaccharides terminating with SO4-4-GalNAc and Sia alpha 2,3Gal, respectively. *J. Biol. Chem.* 268, 795–802
55. Haig, D. (1999) Genetic conflicts of pregnancy and childhood. In *Evolution in Health and Disease* (Stearns, S.C., ed.), pp. 77–90, Oxford University Press
56. Zeleznik, A.J. (1998) In vivo responses of the primate corpus luteum to luteinizing hormone and chorionic gonadotropin. *Proc. Natl. Acad. Sci. U. S. A.* 95, 11002–11007
57. Henke, A. and Grönoll, J. (2008) New insights into the evolution of chorionic gonadotrophin. *Mol. Cell. Endocrinol.* 291, 11–19
58. Furuhashi, M. *et al.* (1995) Fusing the carboxy-terminal peptide of the chorionic gonadotropin (CG) beta-subunit to the common alpha-subunit: retention of O-linked glycosylation and enhanced in vivo bioactivity of chimeric human CG. *Mol. Endocrinol.* 9, 54–63
59. Risma, K.A. *et al.* (1995) Targeted overexpression of luteinizing hormone in transgenic mice leads to infertility, polycystic ovaries, and ovarian tumors. *Proc. Natl. Acad. Sci. U. S. A.* 92, 1322–1326
60. Joshi, L. *et al.* (1995) Recombinant thyrotropin containing a β-subunit chimera with the human chorionic gonadotropin-β carboxy-terminus is biologically active, with a prolonged plasma half-life: role of carbohydrate in bioactivity and metabolic clearance. *Endocrinology* 136, 3839–3848
61. Lapolt, P.S. *et al.* (1992) Enhanced stimulation of follicle maturation and ovulatory potential by long acting follicle-stimulating hormone agonists with extended carboxyl-terminal peptides. *Endocrinology* 131, 2514–2520
62. Fares, F. *et al.* (2007) Development of a long-acting erythropoietin by fusing the carboxyl-terminal peptide of human chorionic gonadotropin β-subunit to the coding sequence of human erythropoietin. *Endocrinology* 148, 5081–5087
63. Fares, F.A. *et al.* (1992) Design of a long-acting follitropin agonist by fusing the C-terminal sequence of the chorionic gonadotropin beta subunit to the follitropin beta subunit. *Proc. Natl. Acad. Sci. U. S. A.* 89, 4304–4308
64. Laman, T. and Scholes, E. (2012) *Birds of Paradise: Revealing the World's Most Extraordinary Birds*, National Geographic Books
65. Nelson, J.E. and Gemmell, R.T. (2003) Birth in the northern quoll, *Dasyurus hallucatus* (Marsupialia: Dasyuridae). *Aust. J. Zool.* 51, 187–198
66. Stephenson, A.G. (1981) Flower and fruit abortion: proximate causes and ultimate functions. *Annu. Rev. Ecol. Syst.* 12, 253–279
67. Lamont, B.B. and Barrett, G.J. (1988) Constraints on seed production and storage in a root-suckering Banksia. *J. Ecol.* 76, 1069–1082
68. Vaughton, G. and Carthew, S.M. (1993) Evidence for selective fruit abortion in *Banksia spinulosa* (Proteaceae). *Biol. J. Linn. Soc.* 50, 35–46
69. McKee, M. (2004) Not everything that counts can be counted; not everything that can be counted counts. *BMJ* 328, 153
70. Braganza, O. (2018) Proxeconomics, an agent based model of Campbell's law in competitive societal systems. *arXiv Prepr. arXiv1803.00345*
71. Fire, M. and Guestrin, C. (2018) Over-Optimization of Academic Publishing Metrics: Observing Goodhart's Law in Action. *arXiv*, 1809.07841
72. Head, M.L. *et al.* (2015) The extent and consequences of p-hacking in science. *PLoS Biol.* 13, e1002106
73. Nguyen, P.K. *et al.* (2016) A systematic comparison of sugar content in low-fat vs regular versions of food. *Nutr. Diabetes* 6, e193
74. Clark, H.L. and Backwell, P.R.Y. (2016) Male mating success in a fiddler crab: a lesson in sample sizes. *J. Ethol.* 34, 119–126
75. Christy, J.H. and Rittschof, D. (2010) Deception in visual and chemical communication in crustaceans. In *Chemical Communication in Crustaceans*, pp. 313–333, Springer
76. Gasparini, C. *et al.* (2013) Do unattractive friends make you look better? Context-dependent male mating preferences in the guppy. *Proc. Biol. Sci.* 280, 20123072
77. Funk, D.H. and Tallamy, D.W. (2000) Courtship role reversal and deceptive signals in the long-tailed dance fly, *Rhamphomyia longicauda*. *Anim. Behav.* 59, 411–421
78. Albo, M.J. *et al.* (2011) Worthless donations: male deception and female counter play in a nuptial gift-giving spider. *BMC Evol. Biol.* 11, 329
79. Preston-Matham, K.G. (1999) Courtship and mating in *Empis (Xanthempis) trigramma* Meig., *E. tessellata* F. and *E. (Polyblepharis) opaca*F. (Diptera: Empididae) and the possible implications of 'cheating' behaviour. *J. Zool.* 247, 239–246
80. Gosling, L.M. and Roberts, S.C. (2001) Scent-marking by male mammals: cheat-proof signals to competitors and mates. *Adv. Study Behav.* 30, 169–217
81. Alberts, A.C. (2002) Constraints on the design of chemical communication systems in terrestrial vertebrates. *Am. Nat.* 139, S62–S89
82. Sharpe, L.L. (2015) Handstand scent marking: height matters to dwarf mongooses. *Anim. Behav.* 105, 173–179
83. Sharpe, L.L. *et al.* (2012) Handstand scent marking in the dwarf mongoose (*Helogale parvula*). *Ethology* 118, 575–583
84. McGuire, B. *et al.* (2018) Urine marking in male domestic dogs: honest or dishonest? *J. Zool.* 306, 163–170
85. Buchinger, T.J. *et al.* (2013) Evidence for a receiver bias underlying female preference for a male mating pheromone in sea lamprey. *Proc. Biol. Sci.* 280, 20131966
86. Christy, J.H. (1995) Mimicry, mate choice, and the sensory trap hypothesis. *Am. Nat.* 146, 171–181
87. Garcia, C.M. and Ramirez, E. (2005) Evidence that sensory traps can evolve into honest signals. *Nature* 434, 501–505
88. Buchinger, T.J. *et al.* (2017) Increased pheromone signaling by small male sea lamprey has distinct effects on female mate search and courtship. *Behav. Ecol. Sociobiol.* 71, 155
89. Brant, C.O. *et al.* (2016) Female sea lamprey shift orientation toward a conspecific chemical cue to escape a sensory trap. *Behav. Ecol.* 27, 810–819
90. Kelley, L.A. and Kelley, J.L. (2014) Animal visual illusion and confusion: the importance of a perceptual perspective. *Behav. Ecol.* 25, 450–463
91. Kelley, L.A. and Endler, J.A. (2012) Illusions promote mating success in great bowerbirds. *Science* 335, 335–338

What is a marmoset?

David Haig



6

Effects of Litter Size and Sex Composition in Callitrichine Monkeys

REPRINTED FROM: McCoy, D.E.*; Frye, B.M.*; Kotler, J.; Burkart, J.M.; Burns, M.; Embury, A.; Eyre, S.; Galbusera, P.; Hooper, J.; Idee, A. and Goya, A.L., 2019. A comparative study of litter size and sex composition in a large dataset of callitrichine monkeys. *American journal of primatology*, 81(9), p.e23038.

ARTICLE AND SUPPLEMENT AVAILABLE AT: <https://doi.org/10.1002/ajp.23038>

A comparative study of litter size and sex composition in a large dataset of callitrichine monkeys

Dakota E. McCoy^{1*}  | Brett M. Frye^{2*}  | Jennifer Kotler^{1,3} | Judith M. Burkart⁵ |
Monika Burns⁶ | Amanda Embury⁴ | Simon Eyre⁷ | Peter Galbusera⁸ |
Jacqui Hooper⁷ | Arun Idoe⁹ | Agustín López Goya¹⁰ | Jennifer Mickelberg¹¹ |
Marcos Peromingo Quesada¹⁰ | Miranda Stevenson¹² | Sara Sullivan¹³ |
Mark Warneke¹⁶ | Sheila Wojciechowski¹³ | Dominic Wormell¹⁴ | David Haig¹  |
Suzette D. Tardif¹⁵ 

¹Department of Organismic and Evolutionary Biology, Harvard University, Cambridge, Massachusetts

²Department of Biological Sciences, Clemson University, Clemson, South Carolina

³Department of Psychology, Harvard University, Cambridge, Massachusetts

⁴Department of Wildlife Conservation and Science, Zoos Victoria, Parkville, Victoria

⁵Department of Anthropology, University of Zurich, Zürich, Switzerland

⁶Division of Comparative Medicine, Massachusetts Institute of Technology, Cambridge, Massachusetts

⁷Wellington Zoo, Newtown, Wellington, New Zealand

⁸Centre for Research and Conservation (CRC), Royal Zoological Society of Antwerp (RZSA), Antwerp, Belgium

⁹Apenheul Primate Park, Apeldoorn, The Netherlands

¹⁰Zoology Department, Faunia-Parques Reunidos, Madrid, Spain

¹¹Animal Collections Department, Zoo Atlanta, Atlanta, Georgia

¹²Bristol Zoological Society, Bristol, UK

¹³Primate Department, Chicago Zoological Society, Brookfield, Illinois

¹⁴Mammal Department, Durrell Wildlife Conservation Trust, Channel Islands, UK

¹⁵Southwest National Primate Research Center, San Antonio, Texas

¹⁶Department of Animal Health, Chicago Zoological Society, Brookfield, Illinois

Correspondence

Dakota E. McCoy, Department of Organismic and Evolutionary Biology, Harvard University, 26 Oxford Street, MCZ #410, Haig Lab, Cambridge, MA 02138.
Email: dakotamccoy@g.harvard.edu

Funding information

Army Research Office; National Defense Science and Engineering Graduate (NDSEG) Fellowship, Grant/Award Number: 32 CFR 168a; Theodore H. Ashford Graduate Fellowship in the Sciences

Abstract

In many birds and mammals, the size and sex composition of litters can have important downstream effects for individual offspring. Primates are model organisms for questions of cooperation and conflict, but the factors shaping interactions among same-age siblings have been less-studied in primates because most species bear single young. However, callitrichines (marmosets, tamarins, and lion tamarins) frequently bear litters of two or more, thereby providing the opportunity to ask whether variation in the size and sex composition of litters affects development, survival, and reproduction. To investigate these questions, we compiled a large dataset of nine species of callitrichines ($n = 27,080$ individuals; *Callithrix geoffroyi*, *Callithrix jacchus*, *Cebuella pygmaea*, *Saguinus imperator*, *Saguinus oedipus*, *Leontopithecus chrysomelas*, *Leontopithecus chrysopygus*, *Leontopithecus rosalia*, and *Callimico goeldii*)

*Dakota E. McCoy and Brett M. Frye contributed equally to this work.

from zoo and laboratory populations spanning 80 years (1938–2018). Through this comparative approach, we found several lines of evidence that litter size and sex composition may impact fitness. Singletons have higher survivorship than litter-born peers and they significantly outperform litter-born individuals on two measures of reproductive performance. Further, for some species, individuals born in a mixed-sex litter outperform isosexually-born individuals (i.e., those born in all-male or all-female litters), suggesting that same-sex competition may limit reproductive performance. We also document several interesting demographic trends. All but one species (*C. pygmaea*) has a male-biased birth sex ratio with higher survivorship from birth to sexual maturity among females (although this was significant in only two species). Isosexual litters occurred at the expected frequency (with one exception: *C. pygmaea*), unlike other animals, where isosexual litters are typically overrepresented. Taken together, our results indicate a modest negative effect of same-age sibling competition on reproductive output in captive callitrichines. This study also serves to illustrate the value of zoo and laboratory records for biological inquiry.

KEY WORDS

birth sex ratio, callitrichine, litter size, sibling competition, studbook

1 | INTRODUCTION

Variation in the size and sex composition of litters can have important implications for the developmental, survival, and reproductive outcomes of individual offspring. Sibling number—that is litter size—often matters because individuals compete for a limited pool of parental resources. For example, Northern quoll (*Dasyurus hallucatus*) mothers have only eight teats but give birth to 17 neonates, inevitably generating winners and losers within each litter (Nelson & Gemmell, 2003). Wild European starling (*Sturnus vulgaris*) chicks raised in larger clutches weigh less than chicks raised in smaller clutches, and these disparities have important implications for immune functioning (Nettle et al., 2016). The sex composition of litters also can impose lasting outcomes, but the direction of these effects differs across taxa. In spotted hyenas (*Crocuta crocuta*), a species which exhibits facultative siblicide, all-female and all-male litters exhibit higher rates of aggression than do mixed-sex litters during infancy (Golla, Hofer, & East, 1999). In contrast, among humans, females born with male cotwins exhibit socioeconomic and reproductive shortcomings compared with females born with twin sisters (Bütikofer, Figlio, Karbownik, Kuzawa, & Salvanes, 2019). Thus, comparative study of litter composition may provide insight about the complex interplay of proximate and ultimate factors shaping variation in these traits.

Within primates, several lineages routinely produce litters (Leutenegger, 1979), thereby providing the opportunity to investigate the (a) mechanisms responsible for; (b) constraints associated with; and (c) consequences of varying litter size and sex composition. The callitrichines—marmosets, tamarins, and lion tamarins—are Neotropical monkeys that produce small litters (ranging from 1 to 5 in captivity; with the exception of the singleton-producing genus, *Callimico*) with

twins being the most common litter size (Digby, Ferrari, & Saltzman, 2011; Rutherford & Tardif, 2008; Tardif et al., 2003). Characteristics associated with litter composition can have lasting impacts on survival and reproduction. Indeed, triplets are unusual in the wild (Digby et al., 2011), and they often exhibit higher mortality than do offspring from smaller cohorts (Box & Hubrecht, 1987; Tardif et al., 2003; Ward, Buslov, & Vallender, 2014). However, in some species (i.e., *Callithrix jacchus*), captive mothers routinely produce larger litters because of excess energy stores, which impacts ovulation dynamics (Tardif, Layne, & Smucny, 2002). The sex composition of litters also may mediate individuals' developmental outcomes—for example, via exposure to sex hormones produced by males—but the overall evidence of such sex-related effects on development remains mixed (Bradley et al., 2016; De Moura, 2003; French et al., 2016; Frye, Rapaport, Melber, Sears, & Tardif, 2019; Rutherford, DeMartelly, Layne Colon, Ross, & Tardif, 2014).

Several other aspects of callitrichine biology may provide clues to the evolution and maintenance of particular litter compositions. Callitrichines breed cooperatively, whereby a dominant pair typically monopolizes reproduction and group members delay or forgo reproduction to rear offspring that are not necessarily their own (Digby et al., 2011). Breeding opportunities are thus a limited resource for which close relatives may compete (Henry, Hankerson, Siani, French, & Dietz, 2013; Saltzman, Digby, & Abbott, 2009). Broadly, male-male competition (often between brothers) is low, while many reports cite high levels of female-female competition (Abbott, Barrett, & George, 1993; Bicca-Marques, 2003; French & Inglett, 1989; Garber, Ón, Moya, & Pruetz, 1993; Haig, 1999; Kleiman, 1979; Roda & Pontes, 1998). Callitrichines are unusual among mammals for this intense female-female competition relative to males, accompanied by relatively larger reproductive skews in

females (French, Mustoe, Cavanaugh, & Birnie, 2013). Further, callitrichines are genetic chimeras because they share placental circulation that allows for the exchange of cells with their siblings in utero; this has uncertain implications for the interplay of conflict and cooperation within callitrichine groups (Haig, 1999). For all their unusual characteristics, members of this lineage present an opportunity to investigate the causes and consequences of variation in litter composition (i.e., sex composition and sizes).

Herein, we evaluated large demographic datasets ($n = 27,080$ individuals) of nine species of callitrichines living in captivity to examine multiple features that may be relevant to these traits: birth sex ratios, litter sizes, distributions of isosexual (i.e., all-male and all-female) versus mixed-sex litters, survivorship, and several measures of reproductive potential. Across these analyses, we explored the relationships between sibling sex, litter size, and phenotypic outcomes. We asked whether same- versus opposite-sex siblings impacted each other's phenotypic outcomes. Further, we investigated whether litter size itself, and thus potential sibling competition, shapes survival, and reproductive outcomes. Taken together, this examination of the links between litter composition and later life outcomes may advance our understanding of sibling interactions and intra-familial relationships writ large.

2 | METHODS

2.1 | Study subjects

We analyzed longitudinal demographic records of nine species of captive callitrichine primates: marmosets (*Callithrix geoffroyi*, *Callithrix jacchus*, and *Cebuella pygmaea*), tamarins (*Saguinus imperator* and *Saguinus oedipus*), lion tamarins (*Leontopithecus chrysopygus*, *Leontopithecus chrysomelas*, and *Leontopithecus rosalia*), and *Callimico goeldii*.

We obtained these data from international studbooks, national studbooks, university research programs, and national primate research centers (Table 1). Collectively, these records provide demographic information for captive callitrichines spanning an 80-year period (January 1938 to January 2018). These datasets included detailed demographic information about individuals' births, deaths, parentage, location, and causes of death; from this, we inferred litter sex composition, litter sizes, litter orders, and parity (i.e., primiparous or multiparous).

Much of these data come from zoo populations, which are typically managed through, for example, separating pairs or contraception. When animals are group-living, estimations of paternity are not always certain. Here, for the variables we are interested in, we assume that management practices would not bias our results. In our analyses using litter composition, we designated litters as isosexual (i.e., same-sex) or mixed-sex. We had some data points where one individual in a litter was of "unknown" sex, but the litter could still be designated as "mixed-sex" (e.g., a litter with sexes male, female, and unknown is designated MFU; see Table S1 for the numbers and sexes of individuals included in these analyses). We did not include animals born as singletons in our analyses of litter sex composition, because they likely gestated as twin or triplet litters of which we could not determine sibling sex (Jaquish, Tardif, Toal, & Carson, 1996). *Callimico* predominantly gives birth to singletons (Digby et al., 2011), so we excluded *Callimico* from all analyses of within-cohort sibling competition.

For our analyses of litter size, we compare offspring across four litter size categories: singletons, twins, triplets, and quad + (quadruplets, quintuplets, and sextuplets). We note that the production of triplet and larger litters probably represents an artifact of captivity: heavier, captive mothers ovulate more eggs, leading to the production of supernumerary offspring in energy-rich environments (Tardif

TABLE 1 Sources of data, with basic demographic information, for each species

Species	Common name	Studbook source	F	M	U	Prop. F	Prop. M
<i>Callimico goeldii</i>	Goeldi's marmoset	Chicago Zoological Society	1,427	1,534	504	0.482	0.518
<i>Callithrix geoffroyi</i>	White-headed marmoset	Chicago Zoological Society	1,160	1,283	575	0.475	0.525
<i>Callithrix jacchus</i>	Common marmoset	University of Zurich, Southwest National Primate Research Center, Massachusetts Institute of Technology	1,731	1,800	1,857	0.490	0.510
<i>Cebuella pygmaea</i>	Pygmy marmoset	Australasian Species Management Program	148	147	73	0.502	0.498
<i>Leontopithecus chrysomelas</i>	Golden-headed lion tamarin	European Association of Zoos and Aquaria	1,625	1,795	405	0.475	0.525
<i>Leontopithecus chrysopygus</i>	Black lion tamarin	International Studbook, World Association of Zoos and Aquariums.	187	244	83	0.434	0.566
<i>Leontopithecus rosalia</i>	Golden lion tamarin	Association of Zoos & Aquariums	1,136	1,370	616	0.453	0.547
<i>Saguinus imperator</i>	Emperor tamarin	Chicago Zoological Society	179	217	86	0.452	0.548
<i>Saguinus oedipus</i>	Cotton-top tamarin	Australasian Species Management Program	2,553	2,892	1,453	0.469	0.531
Overall			10,146	11,282	5,652	0.473	0.527

Note: numbers of male (M), female (F), animals of unknown sex (U), and proportions of each sex.

et al., 2002). However, while callitrichine mothers rarely raise more than two infants (Digby et al., 2011), surviving infants exhibit phenotypes that provide clues to the potential constraints stemming from early environments (e.g., Rutherford et al., 2014). Thus, we included triplet and quad+ animals in our sample to provide a complete accounting of reproductive outcomes.

Since our data consisted of archival data, we did not perform an Institutional Care and Use Committee review. However, all the institutions from which the data were sourced adhere to all national, international, and American Society of Primatologists' guidelines for the ethical treatment of nonhuman primates.

2.2 | Population birth sex ratios & litter sizes

To investigate whether sex ratios at birth diverged from an overall 1:1 birth sex ratio (BSR), we employed a χ^2 Goodness-of-Fit test. To calculate the effect size, we used the function `ES.chisq.gof` in the R package "powerAnalysis" (Fan, 2017). We used the same procedure to investigate whether sex ratios differed by litter size.

To supplement these analyses, we examined interspecific variation in BSR and litter sizes using an ancestral state phylogenetic reconstruction, a method which can uncover the likely ancestral state of a continuous trait (Revell, 2012, 2013). We used the maximum-likelihood Callitrichine tree from Garbino and Martins-Junior (2018) as our reference phylogeny, which included all the species studied except *L. chrysopygus*. Therefore, we added a tip for *L. chrysopygus*, relying on the pairwise genetic distances reported from a phylogeny of lion tamarins (Mundy & Kelly, 2001). We then reconstructed the evolutionary history of population BSR (expressed as the proportion of males in the dataset by species) and mean litter sizes via the `contMap` and `fastAnc` functions in `phytools` v. 0.6-44 (Revell, 2012, 2013), including a 95% confidence interval for all inferred node states. Briefly, this program estimates the ancestral value of characters (i.e., how big were litters in the common ancestor of two species?), using maximum likelihood to estimate states at internal nodes, and interpolates these states along internal branches (Felsenstein, 1985).

For our ancestral state reconstruction of litter sizes, we included four noncallitrichine platyrhine species with singleton births as outgroups (to represent that most New World monkeys give birth to singletons); these were *Saimiri sciureus*, *Cebus apella*, *Aotus azarae*, and *Callicebus nigrifrons* (Mittermeier, Rylands, & Wilson, 2013).

2.3 | Litter distributions: sex composition

To investigate whether the distribution of litter sex compositions differed from that which was expected, we first used the overall BSR of each callitrichine species to calculate the expected proportions of each litter type (excluding litters with offspring of unknown sex). Then we used a χ^2 Goodness-of-Fit test to inspect the distributions of both twin (i.e., FF, MF, MM) and triplet (MMM, MMF, MFF, FFF) litters. We hypothesized that divergence between the observed and expected proportions may indicate sex-mediated competition in

utero: for example, disproportionate production of isosexual litters suggests a selective advantage. *Callimico* was excluded from these analyses.

2.4 | Survivorship

We explored how litter composition (sex of siblings) and litter size (number of siblings) impacted survivorship profiles. We restricted our analyses to the period before full-adulthood (sexual maturity), the stage at which both captive and free-ranging callitrichines face the highest risk of death (Kohler, Preston, & Lackey, 2006; Soini, 1982; Ward et al., 2014). In addition, both male and female callitrichines may disperse from natal groups around the time of sexual maturation (Digby et al., 2011). As such, interactions among same-aged siblings may become less important determinants of fitness once siblings have dispersed from natal groups. Finally, for captive monkeys specifically, husbandry and management decisions to transfer animals around the time of sexual maturity (EAZA Husbandry Guidelines, 2010) may confound any findings of survivorship disparities because of transfer-associated mortality. Based on each of the callitrichine genera's different pace of development, we identified life stages and thus ages at which we censored data (Table S2). Despite these stages differing in absolute lengths (in days), each period is a conserved period of ontogenetic development across the callitrichine lineage (Díaz-Muñoz & Bales, 2015; Digby et al., 2011; Garber, Porter, Spross, & Di Fiore, 2015).

We constructed Cox proportional hazards regressions (Cox, 1972; Lee & Wang, 2003) using the "coxph" function in the R package "survival" (Therneau & Grambsch, 2000, 2013). We compared survivorship profiles of callitrichines for males and females that were born into isosexual and mixed-sex litters. We included litter size as a predictor variable to examine possible differences in the survivorship among infants born into a singleton, twin, triplet, or larger-sized litters (Box & Hubrecht, 1987; Rothe, Darms, & Koenig, 1992; Ward et al., 2014). Finally, we clustered individuals by dams to control for nonindependence among siblings, and we included the term "cluster(ID)" to account for any violations of the assumptions of proportional hazards. For post hoc analysis of the groups, we conducted multiple pairwise comparisons of the Kaplan-Meier survival curves using log-rank tests via the "pairwise.survdiff" function in the R package "survminer" (Kassambara & Kosinski, 2018). In these post hoc analyses, we used the Benjamini & Hochberg correction to minimize the risk of Type I errors while maintaining statistical power (Benjamini & Hochberg, 1995).

2.5 | Intergenerational effects

It is likely that a given callitrichine's litter composition at birth impacts its downstream reproductive output, due to developmental or social factors (e.g., Rutherford et al., 2014). To investigate this, we explored the relationships between a monkey's litter size and sex composition at birth and subsequent reproductive performance (measured as (a) whether or not an individual becomes a parent

and (b) the total number of offspring produced). First, we asked whether litter size matters: are singletons at an advantage compared with individuals born to larger litters, due to reduced competition for parental investment? Second, we asked whether litter composition matters: are animals born into a mixed-sex litter at an advantage compared with those in same-sex litters, due to reduced competition among littermates for reproductive opportunities? To answer these questions, for each species we calculated (a) the proportion of singletons in the female population ("Expected Proportion Singletons") and (b) the proportion of isosexual individuals (rather than mixed-sex) in the female population ("Expected Proportion Isosexual"). We did so for males as well. By the null hypothesis, assuming equal reproductive outputs for every individual, the observed proportion of singletons among dams should equal the expected proportion of singletons in the entire female population. Likewise, observed proportions should equal expected proportions for isosexual dams, singleton sires, and isosexual sires. We hypothesized that isosexuals would be underrepresented and singletons overrepresented among parents. To test our hypothesis, we performed χ^2 Goodness of Fit analyses to compare observed versus expected proportions of singletons and isosexual individuals for both dams and sires. To calculate the effect size, we used the function ES.chisq.gof in the R package "powerAnalysis" (Fan, 2017). Finally, we performed these analyses once for unique dams and unique sires (i.e., testing the binary outcome of whether or not an individual became a parent), and once for all dams and all sires allowing double-counting of individual dams and sires (i.e., testing the numerical outcome of the number of offspring produced).

3 | RESULTS

We compiled demographic records for a total of 27,080 individuals from 11 sources (research laboratories and zoos), representing five

genera and nine species of Callitrichinae (Table 1). Within each species, we conducted several analyses of the demographic, survival, and reproductive consequences of sibling competition. The exact sample sizes for each analysis differed, though, because not all animals were reproductively active. We also note that this dataset likely contains some variability stemming from data management protocols across institutions. We, therefore, discuss the outcomes of sibling interactions with the caveat that stochastic processes, including under-reporting of birth events, may impact these results. Table S1 outlines the numbers and sexes of individuals included in each analysis.

3.1 | Population birth sex ratios & litter sizes

All species except the pygmy marmoset (*C. pygmaea*) exhibited an overall male-biased BSR, with between 51 and 56 males being born for every 100 individuals (Table 2). However, the male bias was not statistically different from 1:1 for common marmosets (*C. jacchus*) and emperor tamarins (*S. imperator*). We did not find significant differences in sex ratios (compared with the overall BSR) among different litter sizes (Table S3).

We also performed ancestral state reconstructions to investigate and visualize the variation in population BSR (Figure 1a) and mean litter sizes (Figure 1b) across the callitrichine lineage. This technique can provide information about the inferred evolutionary history of traits. Two lion tamarin species (i.e., *L. rosalia* and *L. chrysopygus*) seemed to have evolved a high skew in overall sex ratio from an evolutionary history of more equal distribution. In contrast to the more divergent *Leontopithecus* spp., *Callithrix* species were closer to 50%.

Regarding litter sizes, callitrichines gave birth to litters ranging from 1 to 6 individuals (Figure 2 and Table S4). At one end of this spectrum, *Callimico* births were predominantly represented by singletons, whereas, *Callithrix* species exhibited the largest litter

TABLE 2 Birth sex ratios and sex ratios for animals that lived at least 14 days

Species	Birth						≥ 14 Days							
	F	M	Prop. F	Prop. M	χ^2	p	W	F	M	Prop. F	Prop. M	χ^2	p	W
<i>Callimico goeldii</i>	1,427	1,534	0.482	0.518	3.867	.049	0.036	1,140	1,195	0.488	0.512	1.296	.255	0.024
<i>Callithrix geoffroyi</i>	1,160	1,283	0.475	0.525	6.193	.013	0.050	1,014	1,052	0.491	0.509	0.699	.403	0.018
<i>Callithrix jacchus</i>	1,731	1,800	0.490	0.510	1.348	.246	0.020	1,507	1,508	0.500	0.500	0.000	.999	0.00
<i>Cebuella pygmaea</i>	148	147	0.502	0.498	0.003	.954	0.003	146	137	0.516	0.484	0.286	.593	0.032
<i>Leontopithecus chrysomelas</i>	1,625	1,795	0.475	0.525	8.450	.004	0.050	1,493	1,583	0.485	0.515	2.633	.105	0.029
<i>Leontopithecus chrysopygus</i>	187	244	0.434	0.566	7.538	.006	0.132	144	192	0.429	0.571	6.857	.009	0.143
<i>Leontopithecus rosalia</i>	1136	1,370	0.453	0.547	21.85	<.001	0.093	908	1,027	0.469	0.531	7.318	.007	0.061
<i>Saguinus imperator</i>	179	217	0.452	0.548	3.647	.056	0.096	124	135	0.479	0.521	0.467	.494	0.042
<i>Saguinus oedipus</i>	2,553	2,892	0.469	0.531	21.106	<.001	0.062	2,185	2,411	0.475	0.525	11.113	<.001	0.049
Overall	10,146	11,282	0.473	0.527				8,661	9,240	0.484	0.516			

Note: The χ^2 goodness-of-fit tests indicate divergence from an overall 1:1 birth sex ratio. We also provide (W) effect size estimates where values of 0.10, 0.30, and 0.50 indicate small, medium, and large effects, respectively (Cohen 1988). F, female; M, male. Bold values indicate $p < 0.05$. Italicized values indicate $p < 0.10$.

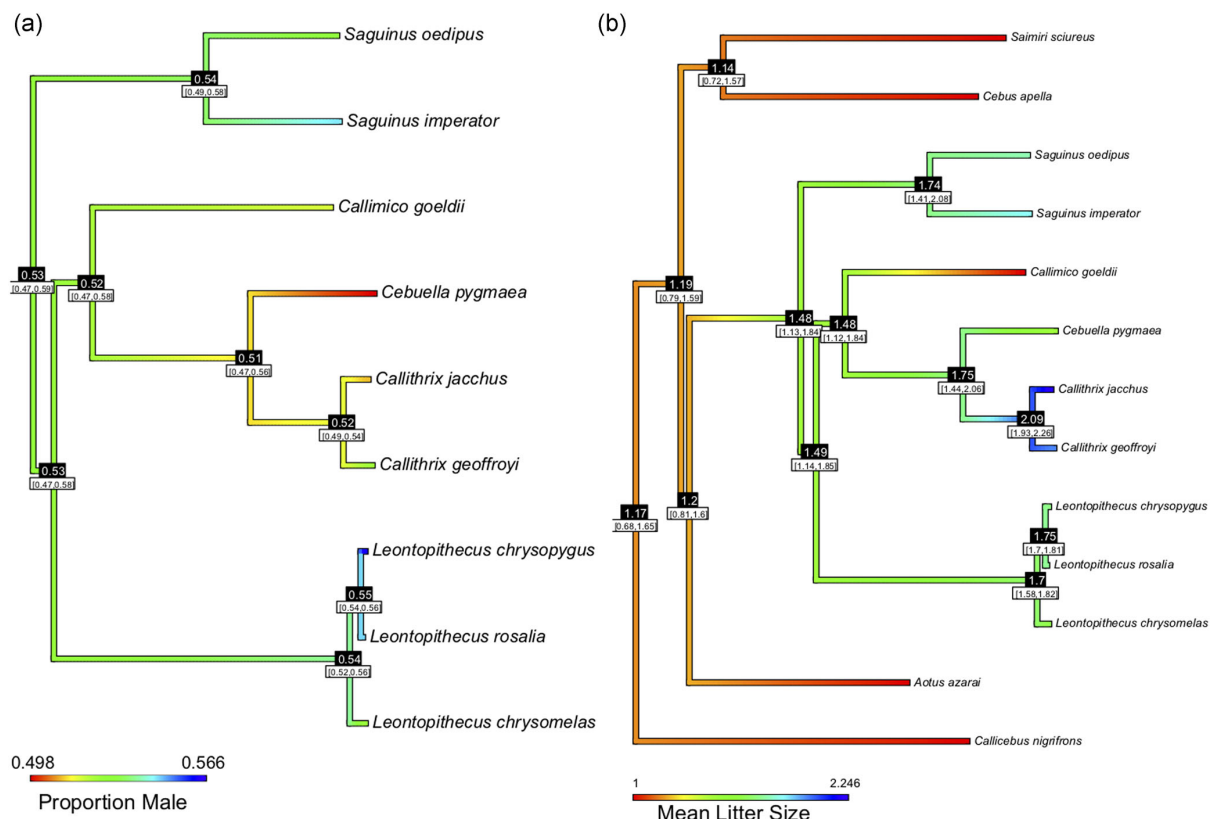


FIGURE 1 Ancestral state reconstruction of (a) sex ratios and (b) mean litter sizes in Callitrichine species on a maximum-likelihood tree from (Garbino & Martins-Junior, 2018), with *Leontopithecus chrysopygus* added from information in (Mundy & Kelly, 2001). (a) Warmer colors indicate birth sex ratios (BSR) that are closer to equality (1:1), whereas cooler colors indicate a male-biased sex ratio. (b) Warmer colors indicate a greater likelihood of producing singletons, whereas cooler colors represent larger litters. Numbers at nodes indicate inferred ancestral states, with a 95% confidence interval in brackets

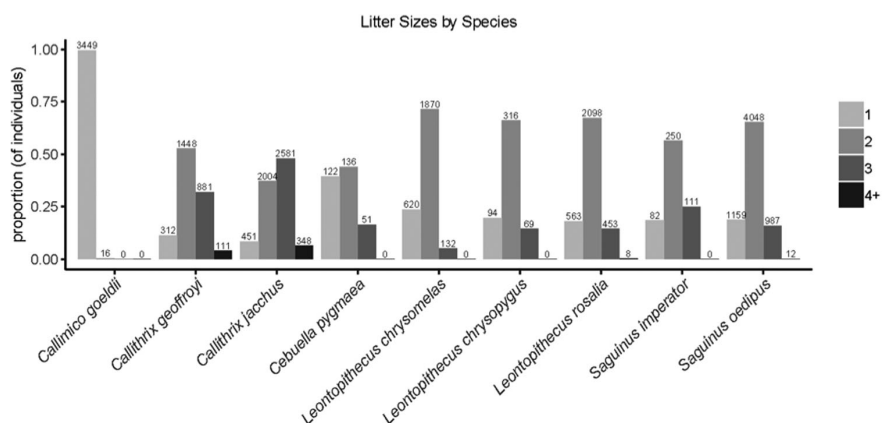


FIGURE 2 Callitrichines frequently have litters of 2–4 offspring. Proportions and counts for individuals born into litter sizes categories (i.e., singleton, twins, triplets, and quad+) by species. “4+” category includes individuals born into quadruplet, quintuplet, and sextuplet litters. Y-axis is the proportion of individuals born (i.e., not the proportion of litters birthed)

TABLE 3 A χ^2 goodness-of-fit test comparing the observed versus the expected counts of twin (i.e., FF, MF, MM) and triplet (i.e., MMM:MMF:MFF:FFF) litters based on the overall birth sex ratios for each species

Species	Prop. males	Prop. females	Twin litters			Triplet litters		
			χ^2	df	p	χ^2	df	p
<i>Callithrix geoffroyi</i>	0.525	0.475	0.793	2	.673	2.069	3	.558
<i>Callithrix jacchus</i>	0.510	0.490	1.343	2	.511	1.059	3	.787
<i>Cebuella pygmaea</i>	0.498	0.502	2.794	2	.247	3.269	3	.352
<i>Leontopithecus chrysomelas</i>	0.525	0.475	0.610	2	.737	1.285	3	.733
<i>Leontopithecus chrysopygus</i>	0.566	0.434	0.765	2	.682	1.637	3	.651
<i>Leontopithecus rosalia</i>	0.547	0.453	2.253	2	.324	0.380	3	.944
<i>Saguinus imperator</i>	0.548	0.452	0.695	2	.706	0.193	3	.979
<i>Saguinus oedipus</i>	0.531	0.469	2.879	2	.237	1.996	3	.573

Note: Litter distributions in callitrichines did not diverge from the expected values.

sizes, with 2.25 representing the average litter size in these genera. The *Saguinus* and *Leontopithecus*, spp. fell between these two extremes. The modal litter size was two in all species except *Callimico* and *Cebuella pygmaea*, for both of whom singleton litters were most common (i.e., in counting litters, litters of one offspring were more common than litters with two offspring).

3.2 | Litter distributions: sex composition

The sex distributions of neither twin nor triplet litters (i.e., MM:MF:FF or MMM:MMF:MFF:FFF) differed from the expected values based on the overall BSR observed in each callitrichine species (Table 3).

3.3 | Survivorship

Litter type (same-sex or mixed-sex) significantly impacted survivorship in a single species—*L. chrysomelas* (Table S5 and Figure S1). For members of this species, isosexual females exhibited significantly higher survivorship than all other groups. Survivorship based on litter types did not differ for the other species. However, while not statistically significant, isosexual females exhibited the highest survivorship probabilities for all the species (Table S6 and Figure S1). Irrespective of litter type, males and females, exhibited differences in the survival in the following species: *C. geoffroyi* and *L. rosalia*. By contrast, survivorship profiles between males and females were indistinguishable for *C. jacchus*, *L. chrysomelas*, *L. chrysopygus*, *C. pygmaea*, *S. imperator*, and *S. oedipus* (Table S7 and Figure 3). In the species in which significant differences in survivorship between the sexes existed, females exhibited a higher probability of surviving to sexual maturity than did males. Litter size was the strongest predictor of survivorship across the callitrichines (Table S5 and Figure S2). In all species surveyed, mortality increased with litter size (Table S8 and Figure S2). Histograms with age at death for each species are shown in Figure S3. The pygmy marmoset (*C. pygmaea*) had unusually high survivorship (Figure 3c), which may be an artefact of the studbook records or of life in captivity.

3.4 | Intergenerational effects

For the majority of callitrichine species, singletons outperformed individuals born in a litter on two measures of reproductive output. In both males and females, singletons gave rise to a disproportional percentage of all offspring and were overrepresented among unique sires and dams compared with litter-born peers (χ^2 Goodness of Fit; Figure 4 and Table S9).

For some, but not all, callitrichine species, isosexually-born individuals significantly underperformed on two measures of reproductive output (χ^2 Goodness of Fit; Figure 5 and Table S10). Isosexual parents gave rise to fewer offspring than expected for four species (dams) and three species (sires), more offspring than expected for *S. imperator* (both sires and dams), and otherwise did not differ from expectations. We also looked at all individuals and whether or not they became parents; we found that the proportion of parents who were born into isosexual litters was lower than expected for *C. jacchus* for both sires and dams. Taken together, this suggests a reproductive disadvantage for individuals born into isosexual litters. In cases where the observed proportion did not significantly deviate from expected, trends in the majority of cases supported this hypothesis.

4 | DISCUSSION

4.1 | Results summary

We analyzed whether litter size and sex composition impact survivorship and reproduction in callitrichine primates, using a large dataset of captive animals from nine species ($n = 27,080$ individuals). Litter size, irrespective of sibling sex, showed the strongest effect on callitrichine survival and reproduction: individuals born as singletons are more likely to survive and reproduce, perhaps due to the absence of sibling competition with litter-born peers or variation in processes associated with maternal energy allocation. In addition to litter size, we found small effects of litter sex composition (isosexual vs. mixed-sex) on reproductive outcomes: isosexual parents gave rise to a significantly lower proportion of offspring than expected for four

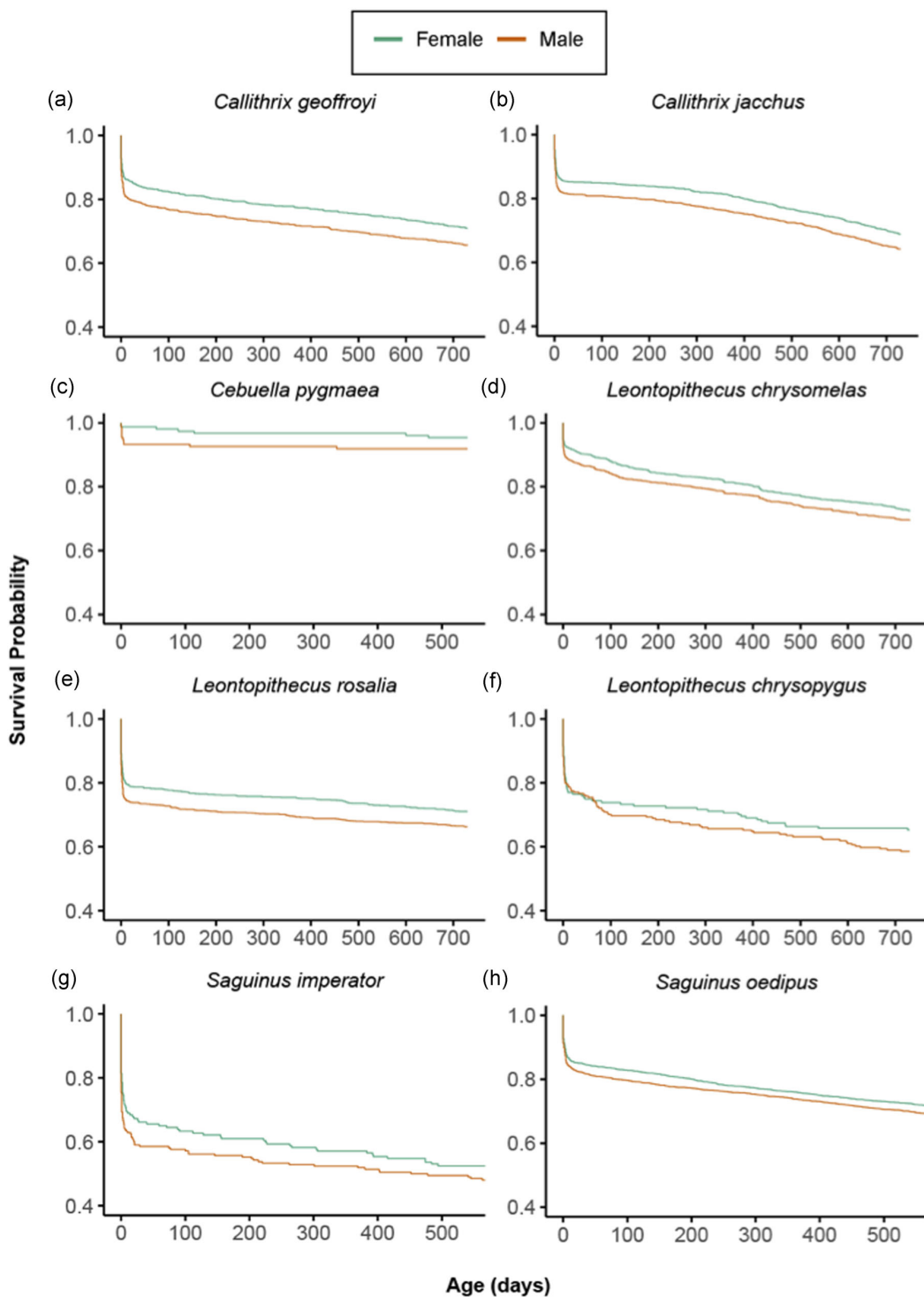


FIGURE 3 Females tend to have higher survivorship than males. Survivorship profiles of males and females from birth to sexual maturity for each callitrichine species: (a) *Callithrix geoffroyi*, (b) *Callithrix jacchus*, (c) *Cebuella pygmaea*, (d) *Leontopithecus chrysomelas*, (e) *Leontopithecus rosalia*, (f) *Leontopithecus chrysopygus*, (g) *Saguinus imperator*, and (h) *Saguinus oedipus*. Females exhibited significantly higher survival probabilities to sexual maturity in *Callithrix geoffroyi* (a) and *Leontopithecus rosalia* (e), whereas survivorship profiles between males and females were statistically indistinguishable for *Callithrix jacchus*, *Leontopithecus chrysopygus*, *Leontopithecus chrysomelas*, *Cebuella pygmaea*, *Saguinus imperator*, and *Saguinus oedipus*.

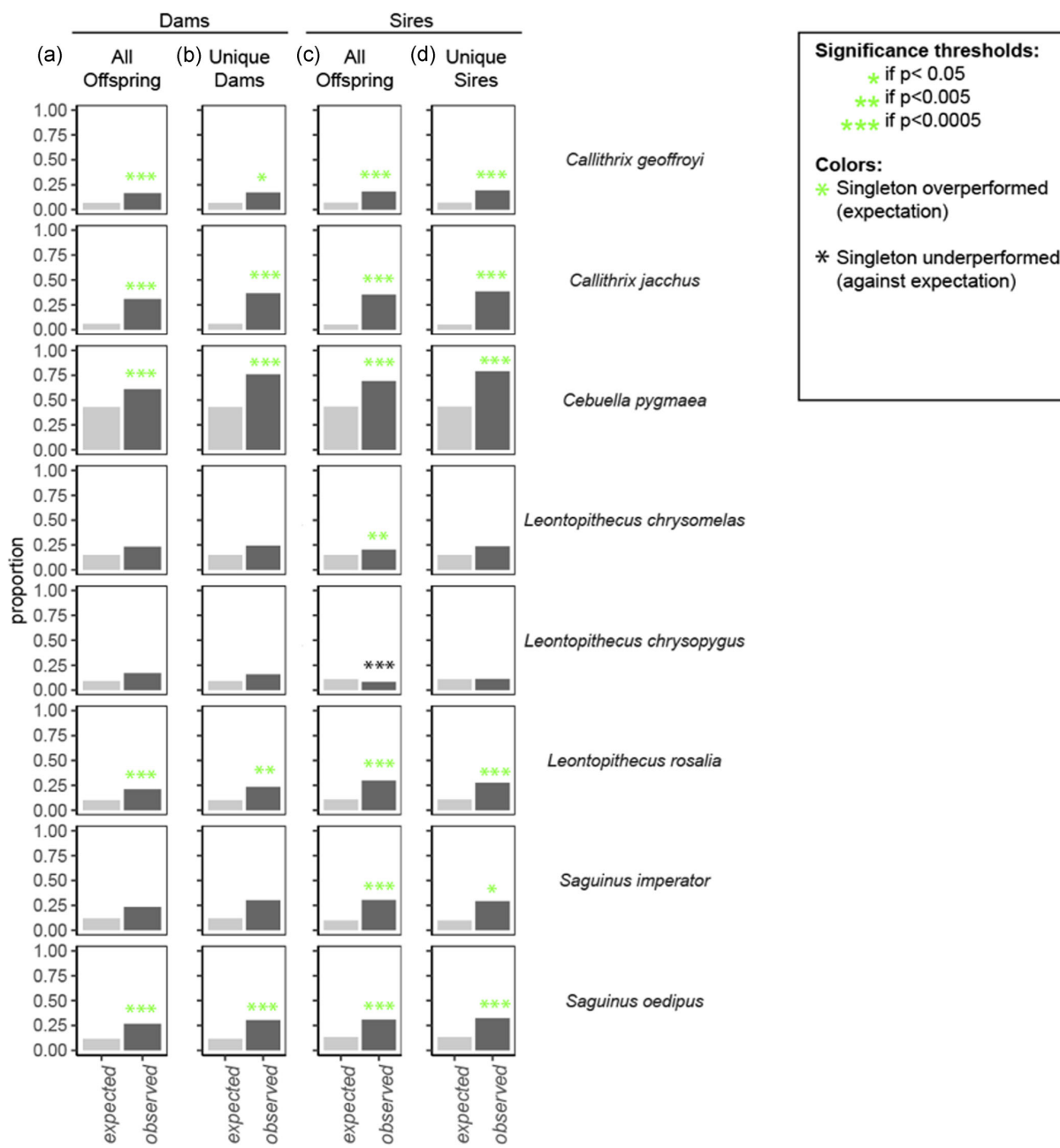


FIGURE 4 For most species, singletons had a better reproductive performance than litter-born individuals. (a) Singleton dams bore more offspring than expected for five species: *Callithrix geoffroyi*, *Callithrix jacchus*, *Cebuella pygmaea*, *Leontopithecus rosalia*, and *Saguinus oedipus*. (b) Singletons were overrepresented among unique dams for five species: *Callithrix geoffroyi*, *Callithrix jacchus*, *Cebuella pygmaea*, *Leontopithecus rosalia*, and *Saguinus oedipus*. (c) Singleton sires fathered more offspring than expected for seven of eight species, with the opposite trend in *Leontopithecus chrysopygus*. (d) Singletons were overrepresented among unique sires for six of eight species: *Callithrix geoffroyi*, *Callithrix jacchus*, *Cebuella pygmaea*, *Leontopithecus rosalia*, *Saguinus imperator*, and *Saguinus oedipus*. For p values, χ^2 statistics, counts, and effect sizes see Table S9.

species (dams) and three species (sires). The majority of nonsignificant trends supported this observation, but in one species with a low sample size (*S. imperator*) isosexual sires and dams significantly overperformed reproductively. Unlike litter size, litter sex composition generally did not impact survivorship from birth to sexual

maturity. Although most mammals have more isosexual litters than expected, here we found that all but one species (*C. pygmaea*) have the expected distributions of litter sex compositions. In addition to analyses of litter characteristics, we confirmed a male-biased BSR for all but three species and found that females had higher probabilities

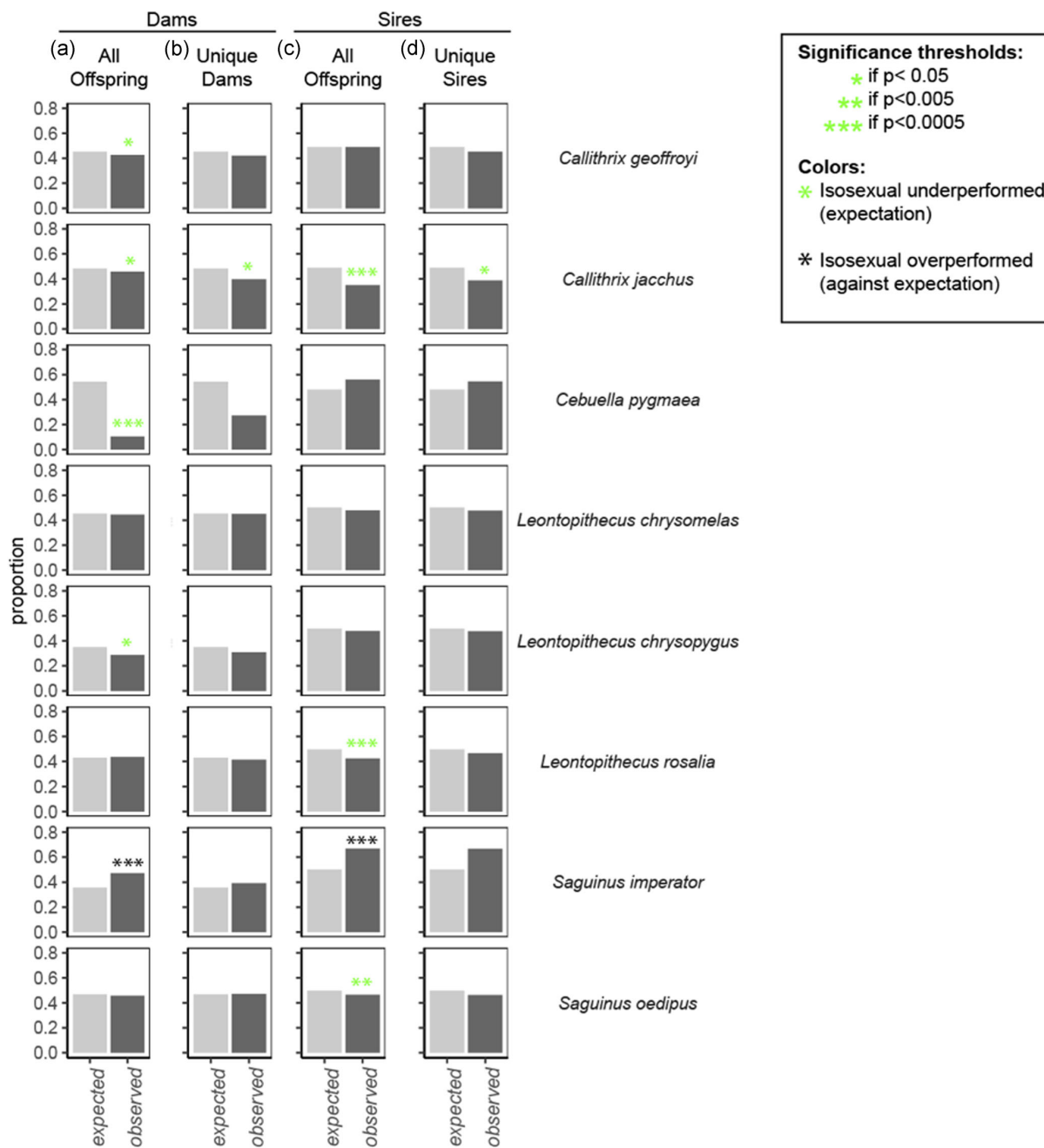


FIGURE 5 For some species, parents born into an isosexual litter had a worse reproductive performance than parents born into a mixed-sex litter. (a) Isosexual dams bore fewer offspring than expected for four species—*Callithrix geoffroyi*, *Callithrix jacchus*, *Cebuella pygmaea*, and *Leontopithecus chrysopygus*—but more than expected for one species, *Saguinus imperator*. (b) Isosexual females became dams at the expected rate for all species except *Callithrix jacchus*, where they were underrepresented. (c) Isosexual sires bore fewer offspring than expected for three species—*Callithrix jacchus*, *Leontopithecus rosalia*, and *Saguinus oedipus* but more than expected for *Saguinus imperator*. (d) Isosexual males became sires at the expected rate for all species except *Callithrix jacchus*, for which they were underrepresented. For p values, χ^2 statistics, counts, and effect sizes see Table S10

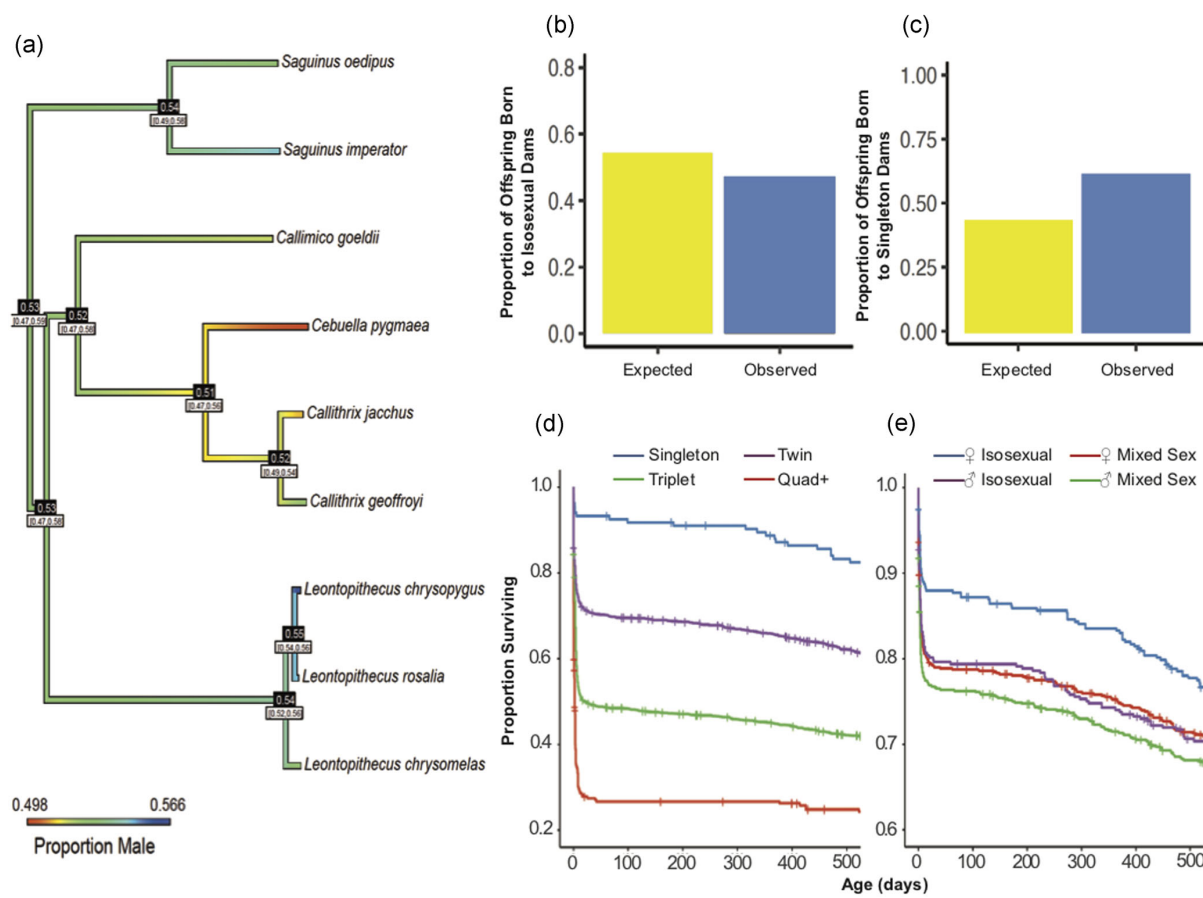


FIGURE 6 Sibling competition shapes survival and reproductive outcomes in captive callitrichine monkeys. (a) Phylogeny of callitrichine species included in this study. (b) Individuals born in a mixed-sex litter outperformed isosexually-born individuals (i.e., those born in all-male or all-female litters): i.e., isosexual monkeys were significantly underrepresented among parents. (c) Singletons significantly outperformed litter-born individuals in two metrics of reproductive performance: i.e., singletons produced more offspring and were overrepresented as parents compared with their litter-born peers. (d) From birth to adulthood, the risk of mortality increases with litter size. (e) In contrast to the clear relationship between litter size and mortality risk, the sex composition of litters does not impact survivorship in the majority of captive callitrichines

of survival to sexual maturity (although these differences were statistically significant for only two species: *C. geoffroyi* and *L. rosalia*).

Taken together, these data illuminate cross-species patterns in callitrichine diversity and reveal that sibling interactions may impose lasting effects in litter-bearing primates (Figure 6).

4.2 | Population sex ratios & litter sizes

All but one species in our sample exhibited male-biased BSR, although three species did not significantly diverge from the expected 1:1 BSR (*C. jacchus*, *C. pygmaea*, and *S. imperator*; Table 2). Biased birth sex ratios are typical in mammals (Clutton-Brock & Iason, 1986; Faust & Thompson, 2000; Thogerson et al., 2013), including callitrichines (e.g., *L. rosalia*, Rapaport, Kloc, Warneke, Mickelberg, & Ballou, 2013; *S. oedipus*, Boulton & Fletcher, 2015; *C. jacchus*, Poole & Evans, 1982; but see Rothe et al.,

1992). Some of the callitrichine species surveyed here, though, exhibited skews of relatively large magnitude (Figure 1a; Table 2). Evolutionary processes, including optimal sex allocation strategies (Clark, 1978; Clutton-Brock & Iason, 1986; Fisher, 1930; Hamilton, 1967; Silk, 1984), higher expected fitness returns from males due to male alloparenting (Emlen, 1982; Emlen, Emlen, & Levin, 1986; Silk & Brown, 2008), or higher male mortality (thus selecting for an overproduction of males at birth; Clutton-Brock & Iason, 1986) could be evoked to explain instances of such pronounced skews. However, future surveys exploring the adaptive value of producing sons versus daughters (e.g., via multi-generation pedigrees; Thogerson et al., 2013) are needed to assess whether the skews observed here actually represent adaptive sex allocation strategies rather than conserved mammalian traits.

Altogether, the ancestral state reconstruction on litter size including four outgroup species supported the commonly held notion

that callitrichines evolved twinning from singleton-bearing ancestors and that *Callimico* evolved singleton births secondarily from twinning ancestors (Figure 1b).

4.3 | Relaxation of mixed-sex constraints

Unlike many mammals, isosexual litters are not overrepresented in callitrichines; it is interesting to speculate that this might be evidence that there are few if any, monozygotic twins (which are necessarily same-sex). We did not detect survival or reproductive costs of being born into a mixed-sex litter for either males or females (Figure S1). This finding recapitulates a growing literature which espouses that callitrichines, unlike other litter-bearing mammals (Hackländer & Arnold, 2012; Korsten, Clutton-Brock, Pilkington, Pemberton, & Kruuk, 2009; Monclús & Blumstein, 2012; Ryan & Vandenbergh, 2002), have evolved mechanisms which shield females from brother-derived masculinization (Bradley et al., 2016; French et al., 2016). This is true even in wild golden lion tamarins (*L. rosalia*): individuals from mixed-sex litters were indistinguishable from those from isosexual litters in several morphological (growth to maturity and adult body size), survival (lifetime survivorship), and reproductive metrics (age at first reproduction, reproductive rates, and reproductive tenures; Frye, B.M., Hankerson, Sears, Tardif, & Dietz, n.d.). Taken together, these results suggest that selection has enabled callitrichines to circumvent the detriments of female masculinization that are characteristic of other litter-bearing mammals.

Other work outlines that callitrichines may exhibit subtle, while not necessarily deleterious, differences based on the sex composition of their litters. For example, *C. jacchus* infants from mixed-sex litters weighed less than isosexual monkeys, and both males and females born with brothers exhibit delayed developmental trajectories (Frye et al., 2019). Further, mature *C. jacchus* females born into mixed-sex litters produce proportionally more stillborns than do females born into isosexual litters (Rutherford et al., 2014). Additional research investigating developmental trajectories and fine-scaled measures of reproductive performance (e.g., fetal reabsorption, abortions, and stillbirth) might reveal how such early effects pose lasting constraints across callitrichine species.

4.4 | Intergenerational effects on reproductive output

In general, we found that singletons produced more offspring, and were overrepresented among parents, compared with litter-born peers (Figure 4 and Figure S4 and Table S9). Management practices are unlikely to explain these results. That is, while it is true that many protocols rarely allow more than one individual per litter to breed, owing to genetic or logistical reasons (Ballou, 1996), we cannot identify any reason why singletons would be preferentially selected as breeders. Instead, competition within a group may mean that individuals born with siblings have a lower chance of reproducing than do singletons. Sibling competition for resources and reproduction could explain the relative reproductive advantages of singletons,

who do not have to compete with same-aged littermates at any ontogenetic stage. In addition, singletons tend to be heavier at birth than individuals born with littermates especially triplets and above (*Saguinus spp.* and *C. jacchus*, Jaquish, Gage, & Tardif, 1991; *C. jacchus*, Lunn, 1983; Tardif & Bales, 2004).

Two additional factors may explain the difference between singletons and their litter-born peers. First, singletons may receive significantly more resources from family members than do young that are raised alongside littermates. If so, singleton offspring may enjoy developmental advantages that ultimately translate into superior reproductive performance. Second, perhaps singletons are relatively more robust and high-quality, and thus more reproductively successful. Such "robustness" of singletons may stem from variation in maternal energy allocation. For example, Oftedal, Power, Oftedal, Power, and Layne (2001) discovered that common marmoset twins born to smaller-than-average dams received relatively poorer milk (i.e., lower milk fat and lower gross energy) than twins born to heavier dams (Oftedal et al., 2001). This disparity translated into slower growth for twins. However, maternal size did not impact growth in singletons. These findings suggest that singleton offspring may be less restricted by maternal energy allocation limitations than offspring born with one or more siblings.

In some cases, we found that individuals born in isosexual litters were significantly underrepresented among parents (and all non-significant trends were in this direction; Figure 5 and Table S10). *C. jacchus*, the species for which we had the largest dataset, exhibited the strongest effect: isosexual individuals were underrepresented for both dams and sires (Figure 5). There is one exception: isosexual individuals of *S. imperator* significantly overperformed reproductively (Figure 5). While stochastic variation may explain reproductive underperformance by isosexuals, it also is possible that competition between same-sex siblings limits the reproductive potential of individuals born in isosexual litters compared to those born in mixed-sex litters. There is some evidence from other species for enhanced competition among isosexual litters (hyenas, Golla et al., 1999; humans, Ji et al., 2013; Nitsch, Faurie, & Lummaa, 2012). Through either prenatal biological competition or postnatal social competition, perhaps marmosets born in isosexual litters are disadvantaged. If sibling competition explains why isosexual animals underperform reproductively, why do isosexual male and female *S. imperator* individuals overperform? Is this merely random variation, potentially due to low sample size for this species (N [unique isosexual sires] = 18; N [unique isosexual dams] = 11; Table S10), or does some aspect of *S. imperator* reproduction favor isosexuals? This is a fascinating topic for future research.

4.5 | Limitations and future directions

There are several potential limitations to this study that merit consideration and could be addressed in future work. Foremost, this demographic study is based on captive animals from zoos and laboratories, which are relatively benign environments. These animals may be well-fed and sedentary compared with wild populations where selective forces are different. For example, litter

sizes may be smaller in the wild due to food constraints and the threat of predation. In addition, selective breeding may have impacted reproductive performance for these animals. Future work validating our findings in wild populations is needed to more fully understand the fitness consequences of sibling interactions.

Further, this is a broad-scale demographic analysis, rather than a fine-scale mechanistic analysis. Adding information about individuals' physical traits, health, and social grouping to these data likely would provide additional insights into the mechanisms mediating survival and reproduction.

Other questions may explore whether subtle competition among same-sex litters is driving down the proportion of isosexual litters (compared with what is seen in most other animals). Social grouping data could clarify the differences between same-aged sibling relationships and old-to-young relationships. Further, a detailed analysis of survivorship during specific ontogenetic stages may reveal shifts in mortality risks between the sexes across the life course. Lastly, marmosets have a high degree of microchimerism between siblings; documenting the extent of chimerism and correlating this with measures of reproductive output and lifetime health may answer unresolved questions about the evolutionary impact of extensive chimerism among siblings (Haig, 1999).

Altogether, we document broad demographic trends using an unusually large dataset of captive animals. This adds to a robust literature on captive breeding programs in zoos, which is critical for conservation programs. Further, this work illustrates that carefully kept zoo and laboratory records represent a largely untapped treasure for biological inquiry. Callitrichines are an excellent clade for future investigations of parental allocation strategies and intra-familial cooperation and conflict.

ACKNOWLEDGMENTS

We are very grateful to Rahel Brügger, who assisted with extracting data from the University of Zurich dataset. We would also like to extend our sincere thanks to the animal care staffs and zookeepers who provided and continue to provide excellent care to marmosets, tamarins, and lion tamarins living in captivity. We would also like to thank the Writers Guild at Clemson University for their comments on previous versions of this manuscript. We also extend our thanks to Kathy West for providing the beautiful photo that accompanies this work. DEM conducted this research with Government support under and awarded by DoD, Air Force Office of Scientific Research, National Defense Science and Engineering Graduate (NDSEG) Fellowship, 32 CFR 168a. DEM. is also supported by a Theodore H. Ashford Graduate Fellowship in the Sciences.

ORCID

- Dakota E. McCoy  <http://orcid.org/0000-0001-8383-8084>
- Brett M. Frye  <http://orcid.org/0000-0001-8818-063X>
- David Haig  <http://orcid.org/0000-0001-7377-1605>
- Suzette D. Tardif  <http://orcid.org/0000-0002-3412-7742>

REFERENCES

- Abbott, D. H., Barrett, J., & George, L. M. (1993). Comparative aspects of the social suppression of reproduction in female marmosets and tamarins. In Rylands, A. B. (Ed.), *Marmosets and Tamarins: Systematics, Behaviour and Ecology* (pp. 152–163). Oxford: Oxford Univ. Press.
- Ballou, J. D. (1996). *Small population management: contraception of golden lion tamarins. Contraception in Wildlife* (pp. 349–358). New York: Edwin Mellen Press.
- Benjamini, Y., & Hochberg, Y. (1995). Controlling the false discovery rate: A practical and powerful approach to multiple testing. *Journal of the Royal Statistical Society. Series B (Methodological)*, 57(1), 289–300. <https://doi.org/10.1111/j.2517-6161.1995.tb02031.x>
- Bicca-Marques, J. C. (2003). Sexual selection and foraging behavior in male and female tamarins and marmosets. In Jones, C. B. (Ed.), *Sexual Selection and Reproductive Competition in Primates: New Perspectives and Directions* (pp. 455–475). Norman: American Society of Primatologists.
- Boulton, R. A., & Fletcher, A. W. (2015). Do mothers prefer helpers or smaller litters? Birth sex ratio and litter size adjustment in cotton-top tamarins (*Saguinus oedipus*). *Ecology and Evolution*, 5(3), 598–606. <https://doi.org/10.1002/ece3.1396>
- Box, H. O., & Hubrecht, R. C. (1987). Long-term data on the reproduction and maintenance of a colony of common marmosets (*Callithrix jacchus jacchus*) 1972–1983. *Laboratory Animals*, 21(3), 249–260. <https://doi.org/10.1258/002367787781268747>
- Bradley, B. J., Snowdon, C. T., McGrew, W. C., Lawler, R. R., Guevara, E. E., McIntosh, A., & O'connor, T. (2016). Nonhuman primates avoid the detrimental effects of prenatal androgen exposure in mixed-sex litters: Combined demographic, behavioral, and genetic analyses. *American Journal of Primatology*, 78(12), 1304–1315. <https://doi.org/10.1002/ajp.22583>
- Bütikofer, A., Figlio, D. N., Karbownik, K., Kuzawa, C. W., & Salvanes, K. G. (2019). Evidence that prenatal testosterone transfer from male twins reduces the fertility and socioeconomic success of their female co-twins. *Proceedings of the National Academy of Sciences*, 116, 6749–6753. <https://doi.org/10.1073/pnas.1812786116>
- Clark, A. B. (1978). Sex ratio and local resource competition in a prosimian primate. *Science*, 201(4351), 163–165. <https://doi.org/10.1126/science.201.4351.163>
- Clutton-Brock, T. H., & Iason, G. R. (1986). Sex ratio variation in mammals. *The Quarterly Review of Biology*, 61(3), 339–374. <https://doi.org/10.1086/415033>
- Cox, D. R. (1972). Regression models and life-tables. *Journal of the Royal Statistical Society: Series B (Methodological)*, 34(2), 187–202. <https://doi.org/10.1111/j.2517-6161.1972.tb00899.x>
- Digby, L. J., Ferrari, S. F., & Saltzman, W. (2011). *The role of competition in cooperatively breeding species. Primates in Perspective* (pp. 85–106). New York: Oxford University Press.
- Díaz-Muñoz, S. L., & Bales, K. L. (2015). "Monogamy" in primates: Variability, trends, and synthesis: Introduction to special issue on primate monogamy: primate monogamy. *American Journal of Primatology*, 78(3), 283–287. <https://doi.org/10.1002/ajp.22463>
- EAZA Husbandry Guidelines. (2010). EAZA Husbandry Guidelines for Callitrichidae – 2. Taxon. Retrieved from http://www.marmosetcare.com/downloads/EAZA_HusbandryGuidelines.pdf
- Emlen, S. T. (1982). The evolution of helping. I. An ecological constraints model. *The American Naturalist*, 119(1), 29–39. <https://doi.org/10.1086/283888>
- Emlen, S. T., Emlen, J. M., & Levin, S. A. (1986). Sex-ratio selection in species with helpers-at-the-nest. *The American Naturalist*, 127(1), 1–8. <https://doi.org/10.1086/284463>
- Fan, F. Y. (2017). powerAnalysis: Power Analysis in Experimental Design. R package version 0.2.1.
- Faust, L. J., & Thompson, S. D. (2000). Birth sex ratio in captive mammals: Patterns, biases, and the implications for management and

- conservation. *Zoo Biology*, 19(1), 11–25. [https://doi.org/10.1002/\(SICI\)1098-2361\(2000\)19:1<11::AID-ZOO2>3.0.CO;2-V](https://doi.org/10.1002/(SICI)1098-2361(2000)19:1<11::AID-ZOO2>3.0.CO;2-V)
- Felsenstein, J. (1985). Phylogenies and the comparative method. *The American Naturalist*, 125(1), 1–15. <https://doi.org/10.1086/284325>
- Fisher, R. A. (1930). *The genetical theory of natural selection: A complete variorum edition*. Oxford, UK: Oxford University Press.
- French, J. A., & Inglett, B. J. (1989). Female-female aggression and male indifference in response to unfamiliar intruders in lion tamarins. *Animal Behaviour*, 37, 487–497. [https://doi.org/10.1016/0003-3472\(89\)90095-X](https://doi.org/10.1016/0003-3472(89)90095-X)
- French, J. A., Mustoe, A. C., Cavanaugh, J., & Birnie, A. K. (2013). The influence of androgenic steroid hormones on female aggression in 'atypical' mammals. *Philosophical Transactions of the Royal Society, B: Biological Sciences*, 368, 20130084. <https://doi.org/10.1098/rstb.2013.0084>
- French, J. A., Frye, B., Cavanaugh, J., Ren, D., Mustoe, A. C., Rapaport, L., & Mickelberg, J. (2016). Gene changes may minimize masculinizing and defeminizing influences of exposure to male cotwins in female callitrichine primates. *Biology of Sex Differences*, 7(1), 28. <https://doi.org/10.1186/s13293-016-0081-y>
- Frye, B. M., Hankerson, S. J., Sears, M. W., Tardif, S. D., & Dietz, J. M. (n.d.). Beyond sibling sex: the role of sex allocation in a cooperatively breeding primate. In prep.
- Frye, B. M., Rapaport, L. G., Melber, T., Sears, M. W., & Tardif, S. D. (2019). Sibling sex, but not androgens, shapes phenotypes in perinatal common marmosets (*Callithrix jacchus*). *Scientific Reports*, 9(1), 1100. <https://doi.org/10.1038/s41598-018-37723-z>
- Garber, P. A., Óñ, F. E., Moya, L., & Pruetz, J. D. (1993). Demographic and reproductive patterns in mustached tamarin monkeys (*Saguinus mystax*): Implications for reconstructing platyrhine mating systems. *American Journal of Primatology*, 29, 235–254. <https://doi.org/10.1002/ajp.1350290402>
- Garber, P. A., Porter, L. M., Spross, J., & Di Fiore, A. (2015). Tamarins: Insights into monogamous and nonmonogamous single female social and breeding systems. *American Journal of Primatology*, 78(3), 298–314. <https://doi.org/10.1002/ajp.22370>
- Garbino, G. S. T., & Martins-Junior, A. M. G. (2018). Phenotypic evolution in marmoset and tamarin monkeys (Cebidae, Callitrichinae) and a revised genus-level classification. *Molecular Phylogenetics and Evolution*, 118, 156–171. <https://doi.org/10.1016/j.ympev.2017.10.002>
- Golla, W., Hofer, H., & East, M. L. (1999). Within-litter sibling aggression in spotted hyenas: Effect of maternal nursing, sex and age. *Animal Behaviour*, 58(4), 715–726. <https://doi.org/10.1006/anbe.1999.1189>
- Hackländer, K., & Arnold, W. (2012). Litter sex ratio affects lifetime reproductive success of free-living female Alpine marmots *Marmota marmota*. *Mammal Review*, 42(4), 310–313. <https://doi.org/10.1111/j.1365-2907.2011.00199.x>
- Haig, D. (1999). What is a marmoset? *American Journal of Primatology*, 49(4), 285–296. [https://doi.org/10.1002/\(SICI\)1098-2345\(199912\)49:4<285::AID-AJP1>3.0.CO;2-X](https://doi.org/10.1002/(SICI)1098-2345(199912)49:4<285::AID-AJP1>3.0.CO;2-X)
- Hamilton, W. D. (1967). Extraordinary sex ratios. *Science*, 156, 477–488. <https://doi.org/10.1126/science.156.3774.477>
- Henry, M. D., Hankerson, S. J., Siani, J. M., French, J. A., & Dietz, J. M. (2013). High rates of pregnancy loss by subordinates leads to high reproductive skew in wild golden lion tamarins (*Leontopithecus rosalia*). *Hormones and Behavior*, 63(5), 675–683. <https://doi.org/10.1016/j.yhbeh.2013.02.009>
- Jaquish, C. E., Gage, T. B., & Tardif, S. D. (1991). Reproductive factors affecting survivorship in captive Callitrichidae. *American Journal of Physical Anthropology*, 84, 291–305. <https://doi.org/10.1002/ajpa.1330840306>
- Jaquish, C. E., Tardif, S. D., Toal, R. L., & Carson, R. L. (1996). Patterns of prenatal survival in the common marmoset (*Callithrix jacchus*). *Journal of Medical Primatology*, 25(1), 57–63. <https://doi.org/10.1111/j.1600-0684.1996.tb00194.x>
- Ji, T., Wu, J. J., He, Q. Q., Xu, J. J., Mace, R., & Tao, Y. (2013). Reproductive competition between females in the matrilineal Mosuo of southwestern China. *Philosophical Transactions of the Royal Society of London, Series B: Biological Sciences*, 368(1631), 20130081. <https://doi.org/10.1098/rstb.2013.0081>
- Kassambara, A., & Kosinski, M. (2018). survminer: Drawing Survival Curves Using "ggplot2".
- Kleiman, D. G. (1979). Parent-offspring conflict and sibling competition in a monogamous primate. *The American Naturalist*, 114, 753–760. <https://doi.org/10.2307/2678832>
- Kohler, I. V., Preston, S. H., & Lackey, L. B. (2006). Comparative mortality levels among selected species of captive animals. *Demographic research*, 15, 413–434. <https://doi.org/10.4054/demres.2006.15.14>
- Korsten, P., Clutton-Brock, T., Pilkington, J. G., Pemberton, J. M., & Kruuk, L. E. B. (2009). Sexual conflict in twins: Male cotwins reduce fitness of female Soay sheep. *Biology Letters*, 5(5), 663–666. <https://doi.org/10.1098/rsbl.2009.0366>
- Lee, E. T., & Wang, J. W. (2003). Statistical methods for survival data analysis, *Wiley Series in Probability and Statistics*. Hoboken, NJ: John Wiley & Sons, Inc. <https://doi.org/10.1002/0471458546>
- Leutenegger, W. (1979). Evolution of litter size in primates. *The American Naturalist*, 114(4), 525–531. <https://doi.org/10.1086/283499>
- Lunn, S. F. (1983). Body weight changes throughout pregnancy in the common marmoset *Callithrix jacchus*. *Folia Primatologica*, 41(3-4), 204–217. <https://doi.org/10.1159/000156132>
- Mittermeier, R. A., Rylands, A. B., & Wilson, D. E. (2013). In Mittermeier, R. A., Rylands, A. B., & Wilson, D. E. (Eds.), *Handbook of the Mammals of the World. Volume 3. Primates*. Barcelona: Lynx Edicions.
- Monclús, R., & Blumstein, D. T. (2012). Litter sex composition affects life-history traits in yellow-bellied marmots. *Journal of Animal Ecology*, 81(1), 80–86. <https://doi.org/10.1111/j.1365-2656.2011.01888.x>
- De Moura, A. C. A. (2003). Sibling age and intragroup aggression in captive *Saguinus midas* midas. *International Journal of Primatology*, 24(3), 639–652. <https://doi.org/10.1023/a:1023748616043>
- Mundy, N. I., & Kelly, J. (2001). Phylogeny of lion tamarins (*Leontopithecus* spp) based on interphotoreceptor retinol binding protein intron sequences. *American Journal of Primatology*, 54(1), 33–40. <https://doi.org/10.1002/ajp.1010>
- Nelson, J. E., & Gemmell, N. J. (2003). Birth in the northern quoll, *Dasyurus hallucatus* (Marsupialia: Dasyuridae). *Australian Journal of Zoology*, 51(2), 187–198. <https://doi.org/10.1071/ZO02016>
- Nettle, D., Andrews, C., Reichert, S., Bedford, T., Gott, A., Parker, C., ... Bateson, M. (2016). Brood size moderates associations between relative size, telomere length, and immune development in European starling nestlings. *Ecology and Evolution*, 6, 8138–8148. <https://doi.org/10.1002/ece3.2551>
- Nitsch, A., Faurie, C., & Lummaa, V. (2012). Are elder siblings helpers or competitors? Antagonistic fitness effects of sibling interactions in humans. *Proceedings of the Royal Society B: Biological Sciences*, 280(1750), 20122313. <https://doi.org/10.1098/rspb.2012.2313>
- Oftedal, O., Power, R., Layne, D., Tardif, S., & Power, M. (2001). Lactation, maternal behavior and infant growth in common marmoset monkeys (*Callithrix jacchus*): Effects of maternal size and litter size. *Behavioral Ecology and Sociobiology*, 51(1), 17–25. <https://doi.org/10.1007/s002650100400>
- Poole, T. B., & Evans, R. G. (1982). Reproduction, infant survival and productivity of a colony of common marmosets (*Callithrix jacchus jacchus*). *Laboratory Animals*, 16(1), 88–97. <https://doi.org/10.1258/002367782780908760>
- Rapaport, L. G., Kloc, B., Warneke, M., Mickelberg, J. L., & Ballou, J. D. (2013). Do mothers prefer helpers? Birth sex-ratio adjustment in captive callitrichines. *Animal Behaviour*, 85(6), 1295–1302. <https://doi.org/10.1016/j.anbehav.2013.03.018>
- Revell, L. J. (2012). phytools: An R package for phylogenetic comparative biology (and other things): Phytools: R package. *Methods in Ecology and*

- Evolution*, 3(2), 217–223. <https://doi.org/10.1111/j.2041-210X.2011.00169.x>
- Revell, L. J. (2013). Two new graphical methods for mapping trait evolution on phylogenies. *Methods in Ecology and Evolution*, 4(8), 754–759. <https://doi.org/10.1111/2041-210X.12066>
- Roda, S. A., & Pontes, A. R. M. (1998). Polygyny and infanticide in common marmosets in a fragment of the Atlantic forest of Brazil. *Folia Primatologica*, 69(6), 372–376.
- Rothe, H., Darms, K., & Koenig, A. (1992). Sex ratio and mortality in a laboratory colony of the common marmoset (*Callithrix jacchus*). *Laboratory Animals*, 26(2), 88–99. <https://doi.org/10.1258/002367792780745922>
- Rutherford, J. N., DeMartelly, V. A., Layne Colon, D. G., Ross, C. N., & Tardif, S. D. (2014). Developmental origins of pregnancy loss in the adult female common marmoset monkey (*Callithrix jacchus*). *PLoS One*, 9(5), e96845–e96849. <https://doi.org/10.1371/journal.pone.0096845>
- Rutherford, J. N., & Tardif, S. D. (2008). Placental efficiency and intrauterine resource allocation strategies in the common marmoset pregnancy. *American Journal of Physical Anthropology*, 137(1), 60–68. <https://doi.org/10.1002/ajpa.20846>
- Ryan, B. C., & Vandenberghe, J. G. (2002). Intrauterine position effects. *Neuroscience and Biobehavioral Reviews*, 26(6), 665–678. [https://doi.org/10.1016/S0149-7634\(02\)00038-6](https://doi.org/10.1016/S0149-7634(02)00038-6)
- Saltzman, W., Digby, L. J., & Abbott, D. H. (2009). Reproductive skew in female common marmosets: What can proximate mechanisms tell us about ultimate causes? *Proceedings of the Royal Society B: Biological Sciences*, 276(1656), 389–399. <https://doi.org/10.1098/rspb.2008.1374>
- Silk, J. B. (1984). Local resource competition and the evolution of male-biased sex ratios. *Journal of Theoretical Biology*, 108(2), 203–213. [https://doi.org/10.1016/S0022-5193\(84\)80066-1](https://doi.org/10.1016/S0022-5193(84)80066-1)
- Silk, J. B., & Brown, G. R. (2008). Local resource competition and local resource enhancement shape primate birth sex ratios. *Proceedings of the Royal Society B: Biological Sciences*, 275(1644), 1761–1765. <https://doi.org/10.1098/rspb.2008.0340>
- Soini, P. (1982). Ecology and population dynamics of the pygmy marmoset, *Cebuella pygmaea*. *Folia Primatologica*, 39(1–2), 1–21. <https://doi.org/10.1159/000156066>
- Tardif, S. D., & Bales, K. L. (2004). Relations among birth condition, maternal condition, and postnatal growth in captive common marmoset monkeys (*Callithrix jacchus*). *American Journal of Primatology*, 62(2), 83–94. <https://doi.org/10.1002/ajp.20009>
- Tardif, S. D., Layne, D. G., & Smucny, D. A. (2002). Can marmoset mothers count to three? Effect of litter size on mother-infant interactions. *Ethology*, 108(9), 825–836. <https://doi.org/10.1046/j.1439-0310.2002.00815.x>
- Tardif, S. D., Smucny, D. A., Abbott, D. H., Mansfield, K., Schultz-Darken, N., & Yamamoto, M. E. (2003). Reproduction in captive common marmosets (*Callithrix jacchus*). *Comparative Medicine*, 53(4), 364–368.
- Therneau, T. M., & Grambsch, P. M. (2000). *Expected survival. In modeling survival data: Extending the cox model* (pp. 261–287). New York, NY: Springer.
- Therneau, T. M., & Grambsch, P. M. (2013). Modeling survival data: Extending the Cox model. Springer Science & Business Media.
- Thogerson, C. M., Brady, C. M., Howard, R. D., Mason, G. J., Pajor, E. A., Vicino, G. A., & Garner, J. P. (2013). Winning the genetic lottery: Biasing birth sex ratio results in more grandchildren. *PLoS One*, 8, e67867. <https://doi.org/10.1371/journal.pone.0067867>
- Ward, J. M., Buslov, A. M., & Vallender, E. J. (2014). Twinning and survivorship of captive common marmosets (*Callithrix jacchus*) and cotton-top tamarins (*Saguinus oedipus*). *Journal of the American Association for Laboratory Animal Science: JAALAS*, 53(1), 7–11.

SUPPORTING INFORMATION

Additional supporting information may be found online in the Supporting Information section.

How to cite this article: McCoy DE, Frye BM, Kotler J, et al. A comparative study of litter size and sex composition in a large data set of callitrichine monkeys. *Am J Primatol*. 2019;e23038. <https://doi.org/10.1002/ajp.23038>

Are we smart enough to know how smart animals are?

Frans de Waal



New Caledonian Crows Behave Optimistically after Using Tools

REPRINTED FROM: McCoy, D.E., Schiestl, M., Neilands, P., Hassall, R., Gray, R.D. and Taylor, A.H., 2019. New caledonian crows behave optimistically after using tools. *Current Biology*, 29(16), pp.2737-2742.

ARTICLE AND SUPPLEMENT AVAILABLE AT: <https://doi.org/10.1016/j.cub.2019.06.080>



Current Biology

New Caledonian Crows Behave Optimistically after Using Tools

Highlights

- Wild New Caledonian crows are optimistic after tool use, indicating positive affect
- Crows appear to enjoy, or be intrinsically motivated by, tool use
- Effort cannot explain this; crows are less optimistic after an effortful task
- Intrinsic enjoyment may shape the evolution of complex actions like tool use

Authors

Dakota E. McCoy, Martina Schiestl,
Patrick Neilands, Rebecca Hassall,
Russell D. Gray, Alex H. Taylor

Correspondence

dakotamccoy@g.harvard.edu

In Brief

McCoy et al. find that wild New Caledonian crows are optimistic after tool use. Optimism is an indicator of positive mood; in other words, crows appear to enjoy using tools. This suggests that intrinsic motivation (enjoyment) is a fundamental proximate cause in the evolution of tool use and other complex behaviors.



New Caledonian Crows Behave Optimistically after Using Tools

Dakota E. McCoy,^{1,4,*} Martina Schiestl,^{2,3} Patrick Neilands,² Rebecca Hassall,² Russell D. Gray,^{2,3} and Alex H. Taylor²

¹Department of Organismic and Evolutionary Biology, Harvard University, 26 Oxford Street, Cambridge, MA 02138, USA

²School of Psychology, University of Auckland, 23 Symonds Street, Auckland 1010, New Zealand

³Max Planck Institute for the Science of Human History, Jena 07745, Germany

⁴Lead Contact

*Correspondence: dakotamccoy@g.harvard.edu

<https://doi.org/10.1016/j.cub.2019.06.080>

SUMMARY

Are complex, species-specific behaviors in animals reinforced by material reward alone or do they also induce positive emotions? Many adaptive human behaviors are intrinsically motivated: they not only improve our material outcomes, but improve our affect as well [1–8]. Work to date on animal optimism, as an indicator of positive affect, has generally focused on how animals react to change in their circumstances, such as when their environment is enriched [9–14] or they are manipulated by humans [15–23], rather than whether complex actions improve emotional state. Here, we show that wild New Caledonian crows are optimistic after tool use, a complex, species-specific behavior. We further demonstrate that this finding cannot be explained by the crows needing to put more effort into gaining food. Our findings therefore raise the possibility that intrinsic motivation (enjoyment) may be a fundamental proximate cause in the evolution of tool use and other complex behaviors.

RESULTS AND DISCUSSION

People feel happy when performing certain behaviors. For example, humans improve their affective state by giving altruistically [1], playing sports [2–5], and striving for concrete goals [6–8]. Do animals also feel happy after carrying out certain actions? Despite strong arguments for evolutionary continuity between humans and animals [24–26], research in this area has often been critiqued for being overly anthropomorphic. However, researchers now have the tools to objectively measure the affective state of an animal. The cognitive bias test is based on the finding that animals, like humans, will treat an identical ambiguous stimulus differently depending on their affective state: individuals in a positive state will interpret an ambiguous stimulus as more positive than individuals in a negative state [9, 14, 19, 27–32]. That is, individuals in a positive state act optimistically, and those in a negative state act pessimistically. The terms optimism and pessimism in this context are short-hand labels for responses made to ambiguous cues from which, respectively, positively and

negatively valenced affective states (“dimensional” emotions and/or moods) [32] can be inferred without implying that these are consciously experienced.

To date, studies that have used the cognitive bias test have generally focused on changing the circumstances of an animal by manipulating their environment or the animal themselves. Environmental enrichment is associated with optimism: rats [9–14], starlings [12, 13], and pigs [14] housed with enrichment are optimistic, and those housed without environmental enrichment are pessimistic. Similarly, unpredictable or aversive environmental experiences cause pessimism, such as in rats subject to chaotic housing conditions [28]. Manipulation of animals themselves also changes their cognitive state. Pessimism emerges when peccaries are trapped [15], piglets are handled roughly [16], calves are painfully disbudded [17] or separated from their mothers [18], honeybees [19] and flies are shaken [20], rats are given experience of chronic social defeats [21], chicks are socially isolated [22], and ravens observe a peer in a negative state [33]. Positive manipulation also appears to cause optimism, as exemplified by work showing that tickled rats are more optimistic than peers handled normally [23].

The effect of performing complex, species-specific behavior on animal emotion has received comparatively little attention, despite suggestive evidence that it improves mood in humans [1–5, 8, 34, 35]. To date, only two studies have directly examined whether animals show more positive affect after carrying out complex species-specific behaviors [36, 37]. These studies have found mixed results. When given experience searching for food randomly placed within a maze arena, dogs actually behaved more pessimistically [37]. However, this may have been an artifact of the study design; dogs were interrupted during their search of the maze, which could have promoted a negative affective state (because they were prevented from eating the rest of the food). In another study, when dogs practiced nosework (searching for food using olfactory cues, a species-specific behavior), they became more optimistic, and dogs who practiced heelwork (walking behind their owner) did not change their affective state [36]. Although these results raise the possibility that complex, species-specific behaviors can improve animal affective states, the nosework group were trained to search for food, and the heelwork group were trained not to move freely. This difference may have led the nosework dogs to approach the ambiguous stimulus faster rather than because of a change in their affective state.





At present, therefore, it is not yet clear whether complex, species-specific behaviors lead to positive affective states in animals, as they do in humans. One way to test this hypothesis is to focus on tool-using animals. Previous research suggests that tool-using animals like chimpanzees and New Caledonian crows are intrinsically motivated to use tools [38, 39], but no study has yet directly tested this hypothesis by examining whether tool use leads to a positive affective state. Here, we tested whether tool use—a complex, species-specific behavior in New Caledonian crows—instills positive affect, as indicated through approach speed toward an ambiguous stimulus.

We presented a spatial cognitive bias test [9, 28–31] to fifteen wild New Caledonian crows captured and temporarily housed in an aviary before re-release. These crows had no previous experience in the laboratory before capture. We trained these crows that a box placed on one side of a table contained a large reward and the same box, when placed on the opposite side of the table, contained only a small reward (Figure 1). They had 30 s maximum to approach and open the box. The crows approached the large reward box quickly, anticipating the large reward (mean latency: 3.79 s; SEM = 0.18 s) but moved slowly or not at all to the small reward (mean latency: 25.20 s; SEM = 0.79 s). To measure affective state, we recorded crows' approach times to an ambiguous stimulus: the same box placed halfway in between where the large and small reward boxes had been (Figure 2D).

Figure 1. Spatial Cognitive Bias Test

(A) Experimental aviary setup.

(B–D) Box is placed in one of three locations on the table, along with a wooden marker that does not change location. Birds learned that the box on one side (B) had a large reward (3 meat cubes); the box on the other side (C) had a small reward ($\frac{1}{4}$ of a meat cube). The box in the middle (D) was ambiguous and used to test optimism.

(E–G) Crows (E) fly or walk to table, (F) remove box lid, and (G) retrieve meat from inside.

Quicker approaches imply a relatively more positive affective state, and slower approaches imply a relatively more negative affective state.

We compared latency to approach the ambiguous box after crows encountered one of four conditions, each of which resulted in the same reward amount (Figure 2). We compared (1) tool use, using a stick tool to extract one piece of food from an apparatus (Figure 2A), with (2) no tool, extracting one piece of food with their beak from the front of the same apparatus (Figure 2B). This tested whether crows were more optimistic after using a tool rather than simply after gaining food. It also controlled for the presence of the apparatus itself. However, differences between these two conditions might also

be due to the fact that tool use took more effort than no tool use (the crows were slower to extract meat with a tool than with just their beaks). We therefore also compared (1) effort, traveling to four separate locations in the aviary to get four $\frac{1}{4}$ pieces of food (Figure 2C), with (2) easy, taking four $\frac{1}{4}$ pieces of food directly from the table (Figure 2D). This tested whether approach speed changed when crows had to put more effort into getting food. If tool use led to increased positive affect, we predicted that birds would be more optimistic after using a tool, rather than just their beak, to gain food, but not when putting more effort into gaining food compared to receiving it easily.

We found that recent experiences significantly impact New Caledonian crow affective state, as measured through latency to approach an ambiguous stimulus. We found that the statistical model containing the factors condition (consisting of four levels: tool use, no tool, effort, and easy) and trial order as main effects (with no interaction) was the best fit for the data (repeated-measures Bayesian ANOVA: BF = 17.89; see Table S1 for details on all models fitted). To assess the relative importance of condition and trial order, we compared the fit of the condition-only and trial-order-only models to the condition + trial order model. For this comparison, where we remove a single factor, a BF = 1 indicates no difference in model fit, BF > 3 indicates a substantial improvement, and BF < 0.33 indicates a substantial decrease in model fit. Removing trial order from the model led to no substantial difference in the model's fit to the data (BF = 0.96). This implies

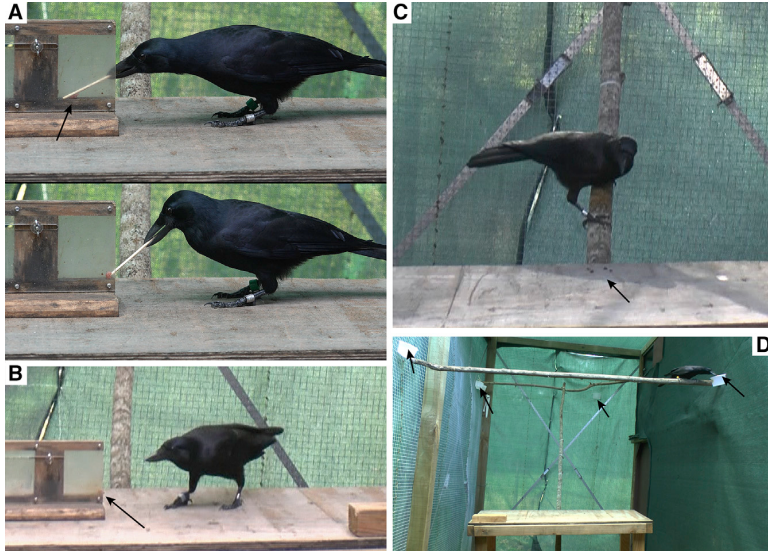


Figure 2. Test Conditions

Optimism was tested after four different experiences (arrows indicate food location).

- (A) “Tool” condition, in which birds used a tool to extract one block of meat from a wood and plexiglass apparatus.
- (B) “No tool” condition, in which birds used their beak to extract one block of meat from within reach in the same apparatus.
- (C) “Easy” condition, in which birds retrieved four $\frac{1}{4}$ block pieces of meat from one location.
- (D) “Effort” condition, in which birds traveled to four locations in the aviary to retrieve four $\frac{1}{4}$ block pieces of meat, placed within sight on the rims of the white dishes.

that the birds did not change their attitude toward the ambiguous stimuli because of repeated exposure (each bird saw the ambiguous stimulus four times total). In contrast, removing condition from the model led to a substantial reduction in the fit of the model ($BF = 0.045$). As such, condition appears to be the main factor driving approach latency to the ambiguous stimulus in crows (see STAR Methods and Table S1).

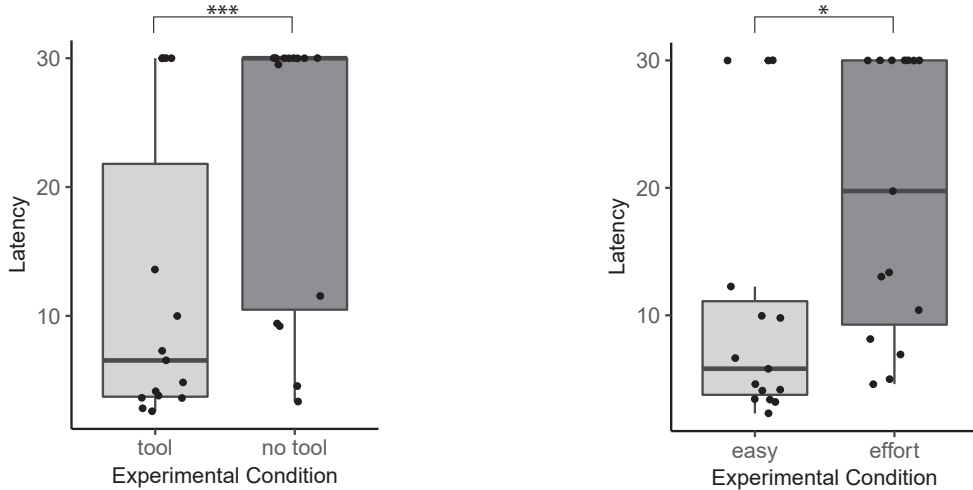
Crows differed in their approach speed between our paired conditions. Crows approached the ambiguous stimulus significantly faster in tool use condition trials, where they used a tool to extract a meat block from an apparatus, than in no tool trials, where they extracted a meat block from the same apparatus using only their beak (Figure 3; Bayesian paired t test: $BF = 28.70$). Crows were also significantly faster after the easy condition, where they retrieved four meat $\frac{1}{4}$ blocks from a single location on the table, compared to the effort condition, where they traveled to four locations in the aviary to retrieve four meat $\frac{1}{4}$ blocks (Figure 4; Bayesian paired t test: $BF = 7.62$). These results show that New Caledonian crows approached ambiguous stimuli faster after (1) using a tool to gain food rather than just their beak and (2) gaining freely available food from one location rather than collecting it from multiple locations.

Our study shows that tool use leads to New Caledonian crows approaching an ambiguous stimulus faster, as do “windfalls,” where an animal gains freely accessible food. In contrast, crows approached an ambiguous stimulus more slowly after extracting food from an apparatus with their beak and after flying to collect food across their aviary. Reward processing includes multiple dissociable components (liking, wanting, and learning) [40, 41]. Measuring approach speed in this spatial paradigm specifically reveals the “wanting” component, from which we can infer affective “liking” [9, 28–31]. Quicker approaches suggest that the crows had liked a prior experience more and so were in a more positive affective state, and slower approaches suggest crows had not liked a prior experience as much, leading them

to be in a relatively more negative affective state. These results therefore suggest that tool use, rather than effort or activity in general, led to increased positive affective state in our study species. This demonstrates that complex, species-specific activities can influence

the positive affect of an animal above and beyond the affect generated by being active or gaining a material reward. Interestingly, we also found that crows acted more optimistically after collecting food from an easily accessible location. This finding supports anecdotes reporting that animals receiving windfalls of food often show an elevated affective state [42].

Our results suggest that intrinsic motivation (internal feelings and predispositions) influences the evolution of tool use. That is, we propose that mechanisms of intrinsic reward evolved to support tool use and have shaped its evolution and development over time. Past work has claimed that both chimpanzees and New Caledonian crows are intrinsically motivated to use tools [38, 39]. This claim is based on two observations, namely (1) the higher rates of unrewarded object-related behavior by individuals of tool-using species compared to related non-tool-using species [38, 39] and (2) the lack of correlation between the presence of tool behavior and ecological resources requiring tool use [38]. This research suggests that, at a behavioral level, reinforcement of tool use is not only derived from external motivators, such as reward, but also from intrinsic, psychological motivators as well. Our results suggest that, at least in New Caledonian crows, positive affect is a key mechanism in creating intrinsic motivation for this species to use tools. That is, because positive affect increases in New Caledonian crows after tool use, above and beyond that created by simply gaining food (i.e., crows gain intrinsic enjoyment from this behavior), they are then intrinsically motivated to perform more of this behavior in the future. Given the evolutionary distance between New Caledonian crows and humans, this therefore suggests that intrinsic motivation is a fundamental proximate cause in the evolution of tool use. However, further work is needed to confirm this. First, in terms of the results here, due to the need to run four conditions, we used only one ambiguous stimulus (middle), rather than three (near-small, middle, and near-large), as has been used in many other studies (e.g., [9, 12, 17, 19, 43]). The five-point methodology is preferred, because it validates that animals view the ambiguous stimuli

**Figure 3. Crows Are Optimistic after Using a Tool to Extract Food**

Crows ($n = 15$) were exposed to one of two experiences just prior to the cognitive bias test (presentation of an ambiguous stimulus): tool refers to using a tool to extract meat from an apparatus and no tool refers to retrieving meat from within reach within the same apparatus (no tool required). Crows were significantly more optimistic (faster to the ambiguous stimulus) in the tool condition versus no tool (Bayesian paired t test; $BF = 28.70$). In each boxplot, the horizontal bar is the median, the box ranges from the 25th to 75th percentile, and the whiskers show the range of data points. See Data S1 for all latency times and Figure S1 for mean latencies (\pm SEM) for all trials.

as relating to the training stimuli (the response curve along a distribution of expected rewards has five, rather than three, points). Logistical considerations led us to use the three-point methodology (STAR Methods). Future testing with this rigorous five-point methodology would therefore be useful to validate these results. Second, although humans are intrinsically motivated to perform many behaviors [44–48], no study has yet examined whether humans are intrinsically motivated to use tools.

Previous work on animals has shown that circumstantial change impacts affective state, such as through environmental enrichment or aversive manipulation. The results reported here show that tool use—a complex, species-specific activity performed by the animals themselves—can improve the affective state of animals. Our research therefore suggests that “occupational” enrichment [49], which encourages animals to exhibit complex, species-specific behaviors, could significantly improve captive animal welfare by increasing the positive affect of animals. Cognitive bias protocols have already been used to test simple welfare interventions, from pharmacological treatment for separation anxiety in dogs [50] to environmental enrichment in a wide variety of animals [12–14, 51, 52]. This work could be extended to test the impact of not only species-specific behaviors but also active, goal-directed enrichment on captive animals with repetitive or negative behavior, akin to problem-solving therapy for humans suffering from depression [53]. Our research, therefore, opens up a promising line of enquiry for future research: the

Figure 4. Crows Are More Optimistic after Receiving an Easily Accessible Meat Reward Rather Than a Reward Requiring Effort

Crows ($n = 15$) were exposed to one of two experiences just prior to the cognitive bias test (presentation of an ambiguous stimulus): easy refers to retrieving meat from the table and effort refers to flying around the aviary to retrieve meat from four locations. Crows were significantly more optimistic (faster to the ambiguous stimulus) in the easy condition versus effort (Bayesian paired t test; $BF = 7.62$). In each boxplot, the horizontal bar is the median, the box ranges from the 25th to 75th percentile, and the whiskers show the range of data points. See Data S1 for all latency times and Figure S1 for mean latencies (\pm SEM) for all trials.

effect of executing complex, species-specific behaviors and goal-directed actions on animal welfare.

STAR★METHODS

Detailed methods are provided in the online version of this paper and include the following:

- KEY RESOURCES TABLE
- LEAD CONTACT AND MATERIALS AVAILABILITY
- EXPERIMENTAL MODEL AND SUBJECT DETAILS
- METHOD DETAILS
- QUANTIFICATION AND STATISTICAL ANALYSIS
- DATA AND CODE AVAILABILITY

SUPPLEMENTAL INFORMATION

Supplemental Information can be found online at <https://doi.org/10.1016/j.cub.2019.06.080>.

A video abstract is available at <https://doi.org/10.1016/j.cub.2019.06.080#mmc5>.

ACKNOWLEDGMENTS

We thank Province Sud for granting us permission to work in New Caledonia and Dean M. and Boris C. for allowing us access to their properties for catching and releasing the crows. D.E.M. is grateful to Mehdi Husain for assistance with videos. We also thank four anonymous reviewers for their helpful comments on our manuscript. This research was supported by DoD, Army Research Office, National Defense Science and Engineering Graduate (NDSEG) Fellowship, 32

CFR 168a, and a Theodore H. Ashford Graduate Fellowship to D.E.M.; a Royal Society of New Zealand Rutherford Discovery Fellowship and a Prime Minister's McDiarmid Emerging Scientist Prize to A.H.T.; and the Max Planck Institute for the Science of Human History to R.D.G.

AUTHOR CONTRIBUTIONS

Conceptualization, D.E.M. and A.H.T.; Methodology, D.E.M., M.S., and A.H.T.; Formal Analysis, P.N. and A.H.T.; Investigation, D.E.M., M.S., and R.H.; Resources and Funding Acquisition, A.H.T. and R.D.G.; Writing – Original Draft, D.E.M. and A.H.T.; Writing – Review & Editing, D.E.M., M.S., P.N., R.H., R.D.G., and A.H.T.; Visualization, D.E.M.; Supervision, A.H.T. and R.D.G.

DECLARATION OF INTERESTS

The authors declare no competing interests.

Received: April 5, 2019

Revised: May 28, 2019

Accepted: June 27, 2019

Published: August 1, 2019

REFERENCES

- Cialdini, R.B., and Kenrick, D.T. (1976). Altruism as hedonism: a social development perspective on the relationship of negative mood state and helping. *J. Pers. Soc. Psychol.* **34**, 907–914.
- Carless, D., and Douglas, K. (2010). Sport and physical activity for mental health. <https://doi.org/10.1002/9781444324945>.
- Lundqvist, C. (2011). Well-being in competitive sports—the feel-good factor? A review of conceptual considerations of well-being. *Int. Rev. Sport Exerc. Psychol.* **4**, 109–127.
- Caddick, N., and Smith, B. (2014). The impact of sport and physical activity on the well-being of combat veterans: a systematic review. *Psychol. Sport Exerc.* **15**, 9–18.
- Caddick, N., Smith, B., and Phoenix, C. (2015). The effects of surfing and the natural environment on the well-being of combat veterans. *Qual. Health Res.* **25**, 76–86.
- Emmons, R.A. (1986). Personal strivings. An approach to personality and subjective well-being. *J. Pers. Soc. Psychol.* **51**, 1058–1068.
- Emmons, R.A., and Kaiser, H.A. (1996). Goal orientation and emotional well-being: linking goals and affect through the self. In *In Striving and Feeling: Interactions among Goals, Affect, and Self-Regulation*, L.L. Martin, and A. Tesser, eds. (Lawrence Erlbaum Associates), pp. 79–98.
- Sheldon, K.M., and Elliot, A.J. (1999). Goal striving, need satisfaction, and longitudinal well-being: the self-concordance model. *J. Pers. Soc. Psychol.* **76**, 482–497.
- Burman, O.H.P., Parker, R., Paul, E.S., and Mendl, M. (2008). A spatial judgement task to determine background emotional state in laboratory rats, *Rattus norvegicus*. *Anim. Behav.* **76**, 801–809.
- Richter, S.H., Schick, A., Hoyer, C., Lankisch, K., Gass, P., and Vollmayr-B. (2012). A glass full of optimism: enrichment effects on cognitive bias in a rat model of depression. *Cogn. Affect. Behav. Neurosci.* **12**, 527–542.
- Brydges, N.M., Leach, M., Nicol, K., Wright, R., and Bateson, M. (2011). Environmental enrichment induces optimistic cognitive bias in rats. *Anim. Behav.* **81**, 169–175.
- Bateson, M., and Matheson, S.M. (2007). Performance on a categorisation task suggests that removal of environmental enrichment induces ‘pessimism’ in captive European starlings (*Sturnus vulgaris*). *Anim. Welf.* **16**, 33–36.
- Matheson, S.M., Asher, L., and Bateson, M. (2008). Larger, enriched cages are associated with ‘optimistic’ response biases in captive European starlings (*Sturnus vulgaris*). *Appl. Anim. Behav. Sci.* **109**, 374–383.
- Douglas, C., Bateson, M., Walsh, C., Bédué, A., and Edwards, S.A. (2012). Environmental enrichment induces optimistic cognitive biases in pigs. *Appl. Anim. Behav. Sci.* **139**, 65–73.
- Nogueira, S.S.D.C., Fernandes, I.K., Costa, T.S.O., Nogueira-Filho, S.L.G., and Mendl, M. (2015). Does trapping influence decision-making under ambiguity in white-lipped peccary (*Tayassu pecari*)? *PLoS ONE* **10**, e0127868.
- Brajon, S., Laforest, J.P., Schmitt, O., and Devillers, N. (2015). The way humans behave modulates the emotional state of piglets. *PLoS ONE* **10**, e0133408.
- Neave, H.W., Daros, R.R., Costa, J.H.C., von Keyserlingk, M.A.G., and Weary, D.M. (2013). Pain and pessimism: dairy calves exhibit negative judgement bias following hot-iron disbudding. *PLoS ONE* **8**, e80556.
- Daros, R.R., Costa, J.H.C., von Keyserlingk, M.A.G., Hötzl, M.J., and Weary, D.M. (2014). Separation from the dam causes negative judgement bias in dairy calves. *PLoS ONE* **9**, e98429.
- Bateson, M., Desire, S., Gartside, S.E., and Wright, G.A. (2011). Agitated honeybees exhibit pessimistic cognitive biases. *Curr. Biol.* **21**, 1070–1073.
- Deakin, A., Mendl, M., Browne, W.J., Paul, E.S., and Hodge, J.J.L. (2018). State-dependent judgement bias in *Drosophila*: evidence for evolutionarily primitive affective processes. *Biol. Lett.* **14**, 20170779.
- Papciak, J., Popik, P., Fuchs, E., and Rygula, R. (2013). Chronic psychosocial stress makes rats more ‘pessimistic’ in the ambiguous-cue interpretation paradigm. *Behav. Brain Res.* **256**, 305–310.
- Salmeto, A.L., Hymel, K.A., Carpenter, E.C., Brilot, B.O., Bateson, M., and Sufka, K.J. (2011). Cognitive bias in the chick anxiety-depression model. *Brain Res.* **1373**, 124–130.
- Rygula, R., Pluta, H., and Popik, P. (2012). Laughing rats are optimistic. *PLoS ONE* **7**, e51959.
- de Waal, F. (2019). *Mama’s Last Hug: Animal Emotions and What They Tell Us about Ourselves* (W.W. Norton & Company).
- Krebs, D.L. (2011). The age of empathy: nature’s lessons for a kinder society. *J. Moral Educ.* **40**, 125–127.
- Darwin, C. (1872). *In The Expression of the Emotions in Man and Animals*, First Edition (John Murray).
- Eysenck, M.W., Mogg, K., May, J., Richards, A., and Mathews, A. (1991). Bias in interpretation of ambiguous sentences related to threat in anxiety. *J. Abnorm. Psychol.* **100**, 144–150.
- Harding, E.J., Paul, E.S., and Mendl, M. (2004). Animal behaviour: cognitive bias and affective state. *Nature* **427**, 312.
- Mendl, M., Brooks, J., Basse, C., Burman, O., Paul, E., Blackwell, E., and Casey, R. (2010). Dogs showing separation-related behaviour exhibit a ‘pessimistic’ cognitive bias. *Curr. Biol.* **20**, R839–R840.
- Mendl, M., Burman, O.H.P., Parker, R.M.A., and Paul, E.S. (2009). Cognitive bias as an indicator of animal emotion and welfare: emerging evidence and underlying mechanisms. *Appl. Anim. Behav. Sci.* **118**, 161–181.
- Paul, E.S., Harding, E.J., and Mendl, M. (2005). Measuring emotional processes in animals: the utility of a cognitive approach. *Neurosci. Biobehav. Rev.* **29**, 469–491.
- Mendl, M., Burman, O.H.P., and Paul, E.S. (2010). An integrative and functional framework for the study of animal emotion and mood. *Proc. R. Soc. B: Biol. Sci.* **277**, 20100303.
- Adriaense, J.E.C., Martin, J.S., Schiestl, M., Lamm, C., and Bugnyar, T. (2019). Negative emotional contagion and cognitive bias in common ravens (*Corvus corax*). *Proc. Natl. Acad. Sci. USA* **116**, 11547–11552.
- Sheldon, K.M., and Lyubomirsky, S. (2006). Achieving sustainable gains in happiness: change your actions, not your circumstances. *J. Happiness Stud.* **7**, 55–86.
- Lyubomirsky, S., Sheldon, K.M., and Schkade, D. (2005). Pursuing happiness: the architecture of sustainable change. *Rev. Gen. Psychol.* **9**, 111–131.
- Duranton, C., and Horowitz, A. (2019). Let me sniff! Nosework induces positive judgment bias in pet dogs. *Appl. Anim. Behav. Sci.* **211**, 61–66.

37. Burman, O., McGowan, R., Mendl, M., Norling, Y., Paul, E., Rehn, T., and Keeling, L. (2011). Using judgement bias to measure positive affective state in dogs. *Appl. Anim. Behav. Sci.* **132**, 160–168.
38. Koops, K., Furuichi, T., and Hashimoto, C. (2015). Chimpanzees and bonobos differ in intrinsic motivation for tool use. *Sci. Rep.* **5**, 11356.
39. Kenward, B., Schloegl, C., Rutz, C., Weir, A.A.S., Bugnyar, T., and Kacelnik, A. (2011). On the evolutionary and ontogenetic origins of tool-oriented behaviour in New Caledonian crows (*Corvus monedulaoides*). *Biol. J. Linn. Soc. Lond.* **102**, 870–877.
40. Berridge, K.C., and Robinson, T.E. (2003). Parsing reward. *Trends Neurosci.* **26**, 507–513.
41. Berridge, K.C., and Kringelbach, M.L. (2008). Affective neuroscience of pleasure: reward in humans and animals. *Psychopharmacology (Berl.)* **199**, 457–480.
42. Balcombe, J. (2006). *Pleasurable Kingdom: Animals and the Nature of Feeling Good* (Macmillan).
43. Doyle, R.E., Lee, C., Deiss, V., Fisher, A.D., Hinch, G.N., and Boissy, A. (2011). Measuring judgement bias and emotional reactivity in sheep following long-term exposure to unpredictable and aversive events. *Physiol. Behav.* **102**, 503–510.
44. White, R.W. (1959). Motivation reconsidered: the concept of competence. *Psychol. Rev.* **66**, 297–333.
45. De Charms, R. (2013). *Personal Causation: The Internal Affective Determinants of Behavior* (Routledge).
46. Deci, E.L., and Ryan, R.M. (1985). Intrinsic Motivation and Self-Determination in Human Behavior (Springer Science & Business Media).
47. Oudeyer, P.Y., and Kaplan, F. (2007). What is intrinsic motivation? A typology of computational approaches. *Front. Neurorobot.* **1**, 6.
48. Ryan, R.M., and Deci, E.L. (2000). Intrinsic and extrinsic motivations: classic definitions and new directions. *Contemp. Educ. Psychol.* **25**, 54–67.
49. Bloomsmith, M.A., Brent, L.Y., and Schapiro, S.J. (1991). Guidelines for developing and managing an environmental enrichment program for nonhuman primates. *Lab. Anim. Sci.* **41**, 372–377.
50. Karagiannis, C.I., Burman, O.H.P., and Mills, D.S. (2015). Dogs with separation-related problems show a “less pessimistic” cognitive bias during treatment with fluoxetine (Reconcile™) and a behaviour modification plan. *BMC Vet. Res.* **11**, 80.
51. Henry, S., Fureix, C., Rowberry, R., Bateson, M., and Hausberger, M. (2017). Do horses with poor welfare show ‘pessimistic’ cognitive biases? *Sci. Nat.* **104**, 8.
52. Löckener, S., Reese, S., Erhard, M., and Wöhr, A.-C. (2016). Pasturing in herds after housing in horseboxes induces a positive cognitive bias in horses. *J. Vet. Behav.* **11**, 50–55.
53. Bell, A.C., and D'Zurilla, T.J. (2009). Problem-solving therapy for depression: a meta-analysis. *Clin. Psychol. Rev.* **29**, 348–353.
54. Hunt, G.R. (2016). Social and spatial reintegration success of New Caledonian crows (*Corvus monedulaoides*) released after aviary confinement. *Wilson J. Ornithol.* **128**, 168–173.
55. Biro, D., Freeman, R., Meade, J., Roberts, S., and Guilford, T. (2007). Pigeons combine compass and landmark guidance in familiar route navigation. *Proc. Natl. Acad. Sci. USA* **104**, 7471–7476.
56. Bingman, V.P. (1990). Spatial navigation in birds. In *Comparative Cognition and Neuroscience*. In *Neurobiology of Comparative Cognition*, R.P. Kesner, and D.S. Olton, eds. (Lawrence Erlbaum Associates), pp. 423–447.
57. Bateson, M., and Nettle, D. (2015). Development of a cognitive bias methodology for measuring low mood in chimpanzees. *PeerJ* **3**, e998.
58. d'Ettorre, P., Carere, C., Demora, L., Le Quinquis, P., Signorotti, L., and Bovet, D. (2017). Individual differences in exploratory activity relate to cognitive judgement bias in carpenter ants. *Behav. Processes* **134**, 63–69.
59. Gamer, M., Lemon, J., Fellows, I., and Singh, P. (2012). Package ‘irr.’ Various coefficients of interrater reliability and agreement. <https://cran.r-project.org/web/packages/irr/irr.pdf>.
60. Morey, R.D., Rouder, J.N., Jamil, T., Urbanek, S., Forner, K., and Ly, A. (2018). Package ‘BayesFactor.’ Computation of Bayes factors for common designs. <https://cran.r-project.org/web/packages/BayesFactor/BayesFactor.pdf>.
61. Wagenmakers, E.J., Marsman, M., Jamil, T., Ly, A., Verhagen, J., Love, J., Selker, R., Gronau, Q.F., Smíra, M., Epskamp, S., et al. (2018). Bayesian inference for psychology. Part I: theoretical advantages and practical ramifications. *Psychon. Bull. Rev.* **25**, 35–57.

STAR★METHODS

KEY RESOURCES TABLE

REAGENT or RESOURCE	SOURCE	IDENTIFIER
Software and Algorithms		
R	The R Foundation	https://www.r-project.org/

LEAD CONTACT AND MATERIALS AVAILABILITY

Further information and requests for resources should be directed to and will be fulfilled by the Lead Contact, Dakota E. McCoy (dakotamccoy@g.harvard.edu). All latency times recorded in this study are available in the Supporting Information file [Data S1](#), and all code used for statistical analyses are available in the Supporting Information file [Methods S1](#).

EXPERIMENTAL MODEL AND SUBJECT DETAILS

Fifteen wild New Caledonian crows (*Corvus monedulaoides*; $n = 7$ in 2016, $n = 8$ in 2018) were captured and housed in an aviary on Grand Terre, New Caledonia for temporary behavioral research purposes before being released back into the wild. Birds were housed in family groups with substantial natural enrichment (logs, bushes, seashells, etc). The birds' daily diet consisted of meat, dog food, eggs, and fresh fruit, with water available *ad libitum*. They were not food-deprived, and birds were maintained at or above their weights at capture. After the research studies were completed, birds were released at their capture sites. Previously, researchers observed that crows housed temporarily in captivity (similarly to the present study) successfully reintegrated into the wild after release [54]. Experiments were conducted in a solo "experimental" aviary, where birds had ample room to fly about but were screened from viewing other birds. The test took place on a table at the front of the experimental aviary, and multiple high perches allowed the birds to remain at the back of the aviary (or elsewhere) when they did not want to participate. One bird, "Jupiter," exhibited signs of nervousness in other experiments and thus was tested in his home compartment. Our work was carried out under the approval of the University of Auckland Animal Ethics Committee (reference no. 001823).

METHOD DETAILS

Birds were trained on a protocol [28, 30, 31] designed to test whether they demonstrate optimistic behavior. The bird's affective state, whether positive or negative, motivates their latency toward an ambiguous stimulus after different experiences. We used a spatial protocol [9, 29] where birds were trained to know that a small tub with a lid contained a large reward if it was placed on one side of the table and a small reward if it was placed on the other side (Figure 1). The large reward was 3 cubes of meat, while the small reward was $\frac{1}{4}$ of a cube of meat. We provided a small reward as contrast, rather than no reward or an aversive stimulus, because these are wild birds who are fed *ad libitum* and participate in our tasks on a voluntary basis. We placed a marker on the table to assist with location memory (since some birds use landmarks for location memory in the wild [55, 56]). We counterbalanced this protocol across birds (half of the birds learned that left was the large reward and right the small reward, and half learned the opposite).

In all phases, birds were given a maximum of 30 s to open the box. During training birds were (i) habituated to the apparatus (ii) given 10 trials of the large reward side and 10 trials of the small reward side (pseudorandomized in blocks of five of the same trial) and (iii) given blocks of 8 trials where trial type (large reward and small reward) was pseudorandomized across trials. We repeated (iii) until birds achieved criterion for two blocks in a row (defined as approaching faster in the final three large reward pseudorandom trials of each block than the final three small reward pseudorandom trials [29]), after which time the bird proceeded to the test phase.

At test, we examined how optimistically a bird behaved after having a particular experience, where relative optimism is indexed by quicker approaches to the ambiguous box and relative pessimism is indexed by slower approaches. For each test block, the bird received 4 refresher trials (two large reward and two small reward presented pseudorandomly), followed by three trials of one of four experience types ("Conditions" in Figure 2), followed by a test trial where the "ambiguous" stimulus was presented (the same box placed in the middle of the table, Figure 1D).

Often in studies using the ambiguous-stimulus framework, researchers present three ambiguous stimuli: near-positive, near-negative, and middle. This rigorous five-point methodology ensures that the animals perceive the ambiguous stimuli as relating to the stimuli from training, because it generates a response curve with five, rather than three, points along a distribution of expected rewards. Here, we used a three-point methodology with only one ambiguous stimulus (middle) because of the logistical constraints of our experimental design, which required testing wild-caught, temporarily captive birds on four conditions (Tool, No Tool, Effort, and Easy; see details below). The crows' average approach time in the refresher trials of the large reward baseline was 3.79 s (SEM = 0.18) and in the refresher trials of the small reward baseline was 25.20 s (SEM = 0.79), demonstrating that the crows continued to distinguish between the large reward and small reward locations before the test trials. The average approach time for ambiguous

trials was 16.19 s (SEM 1.52), which falls almost exactly halfway in between the small and large reward baselines (Figure S1). This suggests that the crows perceived the ambiguous stimulus as relating to the small and large stimuli, but this does need to be validated with a 5-point methodology.

Each experience trial yielded one large total block of meat (equivalent in size to two normal blocks). In the “Tool” condition, the birds conducted standard tool use with a block apparatus to retrieve a single large block of meat. We placed the tool on the table during the test phase when the experience started, and we did not remove it until after the test was concluded. In the “No Tool” condition, crows used their beaks to retrieve a single large block of meat from the tool-use apparatus, without needing nor receiving a tool. In the “Easy” condition, birds retrieved four $\frac{1}{4}$ -block pieces of meat from the table directly, while in the “Effort” condition, birds traveled around the aviary to four locations to retrieve four $\frac{1}{4}$ -block pieces of meat placed within sight. It was necessary to split the meat in this way so it could be distributed around the aviary for the Effort condition. We paired the conditions as Tool – No Tool and Effort – Easy for analysis because the birds received one large block of meat in the former two conditions and four $\frac{1}{4}$ -block pieces of meat in the latter two conditions; although the total reward size was the same, the presentation was not strictly comparable. Additionally, the same tool apparatus was present in both the Tool and No Tool conditions but was not in the other two conditions. Finally, these comparisons directly tested the hypotheses we were interested in. We pseudorandomized the order of these experiences for each bird, but ensured that Tool and No Tool were always adjacent, while Effort and Easy were always adjacent. Prior to the experience trials (at least one half-day before) birds were given one sample trial of each experience to ensure that they were able to complete the experience task.

During test trials, after the “ambiguous” stimulus was presented, we interrupted the bird the moment their beak touched the lid so that they would retreat from the table and thus could not thoroughly explore the box. This ensured the bird did not learn whether the ambiguous stimulus contained food or not across test trials. To ensure that the Test Phase did not confuse the bird’s understanding of the protocol, we repeated the stage (iii) of training between each test trial; that is, after their first test the birds had to achieve criterion for two blocks in a row before they continued with their second test, and so on. We repeated the test protocol four times; that is, each bird saw the ambiguous stimulus four times total, separated by criterion protocols in between each test protocol. We hypothesized that they would not develop negative associations with the ambiguous trial and a lack of reward given that they would only receive four total trials; a similar methodology with chimpanzees found no change in response to ambiguous stimuli over five trials [57]. We included Trial Order as a predictor in our statistical modeling to control for the potential effect of seeing the ambiguous stimulus four times, but it had no explanatory power in the model (see Quantification and Statistical Analysis). This shows that the ambiguous stimulus did not become aversive to the crows over the 4 test trials due to these trials being interrupted.

We measured optimism by scoring the trial in which birds were given an ambiguous stimulus after an experience. We recorded the time it took the bird to approach the stimulus (with a maximum option of 30 s). To ensure consistency of our timing method, we controlled the crows’ approach trajectory by placing a small piece of meat between their upper back perch (a preferred resting location) and the table (the test location). Therefore, birds would consistently fly to this baited portion, pause, and then either go down to the table or not. Using Solomon Coder, we timed the bird’s delay between (i) landing on the perch to retrieve the bait and (ii) descending to the table to open the box and retrieve the reward inside. The moment the bird landed on the table was used as the “end” time, because that is the point at which the bird had decided to investigate the stimulus. If birds chose not to descend to the table after 30 s had elapsed, we assigned a latency time of 30 s [58]. All latency results during test trials are reported in Data S1. To measure interobserver reliability, a second coder unaware of test condition coded 20% of the videos and we calculated intraclass correlation coefficient (ICC, oneway, consistency) using the function `icc` in R package `irr` [59]; there was high agreement (ICC = 0.954, 95% CI = [0.921, 0.974]).

QUANTIFICATION AND STATISTICAL ANALYSIS

All analyses were carried out using the “Bayes Factor” [60] package in R using the `lmBF` and `ttestBF` functions (see Methods S1 for code). We tested $n = 15$ crows, each on the four experimental conditions. In order to analyze whether the crows differed in their approach latency across the four different experimental conditions, we constructed several Bayesian repeated-measures ANOVA models with differing fixed effects (Condition-Only, Trial Order-Only, Condition+Trial Order, and Condition*Trial Order). All models also contained Participant as a random effect to account for the within-subjects nature of the experiment design. Each of the models were compared to a simple model which just included Participant as a random factor, and we selected the model which best explained the data (i.e., had the highest Bayes Factor (BF)). In Bayesian analysis, $BF > 3$ indicate substantial/significant support for the alternative hypothesis whereas $BF < 0.333$ indicate substantial/significant support for the null hypothesis [61]. Each model was constructed with objective priors of prior width $r = 1$ for fixed effects and $r = 0.5$ for random effects. Having established that the Condition+Order model was the best fit for the data (with no interaction; see Table S1 for all models fitted), we directly compared the fit of the Condition-Only model and the Order-Only model to the Condition+Order model. If one factor of these factors was having a larger effect on the crow’s approach latency, removing that factor from the model should reduce the fit of the model to the data more substantially.

To explore our pairwise comparisons, we used Bayesian paired t tests to test between the crows’ approach latencies in the Tool-No Tool conditions and the Easy-Effort conditions. For both t tests, a negative half-Cauchy distribution with $r = 0.707$ and an effect

size centered on 0 was used an objective prior distribution. t test results can be found in [Figures 3 and 4](#) and in the [Results and Discussion](#).

DATA AND CODE AVAILABILITY

All data and code is available as Supporting Information. [Data S1](#) is an excel spreadsheet of crow latency times, and [Methods S1](#) is an annotated HTML document of the code used to run statistical analyses.

References

- [1] Richard O Prum. Aesthetic evolution by mate choice: Darwin's really dangerous idea. *Philosophical Transactions of the Royal Society B: Biological Sciences*, 367(1600):2253–2265, 2012. ISSN 0962-8436.
- [2] Ronald Aylmer Fisher. *The genetical theory of natural selection: a complete variorum edition*. Oxford University Press, 1999. ISBN 0198504403.
- [3] Marian Stamp Dawkins and Tim Guilford. Sensory bias and the adaptiveness of female choice. *American Naturalist*, pages 937–942, 1996. ISSN 0003-0147.
- [4] Geoffrey E. Hill. Sexiness, Individual Condition, and Species Identity: The Information Signaled by Ornaments and Assessed by Choosing Females. *Evolutionary Biology*, 42(3):251–259, 2015. ISSN 00713260. doi: 10.1007/s11692-015-9331-x.
- [5] Ivar Folstad and Andrew John Karter. Parasites, Bright Males, and the Immunocompetence Handicap. *The American Naturalist*, 139(3):603–622, 1992. ISSN 0003-0147. doi: 10.1086/285346.
- [6] Amotz Zahavi. Mate selection—a selection for a handicap. *Journal of theoretical Biology*, 53(1):205–214, 1975. ISSN 0022-5193.
- [7] Alejandro Cantarero, Rafael Mateo, Pablo Camarero, Daniel Alonso, Blanca Fernandez-Eslava, and Carlos Alonso-Alvarez. A mitochondria-targeted antioxidant affects the carotenoid-based plumage of red crossbills. *bioRxiv*, page 839670, 2019.
- [8] Alejandro Cantarero and Carlos Alonso-Alvarez. Mitochondria-targeted molecules determine the redness of the zebra finch bill. *Biology letters*, 2017. ISSN 1744957X. doi: 10.1098/rsbl.2017.0455.
- [9] Geoffrey E. Hill, Wendy R. Hood, Zhiyuan Ge, Rhys Grinter, Chris Greening, James D. Johnson, Noel R. Park, Halie A. Taylor, Victoria A. Andreasen, Matthew J. Powers, Nicholas M. Justyn, Hailey A. Parry, Andreas N. Kavazis, and Yufeng Zhang. Plumage redness signals mitochondrial function in the house finch. *Proceedings of the Royal Society B: Biological Sciences*, 2019. ISSN 14712954. doi: 10.1098/rspb.2019.1354.
- [10] Mirre J.P. Simons, Alan A. Cohen, and Simon Verhulst. What does carotenoid-dependent coloration tell? Plasma carotenoid level signals immunocompetence and

oxidative stress state in birds-a meta-analysis. *PLoS ONE*, 7(8), 2012. ISSN 19326203. doi: 10.1371/journal.pone.0043088.

- [11] Ryan J Weaver, Eduardo S A Santos, Anna M Tucker, Alan E Wilson, and Geoffrey E Hill. Carotenoid metabolism strengthens the link between feather coloration and individual quality. *Nature communications*, 9(1):73, 2018. ISSN 2041-1723.
- [12] John A Endler. Natural and sexual selection on color patterns in poeciliid fishes. In *Evolutionary ecology of neotropical freshwater fishes*, pages 95–111. Springer, 1984.
- [13] Alexandra McQueen, Bart Kempenaers, James Dale, Mihai Valcu, Zachary T. Emery, Cody J. Dey, Anne Peters, and Kaspar Delhey. Evolutionary drivers of seasonal plumage colours: colour change by moult correlates with sexual selection, predation risk and seasonality across passerines, 2019. ISSN 14610248.
- [14] Marian Stamp Dawkins and Tim Guilford. The corruption of honest signalling. *Animal Behaviour*, 41(5):865–873, 1991. ISSN 00033472. doi: 10.1016/S0003-3472(05)80353-7.
- [15] Richard Dawkins and John R Krebs. Animal signals: information or manipulation. In *Behavioural ecology: An evolutionary approach*, volume 2, pages 282–309. 1978.
- [16] Geoffrey E Hill. Trait elaboration via adaptive mate choice: sexual conflict in the evolution of signals of male quality. *Ethology Ecology Evolution*, 6(3):351–370, 1994. ISSN 0394-9370.
- [17] John R Krebs and R Dawkins. Animal signals: mindreading and manipulation. In *Behavioural Ecology: an evolutionary approach*, pages 380–402. Blackwell Scientific Publication, 1984.
- [18] Rebecca E Koch, Andreas N Kavazis, Dennis Hasselquist, Wendy R Hood, Yufeng Zhang, Matthew B Toomey, and Geoffrey E Hill. No evidence that carotenoid pigments boost either immune or antioxidant defenses in a songbird. *Nature communications*, 9(1):491, 2018. ISSN 2041-1723.
- [19] Ryan J Weaver, Rebecca E Koch, and Geoffrey E Hill. What maintains signal honesty in animal colour displays used in mate choice? *Phil. Trans. R. Soc. B*, 372(1724):20160343, 2017. ISSN 0962-8436.
- [20] Innes C. Cuthill, William L. Allen, Kevin Arbuckle, Barbara Caspers, George Chaplin, Mark E. Hauber, Geoffrey E. Hill, Nina G. Jablonski, Chris D. Jiggins, Almut Kelber, Johanna Mappes, Justin Marshall, Richard Merrill, Daniel Osorio, Richard Prum, Nicholas W. Roberts, Alexandre Roulin, Hannah M. Rowland, Thomas N. Sherratt, John Skelhorn, Michael P. Speed, Martin Stevens, Mary Caswell Stoddard, Devi Stuart-Fox, Laszlo Talas, Elizabeth Tibbetts, and Tim Caro. The biology of color. *Science*, 357(6350), 2017. ISSN 10959203. doi: 10.1126/science.aan0221.

- [21] Geoffrey Edward Hill and Kevin J McGraw. *Bird coloration: mechanisms and measurements*, volume 1. Harvard University Press, Cambridge, 2006. ISBN 0674018931.
- [22] Geoffrey Edward Hill and Kevin J McGraw. *Bird coloration: function and evolution*, volume 2. Harvard University Press, Cambridge, 2006. ISBN 0674021762.
- [23] R O Prum. Anatomy, physics, and evolution of avian structural colors, 2006.
- [24] Stéphanie M. Doucet, Matthew D. Shawkey, Geoffrey E. Hill, and Robert Montgomerie. Iridescent plumage in satin bowerbirds: Structure, mechanisms and nanostructural predictors of individual variation in colour. *Journal of Experimental Biology*, 2006. ISSN 00220949. doi: 10.1242/jeb.01988.
- [25] Doekele G. Stavenga, Hein L. Leertouwer, and Bodo D. Wilts. Magnificent magpie colours by feathers with layers of hollow melanosomes. *The Journal of experimental biology*, 2018. ISSN 14779145. doi: 10.1242/jeb.174656.
- [26] Eric R. Dufresne, Heeso Noh, Vinodkumar Saranathan, Simon G.J. Mochrie, Hui Cao, and Richard O. Prum. Self-assembly of amorphous biophotonic nanostructures by phase separation. *Soft Matter*, 2009. ISSN 1744683X. doi: 10.1039/b902775k.
- [27] Todd Alan Harvey, Kimberly S Bostwick, and Steve Marschner. Directional reflectance and milli-scale feather morphology of the African Emerald Cuckoo, <i>Chrysococcyx cupreus</i>. *Journal of The Royal Society Interface*, 10(86):20130391, 2013. ISSN 1742-5689.
- [28] Chad M. Eliason and Julia A. Clarke. Cassowary gloss and a novel form of structural color in birds. *Science Advances*, 2020. ISSN 23752548. doi: 10.1126/sciadv.aba0187.
- [29] Holly L Gorton and Thomas C Vogelmann. Effects of epidermal cell shape and pigmentation on optical properties of Antirrhinum petals at visible and ultraviolet wavelengths. *Plant Physiology*, 112(3):879–888, 1996. ISSN 0032-0889.
- [30] Marlene Spinner, Alexander Kovalev, Stanislav N Gorb, and Guido Westhoff. Snake velvet black: hierarchical micro- and nanostructure enhances dark colouration in <i>Bitis rhinoceros</i>. *Scientific reports*, 3:1846, 2013. ISSN 2045-2322. doi: 10.1038/srep01846.
- [31] Shuliang Dou, Hongbo Xu, Jiupeng Zhao, Ke Zhang, Na Li, Yipeng Lin, Lei Pan, and Yao Li. Bioinspired Microstructured Materials for Optical and Thermal Regulation. *Advanced Materials*, page 2000697, 2020. ISSN 0935-9648.
- [32] D G Stavenga, Sally Stowe, Katharina Siebke, Jochen Zeil, and K Arikawa. Butterfly wing colours: scale beads make white pierid wings brighter. *Proceedings of the Royal Society of London. Series B: Biological Sciences*, 271(1548):1577–1584, 2004. ISSN 0962-8452.

- [33] Joel G Kingsolver. Thermal ecology of Pieris butterflies (Lepidoptera: Pieridae): a new mechanism of behavioral thermoregulation. *Oecologia*, 66(4):540–545, 1985. ISSN 0029-8549.
- [34] Katie Shanks, Sundaram Senthilarasu, and Tapas K Mallick. White butterflies as solar photovoltaic concentrators. *Scientific reports*, 5(1):1–10, 2015. ISSN 2045-2322.
- [35] G J Barber, A Braem, N H Brook, W Cameron, C D'Ambrosio, N Harnew, J Imong, K Lessnoff, R N Martin, and F C D Metlica. Development of lightweight carbon-fiber mirrors for the RICH 1 detector of LHCb. *Nuclear Instruments and Methods in Physics Research Section A: Accelerators, Spectrometers, Detectors and Associated Equipment*, 593(3):624–637, 2008. ISSN 0168-9002.
- [36] Runsheng Tang and Xinyue Liu. Optical performance and design optimization of V-trough concentrators for photovoltaic applications. *Solar Energy*, 85(9):2154–2166, 2011. ISSN 0038-092X.
- [37] David Haig. Genetic Conflicts in Human Pregnancy. *The Quarterly Review of Biology*, 68(4):495–532, 1993. ISSN 0033-5770. doi: 10.1086/418300.
- [38] Helen Wasielewski, Joe Alcock, and Athena Aktipis. Resource conflict and cooperation between human host and gut microbiota: implications for nutrition and health. *Annals of the New York Academy of Sciences*, 2016. ISSN 17496632. doi: 10.1111/nyas.13118.
- [39] David Haig. Altercation of generations: genetic conflicts of pregnancy. *American Journal of Reproductive Immunology*, 35(3):226–232, 1996. ISSN 1046-7408.
- [40] John T Buchholz. Developmental selection in vascular plants. *Botanical Gazette*, 73(4):249–286, 1922. ISSN 0006-8071.
- [41] David Haig. Brood Reduction and Optimal Parental Investment when Offspring Differ in Quality. *The American Naturalist*, 136(4):550–556, 1990. ISSN 0003-0147. doi: 10.1086/285113.
- [42] C J Roberts and C R Lowe. Where have all the conceptions gone? In *Problems of birth defects*, pages 148–150. Springer, 1975.
- [43] Allen J Wilcox, Clarice R Weinberg, John F O'connor, Donna D Baird, John P Schlatner, Robert E Canfield, E Glenn Armstrong, and Bruce C Nisula. Incidence of early loss of pregnancy. *New England Journal of Medicine*, 319(4):189–194, 1988. ISSN 0028-4793.
- [44] Lauren J. Ewington, Shreeya Tewary, and Jan J. Brosens. New insights into the mechanisms underlying recurrent pregnancy loss, 2019. ISSN 14470756.
- [45] Donald R Forsdyke. When few survive to tell the tale: thymus and gonad as auditioning organs: historical overview. *Theory in Biosciences*, pages 1–10, 2019. ISSN 1431-7613.

- [46] David Haig. Cooperation and conflict in human pregnancy. *Current Biology*, 29(11):R455–R458, 2019. ISSN 0960-9822.
- [47] R Michael Roberts. Interferon- τ and Pregnancy. *Journal of interferon cytokine research*, 16(4):271–273, 1996. ISSN 1079-9907.
- [48] John E Nelson and Robert T Gemmell. Birth in the northern quoll, *Dasyurus hallucatus* (Marsupialia: Dasyuridae). *Australian Journal of Zoology*, 51(2):187–198, 2003. ISSN 1446-5698. doi: 10.1071/ZO02016.
- [49] Byron B. Lamont and Gregory J. Barrett. Constraints on Seed Production and Storage in a Root-Suckering Banksia. *The Journal of Ecology*, 1988. ISSN 00220477. doi: 10.2307/2260634.
- [50] Glenda Vaughton and Susan M. Carthew. Evidence for selective fruit abortion in *Banksia spinulosa* (Proteaceae). *Biological Journal of the Linnean Society*, 1993. ISSN 10958312. doi: 10.1111/j.1095-8312.1993.tb00917.x.
- [51] Robyn Hudson and Fritz Trillmich. Sibling competition and cooperation in mammals: challenges, developments and prospects. *Behavioral Ecology and Sociobiology*, 62(3):299–307, 2007. ISSN 0340-5443. doi: 10.1007/s00265-007-0417-z.
- [52] Douglas W Mock and Geoffrey A Parker. The evolution of sibling rivalry. Oxford Series in Ecology and Evolution. 1997.
- [53] Alexandre Roulin and Amélie N Dreiss. Sibling competition and cooperation over parental care, 2012.
- [54] Nick J Royle, Ian R Hartley, Ian P F Owens, and Geoffrey A Parker. Sibling competition and the evolution of growth rates in birds. *Proceedings of the Royal Society of London. Series B: Biological Sciences*, 266(1422):923–932, 1999. ISSN 1471-2954. doi: 10.1098/rspb.1999.0725.
- [55] D D Chapman, S P Wintner, D L Abercrombie, J Ashe, A M Bernard, M S Shivji, and K A Feldheim. The behavioural and genetic mating system of the sand tiger shark, *Carcharias taurus*, an intrauterine cannibal. *Biology Letters*, 9(3):20130003, 2013. ISSN 1744-9561. doi: 10.1098/rsbl.2013.0003.
- [56] W. Golla, H. Hofer, and M. L. East. Within-litter sibling aggression in spotted hyenas: effect of maternal nursing, sex and age. *Animal Behaviour*, 58(4):715–726, 1999. ISSN 0003-3472. doi: 10.1006/anbe.1999.1189.
- [57] S Neuenschwander. Brood size, sibling competition, and the cost of begging in great tits (*Parus major*). *Behavioral Ecology*, 14(4):457–462, 2003. ISSN 1465-7279. doi: 10.1093/beheco/arg025.
- [58] Bart W O’Gara. Unique aspects of reproduction in the female pronghorn (*Antilocapra americana* Ord). *Developmental Dynamics*, 125(2):217–231, 1969. ISSN 1553-0795.

- [59] M. A. Gibson and E. Gurmu. Land inheritance establishes sibling competition for marriage and reproduction in rural Ethiopia. *Proceedings of the National Academy of Sciences*, 2011. ISSN 0027-8424. doi: 10.1073/pnas.1010241108.
- [60] Ting Ji, Jia Jia Wu, Qiao Qiao He, Jing Jing Xu, Ruth Mace, and Yi Tao. Reproductive competition between females in the matrilineal Mosuo of southwestern China. *Philosophical Transactions of the Royal Society B: Biological Sciences*, 368(1631), 2013. ISSN 14712970. doi: 10.1098/rstb.2013.0081.
- [61] Aïda Nitsch, Charlotte Faurie, and Virpi Lummaa. Are elder siblings helpers or competitors? Antagonistic fitness effects of sibling interactions in humans. *Proceedings of the Royal Society B: Biological Sciences*, 280(1750):20122313, 2012. ISSN 0962-8452. doi: 10.1098/rspb.2012.2313.
- [62] Aline Bütkofer, David N. Figlio, Krzysztof Karbownik, Christopher W. Kuzawa, and Kjell G. Salvanes. Evidence that prenatal testosterone transfer from male twins reduces the fertility and socioeconomic success of their female co-twins. *Proceedings of the National Academy of Sciences*, 2019. ISSN 0027-8424. doi: 10.1073/pnas.1812786116.
- [63] Lale Say, Doris Chou, Alison Gemmill, Özge Tunçalp, Ann Beth Moller, Jane Daniels, A. Metin Gülmezoglu, Marleen Temmerman, and Leontine Alkema. Global causes of maternal death: A WHO systematic analysis. *The Lancet Global Health*, 2014. ISSN 2214109X. doi: 10.1016/S2214-109X(14)70227-X.
- [64] David Haig. *From Darwin to Derrida*. 2020. doi: 10.7551/mitpress/12384.001.0001.
- [65] Melissa Bateson, Suzanne Desire, Sarah E. Gartside, and Geraldine A. Wright. Agitated honeybees exhibit pessimistic cognitive biases. *Current Biology*, 21(12):1070–1073, 2011. ISSN 0960-9822. doi: 10.1016/j.cub.2011.05.017.
- [66] Oliver H P Burman, Richard Parker, Elizabeth S. Paul, and Michael Mendl. A spatial judgement task to determine background emotional state in laboratory rats, *Rattus norvegicus*. *Animal Behaviour*, 76(3):801–809, 2008. ISSN 00033472. doi: 10.1016/j.anbehav.2008.02.014.
- [67] Catherine Douglas, Melissa Bateson, Clare Walsh, Anaïs Bédué, and Sandra A. Edwards. Environmental enrichment induces optimistic cognitive biases in pigs. *Applied Animal Behaviour Science*, 139(1-2):65–73, 2012. ISSN 01681591. doi: 10.1016/j.applanim.2012.02.018.
- [68] Michael W. Eysenck, Karin Mogg, Jon May, Anne Richards, and Andrew Mathews. Bias in Interpretation of Ambiguous Sentences Related to Threat in Anxiety. *Journal of Abnormal Psychology*, 100(2):144–150, 1991. ISSN 0021843X. doi: 10.1037/0021-843X.100.2.144.
- [69] Emma J. Harding, Elizabeth S. Paul, and Michael Mendl. Animal behaviour: Cognitive bias and affective state. *Nature*, 427(6972):312–312, 2004. ISSN 0028-0836. doi: 10.1038/427312a.

- [70] Michael Mendl, Oliver H.P. Burman, Richard M.A. Parker, and Elizabeth S. Paul. Cognitive bias as an indicator of animal emotion and welfare: Emerging evidence and underlying mechanisms. *Applied Animal Behaviour Science*, 118(3-4):161–181, 2009. ISSN 01681591. doi: 10.1016/j.applanim.2009.02.023.
- [71] Michael Mendl, Oliver H.P. Burman, and Elizabeth S. Paul. An integrative and functional framework for the study of animal emotion and mood. In *Proceedings of the Royal Society B: Biological Sciences*, 2010. doi: 10.1098/rspb.2010.0303.
- [72] Michael Mendl, Julie Brooks, Christine Basse, Oliver Burman, Elizabeth Paul, Emily Blackwell, and Rachel Casey. Dogs showing separation-related behaviour exhibit a 'pessimistic' cognitive bias, 2010. ISSN 09609822.
- [73] Elizabeth S. Paul, Emma J. Harding, and Michael Mendl. Measuring emotional processes in animals: The utility of a cognitive approach, 2005. ISSN 01497634.
- [74] Melissa Bateson and S. M. Matheson. Performance on a categorisation task suggests that removal of environmental enrichment induces pessimism' in captive European starlings (*Sturnus vulgaris*). *ANIMAL WELFARE-POTTERS BAR THEN WHEATHAMPSTEAD-*, 16(SUPPL.):33, 2007. ISSN 0962-7286.
- [75] Stephanie M. Matheson, Lucy Asher, and Melissa Bateson. Larger, enriched cages are associated with 'optimistic' response biases in captive European starlings (*Sturnus vulgaris*). *Applied Animal Behaviour Science*, 109(2-4):374–383, 2008. ISSN 01681591. doi: 10.1016/j.applanim.2007.03.007.
- [76] Rolnei R Daros, João H C Costa, Marina A G von Keyserlingk, Maria J Hötzl, and Daniel M Weary. Separation from the dam causes negative judgement bias in dairy calves. *PLoS One*, 9(5):e98429, 2014. ISSN 1932-6203.
- [77] Amy L Salmeto, Kristen A Hymel, Erika C Carpenter, Ben O Brilot, Melissa Bateson, and Kenneth J Sufka. Cognitive bias in the chick anxiety–depression model. *Brain research*, 1373:124–130, 2011. ISSN 0006-8993.
- [78] Amanda Deakin, Michael Mendl, William J. Browne, Elizabeth S. Paul, and James J.L. Hodge. State-dependent judgement bias in *Drosophila*: evidence for evolutionarily primitive affective processes. *Biology Letters*, 14(2), 2018. ISSN 1744957X. doi: 10.1098/rsbl.2017.0779.
- [79] Rafal Rygula, Helena Pluta, and Piotr Popik. Laughing Rats Are Optimistic. *PLoS ONE*, 7(12), 2012. ISSN 19326203. doi: 10.1371/journal.pone.0051959.